National Library
of Canada

Acquisitions and
Bibliographic Services Branch

395 Wellington Street
Ottawa, Ontario
K1A 0N4

Bibliothèque nationale
du Canada

Direction des acquisitions et
des services bibliographiques

395, rue Wellington
Ottawa (Ontario)
K1A 0N4

Your file Votre référence

Our file Notre référence

NOTICE

The quality of this microform is heavily dependent upon the quality of the original thesis submitted for microfilming. Every effort has been made to ensure the highest quality of reproduction possible.

If pages are missing, contact the university which granted the degree.

Some pages may have indistinct print especially if the original pages were typed with a poor typewriter ribbon or if the university sent us an inferior photocopy.

Reproduction in full or in part of this microform is governed by the Canadian Copyright Act, R.S.C. 1970, c. C-30, and subsequent amendments.

AVIS

La qualité de cette microforme dépend grandement de la qualité de la thèse soumise au microfilmage. Nous avons tout fait pour assurer une qualité supérieure de reproduction.

S'il manque des pages, veuillez communiquer avec l'université qui a conféré le grade.

La qualité d'impression de certaines pages peut laisser à désirer, surtout si les pages originales ont été dactylographiées à l'aide d'un ruban usé ou si l'université nous a fait parvenir une photocopie de qualité inférieure.

La reproduction, même partielle, de cette microforme est soumise à la Loi canadienne sur le droit d'auteur, SRC 1970, c. C-30, et ses amendements subséquents.

Canada

UNIVERSITY OF ALBERTA

PREDICTING AND IMPROVING SIEVE TRAY EFFICIENCIES IN DISTILLATION

BY

GUANG XIA CHEN

A thesis submitted to the faculty of graduate studies and research in partial fulfillment of the requirements for the degree of **DOCTOR OF PHILOSOPHY**

DEPARTMENT OF CHEMICAL ENGINEERING

EDMONTON, ALBERTA

SPRING 1993

National Library
of Canada

Acquisitions and
Bibliographic Services Branch

395 Wellington Street
Ottawa, Ontario
K1A 0N4

Bibliothèque nationale
du Canada

Direction des acquisitions et
des services bibliographiques

395, rue Wellington
Ottawa (Ontario)
K1A 0N4

Your file *Votre référence*

Our file *Notre référence*

The author has granted an irrevocable non-exclusive licence allowing the National Library of Canada to reproduce, loan, distribute or sell copies of his/her thesis by any means and in any form or format, making this thesis available to interested persons.

L'auteur a accordé une licence irrévocable et non exclusive permettant à la Bibliothèque nationale du Canada de reproduire, prêter, distribuer ou vendre des copies de sa thèse de quelque manière et sous quelque forme que ce soit pour mettre des exemplaires de cette thèse à la disposition des personnes intéressées.

The author retains ownership of the copyright in his/her thesis. Neither the thesis nor substantial extracts from it may be printed or otherwise reproduced without his/her permission.

L'auteur conserve la propriété du droit d'auteur qui protège sa thèse. Ni la thèse ni des extraits substantiels de celle-ci ne doivent être imprimés ou autrement reproduits sans son autorisation.

ISBN 0-315-82038-1

Canada

Department of Chemical Engineering
Room 536 Chemical-Mineral Building
University of Alberta
Edmonton, AB T6G 2G6
1993 04 01

Faculty of Graduate Studies & Research
University Hall
University of Alberta
Edmonton, AB

To whom it may concern:

I hereby grant permission to **Guang X. Chen** to use the information contained in the paper **Performance of Combined Mesh Packing and Sieve Trays in Distillation,** published in the **Canadian Journal of Chemical Engineering,** and **Fouling of Sieve Trays,** submitted to the **Chemical Engineering Communications,** in his thesis entitled **Predicting and Improving Sieve Tray Efficiencies in Distillation.**

Sincerely yours

A. Afacan

Department of Chemical Engineering
Room 536 Chemical-Mineral Building
University of Alberta
Edmonton, AB T6G 2G6
1993 04 01

Faculty of Graduate Studies & Research
University Hall
University of Alberta
Edmonton, AB

To whom it may concern:

I hereby grant permission to **Guang X. Chen** to use the information contained in the paper **Performance of Combined Mesh Packing and Sieve Trays in Distillation,** published in the **Canadian Journal of Chemical Engineering**, in his thesis entitled **Predicting and Improving Sieve Tray Efficiencies in Distillation**.

Sincerely yours

Xu Chongsi

C. Xu

Department of Chemical Engineering
Room 536 Chemical-Mineral Building
University of Alberta
Edmonton, AB T6G 2G6
1993 04 01

Faculty of Graduate Studies & Research
University Hall
University of Alberta
Edmonton, AB

To whom it may concern:

I hereby grant permission to **Guang X. Chen** to use the information contained in the paper **Performance of Combined Mesh Packing and Sieve Trays in Distillation,** published in the **Canadian Journal of Chemical Engineering,** and **Prediction of Point Efficiency for Sieve Trays in Distillation,** submitted to the **Industrial & Engineering Chemistry Research,** and **Fouling of Sieve Trays,** submitted to the **Chemical Engineering Communications,** in his thesis entitled **Predicting and Improving Sieve Tray Efficiencies in Distillation.**

Sincerely yours

KT Chuang

K.T. Chuang

UNIVERSITY OF ALBERTA

FACULTY OF GRADUATE STUDIES AND RESEARCH

The undersigned certify that they have read, and recommend to the Faculty of Graduate Studies and Research for acceptance, a thesis entitled **PREDICTING AND IMPROVING SIEVE TRAY EFFICIENCIES IN DISTILLATION** submitted by **GUANG XIA CHEN** in partial fulfillment of the requirements for the degree of **DOCTOR OF PHILOSOPHY**

K T Chuang

Dr. K. T. Chuang (supervisor)

K Nandakumar

Dr. K. Nandakumar

P J Crickmore

Dr. P. J. Crickmore

Dr. N. O. Egiebor

James R. Fair

Dr. J. R. Fair (external examiner)

DATE April 16, 1993

UNIVERSITY OF ALBERTA

RELEASE FORM

NAME OF AUTHOR: **Guang Xia Chen**

TITLE OF THESIS: **Predicting and Improving Sieve Tray Efficiencies in Distillation**

DEGREE: **Doctor of Philosophy**

YEAR THIS DEGREE GRANTED: **Spring 1993**

Permission is hereby granted to the University of Alberta library to reproduce single copies of this thesis and to lend or sell such copies for private scholarly or scientific research purposes only.

The author reserves all other publication and other rights in association with the copyright in the thesis, and except as hereinbefore provided neither the thesis nor any substantial portion thereof may be printed or otherwise reproduced in any material form whatever without the author's prior written permission.

Signed Guang Xia Chen

Department of Chemical Engineering
University of Alberta
Edmonton, Alberta, Canada, T6G 2G6

DATE: April 21, 1993

ABSTRACT

A reliable and accurate tray efficiency model is of primary economic importance. Based on the dispersion theory and the penetration theory, a new point efficiency model has been developed. The model was verified by experimental data obtained from commercial-scale sieve trays under distillation conditions. The numbers of individual phase mass transfer units have been accurately determined from distillation data. Based on the determined number of individual phase mass transfer units, it was found that surface tension and its gradient have great effects on the number of mass transfer units, hence on the point efficiency. Correlations have been obtained to account for these effects on the point efficiency.

To meet the new demand in distillation, a packed tray with improved performance has been developed by combining sieve trays with a bed of mesh packing. The hydraulic and mass transfer performance of this packed tray has been studied in a distillation and an air/water column. It was found that by adding a shallow bed of packing, the Murphree tray efficiency increases by 40 to 50% over a wide range of flow rates and system properties in a small column. This increase in the efficiency can be attributed to smaller and more uniform bubbles and more stable hydraulic conditions generated on the packed trays. Hydraulic tests on an air/water system have shown that the packing can effectively reduce the tray entrainment and weeping. Consequently, the packing can increase the tray vapour capacity by 50 to 80%. However, the packing also results in a 15% increase in the total tray pressure drop and a 40 to 75% reduction of the tray's lifetime in fouling situations. Correlations have been obtained for estimating the packing effects on the tray efficiency, entrainment and pressure drop.

ACKNOWLEDGEMENTS

The author wishes to thank Dr. K.T. Chuang for his guidance and encouragement throughout this program.

The author would also like to thank Mr. A. Afacan for his assistance in the experimental work. The co-operation of the Chemical Engineering Workshop under the supervision of Mr. K. Faulder and that of the Instrument Shop under the supervision of Mr. W. Boddez are sincerely appreciated.

The author is sincerely grateful for the following financial support:

1. **The Natural Sciences and Engineering Research Council of Canada** through the NSERC PGS 4 and PGS 5 awards (1991 - 1993).
2. **The Education Commission of China** through Graduate Scholarships.
3. Dr. **Myer Horowitz** through The Myer Horowitz Graduate Scholarship.
4. **The Department of Chemical Engineering**, University of Alberta, through **The Captain Thomas Farrell Greenhalgh** Graduate Memorial Scholarships (1990 - 1993).
5. **The Faculty of Graduate Studies and Research**, University of Alberta, through **The Walter H. Johns** Graduate Fellowship (1991 - 1993).

TABLE OF CONTENTS

CHAPTER		PAGE
1.	**INTRODUCTION**	1
	1.1 INTRODUCTION	1
	1.2 PREDICTING TRAY EFFICIENCY	2
	1.3 IMPROVING TRAY EFFICIENCY	3
	1.4 LITERATURE CITED	6
2.	**PREDICTING POINT EFFICIENCIES FOR SIEVE TRAYS IN DISTILLATION**	8
	2.1 INTRODUCTION	8
	2.2 THEORY	10
	2.3 MODEL DEVELOPMENT	11
	2.4 DETERMINING CONSTANTS C_1 AND C_2	18
	2.5 PREDICTING POINT EFFICIENCIES	20
	2.6 LIQUID PHASE RESISTANCE	20
	2.7 COMPARISON WITH OTHER MODELS	21
	2.8 DISCUSSION	23
	2.9 CONCLUSIONS	25
	2.10 NOMENCLATURE	25
	2.11 LITERATURE CITED	37
3	**DETERMINING N_G AND N_L FROM E_{OG}**	44
	3.1 INTRODUCTION	44
	3.2 BASIC RELATIONS	44

3.3 EXISTING MODELS 45

3.3.1 Method 1: Slop and Intercept Method 45

3.3.2 Method 2: Based on Penetration Theory 45

3.3.3 Method 3: Based on Two Bubble Size and Improved Penetration Theory 47

3.4 METHOD 4: NEW MODEL 49

3.5 EXPERIMENTAL EFFICIENCY DATA 51

3.6 RESULTS AND DISCUSSION 51

3.6.1 Cyclohexane/N-heptane System 51

3.6.2 Methanol/Water System 53

3.6.3 Acetic Acid/Water System 54

3.7 CONCLUSIONS 56

3.8 NOMENCLATURE 57

3.9 LITERATURE CITED 71

4. THE EFFECTS OF SURFACE TENSION ON THE NUMBER OF MASS TRANSFER UNITS 73

4.1 INTRODUCTION 73

4.2 THEORY 74

4.2.1 Basic Relations 74

4.2.2 Efficiency Models Not Including Surface Tension 74

4.2.3 Efficiency Models Including Surface Tension 77

4.3 EXPERIMENTAL 78

4.4 RESULTS AND DISCUSSION 79

4.4.1 Murphree Vapour Phase Point Efficiency 79

4.4.2 Surface Tension Effects on The Number of Mass Transfer Units 79

4.4.3 Marangoni and Surface Renewal Effects 82

4.5 COMPARISON OF EFFICIENCY PREDICTION METHODS 83

4.5.1 Cyclohexane/N-heptane System 84

4.5.2 Acetic Acid/Water System 84

4.5.3 Methanol/Water System 85

4.6 CONCLUSIONS 86

4.7 NOMENCLATURE 86

4.8 LITERATURE CITED 106

5. THE EFFECTS OF A SURFACE TENSION GRADIENT ON THE NUMBER OF MASS TRANSFER UNITS 110

5.1 INTRODUCTION 110

5.2 THEORY 111

5.3 EXPERIMENTAL TRAY EFFICIENCY DATA 116

5.4 THE MARANGONI-INDEX 117

5.5 ENHANCEMENT FACTOR Φ 119

5.6 PARAMETER β 119

5.7 CONCLUSIONS 121

5.8 NOMENCLATURE 121

5.9 LITERATURE CITED 133

6. IMPROVING SIEVE TRAY PERFORMANCE WITH MESH PACKING 135

6.1 INTRODUCTION 135

6.2 EXPERIMENTAL 137

6.3 RESULTS AND DISCUSSION 138

6.3.1 Sieve Tray Efficiency 139

6.3.2 Effect of Mesh Packing on Tray Efficiency 140

6.3.3 Mass Transfer Mechanism 141

6.3.4 Tray Hydraulics 143

6.4 CONCLUSIONS 144

6.5 NOMENCLATURE 145

6.6 LITERATURE CITED 154

7. MASS TRANSFER AND HYDRAULICS OF PACKED SIEVE TRAYS 156

7.1 INTRODUCTION 156

7.2 EXPERIMENTAL 157

7.3 RESULTS AND DISCUSSION 158

7.3.1 Mass Transfer Efficiency 158

7.3.2 Interfacial Area 159

7.3.3 Surface Tension Effect 160

7.3.4 Capacity and Entrainment 162

7.3.5 Pressure Drop 164

7.4 CONCLUSIONS 165

7.5 NOMENCLATURE 166

7.6 LITERATURE CITED 180

8. PREDICTING POINT EFFICIENCIES FOR PACKED TRAYS IN DISTILLATION 182

8.1 INTRODUCTION 182

8.2 MODEL DEVELOPMENT 184

8.3 EXPERIMENTAL 187

8.4 RESULTS AND DISCUSSION 187

8.4.1 Point Efficiency 187

8.4.2 Bubble Diameter 188

8.4.3 Parameter Fitting for The Tray Without Packing 188

8.4.4 Predicting Efficiency for The Packed Tray 190

8.5 CONCLUSIONS 192

8.6 NOMENCLATURE 193

8.7 LITERATURE CITED 208

9. FOULING OF SIEVE TRAYS 210

9.1 INTRODUCTION 210

9.2 BACKGROUND 211

9.3 EXPERIMENTAL 212

9.4 RESULTS AND DISCUSSION 213

9.4.1 Particulate Fouling 213

9.4.2 Crystallisation Fouling 214

9.4.3 Mathematical Modelling 217

9.5 CONCLUSIONS 221

9.6 NOMENCLATURE 222

9.7 LITERATURE CITED 236

10. CONCLUSIONS AND RECOMMENDATIONS 237

10.1 INTRODUCTION 237

10.2 PREDICTING POINT EFFICIENCIES 237

10.3 DETERMINING N_G AND N_L FROM E_{OG} 238

10.4 THE EFFECT OF SURFACE TENSION ON TRAY EFFICIENCIES 238

10.5 THE EFFECT OF A SURFACE TENSION GRADIENT ON TRAY EFFICIENCIES 239

10.6 MESH PACKING EFFECTS ON SIEVE TRAY PERFORMANCE 239

10.6.1 Mass Transfer Performance 239

10.6.2 Interfacial Area and Sauter-Mean Bubble Diameter 240

10.6.3 Entrainment and Vapour Capacity 240

10.6.4 Dry Pressure Drop and Total Pressure Drop 241

10.6.5 Weeping and Turndown Ratio 241

10.6.6 Other Observations 241

10.7 FOULING OF SIEVE TRAY WITH AND WITHOUT PACKING 242

10.8 RECOMMENDATIONS FOR FUTURE WORK 242

10.8.1 Mesh Packing Effect on Liquid Mixing 242

10.8.2 Effect of Mesh Packing on Tray Efficiencies in Other Flow Regimes 243

10.8.3 Development of Other Kind of Packed Trays 244

10.9 LITERATURE CITED 244

APPENDICES

A. THE TOP VIEW OF FROTHS ON THE TRAY WITHOUT AND WITH A BED OF MESH PACKING 245

LIST OF TABLES

		PAGE
Table 1-1	List of Parameter Rating for Various Contactors	5
Table 5-1	Comparison of Trays and Physical Properties	124
Table 6-1	Column and Tray Dimensions	146
Table 7-1	Column and Tray Dimensions	168
Table 8-1	Experimental Data for Methanol/Water System	196
Table 8-2	Experimental data for Acetic Acid/Water System	197
Table 8-3	Parameter Values of AJ	198
Table 9-1	Column and Tray Dimensions	224
Table 9-2	Run Conditions	225

LIST OF FIGURES

		PAGE
Figure 2-1	Comparison of Predicted and Measured Point Efficiency for C6/C7	28
Figure 2-2	Comparison of Predicted and Measured Point Efficiency for C6/C7 Under Reduced Pressure at 34 kPa	29
Figure 2-3	Comparison of Predicted and Measured Point Efficiency for Isobutane/N-butane System at three different pressures	30
Figure 2-4	Comparison of Predicted and Measured Point Efficiency Ethylbenzene/Styrene System Under Reduced Pressure at 13.3 kPa	31
Figure 2-5	Calculated Percent Liquid Phase Resistance for Three Systems at Different Pressures	32
Figure 2-6	Comparison of Point Efficiency Obtained by Various Models	33
Figure 2-7	Comparison of Number of Vapour Phase Mass Transfer Units Obtained by Various Models	34
Figure 2-8	Comparison of Number of Liquid Phase Mass Transfer Units Obtained by Various Models	35
Figure 2-9	Comparison of Percent of Liquid Phase Resistance Obtained by Various Models	36
Figure 3-1	Point Efficiency of Cyclohexane/N-heptane System	59
Figure 3-2	Point Efficiency of Methanol/Water System	60

Figure 3-3 Point Efficiency of Acetic Acid/Water System 61

Figure 3-4 Comparison of Determined N_G by Four Methods for Cyclohexane/N-heptane System 62

Figure 3-5 Comparison of Determined N_L by Four Methods for Cyclohexane/N-heptane System 63

Figure 3-6 Comparison of Determined LPR by Four Methods for Cyclohexane/N-heptane System 64

Figure 3-7 Comparison of Determined N_G by Four Methods for Methanol/Water System 65

Figure 3-8 Comparison of Determined N_L by Four Methods for Methanol/Water system 66

Figure 3-9 Comparison of Determined LPR by Four Methods for Methanol/Water system 67

Figure 3-10 Comparison of Determined N_G by Four Methods for Acetic Acid/Water System 68

Figure 3-11 Comparison of Determined N_L by Four Methods for Acetic Acid/Water System 69

Figure 3-12 Comparison of Determined LPR by Four Methods for Acetic Acid/Water System 70

Figure 4-1 Surface Tension as a Function of Composition 89

Figure 4-2 Point Efficiency as a Function of Compositions for Cyclohexane/N-heptane System 90

Figure 4-3 Point Efficiency as a Function of Compositions for Acetic Acid/Water System 91

Figure 4-4 Point Efficiency as a Function of Compositions for Methanol/Water System 92

Figure 4-5 Number of Mass TRansfer Units as a Function of Surface Tension for Three Systems 93

Figure 4-6 Number of Mass TRansfer Units as a Function of Surface Tension for Cyclohexane/N-heptane System 94

Figure 4-7 Number of Mass TRansfer Units as a Function of Surface Tension for Acetic Acid/Water System 95

Figure 4-8 Number of Mass TRansfer Units as a Function of Surface Tension for Methanol/Water System 96

Figure 4-9 Comparison of Number of Liquid Phase Mass Transfer Units for Three Systems 97

Figure 4-10 Comparison of LPR for Three Systems 98

Figure 4-11 Comparison of Measured and Predicted Point Efficiency for Cyclohexane/N-heptane System 99

Figure 4-12 Comparison of Determined and Predicted N_G for Cyclohexane/N-heptane System 100

Figure 4-13 Comparison of Determined and Predicted N_L for Cyclohexane/N-heptane System 101

Figure 4-14 Comparison of Measured and Predicted Point Efficiency for Acetic Acid/Water System 102

Figure 4-15 Comparison of Determined and Predicted N_G for Acetic Acid/Water System 103

Figure 4-16 Comparison of Determined and Predicted N_L for Acetic Acid/Water System 104

Figure 4-17 Comparison of Measured and Predicted Point Efficiency for Methanol/Water System 105

Figure 5-1 Sketch of Roll Cells 125

Figure 5-2 Comparison of Measured and Predicted Efficiency 126
Figure 5-3 Comparison of Various M-Index 127
Figure 5-4 M-Index Used in This study 128
Figure 5-5 Comparison of Number of Mass Transfer Units 129
Figure 5-6 Measured Enhancement Factor 130
Figure 5-7 Comparison of Measured and Calculated Enhancement Factor 131
Figure 5-8 Comparison of Measured and Calculated Point Efficiency 132
Figure 6-1 Schematic Diagram of Experimental Apparatus 147
Figure 6-2 Murphree Tray Efficiency as a Function of Fa-factor 148
Figure 6-3 Murphree Tray Efficiency as a Function of Average Concentration on the Test Tray 149
Figure 6-4 Effect of Packing Height on Murphree Tray Efficiency 150
Figure 6-5 Tray Pressure Drop at Various F-factors 151
Figure 6-6 Froth Height at Various F-factor 152
Figure 6-7 Effect of Packing Height on Tray Pressure Drop and Froth Height 153
Figure 7-1 Murphree Tray Efficiency as a Function of Fa-factor 169
Figure 7-2 Murphree Tray Efficiency as a Function of Average Concentration on the Test Tray 170
Figure 7-3 Interfacial Area and Sauter Mean Bubble Diameter as a Function of F-factor 171
Figure 7-4 Murphree Tray Efficiency for Both Systems at the Same Water Concentration 172

Figure 7-5 Entrainment as a Function of Vapour Velocity 173
Figure 7-6 Entrainment as a Function of Vapour Velocity 174
Figure 7-7 Entrainment as a Function of Vapour Velocity at Different Liquid Flow Rate 175
Figure 7-8 Entrainment as a Function of Vapour Velocity for Different Hole Size 176
Figure 7-9 Total Pressure Drop as a Function of Vapour Velocity 177
Figure 7-10 Dry Pressure Drop as a Function of Vapour Velocity 178
Figure 7-11 Total Pressure Drop as a Function of Vapour Velocity for Different Size 179
Figure 8-1 Hydraulic Model of the Dispersion Above a Sieve Tray 199
Figure 8-2 Number of Mass Tranfer Units Above a Sieve Tray 200
Figure 8-3 Comparison of Experimental and Calculated mass Transfer Efficiency 201
Figure 8-4 Comparison of Experimental and Calculated mass Transfer Efficiency 202
Figure 8-5 Plot of AJ vs Surface Tension 203
Figure 8-6 Comparison of Experimental and Calculated mass Transfer Efficiency 204
Figure 8-7 Comparison of Experimental and Calculated mass Transfer Efficiency 205
Figure 8-8 Correlation of Tray Efficiency Parity Plot 206
Figure 8-9 Correlation of Tray Efficiency Parity Plot 207
Figure 9-1 Schematic Diagram of Experimental Apparatus 226

Figure 9-2 Pressure Drop Ratio vs Time for Tray 1 in the Column for Crystallisation fouling 227

Figure 9-3 Pressure Drop Ratio vs Time for Tray 2 in the Column for Crystallisation fouling 228

Figure 9-4 Pressure Drop Ratio vs Time for Tray 3 in the Column for Crystallisation fouling 229

Figure 9-5 Schematic of Visual Observation of fouling Processes of a Sieve Tray 230

Figure 9-6 Crystallisation Fouling Mechanism in a Tray Hole for the Proposed Model 231

Figure 9-7 Pressure Drop Ratio for Tray 1 at Two Temperatures in the Column for Crystallisation fouling 232

Figure 9-8 Comparison of Experimental and Calculated results for Tray 1 in the Column for Crystallisation fouling 233

Figure 9-9 Comparison of Experimental and Calculated results for Tray 2 in the Column for Crystallisation fouling 234

Figure 9-10 Comparison of Experimental and Calculated results for Tray 3 in the Column for Crystallisation fouling 235

Chapter 1

INTRODUCTION

1.1 Introduction

Separation processes play a key role in the chemical and petroleum industries. These processes, which include distillation, extraction, adsorption, crystallisation and membrane-based separations, account for 40 to 70% of both capital and operating costs of a broad range of industries (Humphrey and Seibert, 1992). Distillation is clearly the most common separation process and accounts for more applications than all the other separation processes combined because of its simplicity, low capital investment and low risk potential. Without question, distillation will remain the key separation method against which any alternate method must be judged, particularly in large-scale applications (Fair, 1990). Therefore, it is important to continue the development of distillation technologies and devices.

Distillation is carried out in distillation columns which contain various internals. Fair (1983) has done a comprehensive review of the historical development of column internals. The two dominant classes of column internals used today are trays and packings. Comparisons of trays and packings have been made by many researchers (e.g., Fair, 1970; Xu and Chuang, 1989). Selecting the best internals under given conditions is not an easy task, and no clear algorithm is available because there are no rigid lines of demarcation among internals. Table 1-1 provides a summary of the basic rules for selecting internals obtained from the literature (Frank, 1977) and from vendors. It can be seen from this table that the sieve tray

is the most versatile and most-often-used internal. It has been estimated that currently about 90% of installed distillation columns contain trays, and sieve trays are the most widely used non-proprietary trays (Krummrich, 1984). Therefore, numerous attempts have been made to understand and improve sieve tray performance.

1.2 Predicting Tray Efficiency

In the design of sieve trays, the most important task is the conversion of theoretical plates to actual plates by using tray efficiency. The number of theoretical stages can be obtained quite accurately by modern computers, but the problem of predicting tray efficiency with any degree of confidence is far from solved. Fair (1987) wrote: "This has long been a nebulous area for the design of distillation columns, and it would appear that improved models for contacting efficiency can represent major advances in the state of distillation design technology." Efficiency models currently available in the literature are developed based on data from absorption, stripping and humidification, but not distillation. They are empirical and have little relationship to system physical properties and fluid mechanics existing on the tray. There is almost no accurately determined number of individual phase mass transfer units in distillation to verify the existing models. Furthermore, the effect of surface tension and its gradient on efficiency, which is, as Lockett (1986) indicated, the only really confused area in prediction of tray efficiency, is still uncertain today because of lack of experimental data. Recently, Fair (1992) concluded that prediction of tray efficiency is the only remaining challenge in the prediction of tray performance.

The availability of a reliable and accurate model for predicting tray efficiencies and the numbers of actual stages is of primary economic importance. Therefore, the first part of this study (Chapters 2 to 5) will be devoted to the prediction of tray efficiencies. A new efficiency model based on distillation data from commercial-scale columns in the literature is presented in Chapter 2. In order to relate the physical properties, the interfacial area of dispersion used in the new model is estimated by the Levich theory (Levich, 1962). In Chapter 3, by using the new model, a new method for determining the number of liquid and vapour phase mass transfer units is introduced and compared with those available in the literature. The number of liquid and vapour phase mass transfer units for three distillation systems is then determined. Based on the determined number of mass transfer units, the effect of surface tension on the number of mass transfer units and the tray efficiency is investigated and determined in Chapter 4. Various efficiency models, with and without including the effect of surface tension, are also compared. Based on the results from Chapters 2 to 4, a new model for estimating the effect of the surface tension gradient on the point efficiency is developed in Chapter 5.

1.3 Improving Tray Efficiency

Because of the massive scale of sieve tray columns in use, even a small improvement in mass transfer performance can have significant economic advantages. Therefore, much effort has been expended to improve the performance of existing sieve trays and to develop new types of trays which more closely approach 100% efficiency. Although many types of sieve trays have been invented, as summarized by Jamal (1981), the mass transfer

efficiency of sieve trays is still relatively low and leaves much room for improvement.

It is very desirable to develop a new method of improving sieve tray performance at minimum cost and risk. In the second part of this study (Chapters 6 to 9), a new kind of sieve tray, called a packed tray, will be described. In order to understand the performance of this packed tray, experimental studies are carried out and described in subsequent chapters. In Chapter 6, the mass transfer performance of packed trays under the distillation of a surface tension positive system (Zuiderweg and Harmens, 1958) with methanol/water mixtures is studied in a 153 mm diameter distillation column. In Chapter 7, instead of a surface tension positive system, a surface tension negative system with acetic acid/water mixtures is used to investigate the effect of mesh packing on the performance of sieve trays. The effects of installing a thin layer of mesh packing on the tray capacity, entrainment, and pressure drop with an air/water system are also quantitatively determined and described in Chapter 7. In Chapter 8, a method is introduced for estimating the mass transfer efficiency of packed trays from that of trays without packing. In Chapter 9, fouling of sieve trays and packed trays with different hole sizes is studied in an air/water column. A mathematical model is developed for predicting the fouling rate for crystallisation fouling.

The main body of the text consists of eight chapters. Each chapter is self-contained and presented as a paper.

Table 1-1
List of Parameter Rating for Various Contactors

Design Parameter	Sieve	Valve	Bubble Cap	Random Packing	Structured Packing	Dual Flow Tray
Tower Pressure: < 13.3 kPa	2	1	1	4	6	0
Moderate	6	6	4	4	2	2
> 50% of Critical	6	6	4	4	0	4
Turndown Ratio: > 3	4	5	6	2	4	0
Liquid Rates: High	4	4	2	6	0	6
Low	2	2	6	2	4	0
Tower Diameter: Small < 0.6 m	2	2	2	6	4	6
Medium	6	6	4	4	4	4
Larger > 3 m	6	4	4	4	4	4
Low Pressure Drop Required	2	1	0	4	6	0
Number of Equilibrium Stage Required > 300	2	2	2	4	6	2
Foaming System	4	4	2	6	0	4
Fouling System	6	0	0	0	0	6
Low Liquid Holdup	2	2	2	4	6	2
Viscous Fluids at Boiling Point	4	4	2	6	0	2
Corrosive Fluids	4	3	2	6	2	4
Solids Present	4	3	2	2	0	6
Dirty Solution	4	4	2	2	0	6
Polymerizing Solution	4	4	2	2	0	6
More Than one Liquid Phase	0	0	0	4	6	6
Internal Heat Transfer Required	4	4	6	2	0	2
Multiple Feeds and Sidestrems	6	6	6	4	4	4
Capacity Expansion Required	4	4	0	4	6	4
Cost important	4	3	2	4	2	6
Design Procedure Reliability	6	6	4	4	3	2

Key: 6: Best Selection 0: Reject

1.4 Literature Cited

AIChE, "Bubble Tray Design Manual", New York (1958).

Fair, J.R., "Historical Development of Distillation Equipment", AIChE Symposium Series, Diamond Jubilee Historical/Review Volume, P.1. (1983).

Fair, J.R., "Comparing Trays and Packings", Chem. Engng. Prog. 66(3), 45 (1970).

Fair, J.R., "Distillation: Whither, not Whether", The Inst. of Chem. Engr. Symp. Ser. No.**104**, 613 (1987).

Fair, J.R., Chem. Proc. Sept. 1990, 23.

Fair, J.R., "What are the Remaining Challenges in the Prediction of Tray Performance", AIChE Annaul Meeting, Miami, FL, Paper 6a (1992).

Forbes, R.J., "A Short History of the Art of Distillation", E.J. Brill, Leiden, Netherlands (1948).

Frank, O., "Short - Cuts for Distillation Design", Chemical Engineering **84** (6), 110 (1977).

Higbie, R., "The rate of absorption of a pure gas into a still liquid during short periods of exposure", Trans. Am. Inst. Chem. Engrs., **31**, 365 (1935).

Humphrey, J.L., and A.F. Seibert, "New Horizons in Distillation", Chem. Eng. Dec. 1992, 86-98 (1992).

Jamal, A., M.Sc. Dissertation, University of Manchester Institute of Science and Technology, (1981).

Krummrich, K., Quoted in Chemical Week, **134** (24), 18 (1984).

Levich, V.G., "Physicochemical Hydrodynamics", Prentice-Hall, Englewood Cliffs, NJ (1962)

Lockett, M.J., "Distillation Tray Fundamentals," Cambridge University Press (1986)

Zuiderweg, F.J., "Distillation - Science and Business", The Chem. Eng. 404, (1973).

Zuiderweg, F.J. and A. Harmens, "The Influence of Surface Phenomena on the Performance of Distillation Columns", Chem. Eng. Sci. 9, 89 (1958).

Xu, C. and K.T. Chuang, "Comparison and Improvement of Distillation Columns", The Petroleum Engineering Equipment (China), 2-6 (1989).

Chapter 2

PREDICTING POINT EFFICIENCIES FOR SIEVE TRAYS IN DISTILLATION

2.1 Introduction

In the design of sieve tray columns for distillation, a tray efficiency is used to convert the number of theoretical stages to actual plates. The number of theoretical plates can be calculated accurately with modern computer methods, but the method for predicting the tray efficiency does not always give satisfactory results. The problem can be divided into two parts: the prediction of a point efficiency, and the relation of the point efficiency to the tray efficiency. The latter has been a subject of many studies (Porter et al., 1972; Lockett et al., 1973; Lockett and Safekourdi, 1976; Lim et al., 1974) and was found that reliable calculations can be made (Biddulph et al., 1991). On the other hand, the prediction of the point efficiency remains uncertain and little real progress has been achieved since the AIChE Bubble Tray Design Manual was published more than thirty years ago (AIChE, 1958). Recently, Fair (1987, 1992) pointed out that new improved models for the point efficiency could represent major advances in the state of distillation design technology.

Many methods for predicting mass transfer efficiencies have been proposed. These methods are based either on empirical correlations or on semi-empirical correlations. Examples of empirical correlations are those of Drickamer and Bradford (1943), O'Connell (1946), and Bakowski (1969). These

---

A version of this chapter has been accepted for publication. Chen, G.X. and K.T., Chuang 1993. Ind. Eng. Chem. Res. **32**(4) *(in press).*

correlations have not always been validated and the results are usually very conservative. The most often used semi-empirical correlation is the AIChE method, although it has been criticized by many authors for being unreliable (Lashmet and Szezepanski, 1974; Hughmark, 1971; Strand, 1963; and Neuburg and Chuang, 1982). Other correlations include those of Harris (1965), Asano and Fujita (1966), Jeromin et al. (1969), and Hughmark (1965). All of these models are developed based on data from absorption, stripping and humidification, but not distillation. Chan and Fair (1984) proposed a new correlation for N_G in the AIChE model by using distillation data. Zuiderweg (1982) reviewed sieve tray performance and developed a correlation for predicting point efficiencies based on the FRI results (Sakata and Yanagi, 1979; Yanagi and Sakata, 1982) by using the slope and intercept method. However, the systems involved have a narrow range in the slope of the vapour-liquid equilibrium line (m). Therefore, the analysis may not be accurate. Later, Zuiderweg (1986) indicated that his model is possibly not more reliable than alternative models. Apart from the above methods, there is another group of models aimed at individually predicting the mass transfer coefficients and interfacial area. This approach has been reported regularly over the years (Geddes, 1946; West et al., 1952; Garner and Porter, 1960; Calderbank and Moo-Young 1960, Andrew, 1961; Goederen, 1965, Fane and Sawistowski, 1969; Stichlmair, 1978; Neuburg and Chuang, 1982), but none of them have gained practical acceptance. Most recently, Prado and Fair (1990) developed another semi-empirical model, which is also based on information from absorption and humidification in an air/water system (Fair and Prado, 1987).

The purpose of this research is to develop correlations for predicting

the number of individual mass transfer units and the liquid phase resistance consistent with mass transfer theories, and to compare the prediction with distillation data measured from commercial-size sieve tray columns.

2.2 Theory

Based on the two-film or two-resistance theory, the following equation is obtained:

$$1/K_{OG} = 1/k_G + (m\rho_G M_L)/(k_L \rho_L M_G) \qquad (1)$$

Dividing equation (1) by (at_G) gives:

$$1/N_{OG} = 1/N_G + \lambda/N_L \qquad (2)$$

where:

$$N_{OG} = aK_{OG}t_G \qquad (3)$$

$$N_G = ak_G t_G \qquad (4)$$

$$N_L = ak_L t_L \qquad (5)$$

and

$$t_G = h_f/u_s \qquad (6)$$

$$t_L = (G\ t_G\ \rho_L M_G)/(L\ \rho_G M_L) \qquad (7)$$

$$\lambda = mG/L \qquad (8)$$

It should be noted that N_{OG}, N_G and N_L are based on the same effective interfacial area "a". If N_G and N_L are determined separately by different absorption, stripping and humidification experiments using gas and liquid phase controlled systems, equation (2) is no longer valid because N_G and N_L may not be based on the same interfacial area. Since this is the case for the models reported previously, those models for N_G and N_L may be

fundamentally incorrect. Equation (2) should be valid only if N_G and N_L are determined simultaneously under distillation conditions. It can also be seen from equation (7) that t_L and t_G are mutually related.

The overall number of mass transfer units can be related to the point efficiency by:

$$E_{OG} = 1 - \exp(-N_{OG}) \qquad (9)$$

The value of E_{OG} can be obtained from the measured Murphree efficiency E_{MV} as outlined by Chan and Fair (1984). In this study, the eddy diffusion coefficient, D_E, is predicted by the experimental correlation of Barker and Self (1962) as suggested by Chan and Fair (1984):

$$D_E = 0.00675\ u_a^{1.44} + 0.000922\ h_L' - 0.00562 \qquad (10)$$

where h_L' is estimated by equations given by Bennett et al.(1983).

The N_{OG} calculated from equation (9) at different slopes "m" can be used to determine the number of mass transfer units N_G and N_L by equation (2). Correlations for N_G and N_L can then be developed.

The percent of liquid phase resistance over the total mass transfer resistance (LPR%) can be defined as:

$$LPR\% = (\lambda/N_L)/(1/N_G + \lambda/N_L)\ 100\% \qquad (11)$$

2.3 Model Development

(A) Clear liquid height h_L

The clear liquid height on a sieve tray plays an important role in mass transfer because of its influence on t_L and t_G. Nearly all of tray performance correlations include clear liquid height as a variable. Many correlations for h_L are available (Hofhuis and Zuiderweg, 1979; Brambilla et

al., 1969; Dhulesia, 1984; Colwell, 1979; Bennett et al., 1983; Hofhuis, 1980). In this study the correlation of Hofhuis (1980) as recommended by Zuiderweg (1982) is chosen. Under total reflux conditions, the correlation is given by:

$$h_L = 0.6\ h_W^{0.5} p^{0.25} ((\rho_G/\rho_L)^{0.5}/b)^{0.25} \qquad (12)$$

for $25\ mm < h_W < 100\ mm$

(B) Mass transfer coefficients k_G and k_L

Based on the results of Lockett et al. (1979) and Mehta & Sharma (1966) and Petty (1975), k_G may be given by:

$$k_G \propto (D_G)^{0.5} \qquad (13a)$$

A dimensional analysis will give following equation from equation (13a):

$$k_G \propto (D_G/\theta_G)^{0.5} \qquad (13)$$

where θ_G may be considered to be a contact time of an gas element at the gas-liquid interface. For sieve tray dispersion we assume that:

$$\theta_G \propto h_L/u_s = t'_G \qquad (14)$$

If it is further assumed that:

$$t_G \propto t'_G \qquad (15)$$

then we can obtain the following equation by combining equations (13), (14) and (15):

$$k_G t_G \propto (D_G t'_G)^{0.5} \qquad (16)$$

Based on the Higbie penetration theory (Higbie, 1935), k_L can be expressed:

$$k_L = 2(D_L/\pi\theta_L)^{0.5} \qquad (17)$$

where θ_L is the time during which the liquid element has been exposed at the interface. If it is assumed for sieve tray dispersion that:

$$\theta_L \propto (h_L \rho_L / u_s \rho_G) = t_L' \tag{18}$$

then $$t_L = (M_G G)/(M_L L)\ (t_G \rho_L)/\rho_G \propto (t_G' \rho_L / \rho_G)(M_G G)/(M_L L)$$

$$= t_L' (M_G G)/(M_L L) \tag{19}$$

and equation (20) is obtained:

$$k_L t_L \propto (M_G G / M_L L)(D_L t_L')^{0.5} \tag{20}$$

where $t_L' = t_G'\ \rho_L / \rho_G$.

Equations (16) and (20) will be used to obtain N_G and N_L.

(C) Interfacial area "a"

Neuburg and Chuang (1982) concluded that no satisfactory correlations existed for the prediction of bubble diameter and interfacial area. Therefore in this study, new correlations for Sauter mean bubble diameter d_{32} and interfacial area had to be developed. If the bubble size distribution is assumed to be independent of the Sauter mean bubble diameter, then the ratio of d_{32}/d_{max} is a constant. This is similar to what is found for stirred vessels (Mersmann and Grossman. 1982; Hesken et al., 1987; Parthasarathy et al., 1991). Therefore, d_{max} is needed in order to obtain the interfacial area.

The fundamental work in dispersion theory in turbulent flow was conducted by Kolmogoroff (1949) and Hinze (1955). The bubble size was found to be controlled by inertial forces (due to dynamic pressure fluctuations) and surface tension forces. The inertial forces tend to deform the bubbles whereas the surface tension forces resist the deformation. The maximum

stable spherical bubble size d_{max} could be determined by the balance between these two forces. A bubble would break up if the ratio of the inertial and surface tension forces, in the form of the Weber number, exceeded a critical value. The critical Weber number is given as:

$$We_c = \tau\, d_{max}/\sigma \qquad (21)$$

Levich (1962) suggested a similar force balance. He considered the balance of the internal pressure with the capillary pressure of a deformed bubble. The dispersed phase density is included through the internal pressure force term. The capillary pressure is determined from the shape of the deformed bubble rather than the spherical bubble. His theory leads to a critical Weber number:

$$We_c = \frac{\tau}{\sigma/d_{max}} \left(\rho_G / \rho_L \right)^{1/3} \qquad (22)$$

The dynamic pressure force of the continuous phase can be obtained by equation (23) (Hinze, 1955):

$$\tau = \rho_L \, \bar{u}^2 \qquad (23)$$

where $\bar{u}^2$ is the mean square velocity difference over a distance equal to the maximum bubble diameter (d_{max}). An expression for $\bar{u}^2$ was obtained by Batchelor (1959):

$$\bar{u}^2 = 2 \left(\omega\, d_{max} \right)^{2/3} \qquad (24)$$

Substituting τ and $\bar{u}^2$ into equations (21) and (22), the following equations can be obtained:

$$d_{max} \propto (\sigma/\rho_L)^{0.6}(\omega)^{-0.4} \qquad (25)$$

and

$$d_{max} \propto \sigma^{0.6}(\rho_L^2\rho_G)^{-0.2}(\omega)^{-0.4} \qquad (26)$$

These two equations have been successfully used to predict the maximum bubble diameter and Sauter-mean bubble diameter in stirred vessels (Kawase and Moo-Young, 1990). However, they have not been used to predict the bubble diameter in sieve tray dispersions.

Calderbank (1958) proposed an empirical correlation for the gas-liquid interfacial area in an aerated mixing vessel:

$$a \propto (\omega)^{0.4}\ \rho_L^{0.6}\ u_s^{0.5}/\ \sigma^{0.6} \qquad (27)$$

The form of this equation is very similar to that in equations (25) and (26) and it is likely that equation (27) was also based on the dispersion theory. Later, Calderbank and Moo-Young (1960) found that equation (27) also applied to sieve tray dispersions. Their measured interfacial area for air/water system using several sieve trays of different designs showed a remarkable agreement with equation (27). This indicated that the dispersion theory is also valid for the sieve tray dispersion, and equations (25) and (26) could be used to predict the maximum bubble diameter for sieve trays. Experimental observations indicated that the bubbles on sieve trays are highly deformed, and not in spherical shape (Lockett et al., 1979; Burgess and Calderbank, 1975; Calderbank and Pereira, 1979; Porter et al., 1967; Kaltenbacher, 1983). Therefore, equation (26) is used in this study. The energy dissipation per unit mass of liquid on a sieve tray is given by (Calderbank, 1960; Geary and Rice, 1991):

$$\omega = u_s g \tag{28}$$

Substituting equation (28) into equation (26) gives:

$$d_{max} \propto \sigma^{0.6}(\rho_L^2 \rho_G)^{-0.2}(u_s)^{-0.4} \tag{29}$$

Equation (29) assumes that only surface tension forces resist dispersion, but as shown by Calderbank (1956), viscous forces also begin to resist dispersion as the ratio of viscosity to surface tension rises. Bhavaraju et al. (1978) proposed a correlation for bubble size including the viscosity effect. They found experimentally that d_{max} is proportional to $(\mu)^{0.1}$ in stirred vessels. If their results are assumed to apply for the sieve tray dispersion, then equation (29) becomes:

$$d_{max} \propto \sigma^{0.6}\ \mu^{0.1}\ (\rho_L^2 \rho_G)^{-0.2}(u_s)^{-0.4} \tag{30}$$

Then the interfacial area can be obtained by:

$$a = \frac{6\varepsilon}{d_{32}} \propto \frac{6\varepsilon}{d_{max}} \propto \frac{\varepsilon\ (\rho_L^2 \rho_G)^{0.2}\ u_s^{0.4}}{\sigma^{0.6}\ \mu^{0.1}} \tag{31}$$

where ε is the mean void fraction, and can be estimated by many empirical correlations (Gardner and Mclean, 1969; Kastanek, 1970; Colwell, 1979; Stichlmair, 1978). The correlation of Stichlmair (1978) is chosen as shown in equation (32):

$$\varepsilon = \left(\frac{F_s}{F_{smax}}\right)^{0.28} = \left[\frac{u_s\ \rho_G^{0.5}}{2.5(\phi^2 \sigma(\rho_L - \rho_G)g)^{0.25}}\right]^{0.28}$$

$$\text{or} \quad \varepsilon \propto \left[\frac{u_s\ \rho_G^{0.5}}{(\phi^2 \sigma\ \rho_L)^{0.25}}\right]^{0.28} \tag{32}$$

Substituting ε into equation (31) gives:

$$a = \frac{6\varepsilon}{d_{32}} \propto \frac{(\rho_L^2 \rho_G)^{0.2}\, u_s^{0.4}}{\sigma^{0.6}\, \mu^{0.1}} \; \frac{u_s^{0.28}\, \rho_G^{0.14}}{\phi^{0.14}\, \sigma^{0.07}\, \rho_L^{0.07}}$$

$$\text{or} \quad a \propto \frac{\rho_L^{0.33}\, \rho_G^{0.34}\, u_s^{0.68}}{\phi^{0.14}\, \sigma^{0.67}\, \mu^{0.1}} \approx \frac{1}{\mu^{0.1}\, \phi^{0.14}} \left[\frac{F_s^2\, \rho_L}{\sigma^2} \right]^{1/3} \tag{33}$$

(D) The number of mass transfer units N_G and N_L

Combining equations (16), (20) and (33) gives the final correlations for the number of mass transfer units.

$$N_G = a k_G t_G = C_1 \frac{1}{\mu^{0.1}\, \phi^{0.14}} \left[\frac{\rho_L\, F_s^2}{\sigma^2} \right]^{1/3} (D_G t_G')^{0.5} \tag{34}$$

$$N_L = a k_L t_L = C_2 \frac{1}{\mu^{0.1}\, \phi^{0.14}} \left[\frac{\rho_L\, F_s^2}{\sigma^2} \right]^{1/3} (M_G G / M_L L)\, (D_L t_L')^{0.5} \tag{35}$$

where $t_G' = h_L / u_s$, and $t_L' = t_G'\, \rho_L / \rho_G$

$$F_s = u_s (\rho_G)^{0.5}$$

and C_1 and C_2 are constants to be found by fitting with experimental data.

(E) Percent liquid phase resistance LPR%

The percent liquid phase resistance could be obtained by substituting equations (34) and (35) into equation (11):

$$LPR\% = \frac{\lambda/N_L}{1/N_G + \lambda/N_L} = \frac{\lambda}{\frac{C_2}{C_1}\left(\frac{D_L\rho_L}{D_G\rho_G}\right)^{0.5}\left(\frac{M_G G}{M_L L}\right) + \lambda} 100\% \quad (36)$$

2.4 Determining Constants C_1 and C_2

In order to find the values for C_1 and C_2, experimentally measured efficiency data have to be used. Because C_1 and C_2 are constants and independent of system properties and tray geometry, they can be determined from one data point in theory. Since experimental data are seldom accurate enough, a series of test results would be required for the evaluation of C_1 and C_2.

Point efficiencies from small columns are often lower than that from large columns (Dribika and Biddulph, 1986; Biddulph et al., 1991), so these data should be avoided. Many efficiency data from large columns are now available in the open literature and have been summarized by Chan and Fair (1984). However, only those data measured as a function of the concentration of mixtures are suitable to evaluate C_1 and C_2. Efficiency data published by FRI may be considered to be most reliable. In 1979, Sakata and Yanagi reported results on two test mixtures, cyclohexane/n-heptane and isobutane/n-butane, at five different pressures. Later, they (Yanagi and Sakata, 1982) published results for three of five systems but with a different tray geometry. Therefore, their efficiency data of cyclohexane/n-heptane obtained in a 1.22 m diameter column at 165 kPa pressure was selected to determine the values of C_1 and C_2. The others will be used to test the efficiency models obtained.

In order to evaluate N_G and N_L, the reported tray efficiency should be

converted to the point efficiency by using the AIChE model as suggested by Chan and Fair (1984). The AIChE model assumed partial mixing of liquid on the tray and was found to agree with experimental results for column diameters below 5 meters (Porter et al., 1972; Yanagi and Scott, 1973; Fair, 1987; Biddulph et al., 1991). The N_{OG} obtained from equation (9) as a function of m can be used to obtain N_G and N_L by using the slope and intercept method (Lockett and Ahmed, 1983; Zuiderweg, 1982) if the m value varies significantly with the concentration. In fact, N_G and N_L may also vary with m. Thus the slope and intercept method may lead to wrong results (Lockett and Plaka, 1983). The cyclohexane/n-heptane data used in this study have only a narrow range of m values. Therefore, a great error would be introduced if the slope and intercept method were used. Alternatively, C_1 and C_2 can be obtained by combining equations (2), (34) and (35) as follows:

$$N_{OG} = \frac{N_G}{1 + \lambda N_G/N_L} = \frac{C_1 \dfrac{1}{\mu^{0.1}\phi^{0.14}} \left[\dfrac{\rho_L F_s^2}{\sigma^2} \right]^{1/3} (D_G t'_G)^{0.5}}{\lambda \dfrac{C_1}{C_2} \left(\dfrac{D_G \rho_G}{D_L \rho_L} \right)^{0.5} \left(\dfrac{M_L L}{M_G G} \right) + 1} \qquad (37)$$

By fitting the above equation to the experimental N_{OG} data as a function of m, the values of C_1 and C_2 have been found to be 11 and 14, respectively. Only data free of weeping and entrainment according to Biddulph et al. (1991) were used. Figure 2-1 compares predicted point efficiencies by equation (37) with the experimental data as a function of F-factors.

2.5 Predicting Point Efficiencies

To confirm the validity of the correlations, equations (34) and (35) were used to predict the number of mass transfer units, point efficiency, and LPR% for other systems under different operating conditions. Figure 2-2 shows the experimentally determined point efficiency and that calculated by the new correlations for the cyclohexane/n-heptane system at 34 kPa in the FRI 1.22 m column (Sakata and Yanagi, 1979). It can be seen that the prediction agrees very well with the experimental data. Figure 2-3 shows the comparison for the isobutane/n-butane system at three different pressures. The measured efficiencies at 2068 kPa and 2758 kPa have been corrected for the entrainment of vapour with the downflow liquid according to the method provided by Hoek and Zuiderweg (1983). The results indicated that all predicted point efficiencies agree with the experimental values within 5% error. An additional comparison was made with data obtained by Billet et al. (1969) who measured sieve tray efficiency for the ethylbenzene/styrene system under vacuum conditions (13.3 kPa) in a 0.79 meter diameter column. Figure 2-4 compares the point efficiency from their measured Murphree tray efficiency with that predicted by the new correlations. Again, the absolute error is within 5%.

7.6 Liquid Phase Resistance

The percent liquid phase resistance, LPR%, can be obtained by substituting λ into equation (36) to give:

$$LPR\% = \frac{mG/L}{\frac{C_2}{C_1}\left(\frac{D_L\rho_L}{D_G\rho_G}\right)^{0.5}\left(\frac{M_G G}{M_L L}\right) + mG/L} = \frac{m\ 100\%}{\frac{C_2}{C_1}\left(\frac{D_L\rho_L}{D_G\rho_G}\right)^{0.5}\left(\frac{M_G}{M_L}\right) + m} \qquad (38)$$

This equation shows that the percent liquid phase mass transfer resistance is a function of system properties only. Neither the (G/L) ratio nor the tray geometry can affect the value of LPR%. It is system properties that determine which phase is the mass transfer controlling phase. Once the number of individual phase mass transfer units is obtained by equations (34) and (35), the LPR% can also be determined by equation (11). Figure 2-5 shows the calculated LPR% for the above mentioned three systems at different pressures. It can be seen that for these three systems the liquid phase resistance is significant, in the range of 40% to 60%. It can also be seen that for the cyclohexane/n-heptane and isobutane/n-butane systems the liquid phase resistance decreases with increasing pressure. This may be attributed to the changes in diffusivities and densities in the vapour and liquid phases. The liquid phase diffusivity increases with increasing pressure due to temperature effect, whereas the opposite is true for the vapour phase diffusivity.

2.7 Comparison With Other Models

Porter and Jenkins (1979) pointed out that, at total reflux, all system properties can be expressed as a function of the flow parameter, $FP=(\rho_G/\rho_L)^{0.5}$. Therefore, it is convenient to use the flow parameter as a variable for the comparison of the point efficiency and number of mass transfer units predicted by existing models. Figure 2-6 shows point efficiencies calculated by equation (37) as well as those reported by Lockett (1986) using different models as a function of the flow parameter, at m=1 in a 2 meter diameter column. It can be seen from Figure 2-6 that the results of the new model are close to those of Chan and Fair's model (1984)

which was obtained by using their distillation efficiency data bank to modify the AIChE model. As shown in Figure 2-6, the new model also gives a correct efficiency trend. When the flow parameter approaches unity, the point efficiency should equal 100% (Hoek and Zuiderweg, 1982). For comparison, the point efficiency from experimental data are also shown in this figure.

Figures 2-7 and 2-8 show the number of individual phase mass transfer units calculated by the various models. The results indicate that the new model, unlike existing models, will predict an infinite value for N_G and N_L at FP=1 where the surface tension disappears. It can also be seen from Figure 2-8 that N_L predicted by the AIChE model and Chan and Fair's model is much higher than that by equation (35). This suggests that the AIChE model and Chan and Fair's model may over-predict the point efficiency for liquid phase controlled systems. Although Chan and Fair's model may predict a correct point efficiency for systems within the range of their data bank, these correct results may be obtained through a wrong route, and their model may not predict the individual N_G and N_L accurately. Their model is open to the same criticism as the AIChE model.

The calculated percent liquid phase resistance by the various models is shown in Figure 2-9. It can be seen that the new model predicts a different trend of liquid phase resistance from other models. It seems unreasonable that liquid phase resistance increases with increasing pressure because the liquid phase diffusivity is higher at a higher pressure because of temperature effect, whereas the vapour phase diffusivity is lower at a higher pressure. It should be noted that in Figure 2-9, when FP or pressure increases, the temperature also increases. The changes in pressure and

temperature with FP will affect the diffusivities and densities of vapour and liquid phases. These variations of diffusities and densities with FP determines the trend of changes in LPR% with FP as indicated in equation (36). In small FP range, the new model predicts a much higher LPR% than all other models as shown in Figure 2-9. It has been known that the AIChE model usually over-predicts the point efficiency for liquid phase controlled systems because it over-predicts N_L. Therefore, it is expected that the new model may overcome the deficiency of the AIChE model for liquid phase controlled systems. The O'Connell equation (1946) has been recommended by Kister (1992) as the standard of the industry for predicting efficiency. It should be noted that the O'Connell equation makes sense only when liquid phase resistance is large because the equation includes only liquid viscosity and relative volatility. This is another indication that liquid phase resistance is considerably large in distillation systems.

2.8 Discussion

Although the new model has been tested against only three systems, at six widely different pressure levels, the three systems cover a wide range of physical properties, and can be considered six different systems. It is found that diffusivities, vapour densities, and surface tensions of these three systems vary more than 10 times between low and high pressures. Therefore, the model should be applicable to other systems, at least for hydrocarbons. The effect of tray geometry on the point efficiency is tested for three tray designs in this study. However, the model includes the most important variable, h_L, which is mainly a function of tray geometry as indicated by equation (12) and which may include the effect of tray geometry

on the point efficiency. Furthermore, the point efficiency is not sensitive to tray geometry, as indicated by the O'Connell correlation (1946). Thus, the present model should be adequate for use with most tray designs.

The model was obtained based on the theory for the froth regime only, therefore, a different model will be required for the spray regime. Fortunately, the changes in the point efficiency between the two regimes are gradual according to the FRI test results and Prado and Fair's results (1990). The calculated transition point based on the correlation of Loon et al. (1973) is shown in Figure 2-1. It can be seen from Figure 2-1 that there is almost no efficiency difference between the two regimes. Therefore, the new model might also be used to estimate the efficiencies in spray regime.

The new model also includes the fractional open hole area (ϕ) as shown in equation (37). This is consistent with FRI results by Yanagi and Sakata (1982). They found that 14% open hole area sieve trays have a lower efficiency than that of 8% open hole area sieve trays. The new model does not include the effect of hole sizes like most other models. It may, therefore, under-predict the point efficiency for sieve trays having very small hole diameters (less than 4 mm), which show a higher efficiency than normal hole size trays (Biddulph and Dribika, 1986).

The new model includes the effect of surface tension as shown in equations (34) and (35), N_G and $N_L \propto (\sigma)^{-2/3}$, which is similar to that of Stichlmair's and Zuiderweg's models. All other models including the AIChE model do not include the effect of surface tension. The inclusion of surface tension is open to debate. Although the new model shows good results for the cyclohexane/n-heptane and isobutane/n-butane systems at different pressures where surface tension changes widely, physical properties of these two

systems tend to change in unison. Thus, a definite conclusion about the effect of surface tension on the point efficiency is still uncertain. The best way to verify this effect is to determine the mass transfer units experimentally as a function of surface tension while keeping other properties constant for both surface tension positive and negative systems in distillation. This work is going to be discussed in the next three Chapters.

2.9 Conclusions

New correlations for predicting the number of mass transfer units, hence the point efficiency, of sieve trays have been developed in this study. In the new model, the interfacial area of sieve tray dispersion is estimated by the Levich theory (1962), and the mass transfer coefficients are obtained based on the Higbie penetration theory (Higbie, 1935). The final model is obtained by fitting the correlations to the FRI measured tray efficiencies in a commercial-size distillation column. It has been shown that the new model is able to predict accurately the point efficiency for hydrocarbon systems under different pressures. The correlation should generally be applicable for the prediction of sieve tray efficiencies in distillation.

2.10 Nomenclature

A_b = bubbling area, m^2

a = interfacial area per unit volume of two phase dispersion, 1/m

b = weir length per unit bubbling area, 1/m

C_1 = constant in equation (38)

C_2 = constant in equation (39)

D_E = eddy diffusivity for liquid mixing, m^2/s

D_G = vapour phase molecular diffusivity, m^2/s

D_L = liquid phase molecular diffusivity, m^2/s

d_{max} = maximum bubble diameter, m

d_{32} = Sauter mean bubble diameter, m

E_{MV} = Murphree vapour phase tray efficiency

E_{OG} = Murphree vapour phase point efficiency

FP = $(\rho_G/\rho_L)^{0.5}$, flow parameter under total reflux conditions

F_s = superficial F-factor, $u_s(\rho_G)^{0.5}$, $kg^{0.5}/m^{0.5}s$

G = vapour flow rate, kmol/s

g = gravitational constant, m/s^2

h_f = froth height, m

h_L and h_L' = liquid holdup, m

h_W = outlet weir height, m

k_G = vapour phase mass transfer coefficient, m/s

k_L = liquid phase mass transfer coefficient, m/s

K_{OG} = overall mass transfer coefficient based on vapour, m/s

L = liquid flow rate, kmol/s

LPR% = percent liquid phase mass transfer resistance, %

m = slope of vapour-liquid equilibrium line

M_G = vapour phase molecular weight, kg/kmol

M_L = liquid phase molecular weight, kg/kmol

N_G = number of vapour phase mass transfer unit

N_L = number of liquid phase mass transfer unit

N_{OG} = number of overall vapour phase mass transfer unit

p = pitch of holes in sieve tray, m

Q_G = vapour flow rate, m^3/s

Q_L = liquid flow rate, m^3/s

t_G = defined as equation (6), s

t_L = defined as equation (7), s

t'_G = vapour contact time defined as equation (14), s

t'_L = Liquid contact time defined as equation (18), s

$\overline{u^2}$ = $\overline{(u(x+d_{max},\ t)-u(x,\ t)^2}$, m^2/s^2

u_s = superficial vapour velocity based on bubbling area A_b, m/s

We_c = critical Weber number

Greek Letters

ε = void fraction in dispersion

θ = contact time in equations (18) and (22), s

λ = mG/L

μ = liquid viscosity, Ns/m^2

ρ_G = vapour density, kg/m^3

ρ_L = liquid density, kg/m^3

σ = interfacial surface tension, N/m

τ = dynamic pressure fluctuations, N/m^2

ϕ = fractional perforated tray area

ω = local energy dissipation per unit mass, w/kg

Figure 2-1
Comparison of Predicted and Measured
Point Efficiency for C6/C7
(Sakata and Yanagi, 1979)

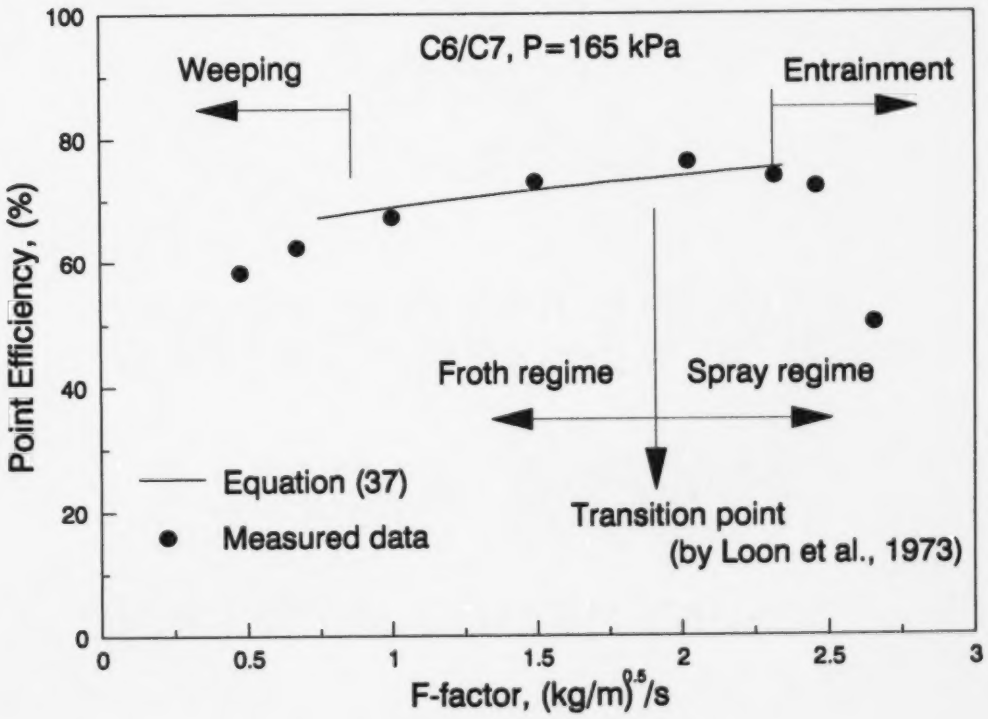

Figure 2-2
Comparison of Predicted and Measured Point Efficiency for C6/C7 Under Reduced Pressure at 34 kPa
(Sakata and Yanagi, 1979)

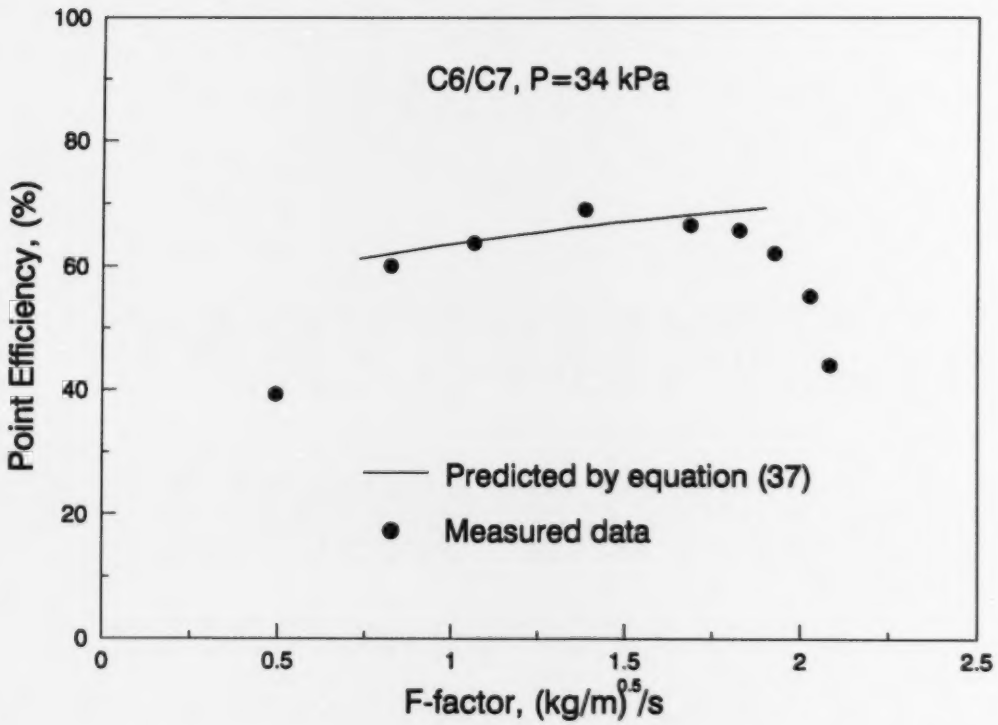

Figure 2-3
Comparison of Predicted and Measured Point Efficiency for Isobutane/N-butane System at Three Different Pressures (Sakata and Yanagi, 1979)

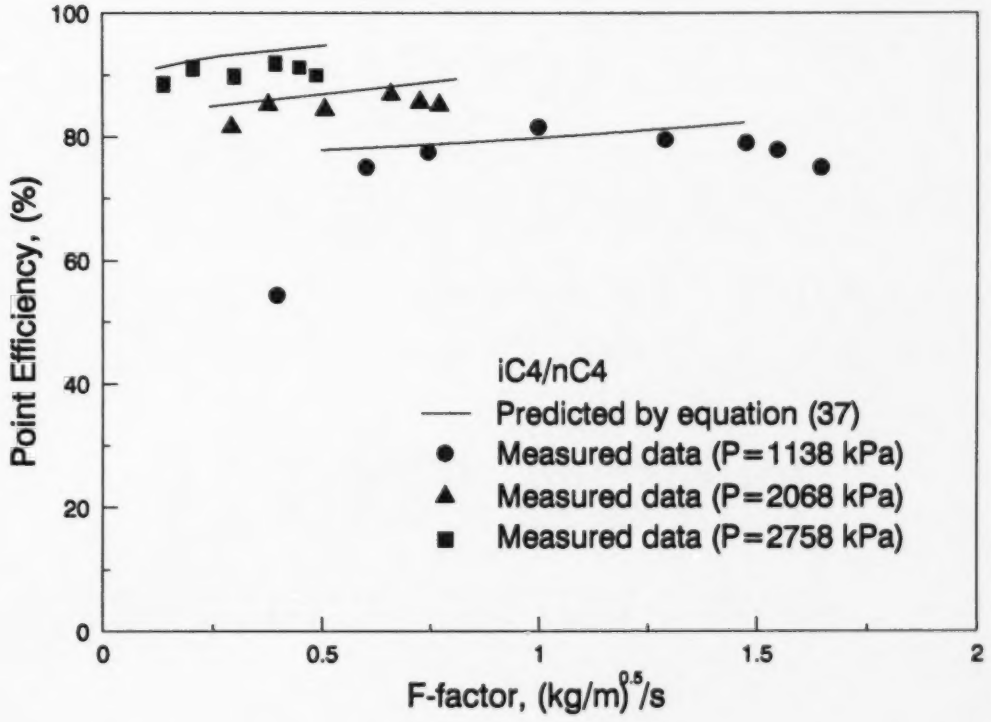

Figure 2-4
Comparison of Predicted and Measured Point Efficiency for ethylbenzene/Styrene System Under reduced Pressure at 13.3 kPa (Billet et al., 1969)

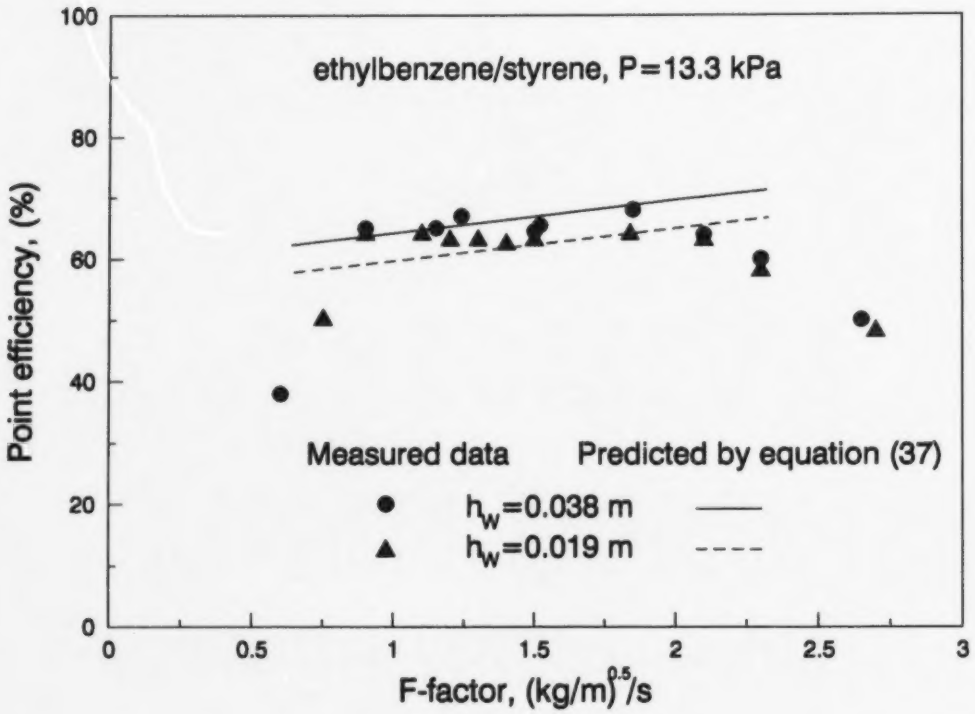

Figure 2-5
Calculated Percent Liquid Phase Resistance
for Three Systems at Different Pressures

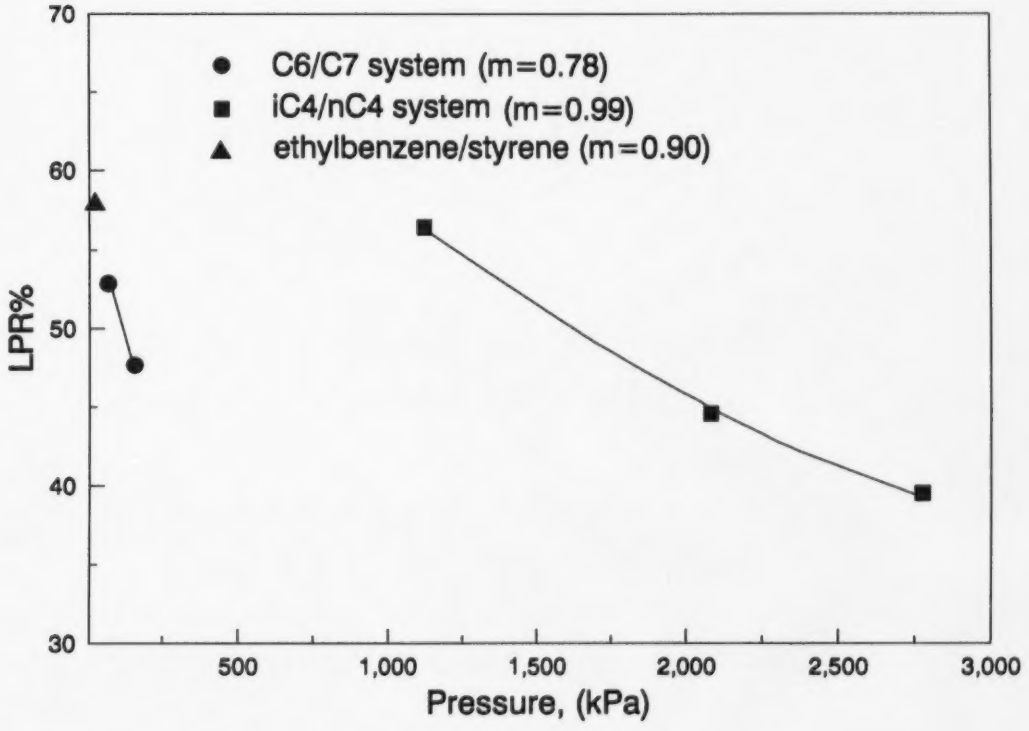

Figure 2-6
Comparison of Point Efficiency Obtained
by Various Models

(Physical Properties from Porter and Jenkins, 1979;
Part of Results Were Obtained by Lockett, 1986)

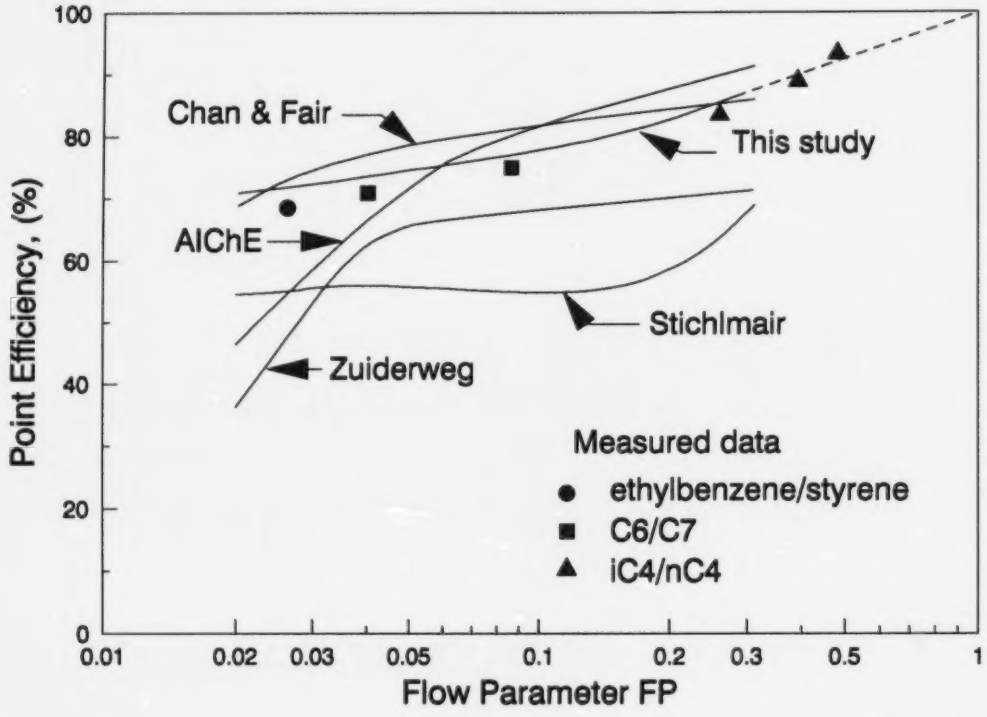

Figure 2-7
Comparison of Number of Vapour Phase Mass Transfer Units Obtained by Various Models

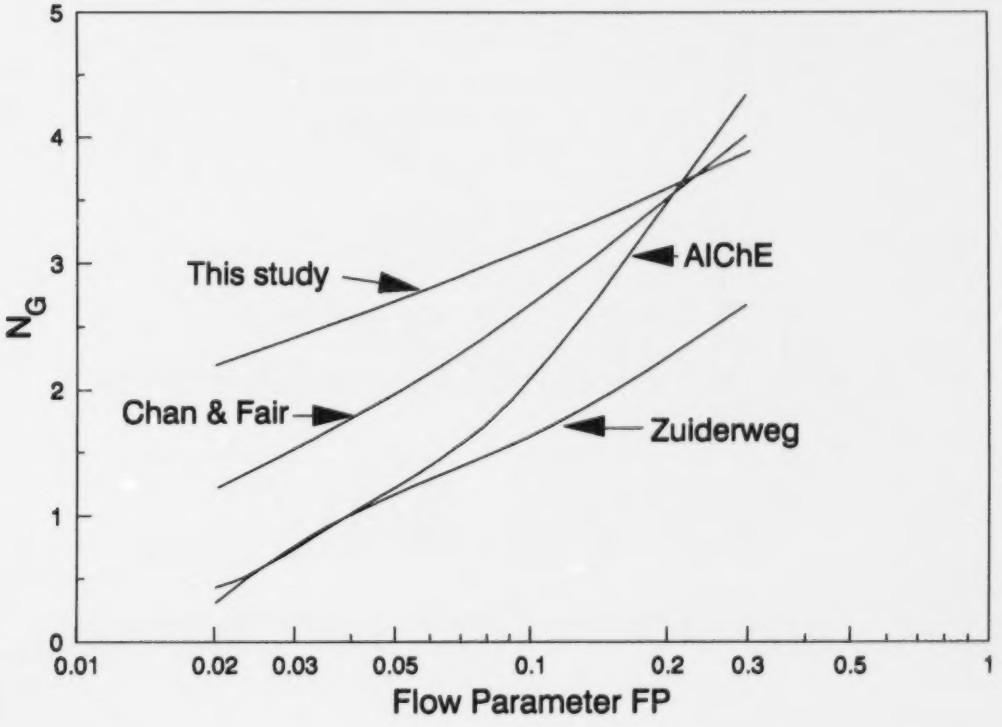

Figure 2-8
Comparison of Number of Liquid Phase Mass Transfer Units Obtained by Various Models

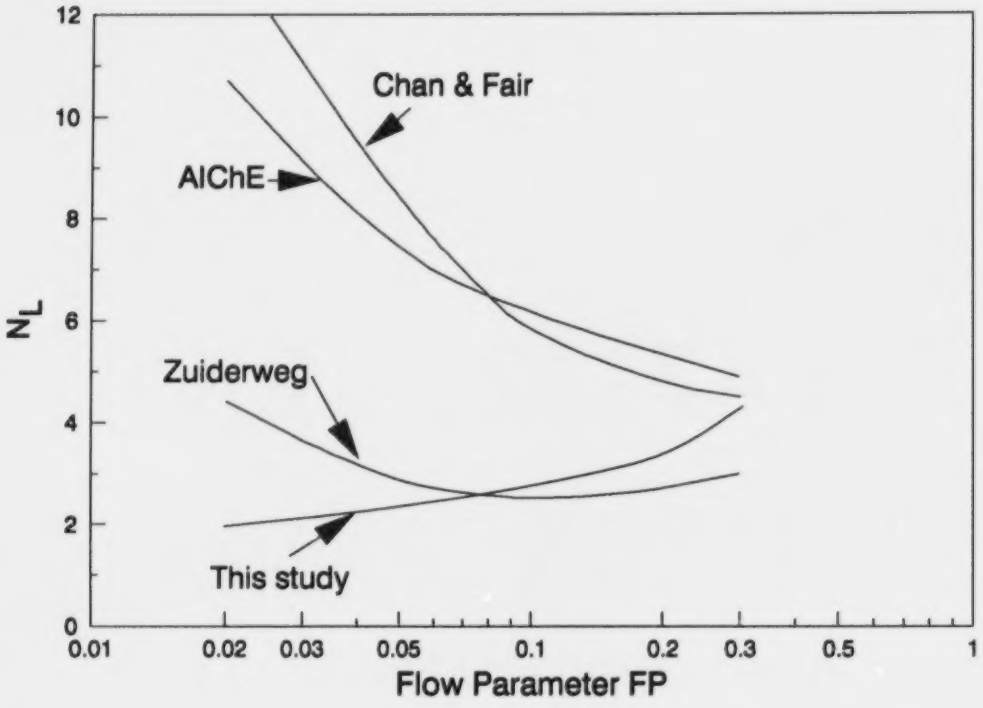

Figure 2-9
Comparison of Percent Liquid Phase Resistance
Obtained by Various Models

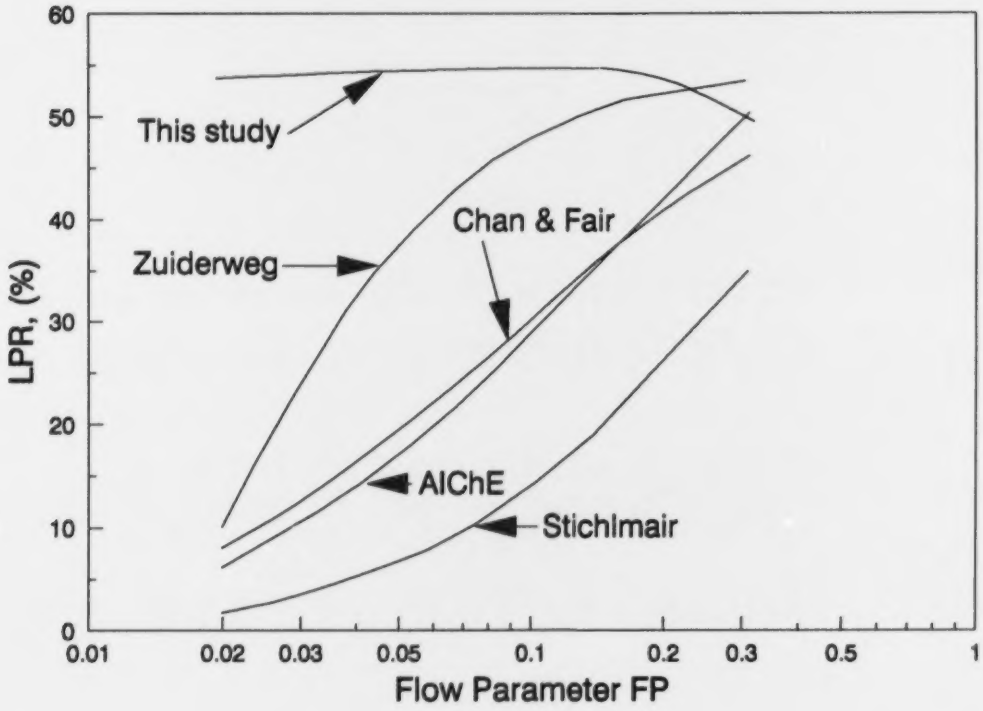

2.11 Literature Cited

AIChE, "Bubble Tray Design Manual," New York (1958).

Andrew, S.P.S., "Aspects of gas-liquid mass transfer," Alta Tecnologia Chimica, 153 (1961).

Asano, K., and S. Fujita, "Vapour and liquid phase mass transfer coefficients in tray towers," Kagaku Kogaku, **4**, 330 and 369 (1966).

Ashley, M.J., and G.G. Haselden, "Effectiveness of vapour-liquid contacting on a sieve plate," Trans. Inst. Chem. Engrs., **50**, 119 (1972).

Bakowski, S., "Efficiency of sieve-tray columns," Br. Chem. Eng., **14**, 945 (1969).

Barker, P.E., and M.F. Self, "The evaluation of liquid mixing effects on sieve plate using unsteady and steady state tracer techniques," Chem. Eng. Sci., **17**, 541 (1962).

Batchelor, G., "Theory of Homogeneous Turbulence," Cambridge, 122 (1959).

Bennett, D.L., R. Agrawal, and P.J. Cook, "New pressure drop correlation for sieve tray distillation columns," AIChE J., **29**(3), 439 (1983).

Bhavaraju, S.M., T.W.F. Russell, and H.W. Blanch, "The design of gas sparged devices for viscous liquid systems," AIChE J., **24**(3), 454 (1978).

Biddulph, M.W., J.A. Rocha, J.L. Bravo, and J.R. Fair, "Point efficiencies on sieve tray," AIChE J., **37**(8), 1261 (1991).

Billet, R., S. Conrad, and C.M. Grubb, "Some aspects of the choice of distillation equipment," Inst. Chem. Engr. Symp. Ser., No. **32**, 5:111 (1969).

Brambilla, A., G. Nardini, G.F. Nencetti, and S. Zanelli, "Hydrodynamic behaviour of distillation columns," Inst. Chem. Engr. Symp. Ser., No.**32**, 2:63 (1969).

Burgess, J.M., and P.H. Calderbank, "The measurement of bubble parameters in two phase dispersion," Chem. Eng. Sci., **30**, 743 and 1107 (1975).

Calderbank, P.H., Br. Chem. Eng., **1**, 206 (1956).

Calderbank, P.H., "Physical rate processes in industrial fermentation, Part 1: The interfacial area in gas-liquid contacting with mechnical agitation," Trans. Inst. Chem. Engrs., **36**, 443 (1958).

Calderbank, P.H., and M.B. Moo-Young, "The mass transfer efficiency of distillation and gas-absorption plate columns - Part 2," Inst. Chem. Engr. Symp. Ser., No. **6**, 59 (1960).

Calderbank, P.H., and J. Pereira, "The prediction of distillation plate efficiencies from froth properties," Chem. Eng. Sci., **32**, 1427 (1977).

Chan, H., and J.R. Fair, "Prediction of point efficiencies on sieve trays," Ind. Eng. Chem. Proc. Des. Dev., **23**, 814 (1984).

Colwell, C.J., "Clear liquid height and froth density on sieve trays," Ind. Eng. Chem. Proc. Des. Dev., **20**(2), 298 (1979).

Dhulesia, H., "Clear liquid height on sieve and valve trays," Chem. Eng. Res. Des., **62**, 321 (1984).

Dribika, M.M., and M.W. Biddulph, "Scale-up distillation efficiencies," AIChE J., **32**(11), 1864 (1986).

Drickamer, H.G., and J. Bradford, "Overall plate efficiency of commercial hydrocarbon fractionating columns as a function of viscosity," Trans. AIChE., **39**, 319 (1943).

Fair, J.R. "Handbook of Separation Process Technology," Edited by Ronald W. Rousseau, John Wiley and Sons, New York, 321 (1987),

Fair, J.R., and M. Prado, " A fundamental model for the prediction of sieve tray efficiency," Inst. Chem. Engr. Symp. Ser., No.**104**, A529 (1987).

Fair, J.R., "Distillation: Whither, not whether," Inst. Chem. Engr. Symp. Ser. No.104, A613 (1987).

Fair, J.R., "What are the remaining challenges in the prediction of tray performance," AIChE Annual Meeting, Miami Beach, FL, 1992.

Fane, A.G., and H. Sawistowski, "Plate efficiencies in the foam and spray regime of sieve-plate distillation," Inst. Chem. Engr. Symp. Ser., No.32, 1:8 (1969).

Gardner, R.G., and A.Y. Mclean, "Effect of system properties on sieve-plate froths," Inst. Chem. Engrs. Symp. Ser., No.32, 2:39 (1969).

Garner, F.H., and K.E. Porter, "Mass transfer stages in distillation," Inst. Chem. Engr. Symp. Ser., No. 6, 43 (1960).

Geary, N.W., and R.G. Rice, "Bubble size prediction for rigid and flexible spargers," AIChE J., 37(2), 161 (1991).

Geddes, R.L., "Local efficiencies of bubble plate fractionators," Trans. Am. Inst. Chem. Engrs., 42, 79 (1946).

Goederen, C.W.J. de, "Distillation tray efficiency and interfacial area," Chem. Eng. Sci., 20, 1115 (1965).

Harris, I.J., "Optimum design of sieve tray," Br. Chem. Eng., 10(6), 377 (1965).

Hesketh, R.P., T.W.F. Russell, and A.W. Etchells, "Bubble size in horizontal pipelines," AIChE J., 33(4), 663 (1987).

Higbie, R., "The rate of absorption of a pure gas into a still liquid during short periods of exposure," Trans. Am. Inst. Chem. Engrs., 31, 365 (1935).

Hinze, J.O., "Fundamentals of the hydrodynamic mechanism of splitting in dispersion processes," AIChE J., 1, 289 (1955).

Hoek, P.J., and F.J. Zuiderweg, "Influence of vapour entrainment on distillation tray efficiency at high pressure," AIChE J., **28**(4), 535 (1982).

Hofhuis, P.A.M., Thesis, TU Delft (1980).

Hofhuis, P.A.M., and F.J. Zuiderweg, "Sieve plates: Dispersion density and flow regimes," Inst. Chem. Engr. Symp. Ser., No. **56**, 2.2/1 (1979).

Hughmark, G.A., "Models for vapour-phase and liquid-phase mass transfer on distillation trays," AIChE J. **17**(6), 1295 (1971).

Hughmark, G.A., "Point efficiencies for tray distillations," Chem. Eng. Prog., **61**(7), 97 (1965).

Jeromin, L., H. Holik, and H. Knapp, "Efficiency calculation method for sieve-plate coulmns of air separation plants," Inst. Chem. Engr. Symp. Ser., No. **32**, 5:45 (1969).

Kalbassi, M.A., M.M. Dribika, M.W. Biddulph, S. Kler, and J.T. Lavin, "Sieve tray efficiencies in the absence of stagnant zones," Inst. Chem. Engr. Symp. Ser., No.**104**, A511 (1987).

Kaltenbacher, E., "On the effect of bubble size distribution and the gas-phase diffusion on the selectivity of sieve trays," Chem. Eng. Fund. 1(1), 47 (1983).

Kastanek, F., "Efficiencies of different types of distillation plate," Coll. Czech. Chem. Comm., **35**, 1170 (1970).

Kawase, Y., and M. Moo-Young, "Mathematical models for design of Bioreactors: Applications of Kolmogoroff's theory of isotropic turbulence," The Chem. Eng. J., **43**, B19 (1990).

Kister, H.Z., "Distillation Design", McGraw-Hill, New York (1992), P378.

Kolmogoroff, A.N., Doklady Akad. Nauk. SSSR, **66**, 825 (1949).

Lashmet, P.K., and S.Z. Szezepanski, "Efficiency uncertainty and distillation column overdesign factors," Ind. Eng. Chem. Process Des. Dev., **13**(2), 103 (1974).

Levich, V.G., "Physicochemical Hydrodynamics," Prentice Hall, Englewood Cliffs, NJ, 464 (1962).

Lim, C.T., K.E. Porter, and M.J. Lockett, "The effect of liquid channeling on two-phase distillation plate efficiency," Trans. Inst. Chem. Engrs. **52**, 193 (1974).

Lockett, M.J., C.T. Lim, and K.E. Porter, "The effect of liquid channeling on distillation column efficiency in the absence of vapour mixing," Trans. Inst. Chem. Engrs. **51**, 61 (1973).

Lockett, M.J., and A. Safekourdi, "The effect of the liquid flow pattern on distillation plate efficiency," Chem. Eng. J. **11**, 111 (1976).

Lockett, M.J., "Distillation Tray Fundamentals," Cambridge University Press, 148 (1986).

Lockett, M.J., and I.S. Ahmed, "Tray and point efficiencies from a 0.6 meter diameter distillation column," Chem. Eng. Res. Des., **61**, 110 (1983).

Lockett, M.J., R.D. Kirkpatrick, and M.S. Uddin, "Froth regime point efficiency for gas-film controlled mass transfer on a two-dimensional sieve tray," Trans. Inst. Chem. Engrs., **57**, 25 (1979).

Lockett, M.J., and T. Plaka, "Effect of non-uniform bubbles in the froth on the correlation and prediction of point efficiencies," Chem. Eng. Res. Des., **61**, 119 (1983).

Loon, R.E., W.V. Pinczewski, and C.J.D. Fell, "Dependence of the froth-to-spray transion on sieve tray design parameters," Trans. Inst. Chem. Engrs., **51**, 374 (1973).

Mehta, V.D., and M.M. Sharma, "Effect of diffusivity on gas-side mass transfer coefficient," Chem. Eng. Sci. **21**, 361 (1966).

Mersmann, A., and H. Grossman, "Dispersion of immiscible liquid in agitated vessels," Int. Chem. Eng., **22**(4), 581 (1982).

Neuburg, H.J., and K.T. Chuang, "Mass transfer modelling for GS heavy water plants. 1: Point efficiency on GS sieve trays," Can. J. Chem. Eng., **60**, 504 (1982a).

Neuburg, H.J., and K.T. Chuang, "Mass transfer modelling for GS heavy water plants. 2: Tray efficiency on GS sieve trays," Can. J. Chem. Eng., **60**, 510 (1982b).

O'Connell, H.E., "Plate efficiency of fractionating columns and absorbers," Trans. AIChE., **42**, 741 (1946).

Parthasarathy, R., G.J. Jameson, and N. Ahmed, "Bubble breakup in stirred vessels - Predicting the Sauter mean diameter," Trans. Inst. Chem. Engrs., **69**, 295 (1991).

Petty, C.A., Chem. Eng. Sci. **30**, 413 (1975).

Porter, K.E., B.T. Davis, and P.F.Y. Wong, "Mass transfer and bubble sizes in cellular foams and froths," Trans. Inst. Chem. Engrs., **45**, T265 (1967).

Porter, K.E., M.J. Lockett, and C.T. Lim, "Effect of liquid channeling on distillation plate efficiency," Trans. Tnst. Chem. Engrs. **50**, 91 (1972).

Porter, K.E., and J.D. Jenkins, "The interrelationship between industrial practice and academic research in distillation and absorption," Inst. Chem. Engr. Symp. Ser., No.**56**, Discussion Volume, 75 (1979).

Prado, M., and J.R. Fair, "Fundamental model for the prediction of sieve

tray efficiency," Ind. Eng. Chem. Res., **29**, 1031 (1990).

Sakata, M., and T. Yanagi, "Performance of a commercial-scale sieve tray," Inst. Chem. Engrs. Symp. Ser., No. **56**, 3.2/21 (1979).

Stichlmair, J., Verlag Chemie: Weinheim, 1978.

Strand, C.P., "Bubble cap tray efficiencies," Chem. Eng. Prog., **59**(4), 58 (1963).

West, F.B., W.D. Gilbert, and T. Shimizu, "Mechanism of mass transfer on bubble plates," Ind. Eng. Chem., **44**, 2470 (1952).

Yanagi, T., and B.D. Scott, "The effect of liquid mixing on sieve trays," Chem. Eng. Prog. 69(10), 75 (1973).

Yanagi, T., and M. Sakata, "Performance of a commercial-scale 14% hole area sieve tray," Ind. Eng. Chem. Proc. Des. Dev., **21**(4), 712 (1982).

Zuiderweg, F.J., "Sieve trays, A view on the state of the art," Chem. Eng. Sci., **37**(10), 1441 (1982).

Zuiderweg, F.J., "Marangoni effect in distillation of alcohol-water mixtures," Chem. Eng. Res. Des., **61**, 388 (1983).

Zuiderweg, F.J., "Influence of the two-phase flow regimes on the separation performance of sieve plates," Int. Chem. Eng. 26(1), 1-10 (1986).

Chapter 3

DETERMINING N_G AND N_L FROM E_{OG}

3.1 Introduction

Although the mass transfer efficiency of sieve trays has been extensively studied, little progress in predicting it has been achieved since the AIChE Bubble Tray Design Manual (1958). Since then, most new efficiency prediction methods have been based on the AIChE method. Because of difficulties encountered in determining the number of individual phase mass transfer units (N_G and N_L) in distillation, there were insufficient experimental data to challenge and verify the efficiency models. Lockett and Ahmed (1983) first reported their determined values (N_G and N_L) for methanol/water distillation in a 0.6 meter diameter column. However, the method they used may not be reliable. They found that there was considerable discrepancy between the experimental data and those predicted by the models, especially for the number of liquid phase mass transfer units. To verify the different efficiency models, it is necessary to determine the number of mass transfer units under distillation conditions.

The main purpose of this study is to compare the various existing methods for determining N_G and N_L from E_{OG} for three different systems with cyclohexane/n-heptane, methanol/water, and acetic acid/water mixtures. The results will be used to develop a new method.

3.2 Basic Relations

The following equations, outlined in Chapter 2, will also be used in this study.

$$1/K_{OG} = 1/k_G + (m\rho_G M_L)/(k_L \rho_L M_G) \qquad (1)$$

$$1/N_{OG} = 1/N_G + m/N_L \qquad (2)$$

$$E_{OG} = 1 - \exp(-N_{OG}) \qquad (3)$$

$$LPR = (m/N_L)/(1/N_G + m/N_L) \qquad (4)$$

The value of E_{OG} can be measured directly or calculated from the vapour phase Murphree efficiency E_{MV} (Chapter 2). When liquid on a tray is completely mixed, as in a small column, E_{OG} would be equal to E_{MV}. Once point efficiency E_{OG} has been obtained as a function of the slope of the vapour-liquid equilibrium line (m), the number of overall mass transfer units N_{OG} as a function of m can be obtained by equation (3). N_G and N_L can then be determined by equation (2) or by other methods.

3.3 Existing Models

3.3.1 Method 1: Slope and Intercept Method

As indicated by equation (2), that $1/N_{OG}$ is plotted against the slope of the equilibrium line (m) gives a straight line if N_G and N_L do not change with m. The slope of this line so obtained gives $1/N_L$, and the intercept $1/N_G$. To use this method, m should be a reasonably strong function of compositions, and N_L and N_G composition-independent. Zuiderweg (1982) and Lockett and Ahmed (1983) used this method to interpret, respectively, the cyclohexane/n-heptane and methanol/water distillation results.

3.3.2 Method 2: Based on Penetration Theory

To account for the variation of N_G and N_L over compositions, another

approach can be developed based on the penetration theory. Rearranging equation (2) gives:

$$N_G = N_{OG} (1 + m N_G/N_L) \qquad (5)$$

and

$$N_L = N_{OG} (m + N_L/N_G) \qquad (6)$$

If the ratio of N_G/N_L is known, N_G and N_L can be obtained from equations (5) and (6). Based on the definitions of N_G and N_L (Chapter 2), one can have:

$$\frac{N_G}{N_L} = \frac{\rho_G k_G}{\rho_L k_L} \qquad (7)$$

In order to obtain the ratio of k_G/k_L, the vapour phase and the liquid phase mass transfer coefficients have to be obtained. The penetration theory (Higbie, 1935) gives:

$$k_L = (4D_L/\pi\theta_L)^{0.5} \qquad (8)$$

and

$$k_G = (4D_G/\pi\theta_G)^{0.5} \qquad (9)$$

It is assumed that the exposure times of the vapour and liquid elements at the interface are equal, i.e., $\theta_L=\theta_G$. This assumption, although rather arbitrary, has been made by many investigators (Calderbank and Pereira, 1977; Stichlmair, 1978; Neuburg and Chuang, 1982). If this assumption is accepted, the ratio of vapour to liquid phase mass transfer coefficients can be given:

$$k_G/k_L = (D_G/D_L)^{0.5} \qquad (10)$$

Equation (10) has also been used by Lockett and Uddin (1980). Substitution of equation (10) into equation (7) gives:

$$N_G/N_L = (\rho_G/\rho_L) (D_G/D_L)^{0.5} \qquad (11)$$

By substituting equation (11) into equations (5) and (6), one obtains:

$$N_G = N_{OG} \left(1 + m \, (\rho_G/\rho_L)(D_G/D_L)^{0.5} \right) \qquad (12)$$

$$N_L = N_{OG} \left(m + (\rho_L/\rho_G)(D_L/D_G)^{0.5} \right) \qquad (13)$$

By knowing N_{OG} at different m, N_G and N_L can then be calculated from equations (12) and (13). This method had been used by Dribika and Biddulph (1986).

3.3.3 Method 3: Based on Two Bubble Sizes and Improved Penetration Theory

The original penetration theory (equations (8) and (9)) does not account for turbulent diffusion and multiple surface renewals. To account for these effects, an enhancement factor is usually introduced (Lockett and Plaka, 1983; Prado and Fair, 1990):

$$k_L = (4\phi_L D_L/\pi\theta_L)^{0.5} \qquad (14)$$

and

$$k_G = (4\phi_G D_G/\pi\theta_G)^{0.5} \qquad (15)$$

The semi-arbitrary assumption of $\theta_L=\theta_G$ is not necessary if one combines ϕ and θ and proposes the following equations involving the unknown hydrodynamic factors, p and q:

$$k_G = p \, (D_G)^{0.5} \qquad (16)$$

$$k_L = q \, (D_L)^{0.5} \qquad (17)$$

In order to obtain the values for p and q, a complete N_{OG} model which can be used to fit the experimental data is required. To complete the N_{OG} model, an interfacial area model is needed.

The most often used interfacial area model is based on the two bubble size distribution model (Lockett and Plaka, 1983; Prado and Fair, 1990; Ashley and Haselden, 1972; Porter et al., 1967; Kaltenbacher, 1983). Ashley and Haselden (1972) proposed that there are two groups of bubbles in froths having diameters d_1=5 mm and d_2=50 mm. The rise velocity of small bubbles u_1 is taken as 0.3 m/s. The small bubble hold-up fraction is $0.7(1-\varepsilon)/0.3$ and that of the large bubbles is $X=(\varepsilon-0.7)/0.3$ where ε is the total gas hold-up fraction. The rise velocity of large bubbles is given by mass balance as $u_2=(u_s-0.7(1-X)u_1)/X$. Clearly, the fraction of the total volumetric vapour flow carried through the froth by small bubbles is $f_1=0.7u_1(1-X)/u_s$, and that carried by large bubbles is $f_2=1-f_1$.

With the knowledge of bubble size distribution, of velocity of bubble ascent and of the mass transfer coefficients, the mass transfer in the froth can be described completely. If plug flow of gas through liquid which is completely mixed vertically is assumed, a mass balance over a differential height of froth, when integrated over the full height of the froth, gives the fraction approach to equilibrium (E_{OG}) of bubbles of diameter d_1 and d_2:

$$E_{OG1} = 1 - \exp\left(- \frac{6h_f K_{OG1}}{d_1 u_1} \right) \qquad (18)$$

$$E_{OG2} = 1 - \exp\left(- \frac{6h_f K_{OG2}}{d_2 u_2} \right) \qquad (19)$$

$$E_{OG} = 1 - f_1 \exp\left(- \frac{6h_f K_{OG1}}{d_1 u_1} \right) - f_2 \exp\left(- \frac{6h_f K_{OG2}}{d_2 u_2} \right) \qquad (20)$$

Comparing equation (20) to equation (3) gives:

$$N_{OG} = - \ln\left[f_1 \exp\left(- \frac{6 h_f K_{OG1}}{d_1 u_1} \right) + f_2 \exp\left(- \frac{6 h_f K_{OG2}}{d_2 u_2} \right) \right] \qquad (21)$$

Combining equations (1), (16), (17) and (21) gives:

$$N_{OG} = - \ln\left[f_1 \exp\left[\frac{- h_f p (D_G)^{0.5}}{d_1 u_1 (1 + m(\rho_G/\rho_L)(p/q)(D_G/D_L)^{0.5})} \right] \right.$$

$$\left. + f_2 \exp\left[\frac{- h_f p (D_G)^{0.5}}{d_2 u_2 (1 + m(\rho_G/\rho_L)(p/q)(D_G/D_L)^{0.5})} \right] \right] \qquad (22)$$

Then hydrodynamic factors p and q can be obtained at fixed Fa-factors by fitting equation (22) to the experimentally determined values of N_{OG} obtained as a function of m. Once p and q are known, N_G and N_L can be calculated by:

$$N_G = N_{OG} \left(1 + m \, (p/q)(\rho_G/\rho_L)(D_G/D_L)^{0.5} \right) \qquad (23)$$

$$N_L = N_{OG} \left(m + (q/p)(\rho_L/\rho_G)(D_L/D_G)^{0.5} \right) \qquad (24)$$

Lockett and Plaka (1983) used equations (23) and (24) to analyze their obtained results for a methanol/water system. They found that the ratio, (p/q), is 5.25 at F-factor=1.26. It can be seen clearly that the results of equations (23) and (24) would be very different from the results of equations (12) and (13).

3.4 Method 4: New Model

The interfacial area obtained by the model used in Method 3 is almost independent of system physical properties because the two bubble sizes are

assumed to be constant. Clearly this assumption is overly idealistic. As discussed in Chapter 2, bubble sizes are a strong function of system physical properties, especially surface tension. The models for N_G and N_L developed in Chapter 2 can be modified for fixed vapour rate conditions as follows:

$$N_G = C_1 \frac{1}{\mu^{0.1}\phi^{0.14}} \left[\frac{\rho_L \rho_G}{\sigma^2}\right]^{1/3} (D_G t_G)^{0.5} \qquad (25)$$

$$N_L = C_2 \frac{1}{\mu^{0.1}\phi^{0.14}} \left[\frac{\rho_L \rho_G}{\sigma^2}\right]^{1/3} (D_L t_L)^{0.5} \qquad (26)$$

$$t_G = h_L/u_s, \quad \text{and} \quad t_L = t_G \rho_L/\rho_G$$

where C_1 and C_2, including the effect of turbulent diffusion and multiple surface renewals, can be found by fitting equations (25) and (26) to the experimentally determined values of N_{OG} obtained as a function of m. Then N_G and N_L can be determined by:

$$N_G = N_{OG} \left(1 + m(C_1/C_2)(\rho_G/\rho_L)^{0.5}(D_G/D_L)^{0.5} \right) \qquad (27)$$

$$N_L = N_{OG} \left(m + (C_2/C_1)(\rho_L/\rho_G)^{0.5}(D_L/D_G)^{0.5} \right) \qquad (28)$$

It can be expected that this new method will give better results than all of the other three methods described above because it includes the effect of physical properties not only on mass transfer coefficients but also on the interfacial area.

3.5 Experimental Efficiency Data

For this study, three distillation systems with a wide range of physical properties have been chosen. They are cyclohexane/n-heptane, methanol/water and acetic acid/water mixtures. The physical properties needed in the calculations are predicted from Reid et al. (1977). The tray efficiency of the cyclohexane/n-heptane system as a function of m at fixed F-factors has been determined by Sakata and Yanagi (1979). Their measured tray efficiency is then converted to the point efficiency by the method used in Chapter 2. The results are shown in Figure 3-1. The froth height h_f and gas hold-up fraction ε of this system are estimated by equations obtained by Colwell (1979). The point efficiencies of the methanol/water and acetic acid/water systems as a function of m at fixed Fa-factors have been obtained in Chapters 6 and 7 and can be used directly. The results are shown in Figure 3-2 for the methanol/water system and Figure 3-3 for the acetic acid/water system, respectively. In these three figures, x is the average mole concentration of more volatile components at the test tray's inlet and outlet. From the point efficiency, N_{OG} is then calculated by equation (3) and the obtained results are used to determine N_G and N_L by the above four methods.

3.6 Results and Discussion

3.6.1 Cyclohexane/N-heptane System

The N_G and N_L obtained from N_{OG} for the cyclohexane/n-heptane system, using the four methods, are shown in Figure 3-4 for N_G and Figure 3-5 for N_L, respectively. It can be seen that, except for method 2, all methods give similar values of N_G and N_L. Because the physical properties of cyclohexane

are very similar to those of n-heptane, the physical properties of the cyclohexane/n-heptane system change little with the tray concentration or m. This means that N_G and N_L remain constant when m changes with the tray concentration as shown in Figures 3-4 and 3-5. Because N_G and N_L are independent of m, method 1 does not introduce any error. Similar results were also obtained by Zuiderweg (1982) for the same system. Methods 3 and 4 also give correct results as shown in Figures 3-4 and 3-5. It can be concluded that the decrease in efficiencies with decreasing concentration shown in Figure 3-1 is due to the liquid phase resistance. Method 2 failed to have correct results simply because the assumptions made to develop this method are not valid. It gives a small liquid phase resistance (large N_L) and a large vapour phase resistance (small N_G). It can be seen that both N_G and N_L from method 2 decrease with decrease in concentration, which is apparently not correct because physical properties remain constant as concentration changes.

The fraction of liquid phase resistance over the total mass transfer resistance (LPR) is calculated from equation (4) and shown in Figure 3-6. It can be found that, except for method 2, all methods give similar results. The decrease in LPR with increasing concentration is due to the decrease in m. At high tray concentrations, m is small, LPR is small (see Figure 3-6) and the tray efficiency is high (see Figure 3-1). On the other hand, at low tray concentrations, m is large, LPR is large (see Figure 3-6) and the tray efficiency is low (see Figure 3-1).

From the above discussions, it can be concluded that method 2 is unreliable and will give incorrect results. Dribika and Biddulph (1986) used this method to interpret their results, and consequently were misled in this

respect. Methods 1, 3 and 4 can be reliably used, at least for systems whose physical properties, or N_G and N_L, do not change with m.

3.6.2 Methanol/Water System

Because the physical properties of water are different from those of methanol, the physical properties of the methanol/water system change widely with concentration and m, especially the surface tension. As a result, N_G and N_L may vary with m, which is different from the cyclohexane/n-heptane system discussed above.

Figures 3-7 and 3-8 show the N_G and N_L obtained by the four methods. It can be seen that the four methods give four different results. There can be only one correct set of results. As discussed in section 3.6.1, method 2 is unreliable. It again gives a small N_G and large N_L, and results in a small liquid phase resistance similar to that of the cyclohexane/n-heptane system. Because the physical properties of the methanol/water system change widely with m, method 1 is also likely to give incorrect results due to changes of N_G and N_L with m. Although method 3 includes the effect of changes of densities and diffusivities of the liquid and vapour phases, the N_G and N_L it gives are similar to those of method 1 (see Figures 3-7 and 3-8). This is because the densities and diffusivities of this system change less than 20% in the concentration range involved. It is not clear so far whether this method is providing correct results. Lockett and Plaka (1983) used this method to analyze their results for the same methanol/water system and obtained similar results to those shown in Figures 3-7 and 3-8.

Method 4, which includes the effect of variations in not only densities

and diffusivities but also the surface tension of the system, gives very different results from those of methods 1 and 3 (see Figures 3-7 and 3-8). The surface tension of this system changes about three times in the concentration range. Because surface tension increases as concentration decreases, method 4 gives small N_G and N_L at the low concentration end and large N_G and N_L at the high concentration end.

Figure 3-9 shows the results of LPR from the four methods. It can be seen that methods 1 and 3 give a large liquid phase resistance. As a result, methods 1 and 3 explain the decrease in the efficiency with decreasing concentration (see Figure 3-2) by the liquid phase resistance only. Method 4 gives a relatively small liquid phase resistance, and explains the decrease in the efficiency with decreasing concentration by an increase in both liquid phase resistance and surface tension.

Based on the results of the methanol/water system alone, one can not tell which method has given the correct results.

3.6.3 Acetic Acid/Water System

The acetic acid/water system is somewhat similar to the methanol/water system. The physical properties of this system also change widely. The difference between these two systems is that water is a less volatile component in the methanol/water system, and a more volatile component in the acetic acid/water system. This results in a difference in the tray efficiency trend as shown in Figures 3-2 and 3-3.

The methods for obtaining N_G and N_L from N_{OG} should be equally applicable to both the methanol/water and the acetic acid/water systems. Figures 3-10 and 3-11 show the N_G and N_L obtained from the four methods.

Method 2 gives a small N_G and a large N_L, and results in a small LPR, which is shown in Figure 3-12. Comparing among Figures 3-6, 3-9 and 3-12, one can find that method 2 has given similar LPRs (less than 10%) for all three systems even though the properties of the three systems are quite different. Since it failed to have correct results for the cyclohexane/n-heptane system, there is no reason for method 2 to give correct results for the acetic acid/water system.

It is even more surprising that method 1 and method 3 give a negative N_L together with a very small N_G for the acetic acid/water system. Since negative N_L is impossible, the assumption used in method 1 that N_G and N_L are independent of m is apparently not valid for this system. These results clearly demonstrate that method 1 is only applicable for systems whose physical properties do not change with m. Therefore, method 1 must also have given wrong results for the methanol/water system because the physical properties of this system also change with m.

Similar to method 1, method 3 also gives a negative N_L with a very small N_G , as shown in Figures 3-10 and 3-11. The reason is that method 3 only accounts for the changes of densities and diffusivities, which actually do not change much with m for this system. It can be concluded that other important physical properties are not accounted for by method 3 because negative N_L is impossible. Because the physical properties of the methanol/water system are similar to those of the acetic acid/water system, method 3 must have given wrong results for the methanol/water system too. Lockett and Plaka (1983) used this method to interpret their experimental results of the methanol/water system and possibly gave wrong results there.

Unlike method 3, method 4 includes the effect of changes of surface

tension, in addition to densities. It gives reasonable N_G and N_L as shown in Figures 3-10 and 3-11. The decrease in N_G and N_L with increasing concentration is mainly due to the effect of surface tension. Consequently, the decrease in the efficiency with increasing concentration (see Figure 3-3) is also due to surface tension. Comparing Figures 3-12 and 3-6, one can find that method 4 gives a similar LPR for this system to for the cyclohexane/n-heptane system. Comparing the N_G and N_L of the three systems obtained by method 4, one can find that N_G has similar values for all three systems, and N_L of the methanol/water system is larger than that of other two systems. The reasons will be discussed in Chapter 5.

3.7 Conclusions

Based on the results for three different distillation systems, it has been shown that method 2 is unreliable for obtaining N_G and N_L from N_{OG}. Methods 1 and 3 are reliable only for systems whose physical properties do not change with m. Only method 4, developed in this study, can be used for all systems. It has taken into account the variation of densities, diffusivities, and the surface tension. Therefore, it is more accurate than any previously proposed method for determining N_G and N_L from experimental distillation data (E_{OG}). Its power lies in the way the effects of compositions and hydrodynamics are separated. The former can easily be accounted for in the model, while the latter are held constant for data obtained at a fixed value of F-factor. Only after N_G and N_L are accurately determined from distillation data can all the efficiency models be verified. A comparison of various efficiency models will be provided in Chapter 4.

3.8 Nomenclature

a = effective interfacial area, m^2/m^3

C_i = constant

D_G = Diffusion coefficient in vapour phase, m^2/s

D_L = Diffusion coefficient in liquid phase, m^2/s

d_i = equivalent spherical bubble diameter, m

E_{MV} = Murphree vapour-phase efficiency

E_{OG} = Murphree vapour-phase point efficiency

Fa, = F factor based on active area, $(kg/m)^{0.5}/s$

F = superficial F factor, $(kg/m)^{0.5}/s$

f_i = fraction of vapour carried by bubbles of diameter d_i

G = Vapour flow rate, kmol/s

h_f = froth height, m

h_L = clear liquid height, m

k_G = gas film mass transfer coefficient, m/s

k_L = liquid film mass transfer coefficient, m/s

K_{OG} = overall mass transfer coefficient, m/s

L = Liquid flow rate, kmol/s

LPR = fraction of liquid phase resistance

m = slope of equilibrium line

N_G = number of gas phase transfer units

N_L = number of liquid phase transfer units

N_{OG} = number of overall gas phase transfer units

p = parameter, $1/s^{0.5}$

q = parameter, $1/s^{0.5}$

t_L = liquid residence time, s

u_s = superficial vapour velocity, m/s

u_l = rise velocity of bubble diameter d_l, m/s

X = holdup fraction of large bubbles

x = mole fraction of MVC in liquid

x_i = mole fraction of MVC in liquid at interface

y = mole fraction of MVC in vapour

y^* = mole fraction of MVC in vapour in equilibrium with liquid

y_i = mole fraction of MVC in vapour at interface

y_n = mole fraction of MVC in vapour for tray above

y_{n-1} = mole fraction of MVC in vapour for tray below

Greek Letters

ε = vapour holdup fraction

θ_G = vapour contact time, s

θ_L = liquid contact time, s

λ = mG/L

μ = liquid phase viscosity, Ns/m^2

ρ_G = vapour density, kg/m^3

ρ_L = liquid density, kg/m^3

σ = surface tension, N/m

ϕ_G = enhancement factor

ϕ_L = enhancement factor

ϕ = percent open hole area

Figure 3-1
Point Efficiency of Cyclohexane/N-heptane System
(Sakata and Yanagi, 1979)

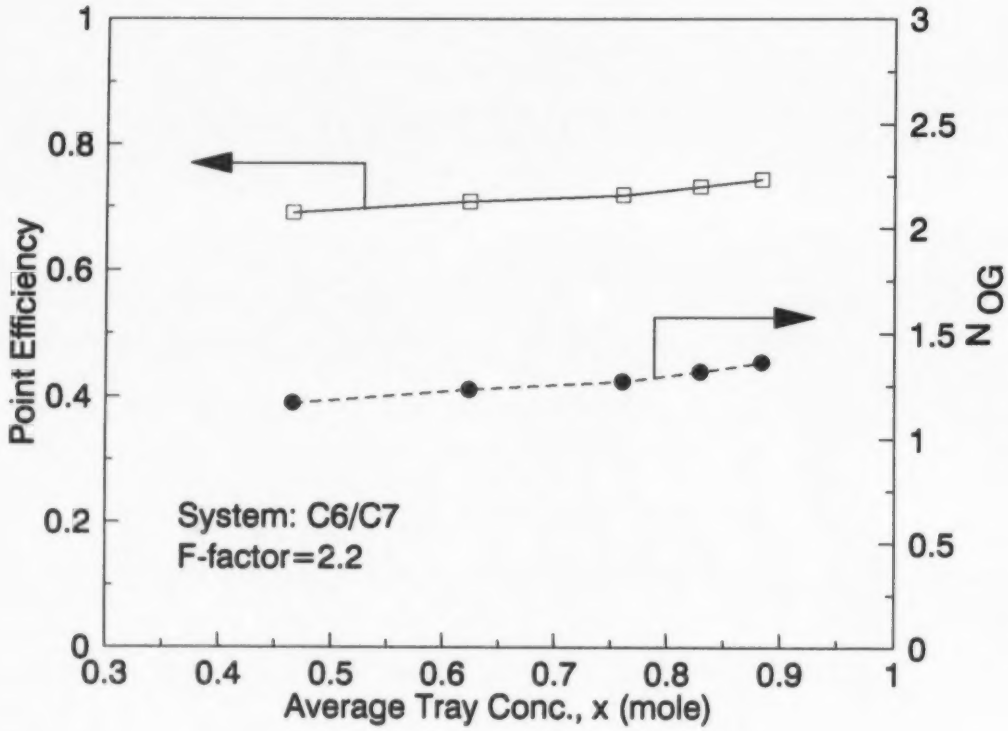

Figure 3-2
Point Efficiency of Methanol/Water System

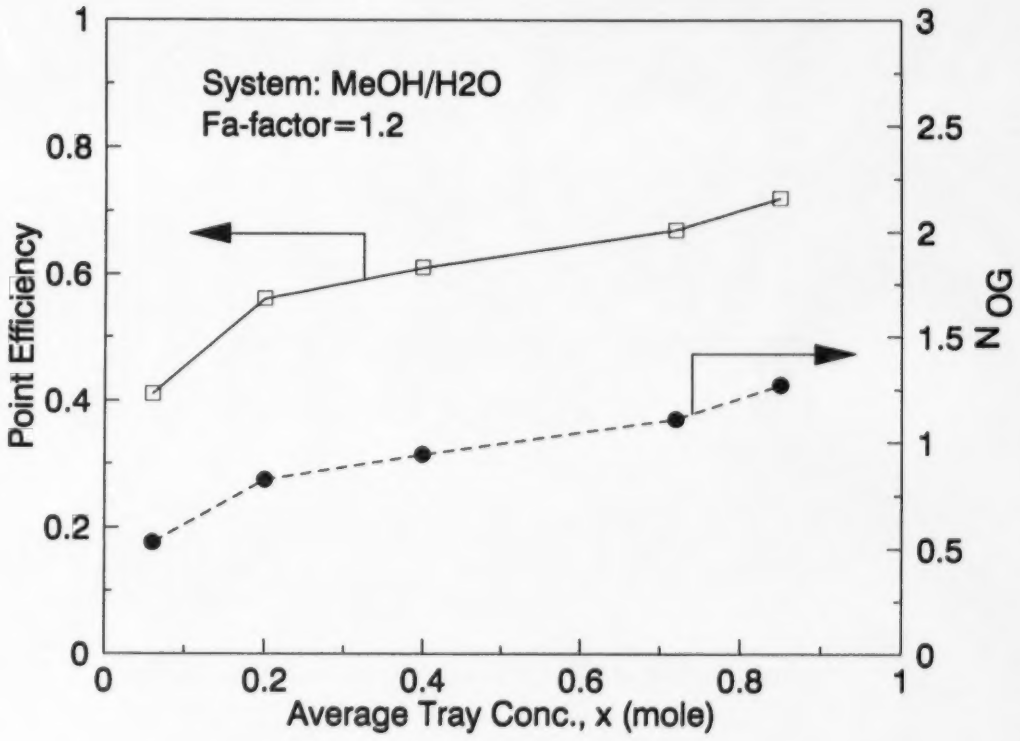

Figure 3-3
Point Efficiency of Acetic Acid/Water System

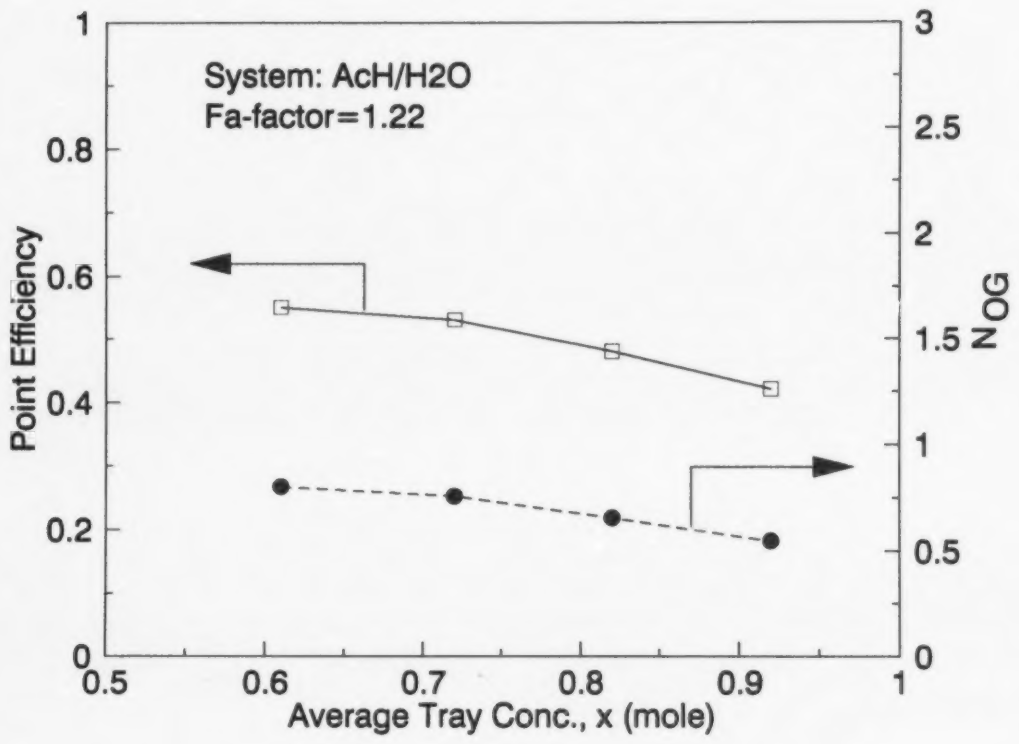

Figure 3-4

Comparison of Determined N_G by Four Methods for Cyclohexane/N-heptane System

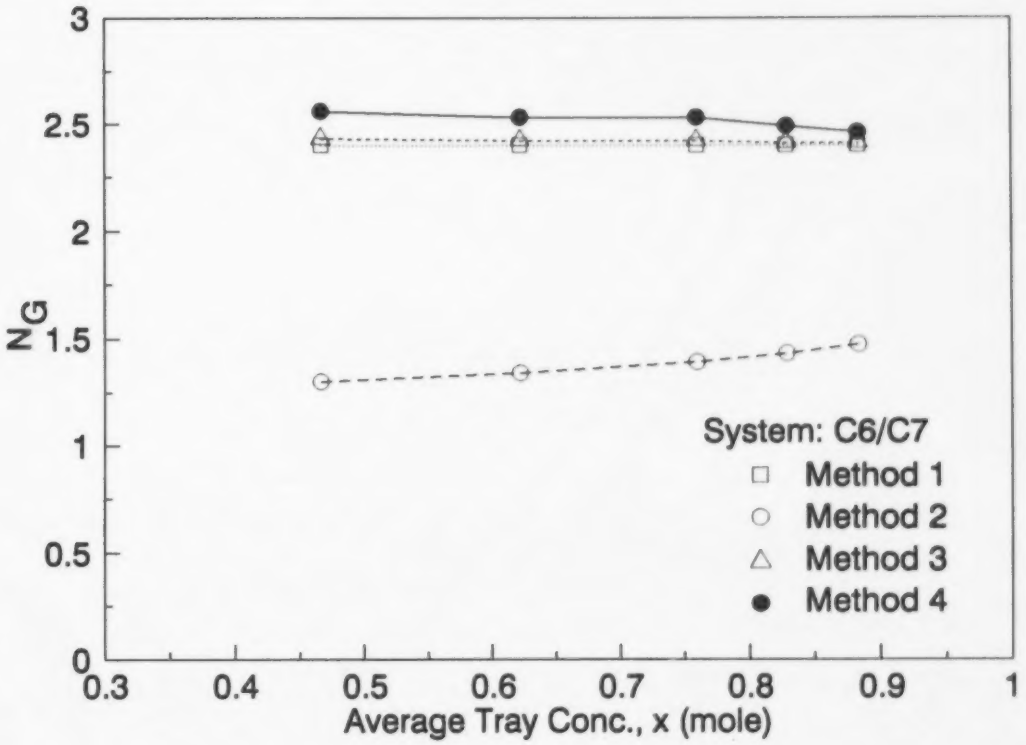

Figure 3-5

Comparison of Determined N_L by Four Methods for Cyclohexane/N-heptane System

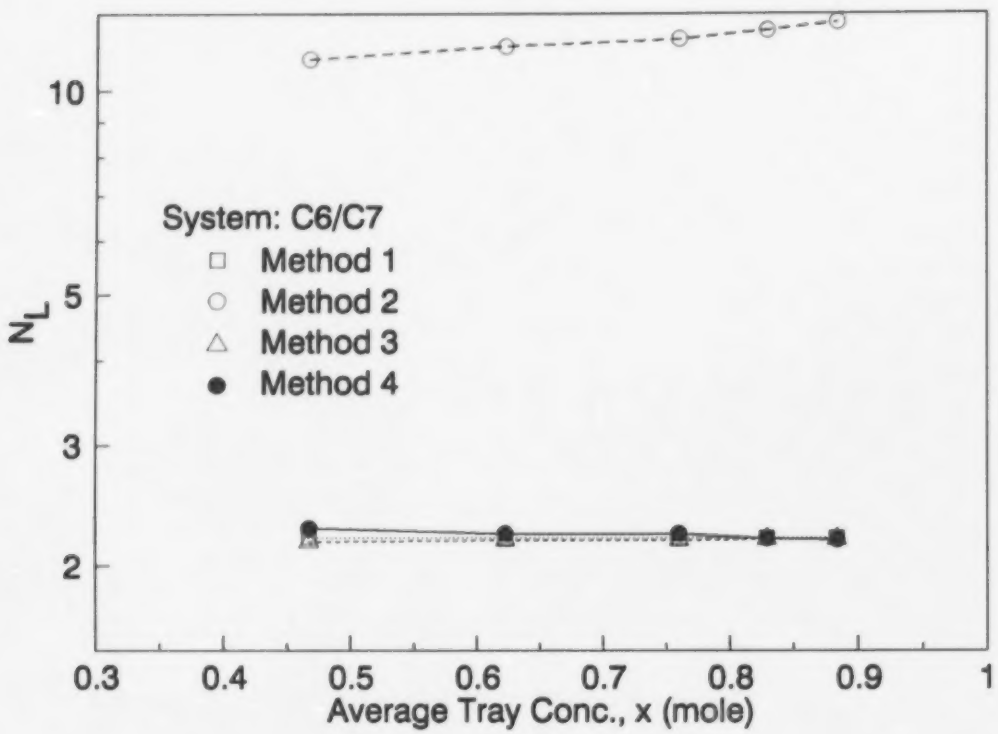

Figure 3-6
Comparison of Determined LPR by Four Methods for Cyclohexane/N-heptane System

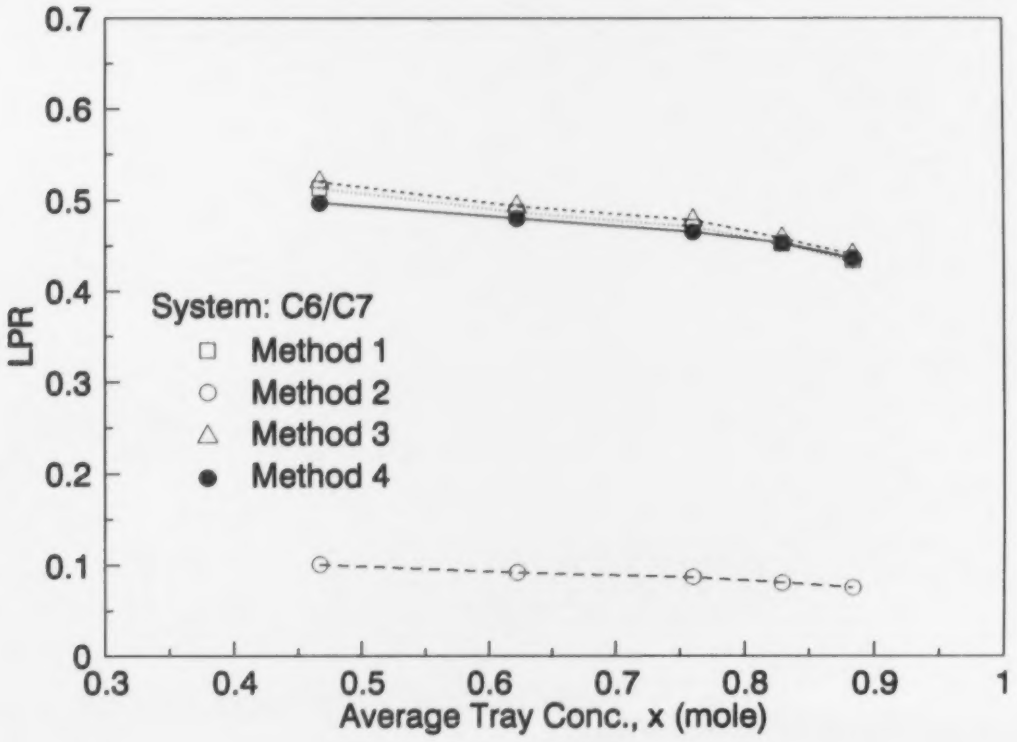

Figure 3-7
Comparison of Determined N_G by Four Methods for Methanol/Water System

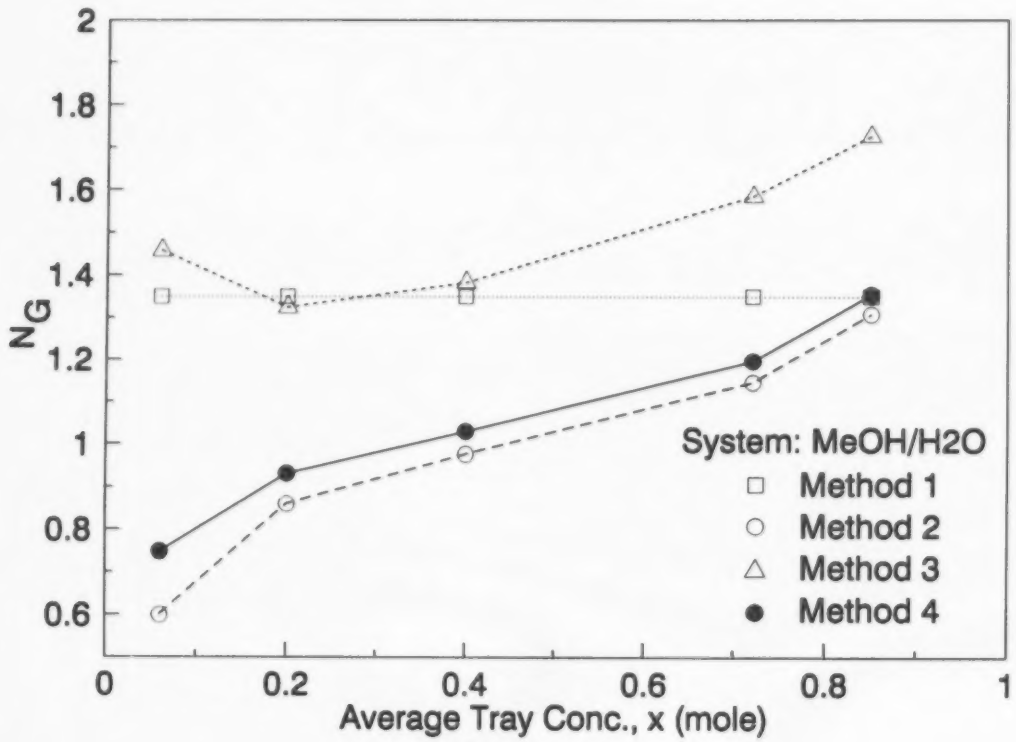

Figure 3-8
Comparison of Determined N_L by Four Methods for Methanol/Water System

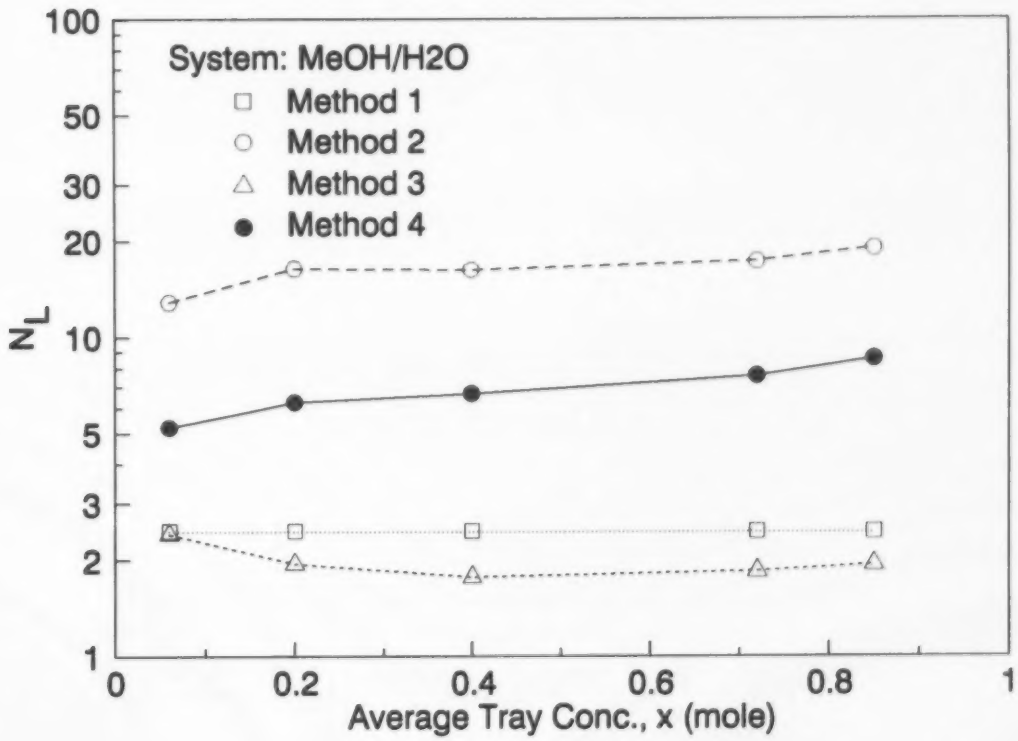

Figure 3-9
Comparison of Calculated LPR by Four Methods for Methanol/Water System

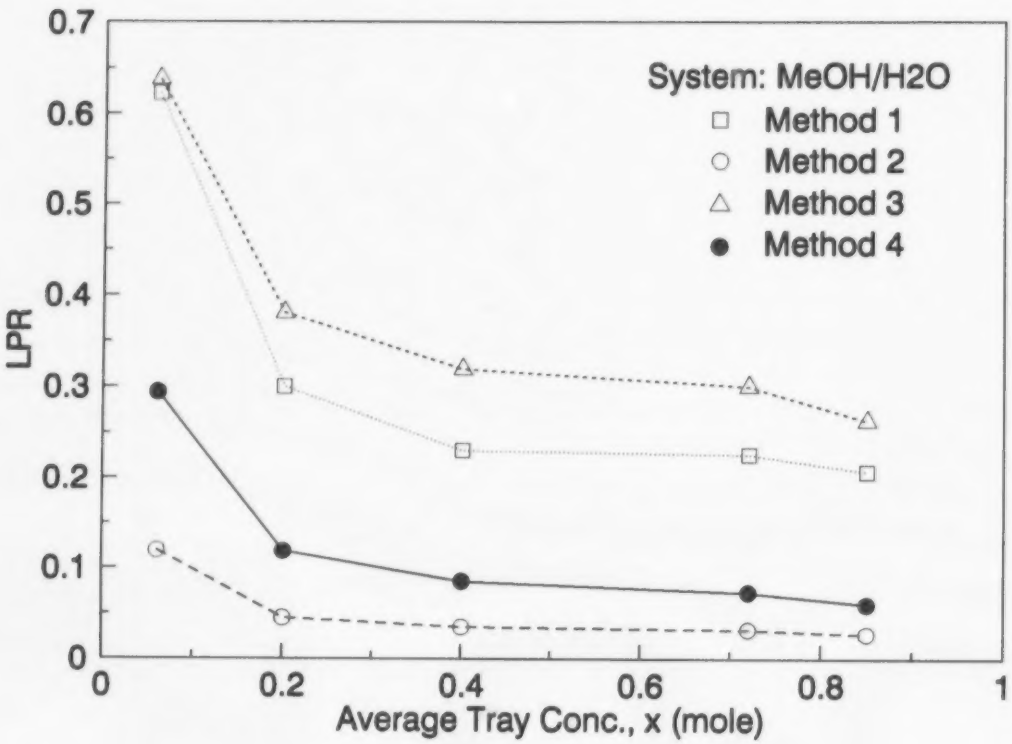

Figure 3-10
Comparison of Determined N_G by Four Methods for Acetic Acid/Water System

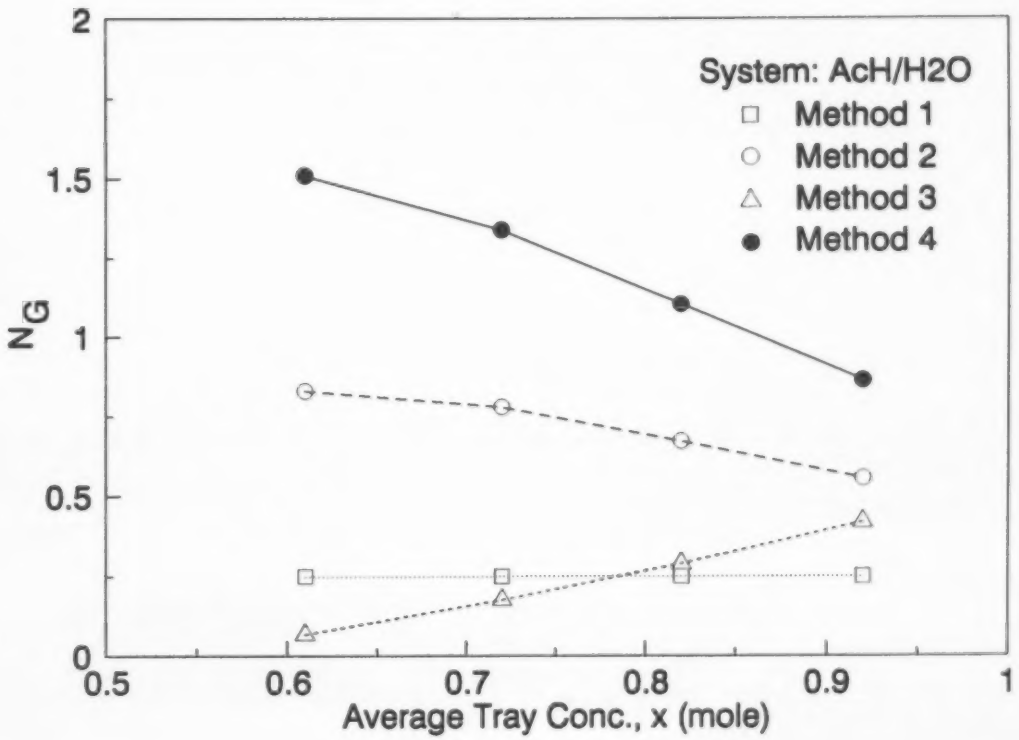

Figure 3-11
Comparison of Determined N_L by Four Methods for Acetic Acid/Water System

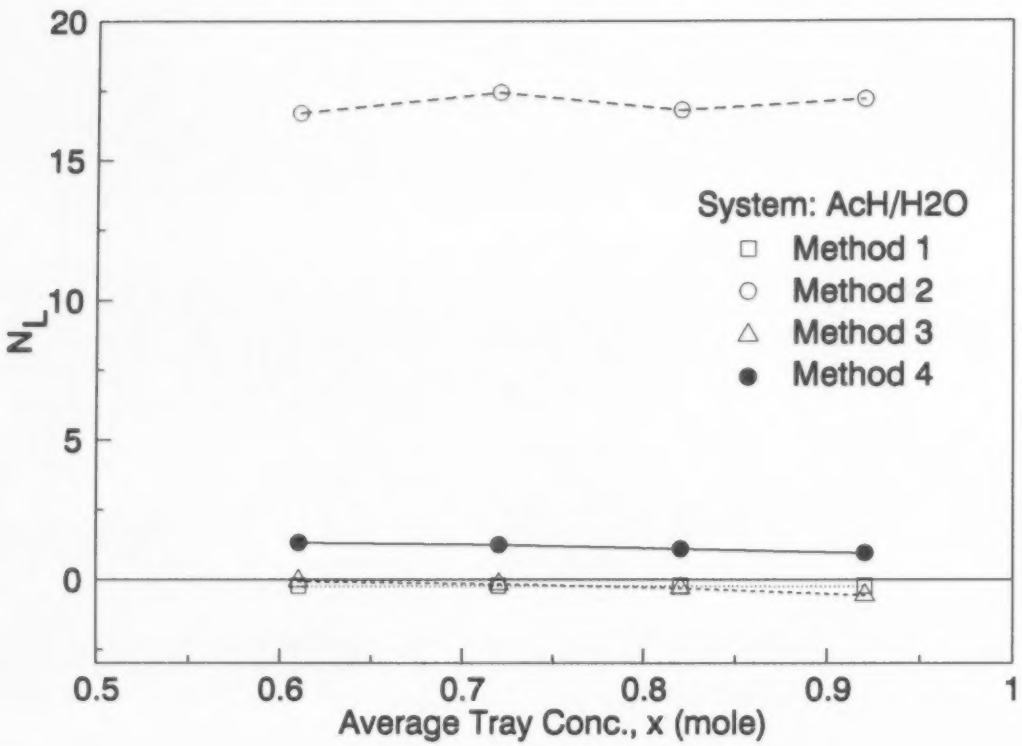

Figure 3-12
Comparison of Determined LPR by Four Methods for Acetic Acid/Water System

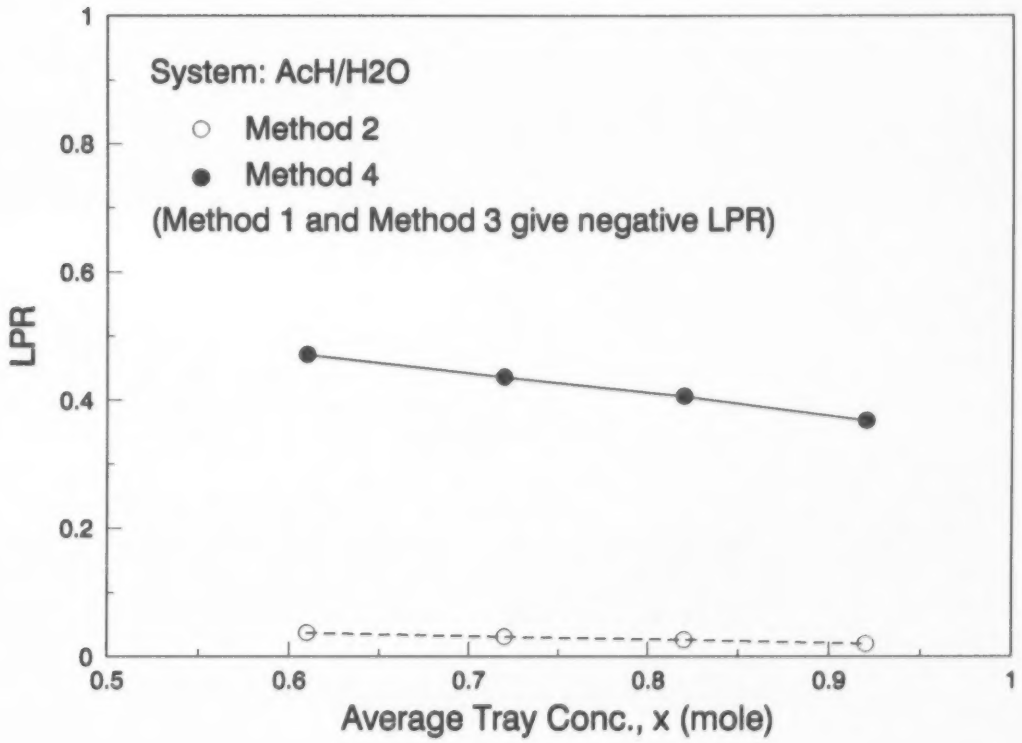

3.9 Literature Cited

AIChE, "Bubble Tray Design Manual," New York (1958).

Ashley, M.J., and G.G. Haselden, "Effectiveness of Vapour-Liquid Contacting on a Sieve Tray," Trans. Inst. Chem. Engrs., **50**, 119 (1972).

Calderbank, P.H., and J. Perira, "The Prediction of Distillation Plate Efficiencies from Froth Properties," Chem. Eng. Sci., **32**, 1427 (1977).

Colwell, C.J., "Clear liquid height and froth density on sieve trays," Ind. Eng. Chem. Proc. Des. Dev. **20**(2), 298 (1979).

Dribika, M.M., and M.W. Biddulph, "Scaling-Up Distillation Efficiencies," AIChE J., **32** (9), 1864 (1986).

Higbie, R., "The rate of absorption of a pure gas into a still liquid during short periods of exposure," Trans. Am. Inst. Chem. Engrs. **31**, 365 (1935).

Kaltenbacher, E., "On the effect of the bubble size distribution and the gas-phase diffusion on the selectivity of sieve trays," Chem. Eng. Fund. **1**(1), 47 (1983).

Lockett, M.J., "Distillation Tray Fundamentals," Cambridge University Press, Cambridge (1986).

Lockett, M.J., and I.S. Ahmed, "Tray and Point Efficiencies from a 0.6 Meter Diameter Distillation Column," Chem. Eng. Res. Des., **61**, 110 (1983).

Lockett, M.J., and T. Plaka, "Effect of Non-Uniform Bubbles in the Froth on the Correlation and Prediction of Point Efficiencies," Chem. Eng. Res. Des., **61**, 119 (1983).

Lockett, M.J., and M.S. Uddin, "Liquid-phase controlled mass transfer in froths on sieve trays," Trans. Inst. Chem. Engrs. **58**, 166 (1980).

Neuburg, H.J., and K.T. Chuang, "Mass transfer modelling for GS heavy water

plants. 1: Point efficiency on GS sieve trays," Can. J. Chem. Eng. **60**, 504 (1982).

Porter, K.E., B.T. Davies, and P.F.Y. Wong, "Mass transfer and bubble sizes in cellular foams and froth," Trans. Inst. Chem. Engrs. **45**, T265 (1967).

Prado, M., and J.R. Fair, "Fundamental model for the prediction of sieve tray efficiency," Ind. Eng. Chem. Res. **29**, 1031 (1990).

Reid, R.C., J.M. Prausnitz, and T.K. Sherwood, "The Properties of Gases and Liquids," McGraw Hill, New York (1958).

Sakata, M., and Y. Yanagi, "Performance of a commercial-scale sieve tray," Inst. Chem. Engrs. Symp. Ser. No. **56**, 3.2/21 (1979).

Stichlmair, J., Bodenkolonne. Verlag Chemie (1978).

Zuiderweg, F.J., "Sieve Trays, a View of the State of the Art," Chem. Eng. Sci., **37**, 1441 (1982)

Chapter 4

THE EFFECTS OF SURFACE TENSION ON THE NUMBER OF MASS TRANSFER UNITS

4.1 Introduction

Many experimentally measured tray efficiencies varied with compositions of distillation mixtures have been reported for different systems (Bainbridge and Sawistoeski, 1964; Fane and Sawistowski, 1968; Zuiderweg, 1983; Ellis and Biddulph, 1967; Moens and Bos, 1972; Moens, 1972; Lockett and Ahmed, 1983; Goederen, 1965; Ruckensten and Smigelschi, 1965). Various reasons have been suggested to explain the variations in mass transfer efficiencies with compositions and none of which alone has provided a complete explanation (Lockett, 1986). The explanations provided were in terms of physical properties, the slope of the equilibrium curve, the interfacial area, mass transfer coefficients, thermal effects, and the most important, the effects of surface tension and its gradient. Recently, more and more attention has been given to the effects of surface tension and its gradient on mass transfer efficiencies, but little progress was made. Most methods for predicting mass transfer efficiencies do not include the effects of surface tension.

Many efficiency models are available now in the literature. It is difficult for a design engineer to select an appropriate model to calculate a value for the plate efficiency, particularly if a new system is being used and efficiency data for a similar system are not available. It is very common that different efficiency models give different values of point efficiencies. Although it was found that the point efficiency changes with

system compositions, most efficiency models rarely predict this composition effect on the point efficiency.

The main purpose of this study was to determine the effects of surface tension on the number of mass transfer units for three different systems. The efficiency models which include the effects of surface tension would be compared with those that do not include these effects. The determined N_G and N_L and measured efficiencies would be compared with those predicted by various models.

4.2 Theory

4.2.1 Basic Relation

The following equations, discussed in Chapter 2, will be used in this study.

$$1/N_{OG} = 1/N_G + m/N_L \qquad (1)$$

$$E_{OG} = 1 - \exp(-N_{OG}) \qquad (2)$$

$$LPR = (m/N_L)/(1/N_G + m/N_L) \qquad (3)$$

The new method of determining N_G and N_L from E_{OG} obtained in Chapter 3 will be used in this study.

4.2.2 Efficiency Models Not Including Surface Tension

Method 1: The AIChE Model (1958)

The AIChE model was the first recognized and the most commonly accepted model in the literature. It is covered well in the standard chemical engineering texts (Smith, 1963; Lockett, 1986). The method is based on the results of the individual number of mass transfer units from experiments

using single phase resistance systems. It has often been criticized for being unreliable (Lashmet and Szezepanski, 1974; Hughmark, 1971; Neuburg and Chuang, 1982; Lockett, 1986).

$$N_G = (0.776 + 4.57h_W - 0.238F_s + 104.8\ Q_L/W)Sc_G^{-0.5} \quad (4)$$

$$N_L = 19700D_L^{0.5}(0.4F_s + 0.17)t_L \quad (5)$$

$$Sc_G = \mu_G/(\rho_G D_G) \quad (6)$$

$$t_L = h_L Z_L W/Q_L \quad (7)$$

$$h_L = 0.725h_W - 0.238h_W F_s + 1.23Q_L/W + 0.006 \quad (8)$$

Equation (4) has no theoretical basis, and does not even include the vapour phase contacting time. The importance of the Schmidt number in equation (4) is open to doubt. In very careful experiments, Mehta and Sharma (1966) found that N_G depends on D_G but not on Sc_G. Equations (4) and (5) do not share a common term for the interfacial area. Because the AIChE model suffered from a fundamental deficiency, many attempts to improve the AIChE model have failed.

Method 2: Chan and Fair's Model (1984)

Chan and Fair (1984) improved the AIChE model to represent most of the efficiency data available for large-scale sieve trays (Jones and Pyle, 1955; Kirschbaum, 1962; Kastanek and Standart, 1967; Billet et al., 1969; Nutter, 1971; Sakata and Yanagi, 1979). Although they retained the same correlation for N_L as the original AIChE model, they improved the N_G correlation by including the vapour phase contacting time and including D_G instead of Sc_G. The volumetric mass transfer coefficients and N_G in the vapour phase were

back-calculated and then correlated in terms of the vapour phase diffusivity, liquid hold-up and fractional approach to flooding.

$$N_L = 19700(0.40F_s + 0.17)D_L^{1/2}t_L \qquad (9)$$

$$N_G = 1000D_G^{1/2}(10.3FF - 8.67FF^2)t_G/h_L^{1/2} \qquad (10)$$

$$t_L = h_L ZW/Q_L \qquad (11)$$

$$t_G = (1-\alpha)h_L/(\alpha u_s) \qquad (12)$$

$$h_L = \alpha\,(h_W + C(Q_L/(W\alpha))^{0.67}) \qquad (13)$$

$$\alpha = \mathrm{Exp}\left[-12.55\,(u_s(\frac{\rho_G}{\rho_L - \rho_G})^{0.5})^{0.91} \right] \qquad (14)$$

$$C = 0.50 + 0.438\,\mathrm{Exp}(-137.8h_W) \qquad (15)$$

where $FF=u_s/u_f$, the fraction approach to the active area gas velocity at flooding. Based on the penetration theory, the interfacial area can be obtained from equation (9):

$$a = C1(0.40F_s + 0.17) \qquad (16)$$

and from equation (10):

$$a = C2(10.3FF - 8.67FF^2)/h_L^{1/2} \qquad (17)$$

It is hardly reasonable that equation (16) would be equivalent to equation (17). Therefore, Chan and Fair's model may be as fundamentally unsound as the AIChE model. Their model does not have the same interfacial area for N_G and N_L.

4.2.3 Efficiency Models Including Surface Tension

Method 3: Zuiderweg's Model (1982)

Zuiderweg (1982) reviewed sieve tray performance and proposed a method of predicting point efficiencies based on the commercial-scale experimental sieve tray efficiency data of Fractionation Research Incorporated reported by Yanagi and Sakata (1982) and Sakata and Yanagi (1979). Independent correlations for the mass transfer coefficients in the vapour and the liquid phases were developed in terms of physical properties. By using the Weber number, values of the interfacial area were correlated with reference to the flow regimes and taking into account the effect of surface tension. The liquid hold-up is evaluated by the Hofhuis's equation. Later, Zuiderweg (1986) stated that his model is possibly not more reliable than alternative models, but it is simpler.

$$K_G = 0.13/\rho_G - 0.065/\rho_G^2 \qquad (18)$$

$$K_L = 0.024\ D_L^{0.25} \qquad (19)$$

For the spray regime: $$ah_f = 40/\phi^{0.3}\ (F_{bba}^2\ h_L FP/\sigma)^{0.37} \qquad (20)$$

For the froth regime: $$ah_f = 43/\phi^{0.3}\ (F_{bba}^2\ h_L FP/\sigma)^{0.57} \qquad (21)$$

$$h_L = 0.6 H_W^{0.5} p^{0.25}\ b^{-0.25} (FP)^{0.25} \qquad (22)$$

For total reflux: $$FP = (\rho_G/\rho_L)^{0.5} \qquad (23)$$

Method 4: New Model Developed in Chapter 2

A new model for predicting point efficiencies (see Chapter 2) has been developed based on the penetration theory and the dispersion theory and by

using the commercial-scale sieve tray data released by Sakata and Yanagi (1979).

$$N_G = 11\ (\rho_L F_s^2/\sigma^2)^{1/3}(D_G t_G)^{0.5}/(\mu_L^{0.1}\phi^{0.14}) \qquad (24)$$

$$N_L = 14\ (\rho_L F_s^2/\sigma^2)^{1/3}(D_L t_L)^{0.5}/(\mu_L^{0.1}\phi^{0.14}) \qquad (25)$$

$$t_G = h_L/u_s \qquad (26)$$

$$t_L = t_G\ \rho_L/\rho_G \qquad (27)$$

where h_L is calculated by equation (22).

4.3 Experimental

The tray efficiency results for three systems obtained in Chapters 3, 6 and 7 will be used in this study. The surface tensions of mixtures at normal temperatures are obtained from the International Critical Tables (1928). The vapour effects on surface tension is negligible (Adamson, 1982), so the surface tension with air was used. Then the surface tensions at boiling point are calculated by the following equation:

$$\sigma = a + b\ T \qquad (28)$$

where a and b are constant and found from the surface tensions at normal temperatures. The surface tensions at boiling point for the three systems are shown in Figure 4-1 as a function of mole fraction of the more volatile components (x). The surface tensions of the methanol/water system are close to those found by Kalbassi et al. (1987). The variations of physical properties with compositions for the three systems are predicted from Reid et al. (1958).

4.4 Results and Discussion

4.4.1 Murphree Vapour Phase Point Efficiency

The experimental efficiency data obtained are shown in Figures 4-2, 4-3 and 4-4 for the three systems as a function of the average test tray concentration x of more volatile components with fixed Fa-factors. It was found that the efficiency of the methanol/water system increases monotonically with x in the test range (see Figure 4-4). Contrary to the efficiency of the methanol/water system, the efficiency of the acetic acid/water system decreases monotonically with x as shown in Figure 4-3. These efficiency data are in good agreement with those of Bennett (1959) and Bahari (1955). The efficiency of the cyclohexane/n-heptane system also increases with increase in x, but not as much as in the methanol/water system, which is shown in Figure 4-2.

4.4.2 Surface Tension Effects on The Number of Mass Transfer Units

Explanations for the effects of mixture compositions on tray efficiencies, as shown in Figures 4-2 to 4-4, have been proposed by many researchers. Ruckenstein and Smigelschi (1965) obtained the same efficiency pattern as shown in Figure 4-4 for the same methanol/water system. They explained this phenomenon in terms of thermal effects. Their equations almost perfectly agreed with their experimental data. But to get these results, they had to assume that about 90% of the resistance to mass transfer lay in the liquid phase, which is very unlikely. Lockett (1986) indicated that their equations can both be faulted because they simply add the effects of heat transfer to mass transfer. Norman (1960) estimated the maximum relative rate of sensible heat transfer was not more than about 5%

of the heat transferred as latent heat. This means that the sensible heat transfer has a negligible effect on distillation tray efficiencies. Sandall and co-workers (Kayihan et al., 1975, 1977, Honorat and Sandall, 1978, Sandall and Dribika, 1979) also concluded that heat transfer effects were negligible in distillation.

The variations of the efficiency shown in Figures 4-3 and 4-4 can not be attributed to the changes in liquid phase resistance either, especially for the acetic acid/water system whose efficiency decreases with decreasing m (see Figure 4-3). Therefore, it can be concluded that neither the thermal effects nor the changes in liquid phase resistance through m can be attributed to the changes in efficiency shown in Figures 4-2 to 4-4. Perhaps the best explanation comes from the changes in physical properties with compositions. By carefully examining the physical properties of the acetic acid/water and methanol/water systems, one can find that only surface tensions change significantly with compositions. All other properties remain quite constant over the composition range involved. Therefore, the efficiency may be a function of system surface tension.

In order to have a more direct connection with physical properties, efficiencies were converted to overall numbers of mass transfer units, N_{OG}, by equation (2). The obtained results are plotted against the surface tension in Figure 4-5 for the three systems. It seems that N_{OG} decreases as surface tension increases. As surface tension changes, however, the slope of the equilibrium line (m) also changes, especially for the methanol/water system. The change in m will also affect N_{OG} as equation (1) indicates. Figure 4-5 makes sense only when liquid phase resistance is small (N_L is large) or m remains constant. As discussed in Chapters 2 and 3, the liquid

phase resistance in a distillation system is comparable to that of the vapour phase. Therefore, it is impossible to draw any conclusion from Figure 4-5 before the effects of surface tension and m on N_{OG} are separated.

To exclude the effect of m, N_G and N_L have to be calculated from N_{OG}. The new method developed in Chapter 3 was used to calculate N_G and N_L from N_{OG} . The obtained results are shown in Figures 4-6 to 4-8 as a function of surface tension for the three systems, respectively. It can be seen from Figures 4-7 and 4-8 that there are definitely some relationships between N_G and N_L and surface tension. Neglecting the effects of properties other than surface tension on N_G and N_L, the following results are obtained by regressions:

For the acetic acid/water system:

$$N_G \propto \sigma^{-0.87}, \qquad N_L \propto \sigma^{-0.60}$$

For the methanol/water system:

$$N_G \propto \sigma^{-0.65}, \qquad N_L \propto \sigma^{-0.53}$$

If it is assumed that surface tension has effects on the interfacial area only, and has no effects on mass transfer coefficients, than surface tension should have the same effects on both N_G and N_L because they are based on the same interfacial area. Averaging the exponent of σ for the two systems gives:

$$N_G \text{ and } N_L \propto \sigma^{-0.73} \qquad \text{for the acetic acid/water system.} \qquad (29)$$

$$N_G \text{ and } N_L \propto \sigma^{-0.59} \qquad \text{for the methanol/water system.} \qquad (30)$$

These results are in good agreement with the previous conclusions in Chapter 2 where it was found from the dispersion theory that N_G and $N_L \propto \sigma^{-2/3}$. The

data of the cyclohexane/n-heptane system were not analyzed because the surface tension range involved is too small to draw any conclusion.

4.4.3 Marangoni and Surface Renewal Effects

A surface tension positive system has a higher point efficiency in the free bubbling or cellular foam regime, while a surface tension negative system has a higher point efficiency in the spray regime, provided that other properties of systems are similar (Zuiderweg and Harmens, 1958). This theory is based on the analysis of Marangoni effects on the interfacial area. Hofhuis and Zuiderweg (1979) found that stable Marangoni-induced foam did not exist in the mixed-froth regime. By applying the equations provided by Hofhuis and Zuiderweg (1979), it was found that when Fa-factor is larger than 0.5, only the mixed-froth regime can exist for the methanol/water and acetic acid/water systems. This was also confirmed by visual observations during the experiments. Therefore, the higher efficiency of the methanol/water system in the froth regime is not due to the Marangoni effects on the interfacial area.

Comparisons among Figures 4-6 to 4-8 show that N_G has similar values for all three systems, but N_L of the methanol/water system is much larger than that of other two systems (see Figure 4-9). If the Marangoni effect had effects on the interfacial area, then both the N_G and N_L of the methanol/water system would be larger than that of other two systems. Thus, the higher efficiency and larger N_L of the methanol/water system might be due only to the surface renewal effects which result in an increase in the liquid phase mass transfer coefficient (k_L). Moens and Bos (1972) studied the surface tension effect in a pool column with a fixed interfacial area.

They found that the N_{OG} of a surface tension positive system was larger than that of a negative system because a positive system has a larger spreading velocity of liquid from eddies arriving at the interface. In other words, the rapid eddy-spreading velocity in a positive system would be expected to reduce the liquid phase resistance, and hence produce a larger N_L. Similar conclusions were also obtained by Ellis and Biddulph (1967). Dribika and Biddulph (1986) found that the enhancement in point efficiencies in the methanol/water system is related to the Marangoni index due to surface renewal effect. The quantitative aspect of this surface renewal effect will be discussed in Chapter 5.

Because of the large values of N_L of the methanol/water system, the fraction of liquid phase resistance over the total mass transfer resistance of this system will be much smaller than that of other two systems. Figure 4-10 compares the LPR results calculated by equation (3) for the three systems. It can be seen that the LPR of the methanol/water system is only about 25% of that of other two systems. It can also be seen that for one system, LPR increases with m as indicated by equation (3).

4.5 Comparison of Efficiency Prediction Methods

It has been shown that surface tension has effects on N_L and N_G. Therefore, efficiency models which do not include the effects of surface tension are likely to predict the efficiency trend incorrectly. It has also been shown that the N_L of a surface tension positive system is much larger than that of other systems due to surface renewal effects. Consequently, a special efficiency model including the surface renewal effect would be needed to predict the point efficiency properly for such systems.

4.5.1 Cyclohexane/N-heptane System

Figure 4-11 compares the measured efficiencies of the cyclohexane/n-heptane system with those of calculated by the four methods as outlined in section **4.2**. Except for method 1, the methods predict the efficiency reasonably well. Because the surface tension of this system changes little with x, as shown in Figure 4-1, it makes no difference whether surface tension is included in the models. Figures 4-12 and 4-13 compare determined N_G and N_L to calculated N_G and N_L. It can be seen from these figures that methods 1 and 2 have failed to predict the individual N_G and N_L correctly. They both have under-predicted the N_G and over-predicted the N_L. As a result, they may over-predict the efficiency for liquid phase controlled systems (Hughmark, 1965). Since method 2 gives reasonable values for the efficiency, as shown in Figure 4-11, it must have been through a wrong route. Overall, method 4 gives the best prediction of N_G and N_L, and of the efficiency.

4.5.2 Acetic Acid/Water System

As shown in Figure 4-1, the surface tension of the acetic acid/water system changes widely with x, so does the efficiency (see Figure 4-3). The measured and predicted efficiencies are compared in Figure 4-14. It can be seen that methods 1 and 2 over-predicted the efficiency, while method 3 under-predicted it. Because the densities and diffusivities of vapour and liquid of this system are similar to those of the cyclohexane/n-heptane system, it is no surprise that methods 1 and 2 gave similar values of efficiency for both the acetic acid/water system and the

cyclohexane/n-heptane system. Furthermore, methods 1 and 2 failed to predict the correct efficiency trend. This is because they do not include the effects of surface tension. On the other hand, method 4, which includes the effect of surface tension, correctly predicted not only the efficiency trend but also the efficiency values. The lower efficiency for the acetic acid/water system as compared to the cyclohexane/n-heptane system is due to the large surface tension, which can be seen in Figure 4-1.

Figures 4-15 and 4-16 show the results for N_G and N_L. Again, methods 1 and 2 over-predicted the N_L. Because methods 1 and 2 do not include the surface tension, they also failed to predict N_G and N_L trends correctly. Method 3, which includes the surface tension, predicted the N_G and N_L trends correctly, but gave incorrect values. Only method 4 predicted both trends and values correctly. Therefore, it can be concluded that without the inclusion of surface tension, it is impossible for a model to predict the point efficiency correctly at least for systems like the acetic acid/water whose surface tension changes significantly with compositions.

4.5.3 Methanol/Water System

As shown in Figure 4-17, all four methods have failed to predict the efficiency correctly for the methanol/water system. The reason is that all four methods do not take the surface renewal effect into consideration. Methods 3 and 4 seem to predict the trend of the variation of efficiency with compositions better than methods 1 and 2, but both under-predicted the efficiency. Zuiderweg (1983) calculated the point efficiency in the methanol/water experiments of Lockett and Ahmed (1983) and found that the predicted point efficiencies were very low as compared with the experimental

results. His explanation was that the efficiency model derived from data on hydrocarbon systems could not be expected to predict the efficiency of the methanol/water system because of the influence of the surface tension gradient effect. This is probably true. But his method also under-predicted the point efficiency of the acetic acid/water system. With this theory, the model should over-predict the efficiency of the acetic acid/water system. Methods 1 and 2 predicted the efficiency trend incorrectly because they do not include surface tension. Therefore, a new special model is needed to include the effects of both surface tension and its gradient for the prediction of the efficiency of positive systems, which will be discussed in Chapter 5.

4.6 Conclusions

For three binary systems, the numbers of individual phase mass transfer units were determined under distillation conditions in the froth regime. It was found that the number of mass transfer units, hence the point efficiency, is a strong function of surface tension. It was also found that only an efficiency model which includes the effect of surface tension is able to predict efficiencies correctly. Comparisons among three distillation systems showed that a surface tension positive system has a smaller liquid phase resistance and a higher point efficiency, mainly due to the surface renewal effect. Special equations are needed for predicting the point efficiency of such systems.

4.7 Nomenclature

a = effective interfacial area, m^2/m^3

b = constant

b = weir length per unit bubbling area, 1/m

C1, C2 = constant

D_E = eddy diffusivity for liquid mixing, m^2/s

D_G = Diffusion coefficient in vapour phase, m^2/s

E_{MV} = Murphree vapour-phase efficiency

E_{OG} = Murphree vapour-phase point efficiency

Fa, F_{bba} = F factor based on active area, $(kg/m)^{0.5}/s$

FP = flow parameter

Fs, F = superficial F factor, $(kg/m)^{0.5}/s$

F_{smax} = defined by Stichlmair (1978)

G = Vapour flow rate, kmol/s

g = acceleration of gravity, m/s^2

h_f = froth height, m

h_L = clear liquid height, m

h_W = weir height, m

k_G = gas film mass transfer coefficient, m/s

k_L = liquid film mass transfer coefficient, m/s

K_{OG} = overall mass transfer coefficient, m/s

L = Liquid flow rate, kmol/s

LPR = fraction of liquid phase resistance

MVC = more volatile component

m = slope of equilibrium line

N_G = number of gas phase transfer units

N_L = number of liquid phase transfer units

N_{OG} = number of overall gas phase transfer units

p = pitch of holes in sieve tray, m

Q_L = liquid flow rate, m^3/s

t_L = liquid residence time, s

u_s = vapour velocity based on bubbling area of tray, m/s

u_f = vapour velocity at flooding, m/s

W = weir length, m

x = mole fraction of MVC in liquid

y = mole fraction of MVC in vapour

y^* = mole fraction of MVC in vapour in equilibrium with liquid

y_n = mole fraction of MVC in vapour for tray above

y_{n-1} = mole fraction of MVC in vapour for tray below

Z_L = liquid flow path length, m

Greek Letters

σ = surface tension, N/m

λ = mG/L

μ_G = vapour viscosity, Ns/m^2

μ_L = liquid viscosity, Ns/m^2

ρ_G = vapour density, kg/m^3

ρ_L = liquid density, kg/m^3

ϕ = relative free area

Figure 4-1
Surface Tension as a Function of Compositions

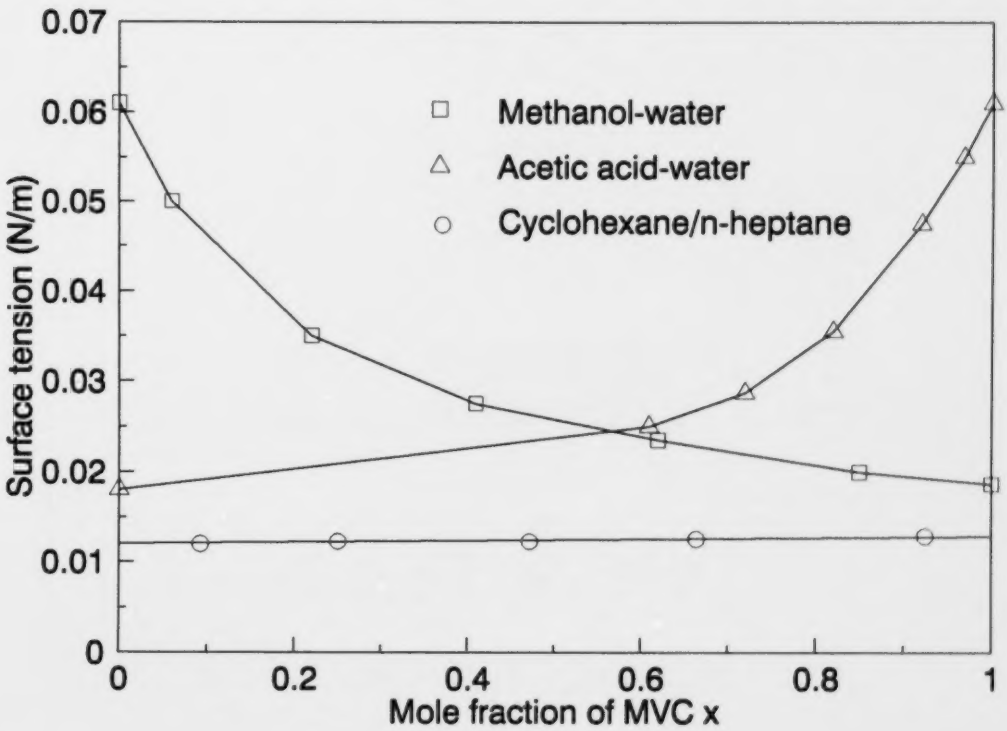

Figure 4-2
Point Efficiency as a Function of Compositions for
Cyclohexane/N-heptane System
(Sakata and Yanagi, 1979)

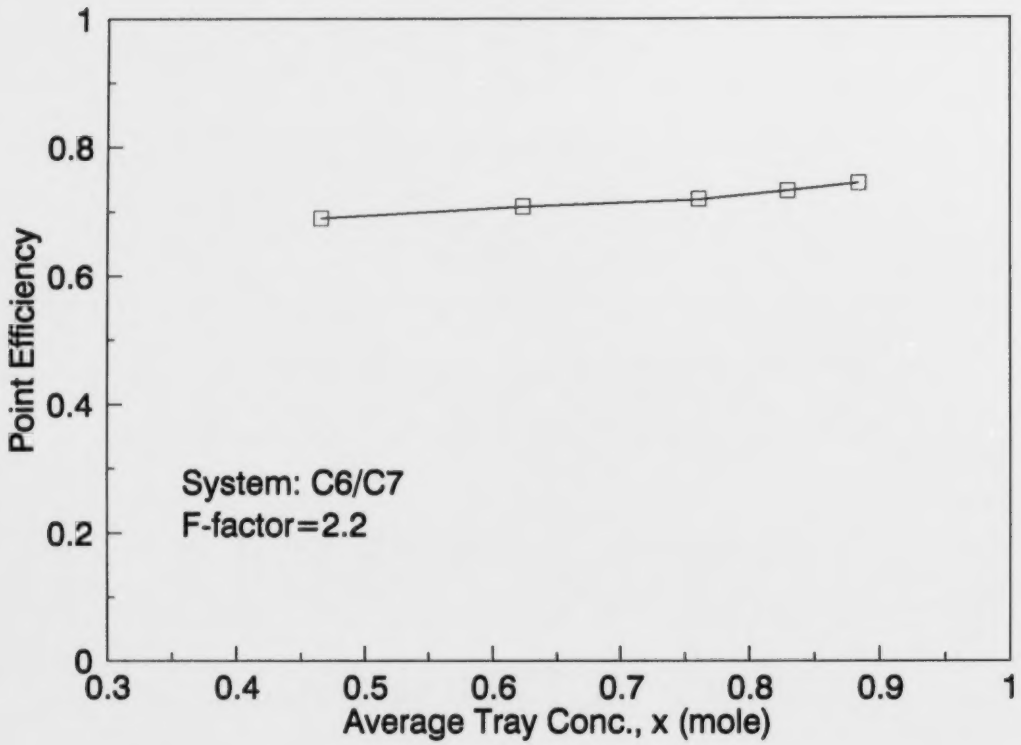

Figure 4-3
Point Efficiency as a Function of Compositions for Acetic Acid/Water System

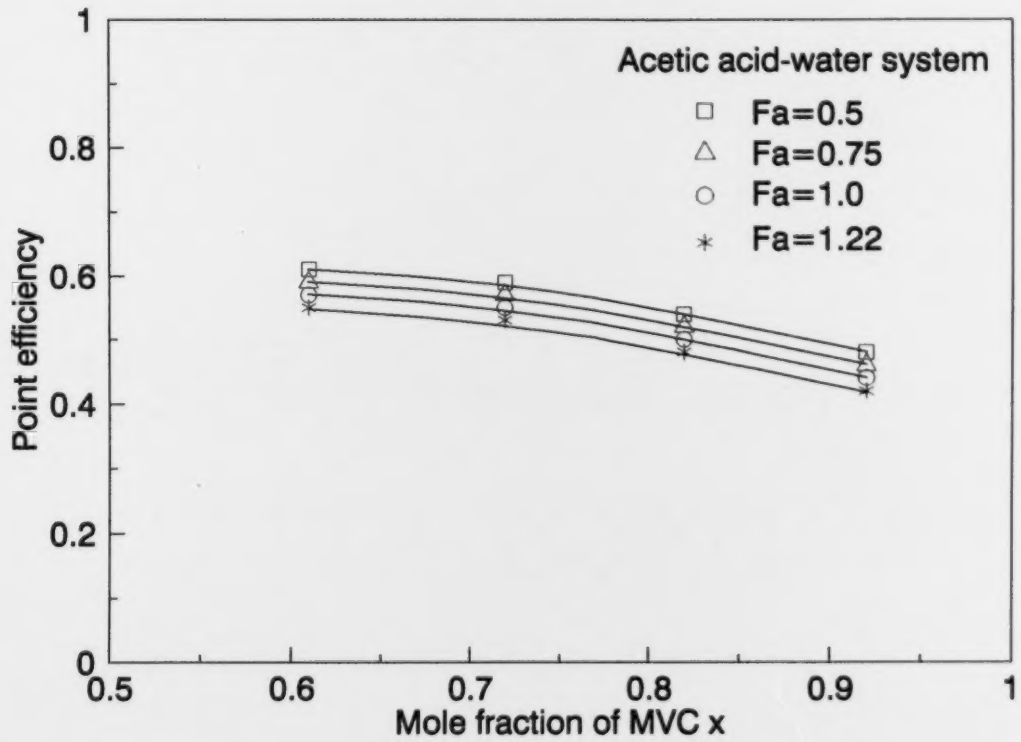

Figure 4-4

Point Efficiency as a Function of Compositions for Methanol/Water System

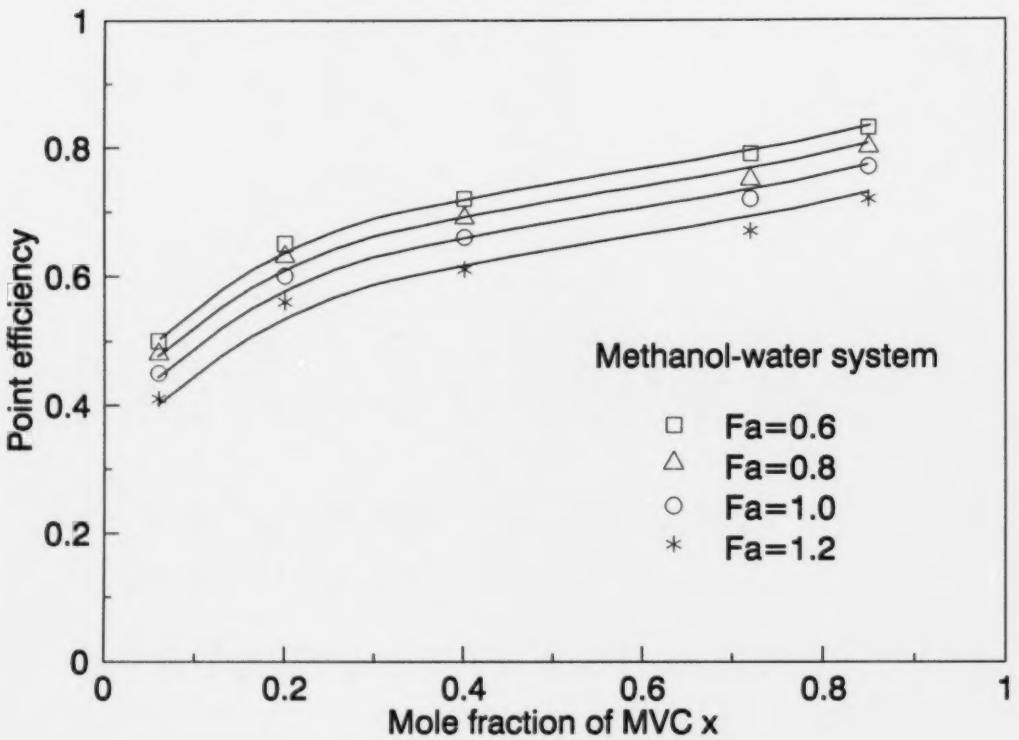

Figure 4-5
Number of Mass Transfer Units as a Function of Surface Tension for Three Systems

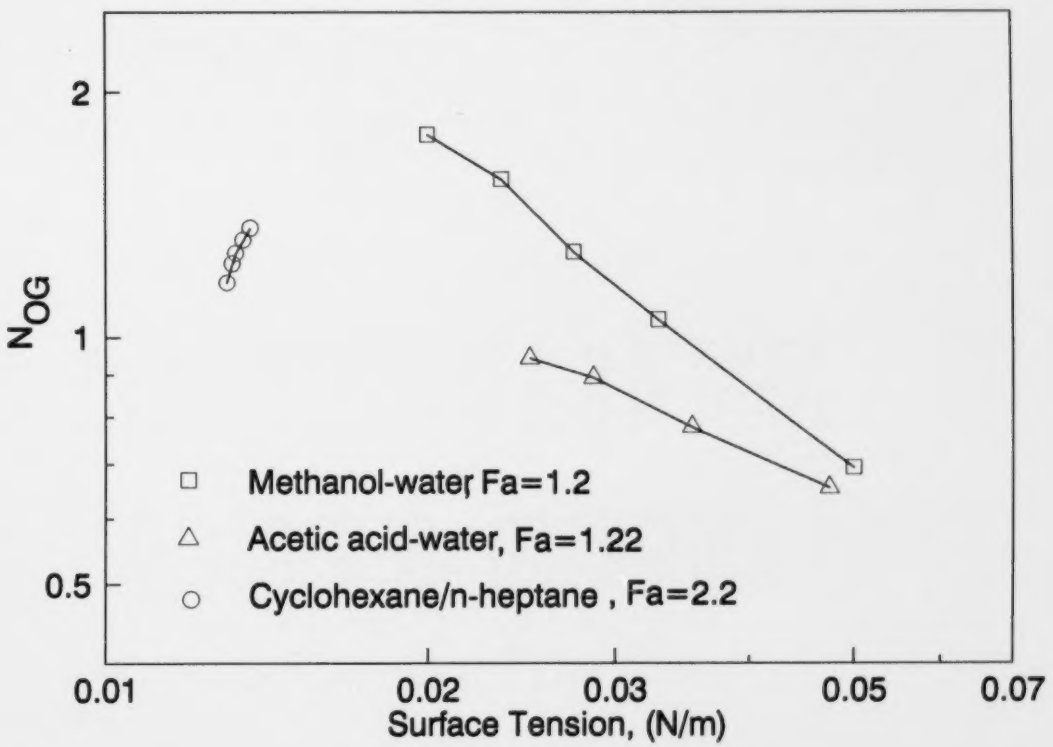

Figure 4-6

Number of Mass Transfer Units as a Function of Surface Tension for Cyclohexane/N-heptane System

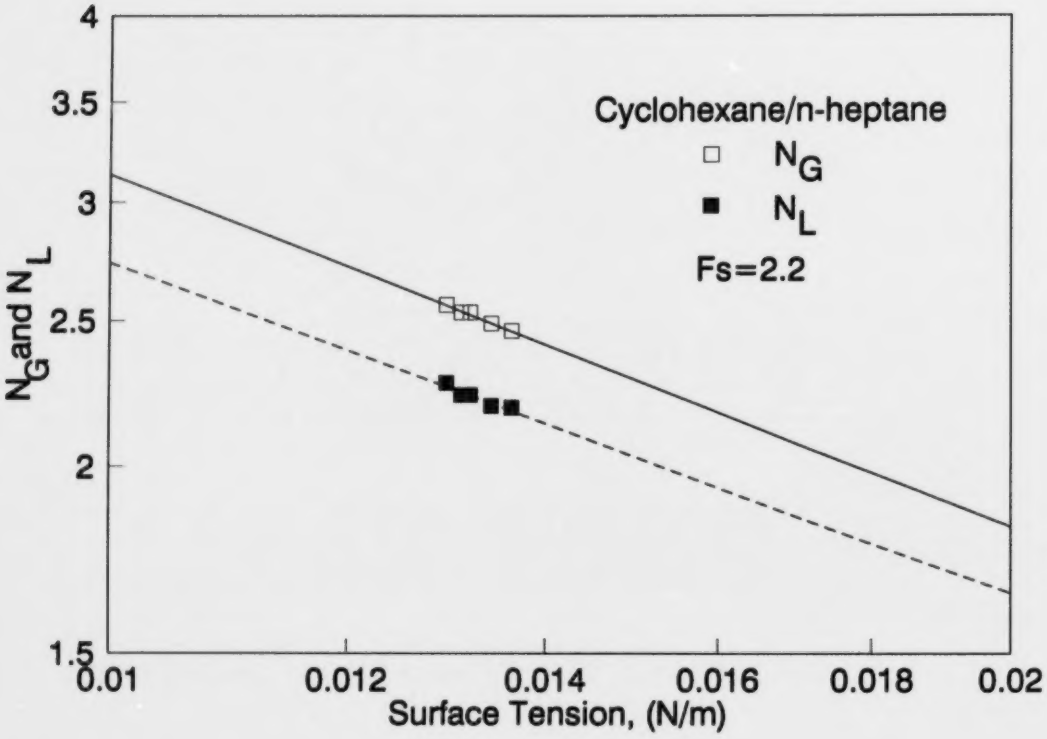

Figure 4-7
Number of Mass Transfer Units as a Function of Surface Tension for Acetic Acid/Water System

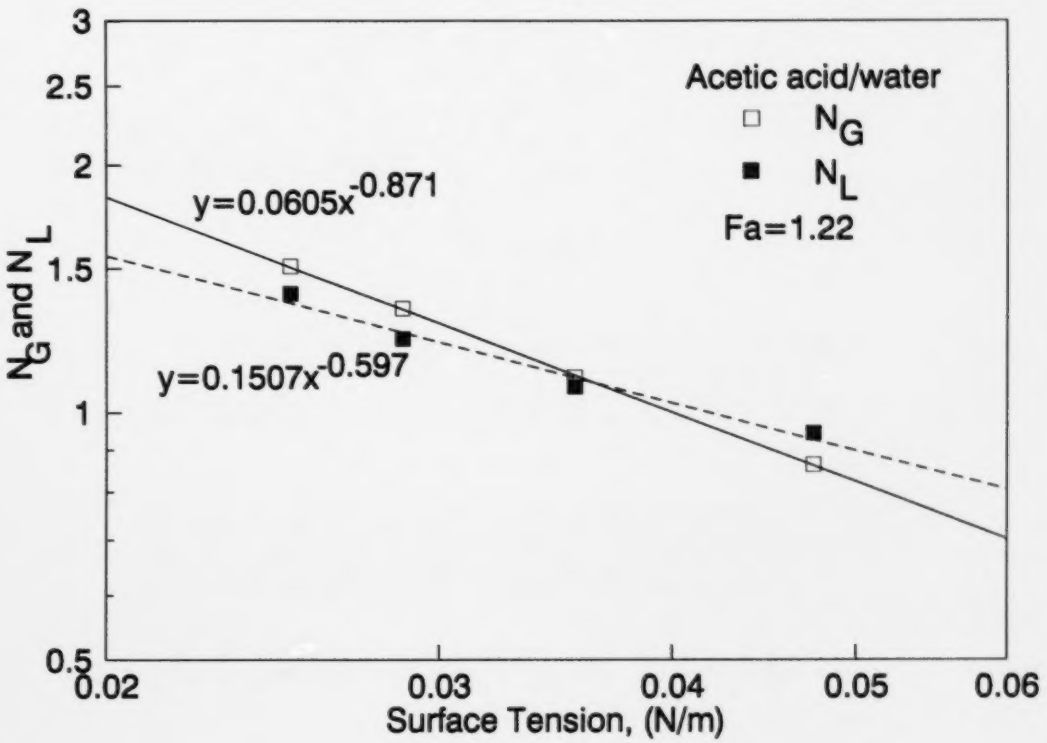

Figure 4-8
Number of Mass Transfer Units as a Function of Surface Tension for Methanol/Water System

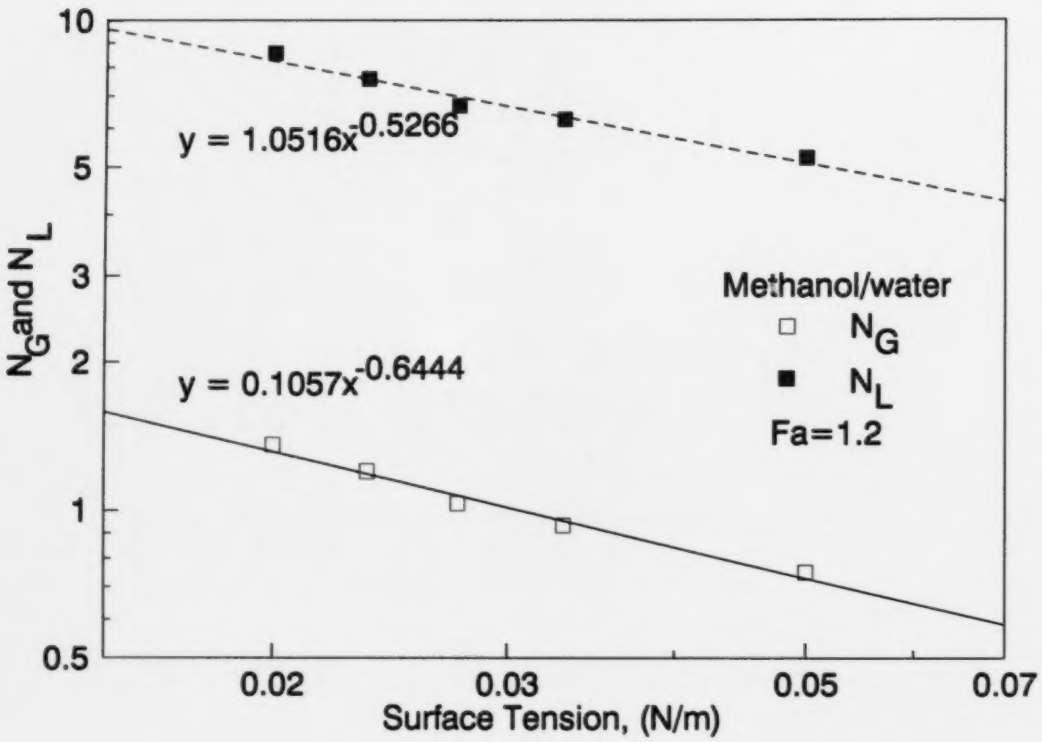

Figure 4-9
Comparison of Number of Liquid Phase
Mass Transfer Units for Three Systems

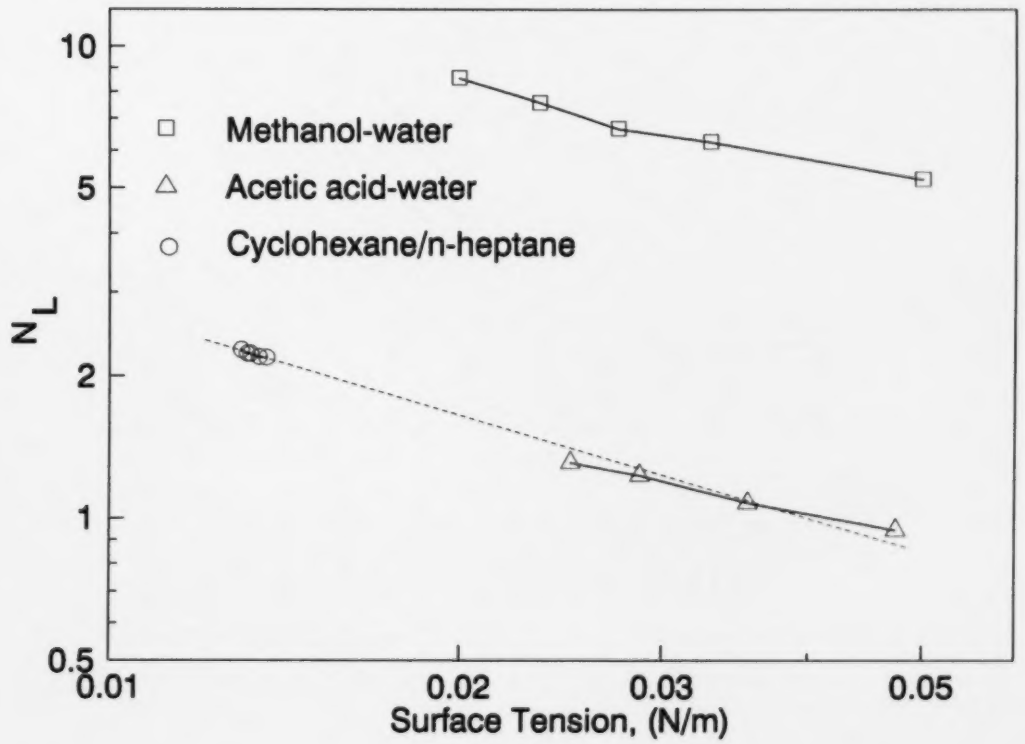

Figure 4-10
Comparison of LPR for Three Systems

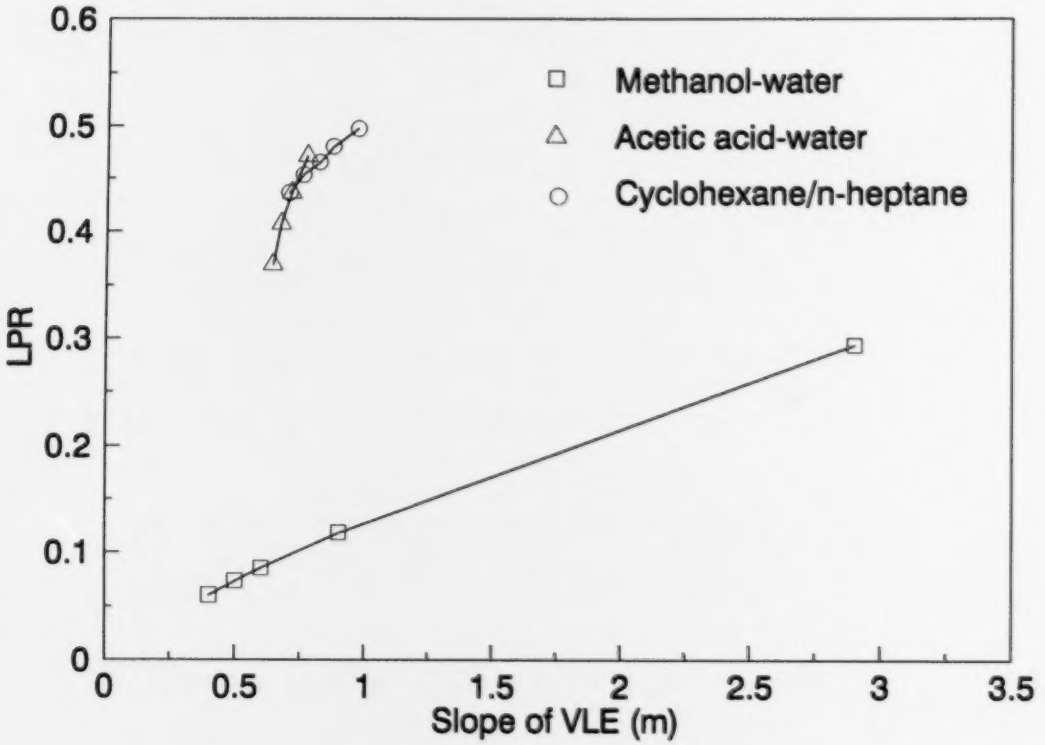

Figure 4-11

Comparison of Measured and Predicted Point Efficiency for Cyclohexane/N-heptane System

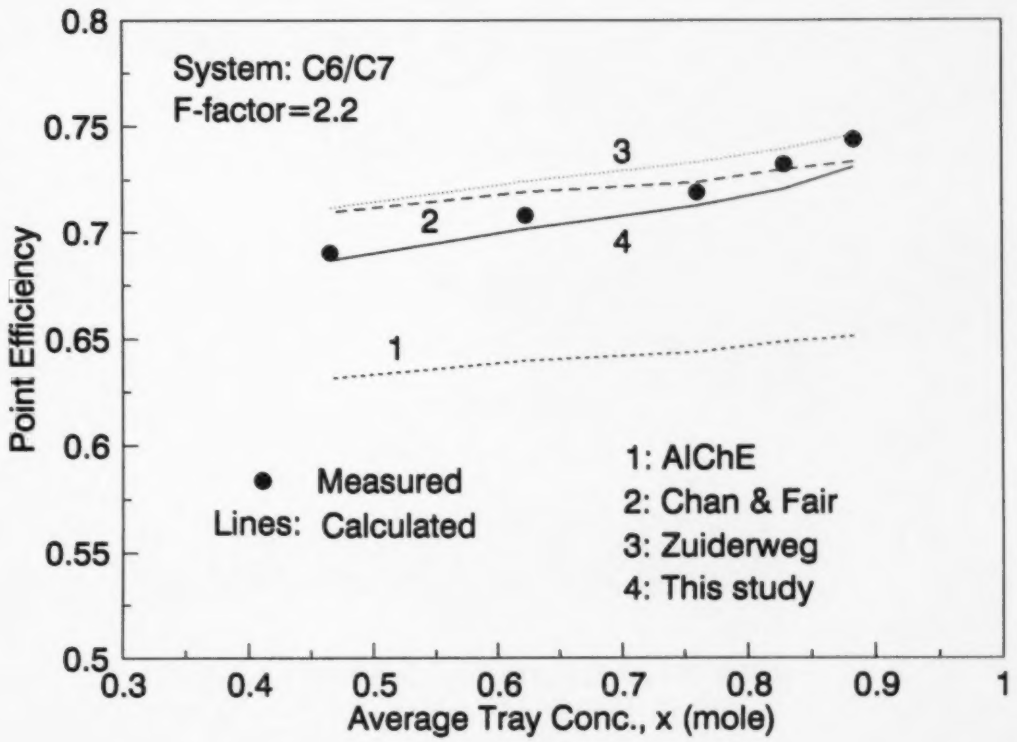

Figure 4-12
Comparison of Determined and Predicted N_G
for Cyclohexane/N-heptane System

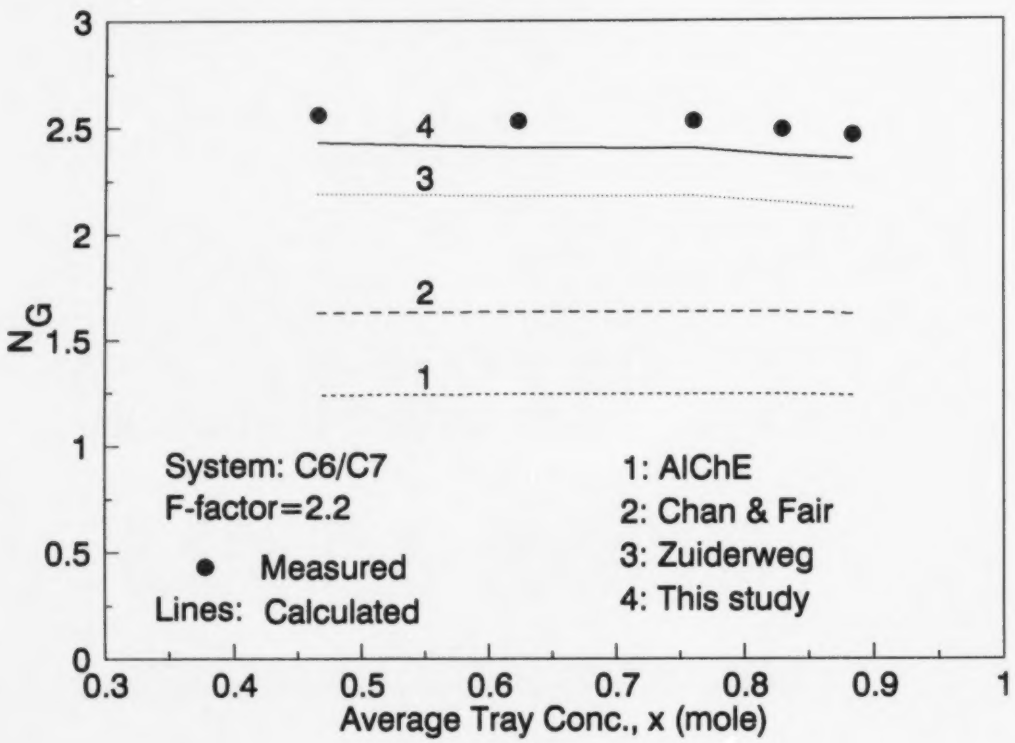

Figure 4-13
Comparison of Determined and Predicted N_L
for Cyclohexane/N-heptane System

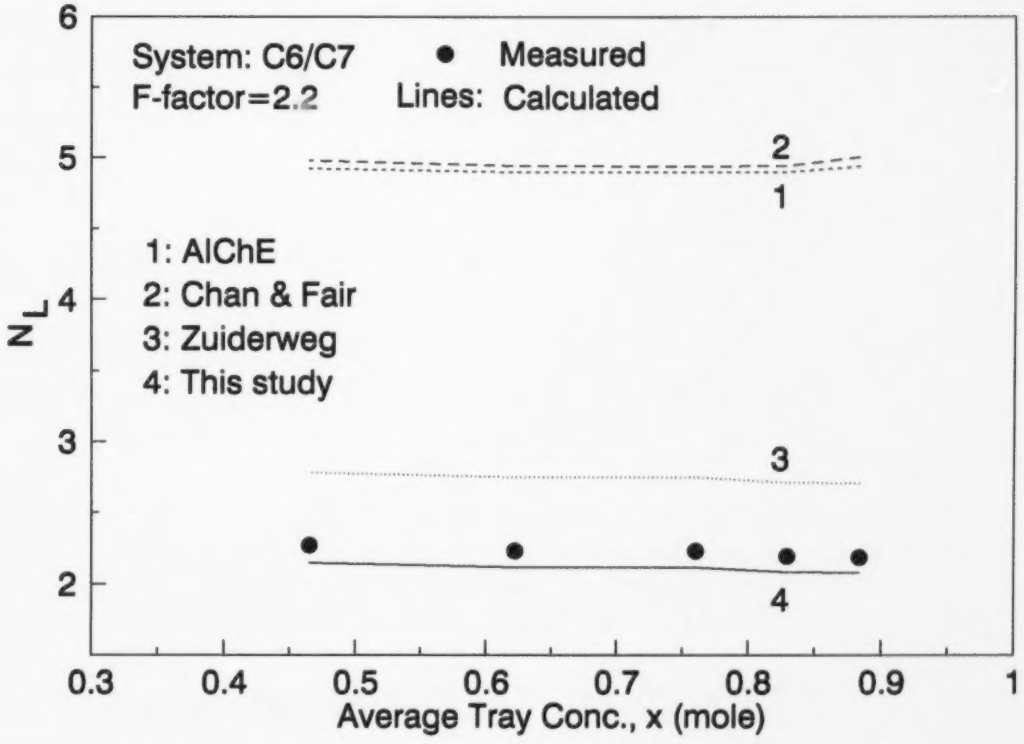

Figure 4-14
Comparison of Measured and Predicted Point Efficiency for Acetic Acid/Water System

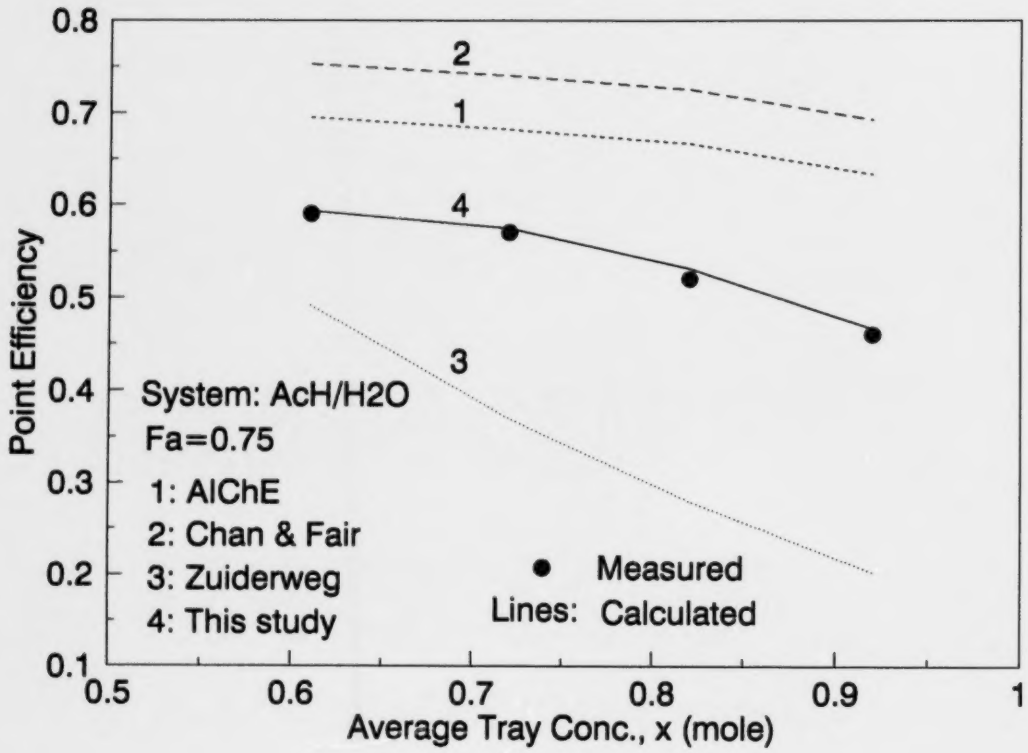

Figure 4-15
Comparison of Determined and Predicted N_G
for Acetic Acid/Water System

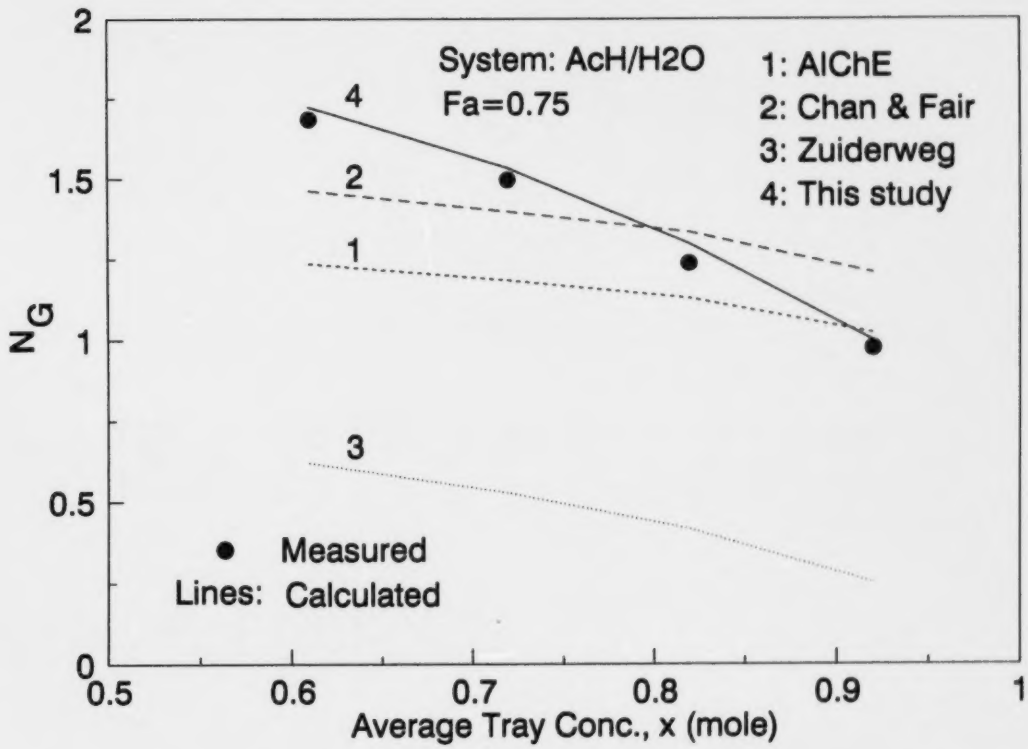

Figure 4-16
Comparison of Determined and Predicted N_L
for Acetic Acid/Water System

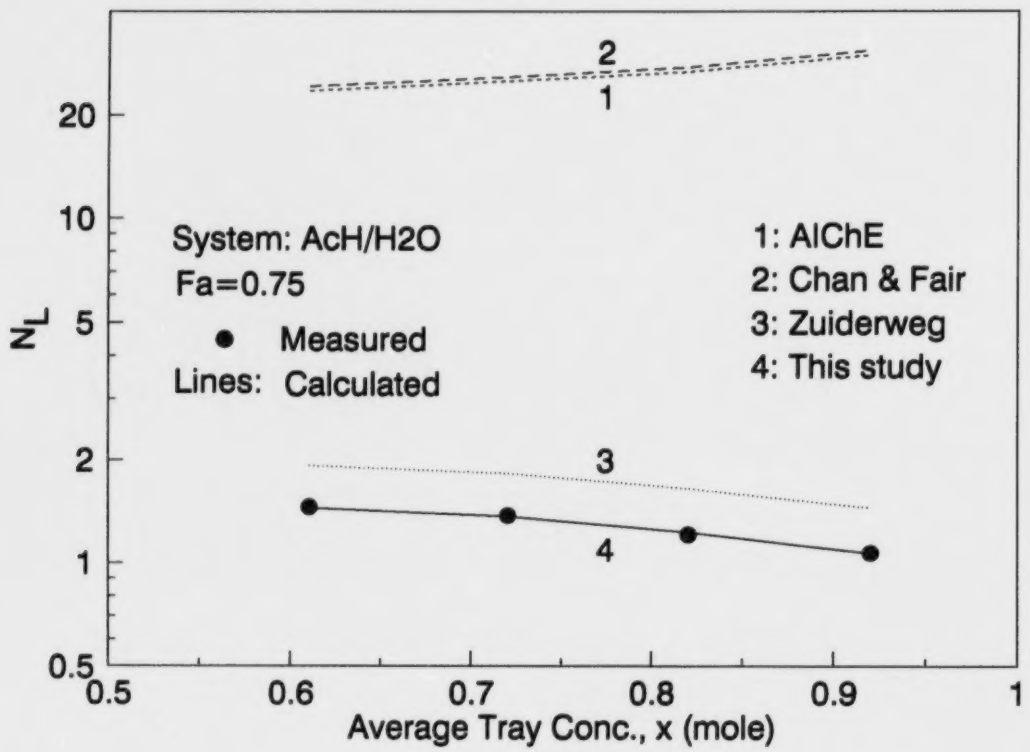

Figure 4-17
Comparison of Measured and Predicted Point Efficiency for Methanol/Water System

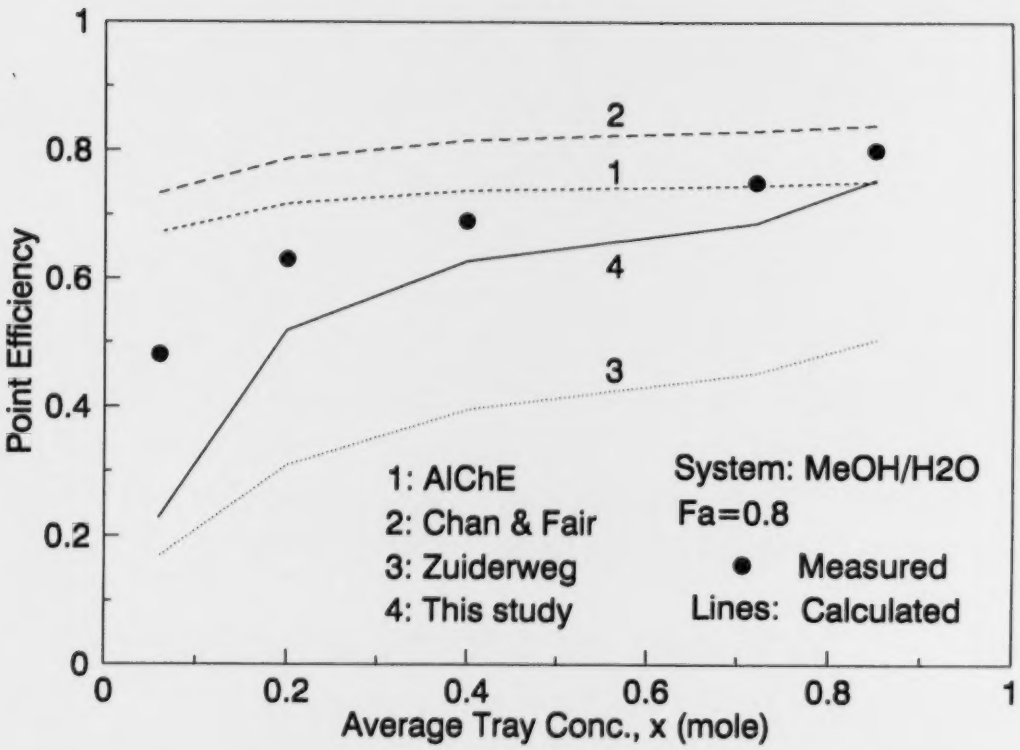

4.8 Literature Cited

Adamson, A.W., "Physical Chemistry of Surfaces," 4th Ed., John Wiley & Sons, New York (1982).

AIChE, "Bubble Tray Design Manual," New York (1958).

Bahari, E.P., Ph.D. Thesis, Univ. Birmingham (1955).

Bainbridge, G.S., Ph.D. Thesis, University of London (1964).

Bainbridge, G.S., and H. Sawistowski, "Surface Tension Effects in Sieve Plate Distillation Columns," Chem. Eng. Sci., **19**, 992 (1964).

Bennett, R.J., Ph.D. Thesis, Univ. Birmingham (1959).

Billet, R., S., Conrad, and C.M. Grubb, "Some aspects of the choice of distillation equipment," Inst. Chem. Engrs. Symp. Ser. **No. 32**, 5:111 (1969).

Chan, H., and J.R. Fair, "Prediction of point efficiencies on sieve trays," Ind. Eng. Chem. Proc. Des. Dev. **23**, 814 (1984).

De Goederen, C.W.J., "Distillation Tray Efficiency and Interfacial Area," Chem. Eng. Sci., **20**, 1115 (1965).

Dribika, M.M., and M.W. Biddulph, "Scaling-Up Distillation Efficiencies," AIChE J., **32** (9), 1864 (1986).

Ellis, S.R.M., and M.W. Biddulph, "The Effect of Surface Tension Characteristics on Plate Efficiencies," Trans. Inst. Chem. Engrs., **45**, T223 (1967).

Fane, A., and H. Swaistowski, "Surface Tension Effects in Sieve-Plate Distillation," Chem. Eng. Sci., **23**, 943 (1968).

Hofhuis, P.A.M., and F.J. Zuiderweg, "Sieve Plates: Dispersion Density and Flow Regimes," Inst. Chem. Engrs. Symp. Series No 56, 2.2/1 (1979).

Honorat, A., and O.C. Sandall, "Simultaneous Heat and Mass Transfer in a

Packed Binary Distillation Column," Chem. Eng. Sci., **33**, 635 (1978).

Hughmark, G.A., "Point Efficiencies for tray distillations," Chem. Eng. Prog. **61**(7), 97 (1965).

Hughmark, G.A., "Models for vapour-phase and liquid-phase mass transfer on distillation trays," AIChE J. **17**(6), 1295 (1971).

Jones, J.B., and C. Pyle, "Relative performance of sieve and bubble cap plates," Chem. Eng. Prog. **51**(9), 424 (1955).

Kalbassi, M.A., M.M. Dribika, M.W. Biddulph, S. Kler, and J.T. Lavin, "Sieve Tray Efficiencies in the Absence of Stagnant Zones," Inst. Chem. Engrs. Symp. Series No. 104, A511 (1987).

Kastanek, F., and G., Standart, "Studies in distillation xx," Sepn. Sci. **2**(4), 439 (1967).

Kayihan, F., O.C. Sandall, and D.A. Mellichamp, "Simultaneous Heat and Mass Transfer in Binary Distillation - 1," Chem. Eng. Sci., **30**, 1333 (1975).

Kayihan, F., O.C. Sandall, and D.A. Mellichamp, "Simultaneous Heat and Mass Transfer in Binary Distillation - 2," Chem. Eng. Sci., **32**, 747 (1977).

Kirschbaum, E., Chem.-Ing.-Tech. **34**, 283 (1962).

Lashmet, P.K., and S.Z. Szezepanski, "Efficiency uncertainty and distillation column overdesign factors," Ind. Eng. Chem. Proc. Des. Dev. **13**(2), 103 (1974).

Lockett, M.J., "Distillation Tray Fundamentals," Cambridge University Press, Cambridge (1986).

Lockett, M.J., and I.S. Ahmed, "Tray and Point Efficiencies from a 0.6 Meter Diameter Distillation Column," Chem. Eng. Res. Des., **61**, 110 (1983).

Mehta, V.D., and M.M. Sharma, "Effect of diffusivity on gas-side mass transfer coefficiencts," Chem. Eng. Sci. **21**, 361 (1966).

Moens, F.P., and R.G. Bos, "Surface Renewal Effects in Distillation," Chem. Eng. Sci., **27**, 403 (1972).

Moens, F.P., "The Effect of Composition and Driving Force on the Performance of Packed Distillation Columns - 1," Chem. Eng. Sci., **27**, 275 (1972).

National Research Council of the United States of America, "International Critical Tables of Numerical Data, Physics, Chemistry and Technology," McGraw-Hill, New York (1928).

Neuburg, H.J., and K.T. Chuang, "Mass transfer modelling for GS heavy water plants. 1: Point efficiency on GS sieve trays," Can. J. Chem. Eng. **60**, 504 (1982).

Norman, W.S., Int. Symp. on Distillation. Inst. Chem. Engrs., Brighton, Contribution to discussion, P.33 (1960).

Nutter, D.E., "Ammonia stripping efficiency studies," Paper 49c, AIChE 68th National Meeting, Houston, Texas (1972).

Reid, R.C., J.M. Prausnitz, and T.K. Sherwood, "The Properties of Gases and Liquids," McGraw Hill, New York (1958).

Ruckenstein, E., and O. Smigelschi, "On Thermal Effects in Rectification of Mixtures," Chem. Eng. Sci., **20**, 66 (1965).

Sakata, M., and Y. Yanagi, "Performance of a commercial-scale sieve tray," Inst. Chem. Engrs. Symp. Ser. **No. 56**, 3.2/21 (1979).

Sandall, O.C., and M.M. Dribika, "Simultaneous Heat and Mass Transfer for Multicomponent Distillation in Continuous Contact Equipment," Inst. Chem. Engrs. Symp. Series No. **56**, 3.2/21 (1979).

Sawistowski, H., "Surface-Tension-Induced Interfacial Convection and its Effects on Rates of Mass Transfer," Chem.-Ing.-Techn. **45**, 1093 (1973).

Sawistowski, H., G.S. Bainbridge, M.J. Stacey, and A. Theobald, Proc.

Symp. on Distillation, Chemical Industries Association, London (1968).

Smith, B.D., "Design of Equilibrium Stage Process," McGraw-Hill, New York, P547 (1963).

Yanagi, T., and M. Sakata, "Performance of a commercial-scale 14% hole area sieve tray," Ind. Eng. Chem. Proc. Des. Dev. **21**(4), 712 (1982).

Zuiderweg, F.J., "Marangoni Effect in Distillation of Alcohol-Water Mixtures," Chem. Eng. Res. Des., **61**, 388 (1983).

Zuiderweg, F.J., "Sieve Trays, a View of the State of the Art," Chem. Eng. Sci., **37**, 1441 (1982)

Zuiderweg, F.J., and A. Harmens, "The Influence of Surface Phenomena on the Performance of Distillation Columns," Chem. Eng. Sci., **9**, 89 (1958).

Zuiderweg, F.J., "Influence of the two-phase flow regimes on the separation performance of sieve plates," Int. Chem. Eng. **26**(1), 1-10 (1986).

Chapter 5

THE EFFECTS OF A SURFACE TENSION GRADIENT ON THE NUMBER OF MASS TRANSFER UNITS

5.1 Introduction

The importance of the effect of a surface tension gradient on tray efficiencies has been discussed in Chapter 4. It has been found that surface tension positive systems have higher mass transfer efficiencies due to the surface renewal effect (Chapter 4; Ellis and Biddulph, 1967; Berg, 1972). Despite this observation, the quantitative aspect of this surface renewal effect on the mass transfer efficiency has not been studied, especially regarding investigation of the mechanism of mass transfer in the presence of roll cells which are observed near the interfaces (Drinkenburg, 1987). An analysis of work studying the effect of a surface tension gradient on the tray efficiency suggests that currently proposed equations for describing this effect reflect the complex character of K_{OG} dependence on the magnitude of the surface tension gradient in a contradictory way. The enhancement factor of the rate of mass transfer due to the effects of a surface tension gradient has been estimated by Sawistowski (1973) to be on the order of 1.6 to 3.2 and by Zuiderweg (1975) to be 1.5 to 2.

Using data from large-scale columns, Zuiderweg (1983) compared the efficiency results from Fractionation Research Incorporated (FRI) reported by Sakata and Yanagi (1979) on the hydrocarbon system cyclohexane/n-heptane with the results of Lockett and Ahmed (1983) on the methanol/water system. This comparison was based on system transport properties and tray dimensions. The two sieve trays were reasonably large. Zuiderweg (1983)

related the efficiency enhancement to the Marangoni index (M) and concluded that Marangoni effects markedly increased the efficiency of the methanol/water system as compared with cyclohexane/n-heptane system. But his explanation was based on his efficiency model (Zuiderweg, 1982) which, as shown in Chapter 4, is generally unreliable. The new model obtained in Chapter 2 was also based on FRI results and showed good results for all systems included in this study except for the methanol/water system. Therefore, a new modified efficiency model including the effect of a surface tension gradient is needed for systems such as methanol/water.

In this study, the effect of a surface tension gradient on the mass transfer efficiency is analyzed. The enhancement factor due to this effect is estimated based on the penetration theory. A new quantitative model for calculating the enhancement factors would be developed, based on the comparison of experimental data obtained by Lockett and Ahmed (1983) for the methanol/water system with that of FRI data for the cyclohexane/n-heptane system (Sakata and Yanagi, 1979).

5.2 Theory

It is widely believed that, in positive systems, the surface tension gradient induced by the mass flux is a destabilizing parameter. As a result, spontaneous circulation flux called roll cells may be induced in both the vapour and liquid phases in the vicinity of the interface which, in fact, enforces liquid exchange in volumes of various concentrations between the interface and the phase bulk. The energy generated in these fluxes, due to the difference in surface tension between the interface and the phase bulk, is dissipated by friction caused by the movement of unit volumes as well as

by shape variations. In principle, the formation of roll cells or other forms of surface convection is possible both in the liquid and in the vapour phases, since the kinematic viscosities of the phases are defined by quantities of a single order of magnitude. However, in the liquid phase one should expect a higher degree of increase in mass transfer as a result of surface convection as compared with mass transfer caused by molecular diffusion, since the magnitude of the diffusion coefficient in the liquid phase is four orders of magnitude less than in the vapour phase. Brian et al. (1971) showed that in the presence of a surface tension gradient along a liquid film, mass transfer of a tracer in the liquid phase was intensified, but in the gas phase it remained unchanged. In Chapter 4, it was also found that only the N_L of a surface tension positive system is considerably larger than of other systems, while the N_G is similar for all systems. On this basis, one may assume that the surface tension gradient affects the rate of mass transfer considerably in the liquid phase, but does not affect the rate of mass transfer in the vapour phase.

To relate the liquid phase mass transfer coefficient to the surface tension gradient, an approach similar to that used to account for the density gradient effect on mass transfer (Link, 1972) will be used. A model of velocity distribution near the interface has to be assumed. Based on the observations in the space lab where there is no gravity (Drinkenburg, 1987), an idealized diagram of velocity distribution near the interface is proposed and shown in Figure 5-1. If there are no roll cells when the surface tension gradient is zero or small, the liquid phase mass transfer coefficient, k_L^0 , can be estimated by penetration theory. This is a common practice in the development of a mass transfer model. It means that liquid elements are

exposed into contact with the gas phase for the time t^0, given by the relation:

$$k_L^0 = \left(\frac{4D_L}{\pi t^0}\right)^{0.5} \qquad (1)$$

If the surface tension difference between the interface and the liquid bulk is sufficient due to mass flux during the exposure time t^0, then two-dimensional roll cells of the size d are formed within the liquid surface element as shown in Figure 5-1. If one assumes that the time needed to form the convective cells is much shorter than the contact time t^0 of the liquid surface element with the gas phase, the velocity u of the surface layer of liquid can be considered constant. If the thickness of the diffusion layer δ is substantially less than the cell size d, a piston flow of liquid along the whole length d can be assumed (see Figure 5-1). The average mass transfer coefficient, k_L, can be obtained by:

$$k_L = \frac{1}{t^0 d} \int_0^{t^0} dt \int_0^d k_L' \, dx \qquad (2)$$

where k_L' is the local mass transfer coefficient, and can be obtained from the solution of the following equation if diffusion in x-direction can be neglected.

$$\frac{\partial c}{\partial t_s} = D_L \frac{\partial^2 c}{\partial y^2} \qquad (3)$$

with the boundary conditions:

$$c = c^0 \text{ at } y = 0, \; t_s \geq 0$$

$$c = c_\infty \text{ at } y = \infty, \; t_s \geq 0$$

$$c = c_\infty \text{ at } y = 0, \; t_s = 0$$

By solving equation (3), k_L' is determined by the local value of exposure time t_s:

$$k_L' = \left(\frac{D_L}{\pi t_s}\right)^{0.5} \qquad (4)$$

When $t < d/u$:

$$t_s = x/u \qquad \text{for } x < tu \qquad (5)$$

$$t_s = t \qquad \text{for } x \geq tu \qquad (6)$$

Substituting equations (5) and (6) into equation (4) gives:

$$k_L' = \left(\frac{D_L u}{\pi x}\right)^{0.5} \qquad (7), \quad \text{for } x < tu$$

$$k_L' = \left(\frac{D_L}{\pi t}\right)^{0.5} \qquad (8), \quad \text{for } x \geq tu$$

When $t \geq d/u$:

$$t_s = x/u \qquad (9)$$

Substituting equation (9) into equation (4) gives:

$$k_L' = \left(\frac{D_L u}{\pi x}\right)^{0.5} \qquad (10)$$

The spatially averaged instantaneous mass transfer coefficients can be calculated from the relation:

$$\bar{k}_L' = \frac{1}{d} \int_0^d k_L' \, dx \qquad (11)$$

Substituting equations (7) and (8) into equation (11) for $t < d/u$ gives:

$$\bar{k}_L' = \frac{1}{d} \left[\int_0^{tu} (D_L u/\pi x)^{1/2} dx + \int_{tu}^{d} (D_L/\pi t)^{1/2} dx \right] \qquad (12)$$

The obtained result from equation (12) is:

$$\bar{k}_L' = (u/d)(D_L t/\pi)^{1/2} + (D_L/\pi t)^{1/2} \qquad (13)$$

Substituting equation (10) into equation (11) for $t \geq d/u$ gives:

$$\bar{k}_L' = \frac{1}{d} \int_0^d (D_L u/\pi x) dx = 2 \, (D_L u/\pi d)^{1/2} \qquad (14)$$

Taking the time average for $t^0 < d/u$ gives:

$$k_L = \frac{1}{t^0} \int_0^{t^0} \left[(u/d)(D_L t/\pi)^{1/2} + (D_L/\pi t)^{1/2} \right] dt \qquad (15)$$

The result from equation (15) is :

$$k_L = k_L^0 \left(1 + \frac{t^0 u}{3d} \right) \qquad (16)$$

where k_L^0 is given by equation (1).

Taking the time average for $t^0 \geq d/u$ gives:

$$k_L = \frac{1}{t^0} \int_0^{d/u} \left[(u/d)(D_L t/\pi)^{1/2} + (D_L/\pi t)^{1/2} \right] dt$$

$$+ \frac{1}{t^0} \int_{d/u}^{t^0} 2(D_L u/\pi d) dt \qquad (17)$$

The result from equation (17) is:

$$k_L = k_L^0 \left[\left(\frac{ut^0}{d}\right)^{1/2} + 1/3 \left(\frac{d}{ut^0}\right)^{1/2} \right] \qquad (18)$$

Let $(t^0 u/d) = \beta$, when $\beta < 1$, equation (16) becomes:

$$\phi = k_L/k_L^0 = 1 + \beta/3 \qquad (19)$$

And $\beta \geq 1$, equation (18) becomes:

$$\phi = k_L/k_L^0 = \beta^{1/2} + \frac{1}{3} \beta^{-1/2} \qquad (20)$$

where ϕ is the liquid phase mass transfer enhancement factor. It can be seen that when enhancement factor ϕ is less than 1.333, equation (19) should be used, and when ϕ is larger than 1.3333, equation (20) should be used.

The problem is not solved so far because β in equations (19) and (20) is unknown. The roll cell size (d) and velocity (u) may be obtained numerically by solving the two-dimensional Navier-Stokes equations governing the convection flow near the interface. However, the contact time t^0 of liquid elements is unknown. The approach taken in this study is to obtain

empirical equations for ϕ. It has been known that ϕ, hence β, is a function of the surface tension gradient between the interface and the phase bulk.

5.3 Experimental Tray Efficiency Data

Lockett and Ahmed (1983) reported efficiency data determined in a semi-commercial column with the methanol/water system. The experimental data were carefully measured on a 0.59 meter column equipped with sieve trays with 4 mm holes and 9.25% open area. A concentration range of about 5 to 45 mol% methanol was covered in the experiments. Their reported efficiencies at F_s=1.54 are shown in Figure 5-2. The average measured froth height was 0.11 meter.

A new efficiency model has been obtained in Chapter 2, based on the efficiency data of the cyclohexane/n-heptane system measured by Fractionation Research Inc. (Sakata and Yanagi, 1979) in a 1.20 meter column. This model fits well with the experimental data on hydrocarbon systems (Chapter 2). However, when this model was applied to the methanol/water system in the 0.59 meter column (Lockett and Ahmed, 1983), the model significantly under-predicted the efficiency (see Figure 5-2). Table 5-1 compares the dimensions of columns and physical properties used in investigations by Lockett and Ahmed (1983) with those used by Sakata and Yanagi (1979). Comparing the two columns, one would expect a low efficiency for the 0.59 meter column because of the longer specific weir length and higher open area. Although the hole size in the 0.59 meter column was smaller, there is no indication that this would influence the tray efficiency positively (Kreis and Raab, 1979). Regarding the physical properties of the two systems, both systems have about the same average

transport properties except for surface tension. The surface tension of the methanol/water system is much larger than that of the cyclohexane/n-heptane system. This should result in a lower efficiency for the methanol/water system (Chapter 4). Because of the higher surface tension of this system, the new model gives a low predicted efficiency (see Figure 5-2). The measured froth height of the methanol/water system is somewhat similar to that of the cyclohexane/n-heptane system. Therefore, the effects of the surface tension gradient on froth height and interfacial area can be excluded. Based on above discussions, the large efficiency of the methanol/water system is apparently due to the effects of the surface tension gradient.

5.4 The Marangoni-Index

There are various ways to account for the effects of a surface tension gradient on the rate of mass transfer. Kalbassi et al. (1986) used the Marangoni stabilizing index M_0 calculated from equation (21), a measure of surface renewal effects, to interpret their experimental results.

$$M_0 = (y - y^*) \frac{d\sigma}{dx} \qquad (21)$$

Hovestreydt (1963) and Moens (1972) suggested employing the "M-index" as a quantitative variable to study the effects of a surface tension gradient on the rate of mass transfer.

$$M_1 = (x - x^*) \frac{d\sigma}{dx} \qquad (22)$$

where $(x-x^*)$ represents the mass transfer driving force and $(d\sigma/dx)$ the change of the surface tension with concentration. Zuiderweg (1983) used equation (22) in analysis of Lockett and Ahmed's results (1983). The

calculated M_1 values for the methanol/water system as a function of concentration are shown in Figure 5-3. As discussed in the theory section, the roll cell size (d) and velocity (u) are related to the surface tension difference between the interface and the phase bulk. This means that one should use M_2 defined by equation (23) instead of equation (22) to account for the effects of the surface tension gradient.

$$M_2 = (x - x_i) \frac{d\sigma}{dx} \qquad (23)$$

where x_i is the concentration at the interface, x concentration at the phase bulk. As a result, M_2 represents the surface tension difference between the interface and the phase bulk. M_2 can be easily related to M_1 by using the following equations:

$$M_2 = \frac{\rho_G \, k_G \, m \, M_1}{\rho_L k_L^0 + \rho_G k_G m} = \frac{M_1}{1 + (\rho_L k_L^0 / \rho_G k_G m)} = \frac{B M_1}{1 + B} \qquad (24)$$

$$B = \frac{m \, k_G \, \rho_G}{k_L^0 \, \rho_L} \qquad (25)$$

where B represents the ratio of the separate mass transfer resistances as Biot number in heat transfer process. The ratio, (k_G/k_L^0), can be obtained by using the penetration theory as suggested by many authors (Calderbamk and Pereira, 1977; Stichlmair, 1978; Neuburg and Chaung, 1982; Lockett and Uddin, 1980; Dribika and Biddulph, 1986):

$$k_G/k_L^0 = (D_G/D_L)^{0.5} \qquad (26)$$

Substituting equation (26) into equation (25) gives:

$$B = (m\rho_G/\rho_L)(D_G/D_L)^{0.5} \qquad (27)$$

The calculated values of M_2 are shown in Figure 5-3. On a cross flow tray the M_2 values are even higher than in a single equilibrium step.

Accordingly, the M_2 has been corrected for cross flow effects by the multiplication with the Lewis Case 1 ratio of (E_{MV}/E_{OG}) to obtain M_3 as suggested by Zuiderweg (1983). The obtained M_3 values are shown in Figure 5-4 and will be used in the analysis of the effects of a surface tension gradient on the rate of mass transfer in cross flow trays.

5.5 Enhancement Factor ϕ

The enhancement of the mass transfer rate by the effects of a surface tension gradient is defined by the enhancement factor ϕ:

$$\phi = (k_L/k_L^0) = (a'k_L t_L)/(a'k_L^0 t_L) = N_L/N_L^0 \qquad (28)$$

where N_L^0 is the number of liquid phase mass transfer units without a surface tension gradient, N_L with a surface tension gradient. N_L^0 can be calculated from equations obtained in Chapter 2. N_L can be obtained from calculated N_G and obtained N_{OG} by equation (29):

$$N_L = (mN_G N_{OG})/(N_G - N_{OG}) \qquad (29)$$

where N_G is calculated from equations obtained in Chapter 2, and N_{OG} can be obtained from the measured point efficiency:

$$N_{OG} = \ln\left(\frac{1}{1-E_{OG}} \right) \qquad (30)$$

The results are shown in Figures 5-5 and 5-6 as functions of concentration.

5.6 Parameter β

As shown in Figure 5-6, the enhancement factor ϕ is larger than 1.333 for the concentration range involved. This means that β is larger than 1 and equation (20) should be used. If it is assumed that $\beta=(aM_3^b)^2$, then equation (20) becomes:

$$\phi = aM_3^b + \frac{1}{3aM_3^b} \qquad (31)$$

Coefficients a and b can be found by fitting equation (31) to the obtained enhancement factor shown in Figure 5-6. The values of a and b have been found to be:

$$a = 27400,\ b = 1.30$$

Then equation (31) becomes:

$$\phi = (10000M_3/3.856)^{1.3} + 1/3\ (3.856/10000M_3)^{1.3} \qquad (32)$$

Figure 5-7 shows how equation (32) fits with the obtained enhancement factor. Figure 5-8 compares the calculated and measured point efficiencies for the methanol/water system using the new model. It can be seen from Figure 5-8 that the new model fits the measured point efficiency very well.

The enhancement factor ϕ is expected to be less in practical distillation at partial reflux because the driving force and M_3 become smaller, and hence there is a decrease in the tray efficiency. This loss in the mass transfer enhancement explains the low efficiency in the partial reflux distillation of the methanol/water system reported by van der Veen et al. (1971). Because the surface renewal effect enhances k_L only, the overall effect on efficiency is dependent on the slope of the equilibrium line (m). For example, if a system has a very small m, the enhancement of k_L has little effect on the N_{OG} and efficiency, no matter how strong the surface renewal effect is. Because the methanol/water system at the low concentration range has a larger m than other systems, the surface renewal effect is more evident in this system.

It should be noted that equation (32) is good only for cases where M_3 is larger than 3.856E-4. For hydrocarbon systems, for example, the

n-heptane/toluene system, M_3 value is about 10-20 times less than that of the methanol/water system. Consequently, equation (32) should not be used. It can also be concluded that the enhancement factor ϕ for hydrocarbon systems will be much less than 1.33. The correlations of ϕ for hydrocarbon systems can also be obtained when experimental data are available. Furthermore, equation (19) should be used to develop such correlations.

5.7 Conclusions

The high efficiency of the methanol/water system at total reflux is most probably due to its large surface tension gradient. It has been shown that the surface tension difference between the interface and the phase bulk can reduce the liquid phase mass transfer resistance by resulting in a convection flow near the interface. New correlations have been obtained for estimating the mass transfer enhancement from the surface tension gradient based on experimental data obtained in semi-commercial columns.

When systems have M-index (M_3) values larger than 3.8E-4, the correlations obtained in this study should be used to calculate the N_L values for such systems. For other systems, the models obtained in Chapter 2 can be used directly. It is expected that the combination of new correlations and new models will predict point efficiencies more accurately than through any previous models and that these models can be used in the design of industrial distillation columns.

5.8 Nomenclature

a = constant

a' = effective interfacial area, 1/m

b = constant

B = ratio of separate phase mass transfer resistance

c = concentration, mole/m^3

d = roll cell size, m

D_G = Diffusion coefficient in vapour phase, m^2/s

D_L = Diffusion coefficient in liquid phase, m^2/s

E_{MV} = Murphree vapour-phase efficiency

E_{OG} = Murphree vapour-phase point efficiency

Fs = superficial F factor, $(kg/m)^{0.5}/s$

k_G = gas film mass transfer coefficient, m/s

k_L = liquid phase mass transfer coefficient, m/s

k_L' = local liquid phase mass transfer coefficient, m/s

$\bar{k}_L'$ = average liquid phase mass transfer coefficient, m/s

k_L^0 = liquid phase mass transfer coefficient, m/s

K_{OG} = overall mass transfer coefficient, m/s

M_0 = M-index, defined by equation (21), N/m

M_1 = M-index, defined by equation (22), N/m

M_2 = M-index, defined by equation (23), N/m

$M_3 = M_2(E_{MV}/E_{OG})$, M-index used in this study, N/m

m = slope of equilibrium line

N_G = number of gas phase transfer units

N_L = number of liquid phase transfer units

N_{OG} = number of overall gas phase transfer units

t^0 = liquid exposure time, s

t = time, s

u = velocity, m/s

x = mole fraction of more volatile component in liquid

x^* = mole fraction of more volatile component in liquid equilibrium with vapour

x_i = mole fraction of more volatile component in liquid at interface

y = mole fraction of more volatile component in vapour

y^* = mole fraction of more volatile component in vapour equilibrium with liquid

Greek Letters

β = $t^0 u/d$

ρ_G = vapour density, kg/m^3

ρ_L = liquid density, kg/m^3

σ = surface tension, N/m

ϕ = enhancement factor

Table 5-1

Comparison of Trays and Physical Properties

	Lockett and Ahmed	FRI
Column diamter (m)	0.59	1.20
Weir length (m)	0.457	0.94
Specific weir length (m)	2.37	1.09
Weir height (m)	0.05	0.05
Liquid flow path length (m)	0.374	0.76
Active area (m^2)	0.20	0.859
Hole area (m^2)	0.0185	0.0715
Open hole area %	9.25	8.32
Hole diamter (mm)	4.8	12.7
Hole pitch (mm)	12.7	38.1
Tray spacing (m)	0.6	0.61
System	MeOH/Water	C6/C7
Vapour density (kg/m^3)	1.0-0.7	1.1
Liquid density (kg/m^3)	925-828	700
Liquid viscosity (mPas)	0.30	0.37
Surface tension (mN/m)	27.5-53	18.5
Liquid diffusivity (m^2/s)	1.8E-9	3.5E-9
Vapour diffusivity (m^2/s)	2.0E-5	1.6E-5
Slope of equilibrium line	3.3-0.6	0.7

Figure 5-1
Sketch of Roll Cells

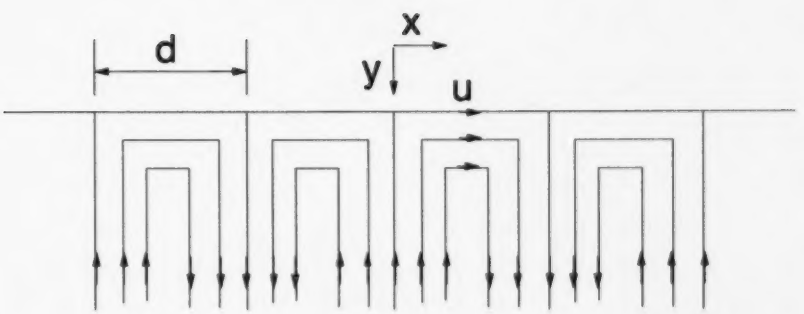

Figure 5-2
Comparison of Measured and Predicted Efficiency
(Lockett and Ahmed, 1983)

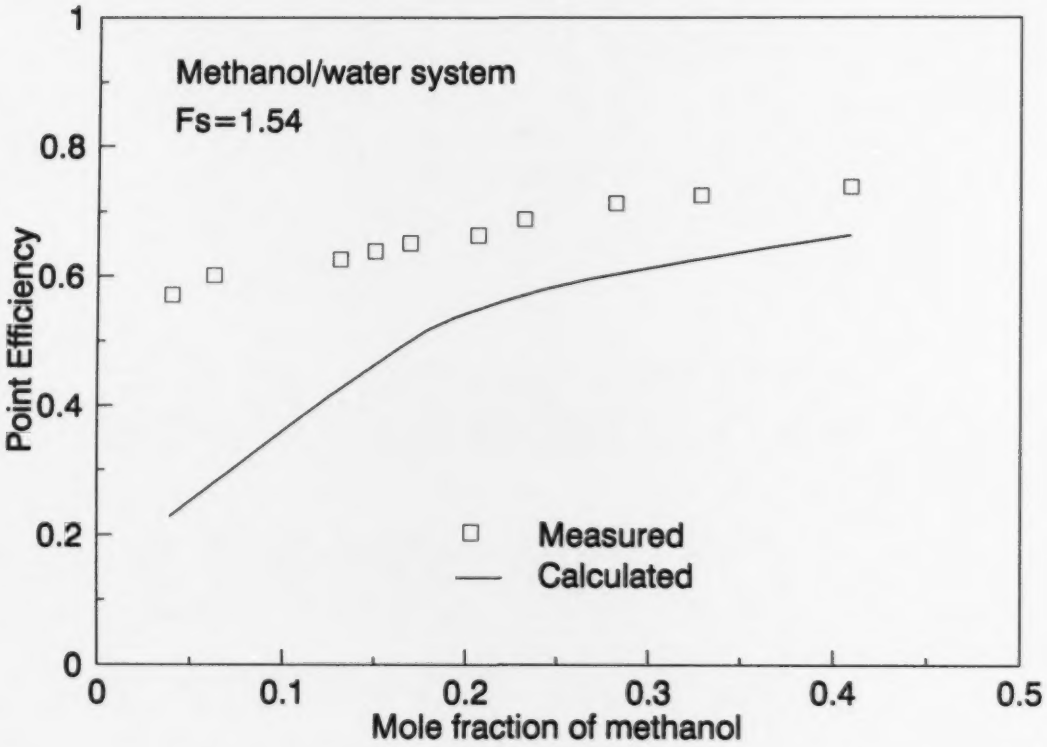

Figure 5-3
Comparison of Various M-index
(Methanol/water system)

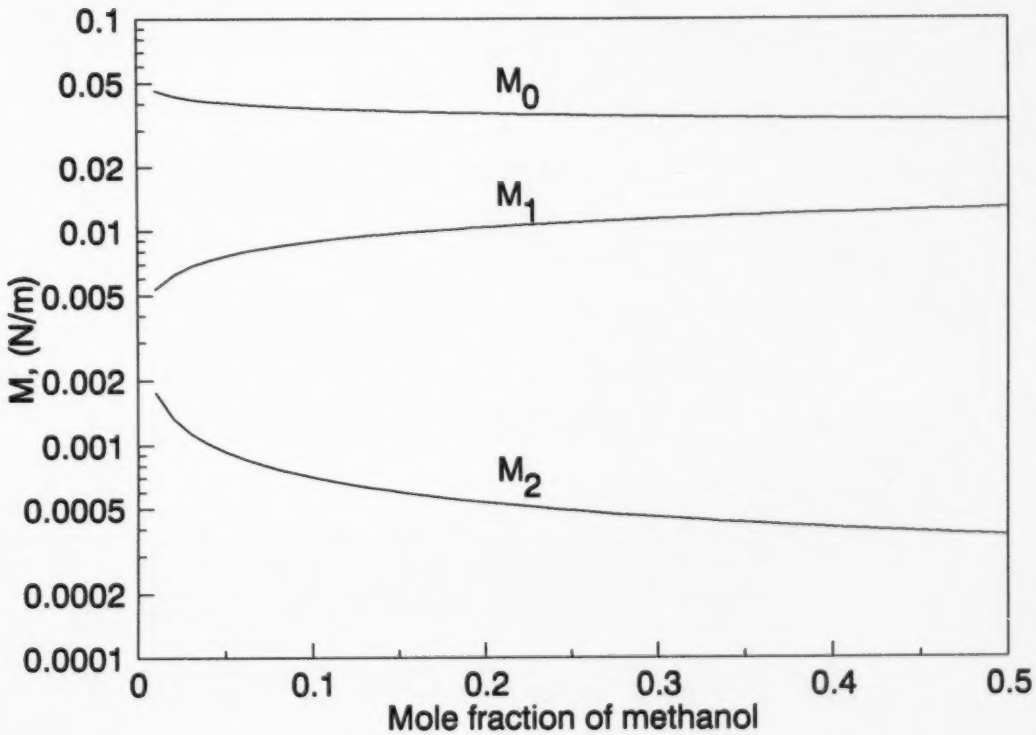

Figure 5-4
M-index Used in This Study
(Methanol/water system)

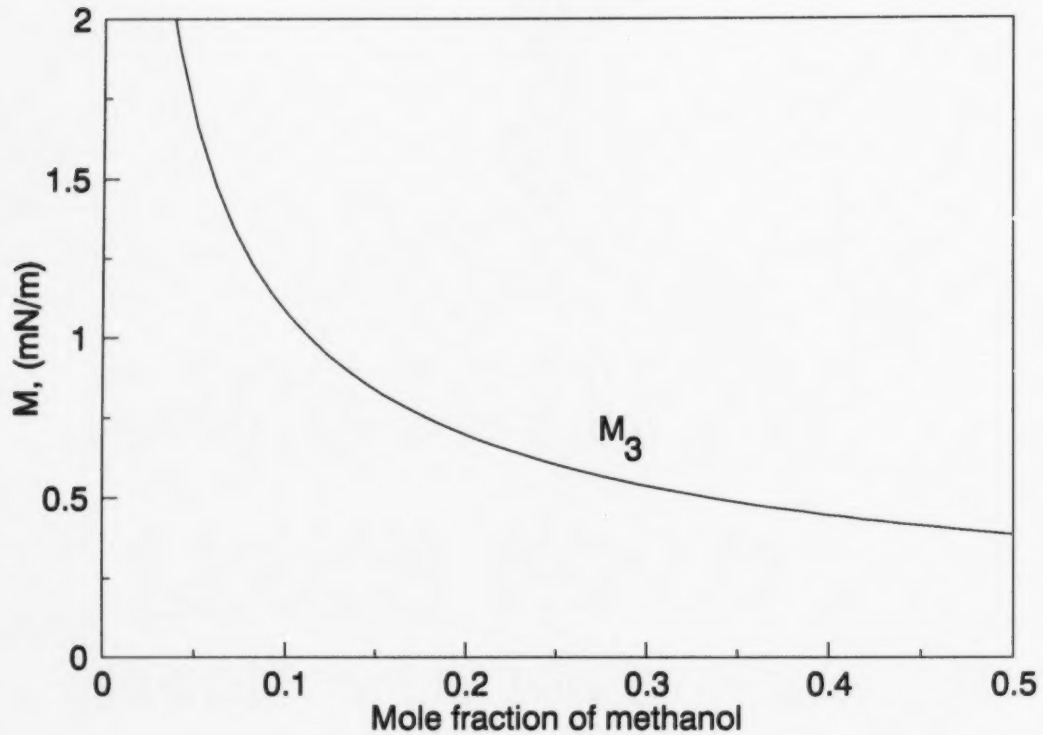

Figure 5-5

Comparison of Number of Mass Transfer Units
(Methanol/water system)

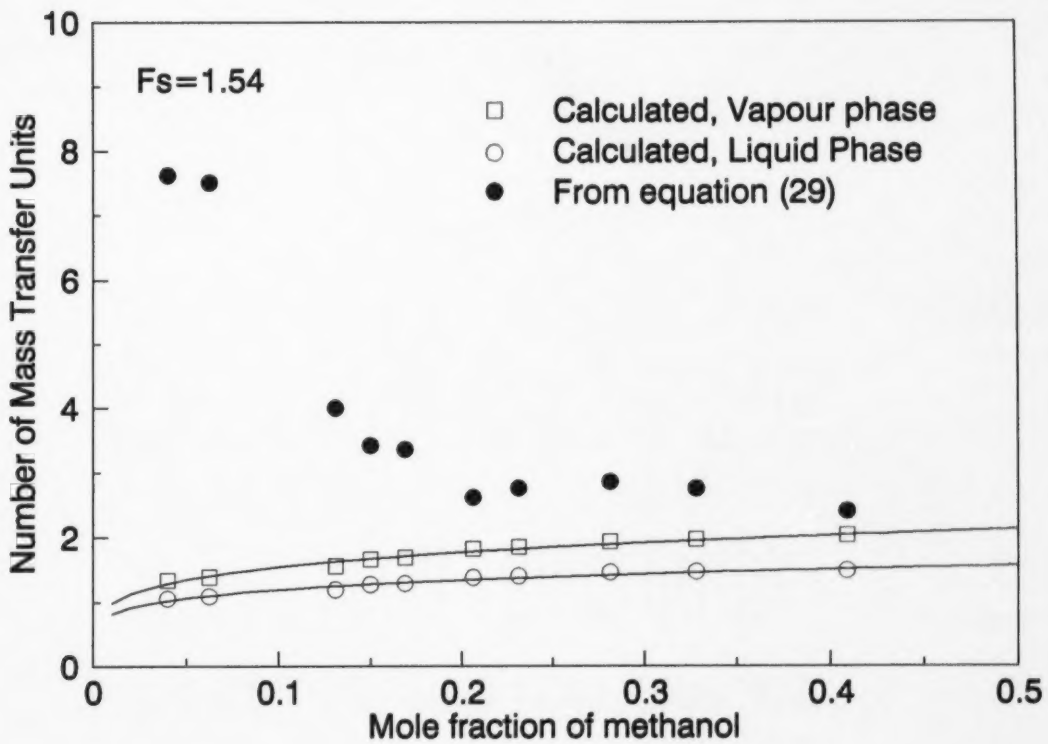

Figure 5-6

Measured Enhancement Factor
(Methanol/water system)

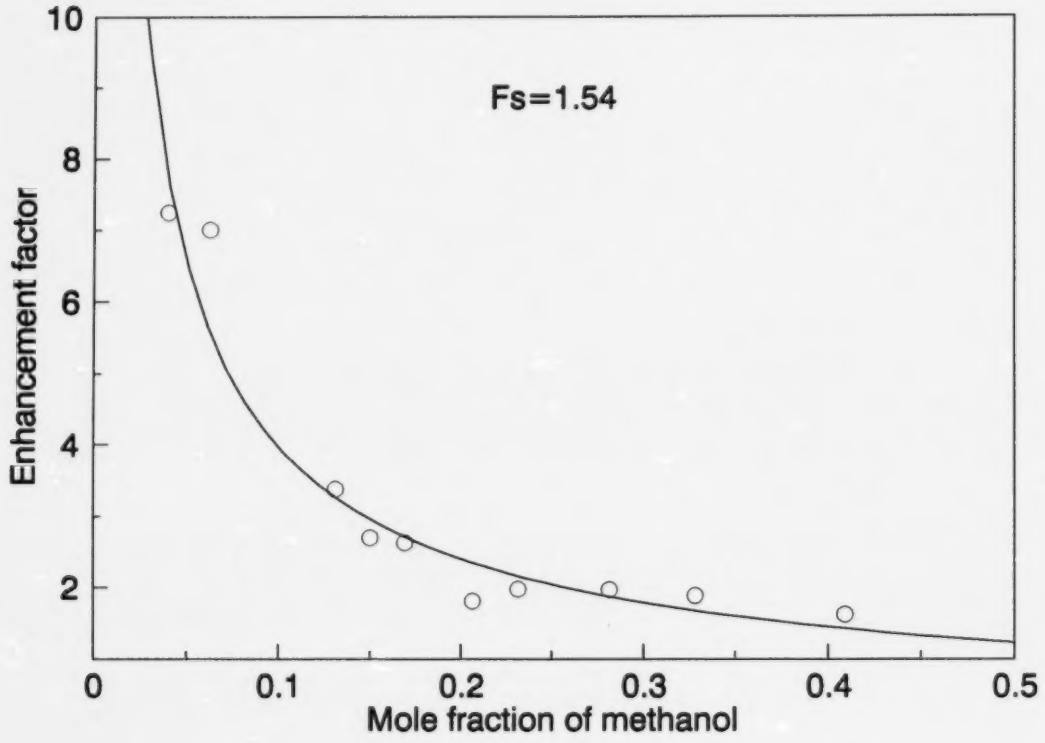

Figure 5-7
Comparison of Measured and Calculated
Enhancement Factor
(Methanol/water system)

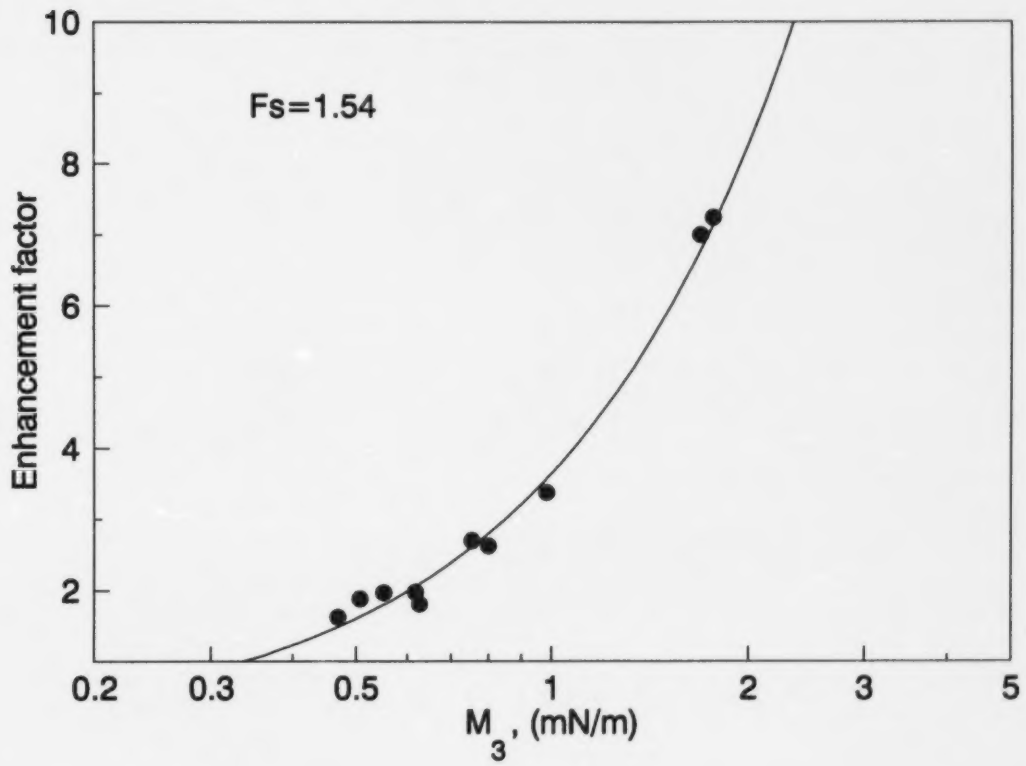

Figure 5-8
Comparison of Measured and Calculated
Point Efficiency
(Methanol/water system)

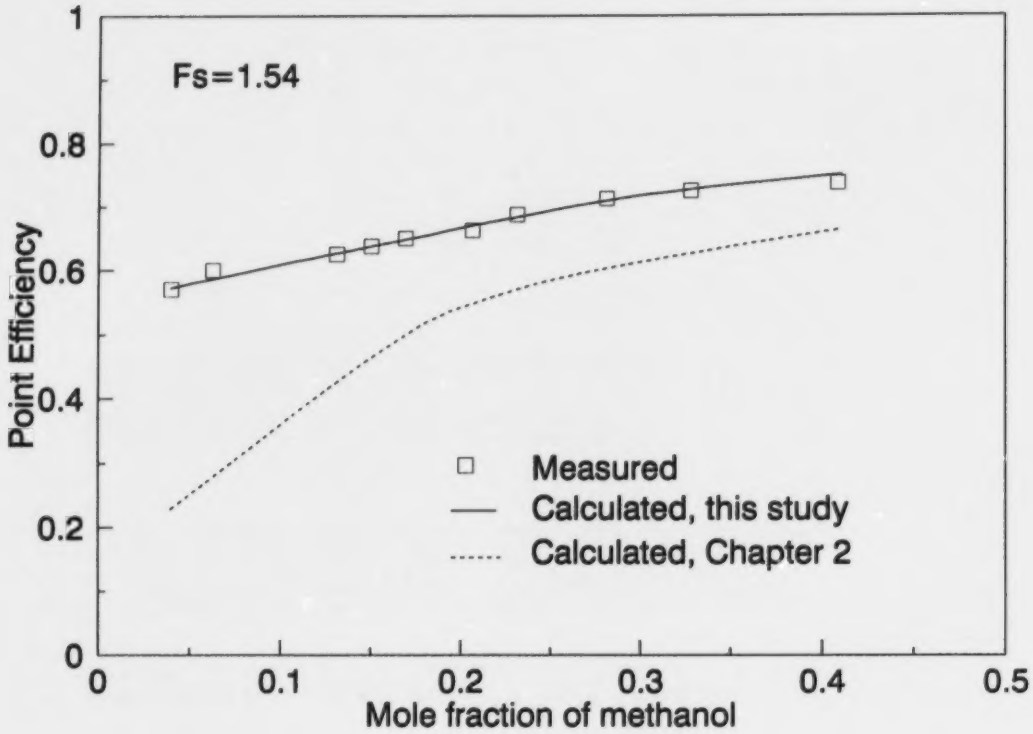

5.9 Literature Cited

Brian, P.L.T.; J.E. Vivian; and S.T. Mayr, "Cellular convection in desorbing surface tension-lowering solutes from water", Ind. Eng. Chem. Fundam. 10(1), 75-83 (1971).

Burg, J.C., "Interfacial phenomena in fluid phase separation processes", Recent Developments in Separation Science **2**, 1-31 (1972).

Calderbank, P.H., and J., Pereira, "The prediction of distillation plate efficiencies from froth properties", Chem. Eng. Sci. **32**, 1427 (1977).

Dribika, M.M., and M.W. Biddulph, "Scaling-Up Distillation Efficiencies," AIChE J., **32** (9), 1864 (1986).

Drinkenburg, A.A.H., "Marangoni convection by evaporation in spacelab", Inst. Chem. Engrs. Symp. Ser. 62, B-179-B191 (1986).

Ellis, S.R.M., and M.W. Biddulph, "The Effect of Surface Tension Characteristics on Plate Efficiencies," Trans. Inst. Chem. Engrs., **45**, T223 (1967).

Hovestreydt, J., "The influence of the surface tension difference on the boiling of mixtures", Chem. Eng. Sci. **18**, 631-639 (1963).

Kalbassi, M.A., M.M. Dribika, M.W. Biddulph, S. Kler, and J.T. Lavin, "Sieve Tray Efficiencies in the Absence of Stagnant Zones," Inst. Chem. Engrs. Symp. Series No. 104, A511 (1987).

Kreis, H, and M. Raab, "Industrial application of sieve trays with hole diameters from 1 to 25 mm with and without downcomers", Inst. Chem. Engrs. Symp. Ser. No. 56, 3.2/63-3.2/83 (1979).

Link, V., "Interfacial turbulence accompanying oxygen absorption in sulphite", Chem. Eng. Sci. **27**, 627-637 (1972).

Lockett, M.J., and I.S. Ahmed, "Tray and Point Efficiencies from a 0.6 Meter

Diameter Distillation Column," Chem. Eng. Res. Des., **61**, 110 (1983).

Lockett, M.J., and M.S. Uddin, "Liquid-phase controlled mass transfer in froths on sieve trays", Trans. Inst. Chem. Engrs. **58**, 166 (1980).

Moens, F.P., "The Effect of Composition and Driving Force on the Performance of Packed Distillation Columns - 1," Chem. Eng. Sci., **27**, 275 (1972).

Neuburg, H.J., and K.T. Chuang, "Mass transfer modelling for GS heavy water plants. 1: Point efficiency on GS sieve trays," Can. J. Chem. Eng. **60**, 504 (1982).

Sakata, M., and Y. Yanagi, "Performance of a commercial-scale sieve tray," Inst. Chem. Engrs. Symp. Ser. **No. 56**, 3.2/21 (1979).

Sawistowski, H., "Surface-Tension-Induced Interfacial Convection and its Effects on Rates of Mass Transfer," Chemie-Ing.-Techn. **45**, 1093 (1973).

Stichlmair, J., Bodenkolonne. Verlag Chemie (1978).

van der Veen, A.J., A.A.H. Drinkenburg, and F.P. Moens, Trans. Inst. Chem. Engrs. **52**, 228 (1974).

Zuiderweg, F.J., 79th National Meeting of the American Institute of Chemical Engineers, Houston, March 1975, B9 (1975).

Zuiderweg, F.J., "Marangoni Effect in Distillation of Alcohol-Water Mixtures," Chem. Eng. Res. Des., **61**, 388 (1983).

Zuiderweg, F.J., "Sieve Trays, a View of the State of the Art," Chem. Eng. Sci., **37**, 1441 (1982)

Chapter 6

IMPROVING SIEVE TRAY PERFORMANCE WITH MESH PACKING

6.1 Introduction

Sieve trays have been widely used in mass and heat transfer applications because of their design reliability and low cost. However a major drawback is their relatively low efficiency among distillation column internals. The rising cost of energy in recent years, has resulted in the use of high efficiency packing instead of sieve trays as the choice for new applications. In addition it is frequently justifiable to replace an existing sieve tray column with a packed column since the cost of revamping can be recovered quickly through lower operating expenses. However this practice is not without problems, on a few occasions, the packing did not perform as expected and the sieve trays had to be reinstalled. Therefore, it is desirable to develop a method to obtain high tray efficiency at minimum risk.

Sieve tray efficiency is not very sensitive to tray design. It appears there is little scope to improve the tray efficiency by design procedure. Bain and Van Winkle (1961) and Smith (1963) found that trays with small hole size provided good vapour-liquid distribution and reduced weeping, while increasing tray efficiency by producing small bubbles with large interfacial area. Lemieux and Scotti (1969) also found that small holes offered an appreciable efficiency advantage especially with positive surface

---

A version of this chapter has been published. Chen, G.X., A. Afacan, C. Xu and K.T. Chuang 1990. Can. J. Chem. Eng. 68, 382-386.

tension systems. However the expense of manufacturing trays with holes smaller than 2 mm and the difficulty in avoiding clogging of these holes limits their applications to a few very clean systems. Spagnolo and Chuang (1984) were the first to report on the performance of sieve trays combined with knitted mesh packing for heavy water production in an absorption column. They found that tray efficiency increased 5% to 40% due to the installation of 30 mm mesh packing on the sieve tray. The enhanced tray efficiency was attributed to smaller bubbles produced which resulted in higher interfacial area. They also found that with mesh packing the sieve tray showed a lower entrainment and higher pressure drop. It has been reported by Salem and Alsaygh (1988) that the efficiency of a 75 mm diameter test column was enhanced with the installation of various kinds of random packings on sieve trays. The largest increase in efficiency was achieved by the addition of 115 mm stacked stainless steel Raschig rings. In this case the overall column efficiency was increased by 21% for the distillation of methanol/water mixture. Haq (1982) showed that the interfacial area of the froth on a sieve tray increased by 8% when adding a simple framework on the tray. The presence of this metal framework was found to have a marked effect on stabilizing the hydrodynamic conditions on the sieve tray. Mix and Erickson (1975) proposed a sieve tray which uses a packing on the tray to limit fluid oscillations and to prevent dumping at low vapour velocities. This is another indication that installing packing on a sieve tray could significantly improve tray efficiency.

The purpose of this study is to investigate the effect of installing a thin layer of mesh packing on the performance of sieve trays under distillation conditions. Since the installation of mesh packing can be

easily carried out at a low cost, this could provide the best method to revamp existing sieve tray columns. The methanol/water system at a wide range of concentrations was chosen for investigation so that the results can be applied to aqueous as well as organic systems.

6.2 Experimental

A schematic diagram of the experimental apparatus is shown in Figure 6-1. The test loop was completely instrumented for continuous unattended operation. The column with a diameter of 153 mm was made of Pyrex glass and contained four identical trays spaced 318 mm apart. The second tray from the top was the test tray which was equipped with pressure taps and sampling points. A total condenser and a thermosiphon partial reboiler completed the distillation system. Detailed dimensions of the column and the tray are shown in Table 6-1. Some test runs were carried out with various layers of stainless steel knitted mesh packing (York Demister style 431) placed on the test tray. The total packing height was varied from 4.2 to 25.4 mm.

An Opto22 process I/O subsystem controlled by IBM personal computer was used to record temperatures, flowrates and liquid levels. The aerated liquid pressure drop and the total pressure drop for the test tray was measured with a manometer and a Capsuhelic differential pressure gauge, respectively. The froth heights on the trays and in the downcomers were obtained from visual observations. When these instruments showed constant signals for a period of 60 minutes, steady state conditions were assumed. Mass and energy balance calculations were performed to ensure that instrumental errors were insignificant (discrepancy $< 5\%$). At this point the vapour and liquid samples at the inlet and outlet of the test tray were taken by a syringe, so

vaporization of liquid samples was completely avoided and the mass transfer contributions from downcomer was also safely excluded. Triplicate samples were taken and analyzed to minimize the error of measurements.

The distillation was conducted at total reflux under ambient pressure with a mixture of methanol and water. The mixture was prepared by mixing distilled water with research grade methanol obtained from Fisher Scientific. A gas chromatograph, (HP 1010 A) was used to measure the compositions of the samples. The Murphree efficiency was calculated from the G.C. results together with the vapour-liquid equilibrium value from Perry's Chemical Engineers' Handbook (1984). The vapour-liquid equilibrium data were also verified by other sources. The efficiency was measured for the test tray with 0.0, 4.2, 12.7, and 25.4 mm of mesh packing at various vapour rates and methanol concentrations.

6.3 Results and Discussion

The main purpose of this investigation was to determine the effect of mesh packing on the tray hydraulic and mass transfer performance of a sieve tray. Careful attention was given to the accurate measurement of liquid holdup, total pressure drop, and vapour and liquid flows and compositions. The reproducibility of individual liquid and vapour composition samples was better than 0.5%. To avoid the mass transfer contributions from the downcomer between trays 2 and 3, the liquid samples for the outlet of the test tray were taken at the outlet weir before the liquid entered the downcomer. The Peclet number for the test system was in the order of 0.2; thus, both vapour and liquid might be assumed to be completely mixed. The Murphree efficiency measured in the test column would be very close to point

efficiency of an industrial size column (Fair, 1987). The tray efficiency of the large column can then be calculated according to the procedure suggested by Fair et al. (1983)

6.3.1 Sieve Tray Efficiency

A series of tests was carried out to measure the Murphree efficiency of the test tray as a function of the F-factor and liquid composition. The results are shown in Figures 6-2 to 6-4. The tests covered the superficial F-factors from 0.6 to 1.2 $(kg/m)^{0.5}s^{-1}$, which correspond to vapour flows from just above the weep point to below the jet flood velocity. It can be seen that the measured tray efficiency decreases with increasing F-factor and these data agree with those reported by Weiss and Longer (1979) for methanol/water distillation using valve trays.

Figure 6-3 shows the variation of E_{MV} with liquid composition on the test tray with and without mesh packing. As the tray concentration increased from 6% to 85% methanol (by mole) the Murphree tray efficiency, E_{MV}, was also increased for both trays with and without packing at constant F-factor of 0.6 and 1.2. Similar effects were also obtained for other F-factors. The major difference in physical properties between these two concentrations is the interfacial tension which decreases from 0.05 N/m to 0.02 N/m as the tray concentration was increased from 6% to 85% methanol. Video pictures of the tray operation suggest that the bubble size decreases with increasing methanol concentration. Consequently, the effective interfacial area is larger at high methanol concentrations. This result is consistent with the observation reported by Lockett and Ahmed 1983.

6.3.2 Effect of Mesh Packing on Tray Efficiency

It has been shown that the York mesh is effective in mist elimination from a gaseous stream by providing a solid surface for the inertial impact of the liquid droplets. Similarly, the mesh should also be effective for breaking up the bubbles before they are fully grown at the orifices of a sieve tray. Tray efficiency appears to be a weak function of tray design. The only factor that a tray designer can choose to enhance sieve tray efficiency is an increase in the outlet weir height. Higher weirs result in higher froth heights which provide longer residence time for the vapour-liquid contact. However, this approach is not very effective because it has been shown by Lockett and Plaka (1983) that there exists a range of bubble sizes, with the smaller bubbles reaching equilibrium long before they leave the froth. As the froth height increases there will be more bubbles playing no part in the mass transfer process for much of their residence time. Photographs show that the bubbles generated on the mesh-packed tray are uniformly smaller in size than those on the sieve tray, which should result in a higher interfacial area. Additionally, these bubbles tend to be more stable, which results in an increase in froth height and thus a longer residence time. The combined effects give much improved tray efficiencies.

Figures 6-2 and 6-3 show the effect of mesh packing on tray efficiency for the entire range of concentration and F-factor. Extensive tests were carried out with a 25.4 mm layer of mesh packing placed on the previously tested tray. It was found that the improvement in tray efficiency due to the installation of the packing is greater than 30 percent. This improvement represents an increase of about 40% at the high efficiency end to over 50% at the low efficiency end. In fact, the efficiencies for most of the runs

with packing were above 90% and, in some cases, were greater then 100% at low F-factors and high concentrations. Normally it is not possible to obtain such high efficiencies for a small diameter column because E_{MV} is about equal to E_{OG}, which should not be greater than 100%. Clearly, the packing must not only increase point efficiency but also reduce back mixing. The latter is significant in that, with a conventional tray, the liquid was assumed to be completely mixed in the vertical direction because of the intense agitation in the froth. With packing, the resistance to the liquid flow may cause a concentration gradient in both the vertical and horizontal direction giving rise to the much improved tray efficiencies.

Although tests with large sieve trays have not been performed, it is quite possible that, in addition to the increase in point efficiency, the packing could also improve the liquid distribution by reducing retrograde flows. Consequently, the tray efficiency enhancement in large diameter columns could be greater than that shown for a small diameter column.

6.3.3 Mass Transfer Mechanism

Test results have clearly shown that the mesh packing is effective in reducing the bubble size on trays. Because the froth height was measured for each run, it is possible to estimate the effect of packing on the overall mass transfer coefficient. Assuming that the liquid is completely mixed and the vapour distribution approaches plug flow in all cases, the following expression can be obtained:

$$E_{OG} = E_{MV} = 1.0 - \exp(-K_y a * h_f / U_v) \qquad (1)$$

where $K_y a$, h_f and U_v are overall mass transfer coefficient, froth height and vapour flow rate, respectively. Rearranging equation (1) gives:

$$K_Y a = (-U_v / h_f) \ln(1-E_{OG}) \quad (2)$$

The mass transfer enhancement factor due to packing is defined as:

$$R = (K_Y a)^* / (K_Y a) \quad (3)$$

where $(K_Y a)^*$ is overall mass transfer coefficient for trays with packing. By using experimental data shown in Table 8-1, the enhancement factor (R) has been calculated and found to be 2.04 on average. The values of $(K_Y a)^*$ calculated are also found to be much higher than that normally reported for a sieve tray (Lockett, 1986). It may be concluded that this magnitude of improvement is likely not achievable by simply varying the tray parameters such as hole size, hole area and weir heights. The effect of height of knitted mesh packing on tray efficiency at different F-factors is shown in Figure 6-4. Increased tray efficiency was obtained with greater packing heights; however after a height of 12.7 mm, since most of the bubbles breakage had taken place, the magnitude of the efficiency increase was less. In the case of packed trays, it is suggested that the effectiveness of vapour-liquid contact is controlled by the mesh packing, giving the designer greater flexibility in choosing tray design. For example, use a larger hole area for vacuum services.

6.3.4 Tray Hydraulics

(a) Pressure drop

Figure 6-5 shows the pressure drops (h_T, h_L) versus F-factors for trays with and without packing. The effect of packing height on h_T and h_L is given in Figure 6-7. It is important for a tray designer to estimate the extra pressure drops caused by packing so that he can properly design the packed

tray to meet the process requirements. It can be seen in Figure 6-5 that, with a 25.4 mm layer of packing, both h_L and h_T increase by about 10% and 20% at low and high F-factors, respectively. The small increase in pressure drop due to the packing may be explained by its high void fraction (97%). Therefore, the packing contributes little additional resistance to the vapour flow. The extra pressure drop is proportional to (F-factor), which agrees with the principle of fluid mechanics. If the h_T needs to be controlled, this extra pressure drop can be compensated for by slightly increasing the hole area. Alternatively, fewer trays can be used to give similar total pressure drop because the increase in efficiency for the packed tray is greater than that in pressure drop.

(b) Froth height

The effect of packing on the froth height is shown in Figure 6-6. The packing caused the froth height to increase by about 15-20% due mainly to the smaller size of bubbles and more stable conditions generated on the packed tray. Figure 6-7 shows that as the packing height increases the froth height on the tray also increases due to smaller diameter bubbles generated by the additional packing.

(c) Turndown ratio

A series of tests was conducted to determine the effect of mesh packing on the turndown ratio. For the sieve tray alone, weeping was noticeable at F-factor = 0.4 and vigorous spraying was seen at F-factor = 1.2. Test results show (Figure 6-2) that the tray efficiency varies by almost 20% between these two operating conditions. Obviously, the sieve tray has a turndown ratio of less than 3, a value similar to those quoted in the literature. When a 25.4 mm layer of packing was placed on the tray, a

uniform froth was observed throughout the entire range of F-factor: no weeping at F-factor = 0.4 and no spraying or entrainment at F-factor = 1.2. When the flows were further increased to F-factor = 1.4, still no spraying above the froth was observed. Because of the limitation of reboiler capacity, a further increase of F-factors could not be achieved. These results suggest that the packing can reduce the weeping and entrainment of a sieve tray. Moreover tray efficiency varied by less than 15%. These results strongly suggest that the packed tray can be designed for a turndown ratio of at least 3.5, a level substantially higher than that for a conventional sieve tray.

6.4 Conclusions

Installation of mesh packing on a sieve tray improved the tray efficiency by as much as 50%. Since the sieve tray design procedure is well established, the combined mesh packing and sieve tray can be applied reliably to distillation and absorption operations. The device is simple and economic, and it should find applications in the areas such as:

(a) revamp of a sieve tray column to increase efficiency and capacity.

(b) use of high hole area to reduce pressure drop.

(c) combined with other high capacity trays, e.g. screen trays, to reduce column height.

6.5 Nomenclature

E_{MV} = Murphree gas-phase tray efficiency, %

E_{OG} = point efficiency, %

F = Active area F-factor, $(kg/m)^{0.5}/s$

h_f = froth height, m

h_L = aerated liquid pressure drop, Pa

h_T = total tray pressure drop, Pa

$K_Y a$ = overall volumetric mass transfer coefficient, $kmol/sm^3$

R = mass transfer enhancement factor due to packing

U_v = vapour flow rate, $kmol/sm^2$

X_A = average test tray concentration, mole fraction of methanol

Table 6-1

Column and Tray Dimensions

Column Diameter	0.153 m
Total Column Cross-sectional Area	0.0184 m^2
Active Area	0.014 m^2
Downcomer Area	0.0022 m^2
Hole Diameter	4.76 mm
Open Hole Area	0.00086 m^2
Tray Thickness	2.5 mm
Outlet Weir Height	0.063 m
Weir Length	0.1104 m
Tray Spacing	0.318 m

Figure 6-1
Schematic Diagram of Experimental Apparatus

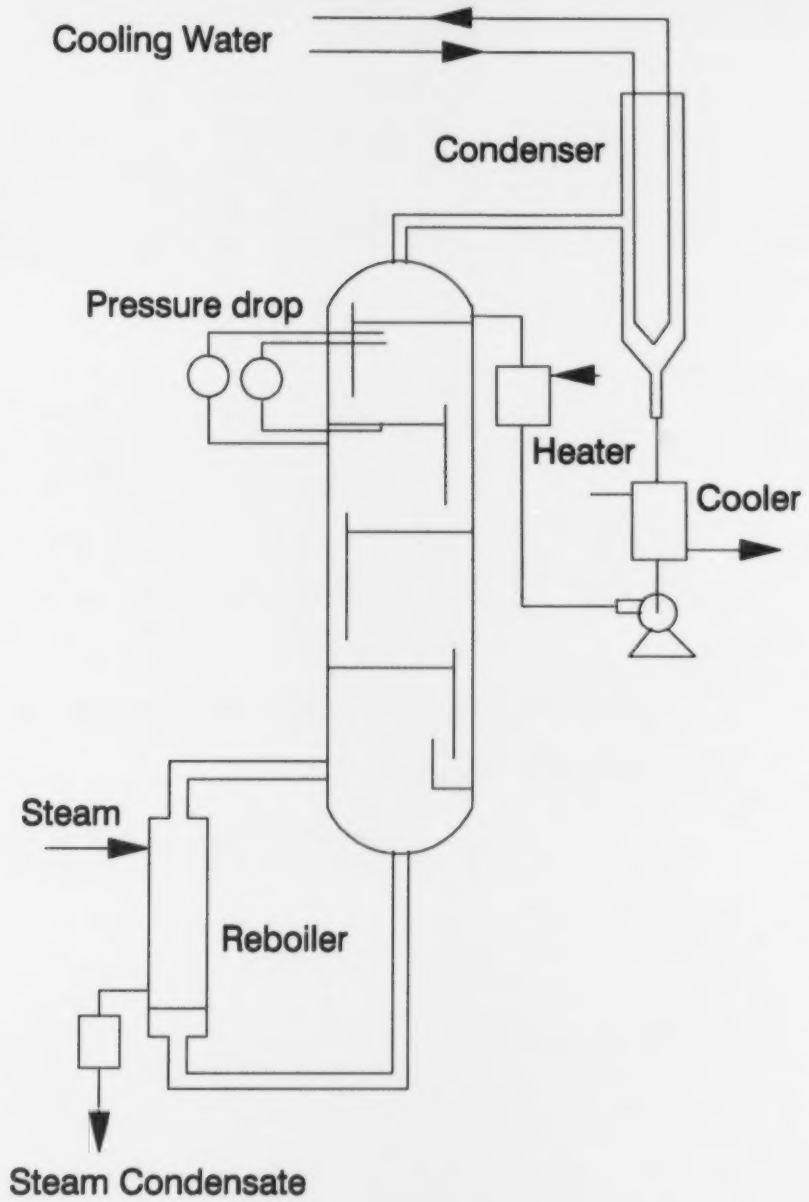

Figure 6-2
Murphree Tray Efficiency as a Function of Fa-factor
(Packing Height = 25.4 mm)
(Methanol/Water System)

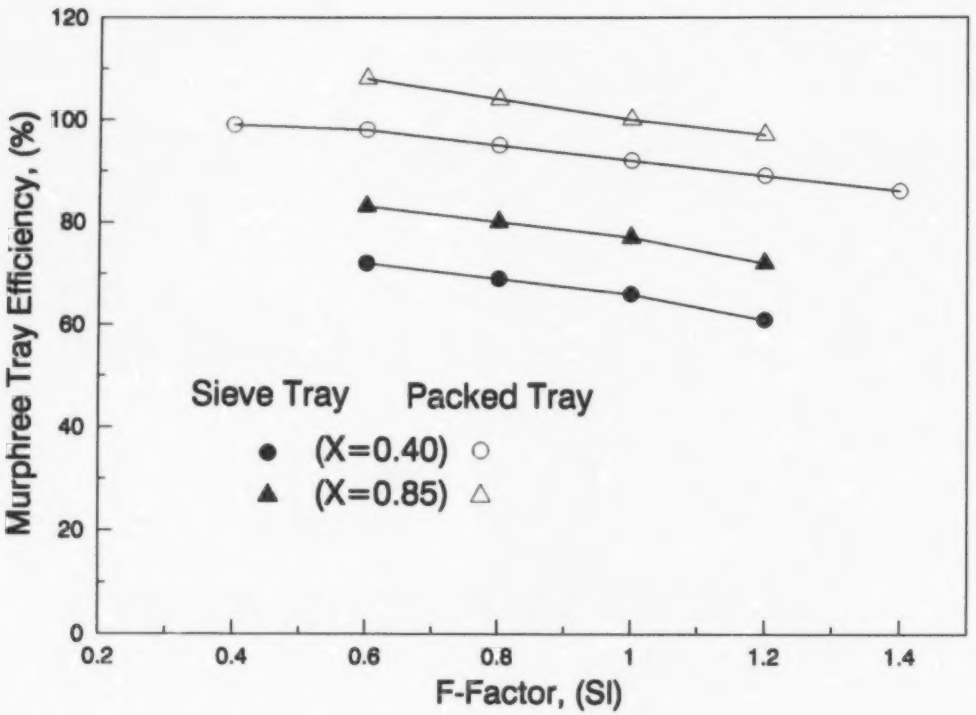

Figure 6-3
Murphree Tray Efficiency as a Function of Average Concentration on the Test Tray
(Packing Height = 25.4 mm)
(Methanol/Water System)

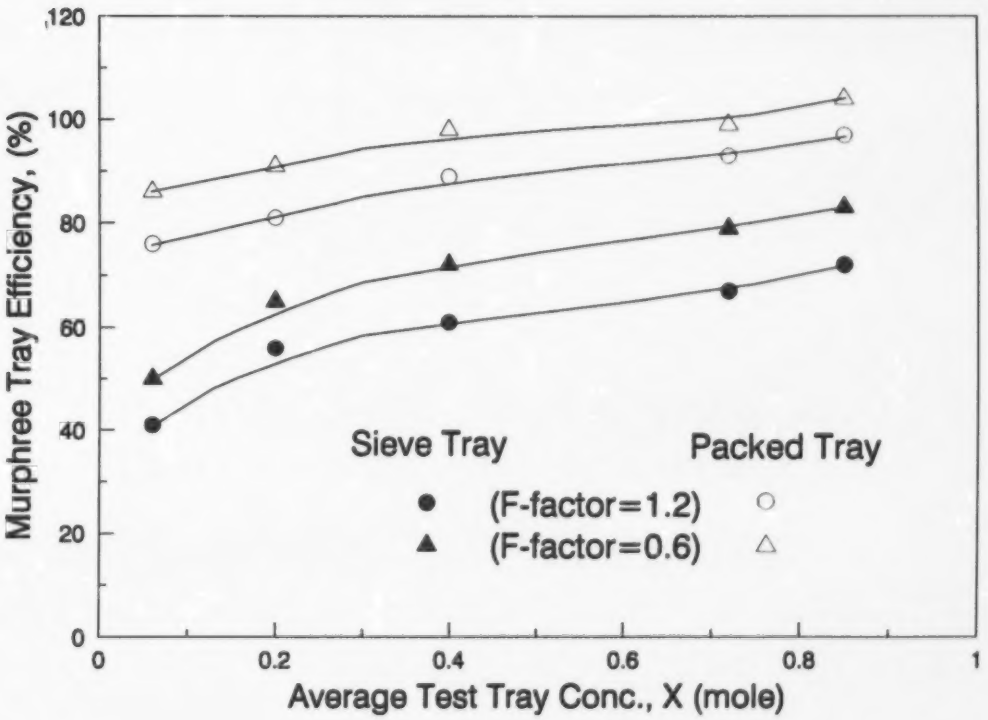

Figure 6-4
Effect of Packing Height on Murphree Tray Efficiency
(X=40% by mole)
(Methanol/Water System)

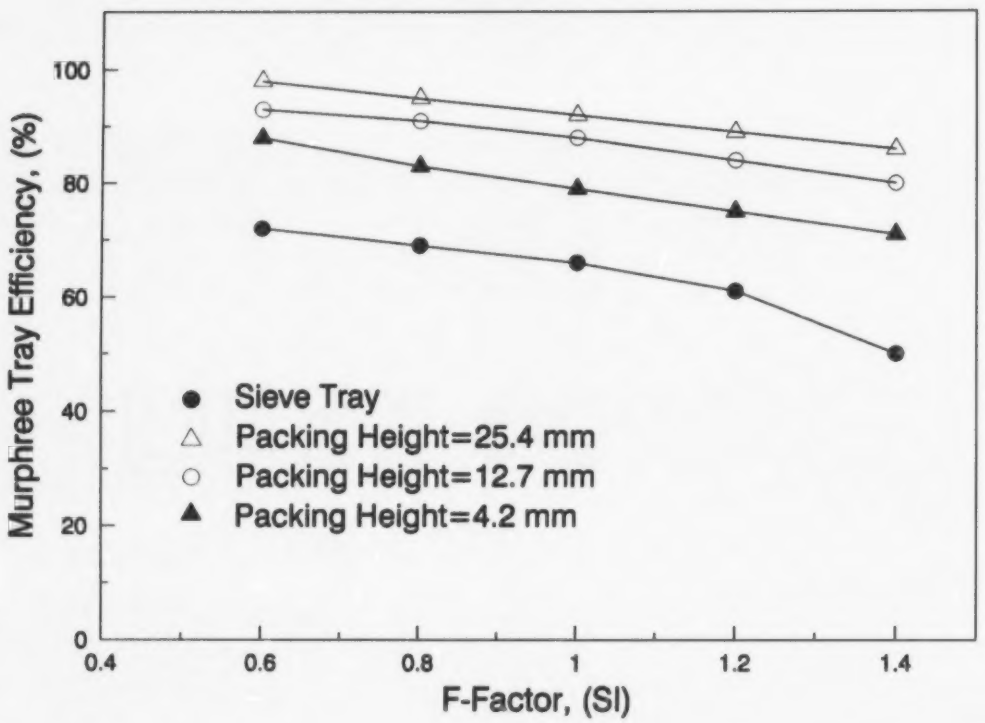

Figure 6-5
Tray Pressure Drop at Various F-factors
(X=40% by mole, Packing Height=25.4 mm)
(Methanol/Water System)

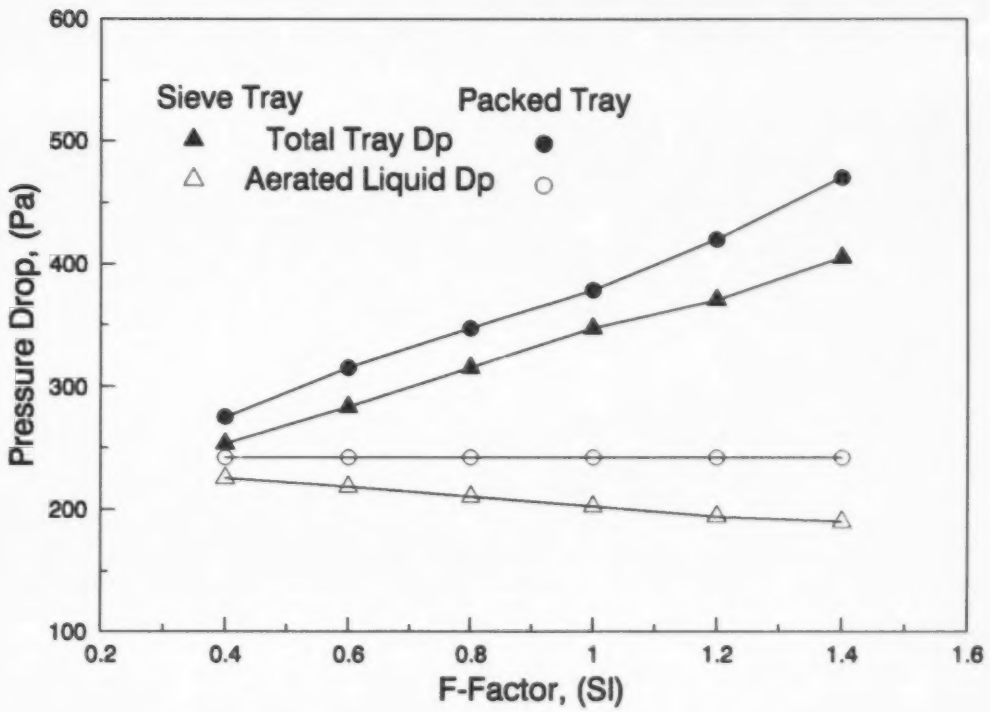

Figure 6-6
Froth Height at Various F-factor
(X=40% by mole, Packing Height=25.4 mm)
(Methanol/Water System)

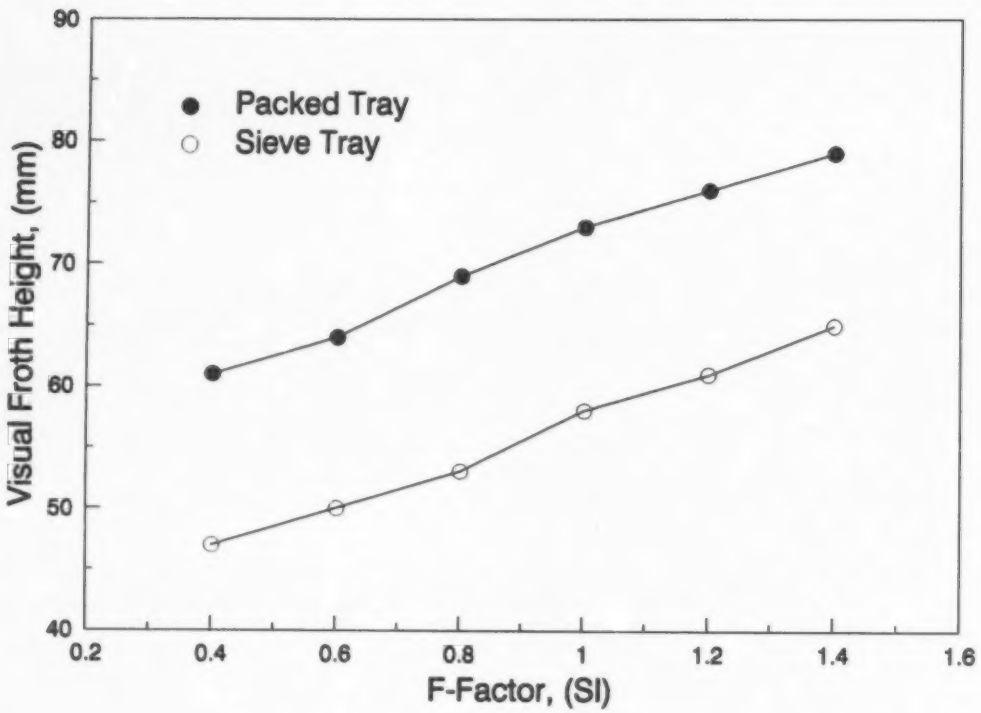

Figure 6-7
Effect of Packing Height on Tray Pressure Drop
and Froth Height
(X=40% by mole, F-factor=1.0)
(Methanol/Water System)

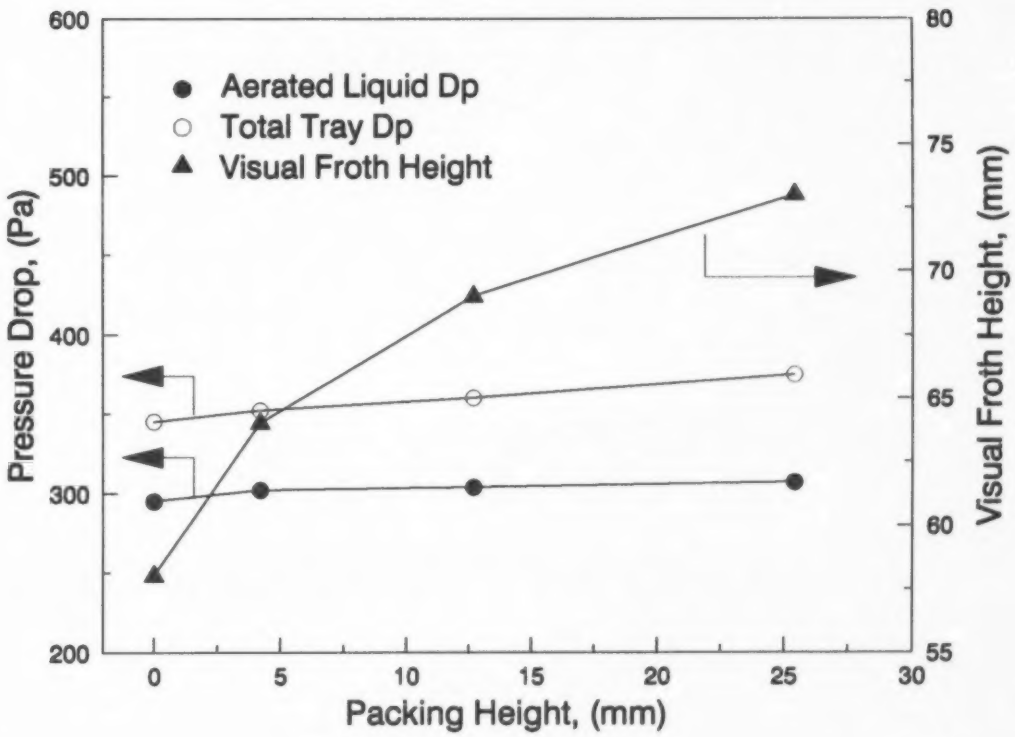

6.6 Literature Cited

AIChE, "Bubble Tray Design Manual", New York (1958).

Bain, J. and M. Van Winkle, "A Study of Entrainment, Perforated Plate Column--Air-Water System", AIChE J. 7, 363-366 (1961).

Fair, J. R., in "Handbook of Separation Process Technology", R. W. Rousseau, Ed., Wiley, New York (1987), p. 317.

Fair, J.R., H. R. Null and W. L. Bolles, "Scale-up of Plate Efficiency from Laboratory Oldershaw Data:, Ind. Eng. Chem. Process. Des. Dev. 22, 53-58 (1983).

Haq, M.A., "Fluid dynamics on sieve tray," Hydrocarbon Processing 61(4), 165-168 (1982).

Lemieux, E. J., and L. J. Scotti, "Perforated Tray Performance", Chem. Eng. Prog. 65(3), 52-58 (1969).

Lockett, M. J. and I. S. Ahmed, "Tray and Point Efficiencies from a 0.6 Meter Diameter Distillation Column", Chem. Eng. Res. Des. 61, 110-118 (1983).

Lockett, M. J., "Distillation Tray Fundamentals", Cambridge University Press (1986).

Lockett, M. J. and T. Plaka, "Effect of Non-uniform Bubbles in the froth on the correlation and Prediction of Point Efficiencies", Chem. Eng. Res. Des. 61, 119-124 (1983).

Mix, T. W. and J. Erickson, "Vapour-Liquid Contacting", U.S. Pat. 3,887,665 (1975).

O'Connell, H. E., "Plate Efficiency of Fractionating Columns and Absorbers", Trans. AIChE 42, 741-755 (1946).

Spagnolo, D. A. and K. T. Chuang, "Improving Sieve Tray Performance with

Knitted Mesh Packing", Ind. Eng. Chem. Proc. Des. Dev. 23, 561-565 (1984).

Salem, A.-B. H. and A. A. Alsaygh, "Better Sieve Tray? Add Packing", Hydrocarbon Processing 67(5), 76-G to 76-H(1988).

Smith, B. D. "Design of Equilibrium Stage Processes", McGraw-Hill, New York (1963).

Weiss, S. and J. Longer, "Mass Transfer On Valve Trays with Modifications of the Structure of Dispersions", Inst. Chem. Eng. Symposium Series 56, 2.3/1-2.3/25, (1979).

Chapter 7

MASS TRANSFER AND HYDRAULICS OF PACKED SIEVE TRAYS

7.1 Introduction

The vapour capacity of a sieve tray is dependent on the system properties, vapour and liquid rates, and tray geometry. For a non-foaming system, tray capacity is usually limited by excessive entrainment if the downcomer is properly designed. Flooding due to massive entrainment or liquid carryover is difficult to overcome. It has been demonstrated that entrainment is dependent on the type of flow regime on the tray (Pinczewski et al., 1975; Lockett et al., 1976; Porter and Jenkin, 1979). In the spray regime, entrainment was found to be much more severe than that in the froth regime. When the froth-to-spray transition criteria (Porter and Jenkin, 1979; Loon et al., 1973) are applied to industrial-scale sieve trays, it is found that most atmospheric and vacuum columns operate in the spray regime. Much attention has been paid in recent years to reducing the entrainment by improving the tray design, but little improvement has been made.

Desirable tray performance characteristics include high efficiency, large capacity, low pressure drop, and high turndown ratio. These characteristics are affected by the tray operating regime, vapour and liquid loads, system properties, and tray geometry. Changing tray geometry can not satisfy both efficiency and capacity. A bed of mesh packing on the sieve tray may increase not only the efficiency but also the capacity. In Chapter 6, it has been shown that a bed of mesh packing can increase the tray efficiency significantly for the distillation of methanol/water mixtures. However, the detail measurement of entrainment for tray with and without

packing was not made there.

The objective of this study is to determine the packed tray efficiency under the distillation of acetic acid/water mixtures in the same column as used in Chapter 6 and to compare the efficiency results with that of methanol/water mixtures (Chapter 6). Hydraulic tests were made to measure quantitatively the effect of mesh packing on the tray capacity, entrainment, and pressure drop in a 600 mm diameter air/water column. The results could then be used to establish the design procedure.

7.2 Experimental

Distillation of acetic acid/water mixtures at total reflux under ambient pressure was effected in the same column as used in Chapter 6 for the distillation of methanol/water mixtures. This allows a direct comparison between the results for the two systems. Schematic diagrams of the experimental apparatus and a complete description of the facilities are given in Chapter 6.

Further hydraulic tests to determine quantitatively the effect of packing on tray pressure drop, entrainment, and capacity were carried out in a 600 mm diameter air-water column. The air supply was provided by a vane blower, and its flow rate was measured by a calibrated orifice meter. The superficial air velocity was varied from 0.4 to 2.5 m/s. The water to the column was supplied by a recirculating pump, and a calibrated rotameter was used to measure the water flow rate from 2.78 to 8.34 m^3/s. The column was made of Pyrex glass and contained four trays spaced 400 mm apart. The first tray from the bottom served as an air distributor, and the second tray from the bottom was the test tray, which was equipped with pressure taps. The top

two trays, equipped with demisters, were used to collect the entrainment. The entrainment was measured by recording time elapsed to fill a container. Three different geometry trays were tested with and without the addition of 15 mm and 30 mm mesh packing. Table 7-1 shows the detail for the three tray designs and the dimensions of this column. The hole spacing for the tray was equilateral triangular pitch. All holes had sharp edges.

7.3 Results and Discussion

7.3.1 Mass Transfer Efficiency

A series of tests was made to measure the Murphree efficiency of the test tray with and without packing under the same operating conditions to determine the effect of mesh packing on the tray mass transfer performance. The measured Murphree tray efficiencies of the test tray with and without a bed of 25.4 mm packing are shown in Figure 7-1 as a function of F-factor, and in Figure 7-2 as a function of liquid composition. It can be seen that the measured tray efficiency decreases with increasing F-factor in the test range (froth regime), and these data without packing agree well with those reported by Jones and Pyle (1955) for the same system. These figures also show that the packed tray efficiency is 40-50% higher than that of the same tray without packing over a wide range of concentrations and flow rates. Compared with the previous data for the methanol/water system (Chapter 6), it is evident that the effect of packing on the tray efficiency is similar for both systems in the froth regime, although the tray efficiency for the acetic acid/water system is lower than that for the methanol/water system. Video pictures taken during the experiments indicate that with packing, bubble sizes are smaller and froth oscillation is reduced. Consequently, it

is expected that packing can cause an increase in interfacial area and vapour-liquid contact time, resulting in a higher mass transfer efficiency.

7.3.2 Interfacial Area

The interfacial area of test tray with and without packing can be estimated by the following equation (Zuiderweg, 1982):

$$a = u_s\left[\frac{1}{k_G} + \frac{1}{k_L}\right]N_{OG} \qquad (3)$$

Assuming that the liquid on the tray is completely mixed in our small column (Biddulph et al., 1991) and the vapour distribution approaches plug flow, then:

$$N_{OG} = -\ln\left(1 - E_{OG}\right) = -\ln\left(1 - E_{MV}\right) \qquad (4)$$

Individual phase mass transfer coefficient k_G and k_L in equation (3) can be determined by equations obtained by Zuiderweg (1982):

$$k_G = \frac{0.13}{\rho_G} - \frac{0.065}{\rho_G^2} \qquad (5)$$

$$k_L = 0.024\, D_L^{0.25} \qquad (6)$$

From the above equations, it may be concluded that mass transfer coefficients, k_G and k_L, are mainly functions of system properties. Therefore, the mesh packing may be assumed to have no effect on mass transfer coefficients. By substituting equations (4), (5) and (6) into equation (3), it is possible to obtain the interfacial area, as shown in Figure 7-3 for trays with and without packing at x=0.61. It was found that packing can increase the interfacial area significantly. The largest improvement is 2.44 times at low F-factors. These results are similar to those reported by Spagnolo and Chuang (1984) for a H_2S/H_2O system and to

what found in Chapter 6 for the methanol-water system. Based on the interfacial area obtained, Sauter mean bubble diameter was estimated, and the results are shown in Figure 7-3. The estimated Sauter mean bubble diameter at F=0.5 was confirmed by photographs taken at the side and top of the test trays with and without packing. These results further illustrate that mesh packing can effectively break up large bubbles and result in an increase in the interfacial area.

7.3.3 Surface Tension Effect

1: Efficiency

The decrease in efficiency with increasing concentrations of the more volatile component for trays both with and without packing was observed, as shown in Figure 7-2. The reduction in efficiency is due to the increase in surface tension as discussed in the first part of this study. Although a previous report (Kumar and Kuloor, 1970) indicated that the size of the bubbles at the formation stage does not depend on surface tension at normal vapour flow rates on sieve trays, the bubble break up, on the other hand, in the intense turbulent velocity field of the froth can be affected by surface tension. It is reasonable to expect that the bubbles in a low surface tension mixture are easier to break up than in a high surface-tension mixture. This phenomenon was also observed in the case of the methanol-water system (Chapter 6), where the efficiency was found to increase with decreasing surface tension. Photographs of the froth showed that the bubble size was larger for the higher surface tension system, confirming the low efficiency observed.

As shown in Figure 7-4, the sieve tray efficiency for the acetic

acid/water system is about 10-15% lower than that for the methanol/water system at the same water concentration. This is attributable to the surface renewal effect discussed in Chapter 5.

2: Froth to Spray Transition

Two types of dispersion were found on sieve trays: a spray type at the relatively high vapour velocities, and a froth type at the lower velocities. In our experiments, the liquid sampler located at the outlet weir could no longer collect the liquid when the test tray was operated in the spray regime. Therefore the tray efficiency measurements were terminated at the froth-to-spray transition. Figure 7-4 shows that for sieve trays at 80% water concentration, the transition point for the methanol-water system was about 20% higher than that for the acetic acid-water system. Prince et al. (1979) observed that the transition was dependent on vapour and liquid density, but substantially independent of surface tension. Since the liquid density at 80% water concentration is similar for both systems, the difference in the transition point between the two systems should be attributable to the differences in surface tension gradient, i.e., surface tension positive vs surface tension negative. For surface tension positive systems, bubbles generated at the holes could be stabilized due to localized mass transfer (Fell and Pinczewski, 1977), whereas the bubbles could be destabilized due to the same mechanism for negative systems. This mechanism may explain our test results, which indicate that at the same water concentration, liquid hold-up and froth height for the positive system were higher than those for the negative system by 12% and 20%, respectively. At higher liquid hold-up, it is more difficult for vapour to penetrate the dispersion, so the spray regime occurs at higher vapour rates. Several

models exist to predict the transition point, all of which indicate liquid hold-up as an important factor. Our results suggest that a portion of the hold-up originates from the effect of surface tension gradient.

For trays with packing, the transition points were found to occur at higher F-factors than those without packing for both systems. This is also shown in Figure 7-4. Photographs taken during experiments show that packing increases the froth height by 10-20%, and in our small column also reduces tray oscillation which is known to cause premature spraying (Bidduph and Stephens, 1974). The combined effect results in a 35% higher transition point for the packed trays.

7.3.4 Capacity and Entrainment

The capacity of the test tray with and without packing for the two distillation systems was found to be limited by flooding due to massive entrainment. Because of small tray spacing in the distillation column, flooding occurred soon after entering the spray regime. If we assume that the limiting vapour capacity is the F-factor at the transition point, the upper-limit F-factor for the acetic acid/water system without packing was 1.2, which is 20% lower than that for the methanol/water system. For trays with packing, this F-factor increased to a value higher than 1.7. The exact flooding point was not determined because of the limitations of the reboiler. The greater than 35% increase in capacity due to packing can be attributed to a lower entrainment and higher froth-spray transition point.

Because of the limitations of the reboiler and the small tray spacing in the distillation column, the definite effect of packing on entrainment and vapour capacity was not obtained. For this reason, further tests in the

600 mm diameter column with an air-water system were made. Tray type 3 (see Table 7-1 for dimensions) and two different packing heights were used to investigate the effect of packing on entrainment and vapour capacity. The results are given in Figures 7-5 and 7-6. Figure 7-5 shows that at a low liquid rate (10 m^3/mh) and with 15 mm height of packing, entrainment is reduced by 50 - 70%, compared with the same tray without packing in the vapour velocity range of 1.2 to 2.3 m/s. The beneficial effect of packing on entrainment becomes more significant with increasing vapour velocity. Figures 7-5 and 7-6 indicate that there is an optimum packing thickness. In our test range, it was found that a packing height of 15 mm had a lower entrainment than that of 30 mm, and only at low liquid loading and high vapour velocity was thicker packing superior. The effect of packing on entrainment could be considered separately for the two operating regimes. It seems that, in the froth regime, the packing continually breaks up the bubbles at the tray floor. This generates more mist when bubbles break up at the top of the froth. This results in increased entrainment, but the absolute value is still very low. In the spray regime, packing could dampen vapour momentum and retard the atomization process and droplet formation, thus reducing the entrainment. In addition, entrainment on packed trays increases with increasing tray hole diameter and decreases with increasing liquid loading. This behavior is similar to that observed for the conventional sieve trays. This is confirmed by the results shown in Figures 7-7 and 7-8. For tray type 3 with and without 15 mm packing. a computerized mathematical analysis gives the correlation of entrainment and vapour velocity as follows.

For tray type 3 without packing for the air/water system:

$$e = k_1 u_s^{5.6} \qquad (L=10\ m^3/mh) \qquad (7)$$

$$e = k_2 u_s^{4.5} \qquad (L=20\text{-}30\ m^3/mh) \qquad (8)$$

where the exponent for u_s is very close to the literature value. For tray type 3 with 15 mm packing for the air/water system:

$$e = k_3 u_s^{3.1} \qquad (L=10\ m^3/mh) \qquad (9)$$

$$e = k_4 u_s^{2.4} \qquad (L=20\text{-}30\ m^3/mh) \qquad (10)$$

From the above equations, it can be seen that packing reduces the exponent of u_s by more than 40%. If a 10% entrainment is defined as the vapour capacity, then the packed tray is found to have a 50-80 % higher capacity than the same tray without packing.

7.3.5 Pressure Drop

Packing has been shown to have beneficial effects on tray efficiency and capacity. The only drawback is the higher pressure drop associated with the installation of packing. For acetic acid/water distillation, it was found that packing increased the total pressure drop by 10 to 20%. Similar results were also found for methanol/water distillation (Chapter 6). It is important to estimate the extra pressure drops caused by packing. Since the measurement of pressure drop in the small distillation column is quite dissimilar to that in the large column, owing to a significant difference in weir loading, detailed measurements were made to obtain the effect of packing on tray pressure drop in the large air-water column. The results at various liquid loadings for different tray designs are shown in Figures 7-9 and 7-10. Figure 7-9 shows the total pressure drops h_T versus vapour

velocity for tray type 3 at a liquid load of 10 m^3/mh. It can be seen that the pressure drop for the 15 mm packed tray is higher by less than 15%. Figure 7-10 shows that packing has no effect on dry tray pressure drop h_D. Thus, the higher h_T can be attributed to the increased liquid holdup h_L and higher residual pressure drop h_R. The higher h_R might result from the extra energy consumed by the packing to break up the bubbles. In addition, when large bubbles break up into smaller ones, the extra surface energy should be absorbed by the extra interface. This energy may be transferred from the vapour kinetic energy and result in a pressure drop. It was also found that the effect of tray hole size on packed tray pressure drop h_T is similar to that of sieve trays. This is shown in Figure 7-11. A computerized regression analysis gave the following correlation for trays with 15 mm packing.

$$h_T(\text{mm of water}) = 4.16 + 17.51\ u_s^2 + 0.55\ L + 2.11\ d \qquad (11)$$

for operations in the range of: u_s= 1.2 to 2.5 m/s, d =7 to 12.5 mm, L = 10 to 30 m^3/mh, b = 15 mm, h_W = 0.05 m.

The total pressure drop h_T can be predicted with an average error of less than 5% for systems similar to the air/water system.

7.4 Conclusions

Performance characteristics of packed trays have been obtained with systems that cover a wide range of properties. It was found that the mass transfer efficiency of packed trays is 40 to 50% higher than that of trays without packing for the distillation of acetic acid/water mixtures. This increase in efficiency is mainly due to the large interfacial area and small bubble diameter resulting from the mesh packing. It was also found that the

phase transition point of the surface tension positive system is about 20% higher than that of the negative system for trays without packing. With packing, the phase transition point is increased by 35% for both systems. It was also found that packing could effectively reduce entrainment. This results in the vapour capacity of packed trays being 50 to 80% higher than that of sieve trays. The total pressure drop of packed trays is about 15% higher than that of trays without packing. Correlations for pressure drop and entrainment of packed trays were determined from data obtained in a 600 mm diameter air/water column. The results may be used for the design of industrial packed-tray columns. The packed tray is simple, economical, and reliable. It could find many industrial applications, especially for the refurbishment of tray columns.

7.5 Nomenclature

a = interfacial area per unit bubbling area

b = packing height, mm

D_L = liquid diffusivity, m^2/s

d = tray hole diameter, mm

E_{MV}= Murphree vapour-phase tray efficiency

E_{OG}= Murphree vapour-phase point efficiency

e = entrainment, kg liquid/kg vapour

F = active area F-factor, $(Kg/m)^{0.5}/s$

h_{DP}= dry tray pressure drop, mm of liquid

h_L = equivalent clear liquid height on the tray, mm of liquid

h_R = residual pressure drop on the tray, mm of liquid

h_T = total pressure drop across wet tray, mm of liquid

h_W = weir height, m

k_i = coefficient

K_G = vapour side mass transfer coefficient, m/s

K_L = liquid side mass transfer coefficient, m/s

L = liquid load, m^3/mh

N_{OG}= number of overall mass transfer units

u_s = superficial vapour velocity, m/s

X_i = mole fraction of more volatile component in liquid phase

Y_i = mole fraction of more volatile component in vapour phase

ρ_G = vapour density, kg/m^3

Table 7-1

Column and Tray Dimensions

Distillation Column:		
Column diameter		0.153 m
Total column cross-sectional area		0.0184 m^2
Active area		0.014 m^2
Downcomer area		0.0022 m^2
Hole diameter		4.76 mm
Open hole Area		0.00086 m^2
Tray thichness		2.5 mm
Outlet weir height		0.063 m
Weir length		0.1104 m
Tray spacing		0.318 m
Air-Water Column:		
Column diameter		0.60 m
Total column cross-sectional area		0.2826 m^2
Active area		0.27 m^2
Downcomer area		0.0014 m^2
Outlet weir height		0.05 m
Weir length		0.17 m
Tray spacing		0.4 m
Tray thichness		2 mm
Hole Diameter	Tray type 1	7 mm
	Tray type 2	10 mm
	Tray type 3	12.5 mm
Open hole area	Tray type 1	0.0273 m^2
	Tray type 2	0.0273 m^2
	Tray type 3	0.0273 m^2

Figure 7-1
Murphree Tray Efficiency as a Function of Fa-factor
(Packing Height = 25.4 mm)
(Acetic Acid/Water System)

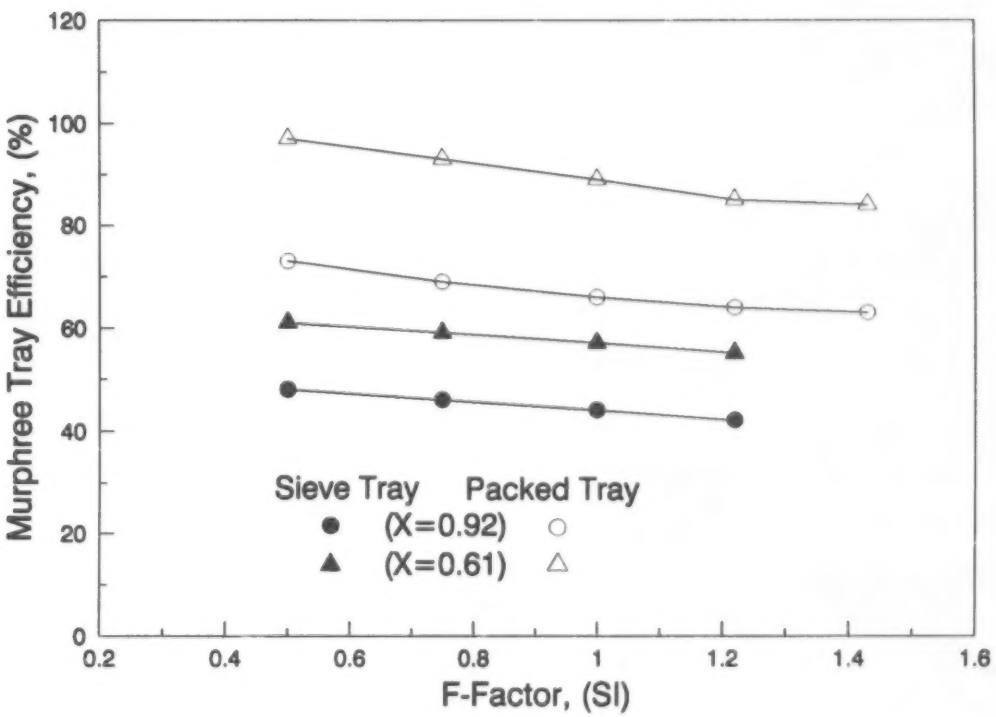

Figure 7-2

Murphree Tray Efficiency as a Function of Average Concentration on the Test Tray (Packing Height = 25.4 mm) (Acetic Acid/Water System)

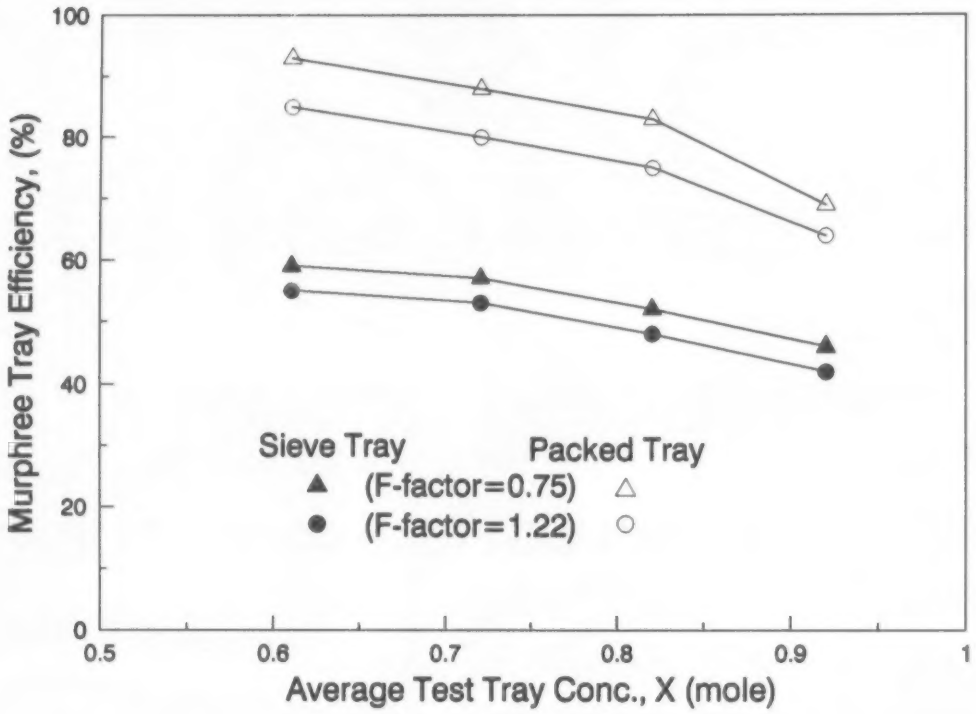

Figure 7-3
Interfacial Area and Sauter Mean Bubble Diameter as a Function of F-factor
(Acetic Acid/Water System)

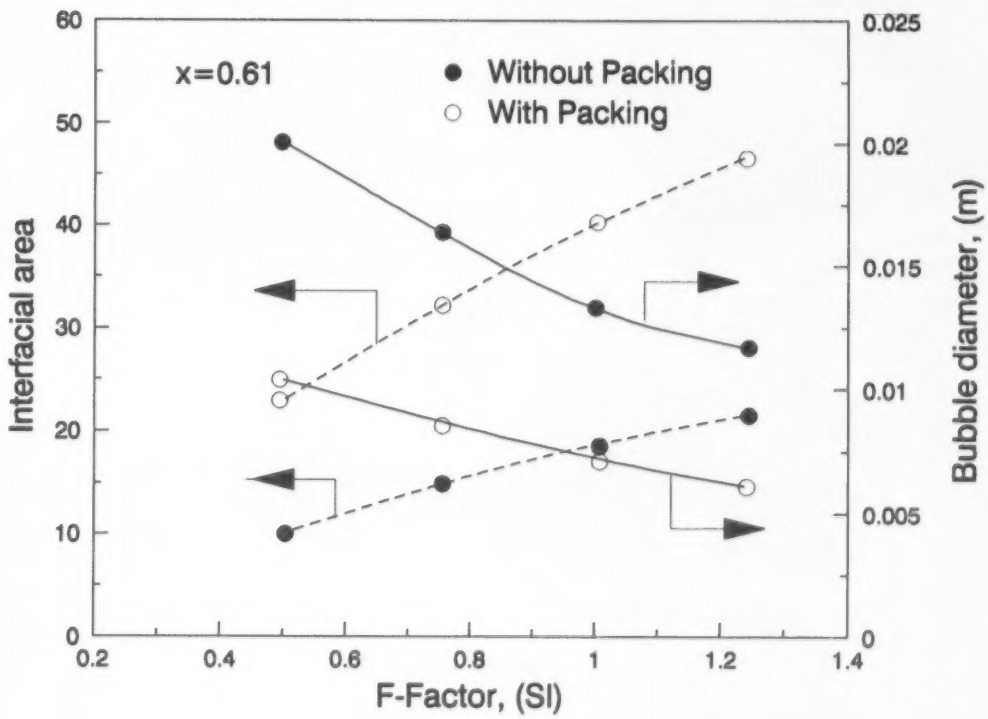

Figure 7-4
Murphree Tray Efficiency for Both Systems
at the Same Water Concentration
(Acetic Acid/Water and Methanol/Water Systems)

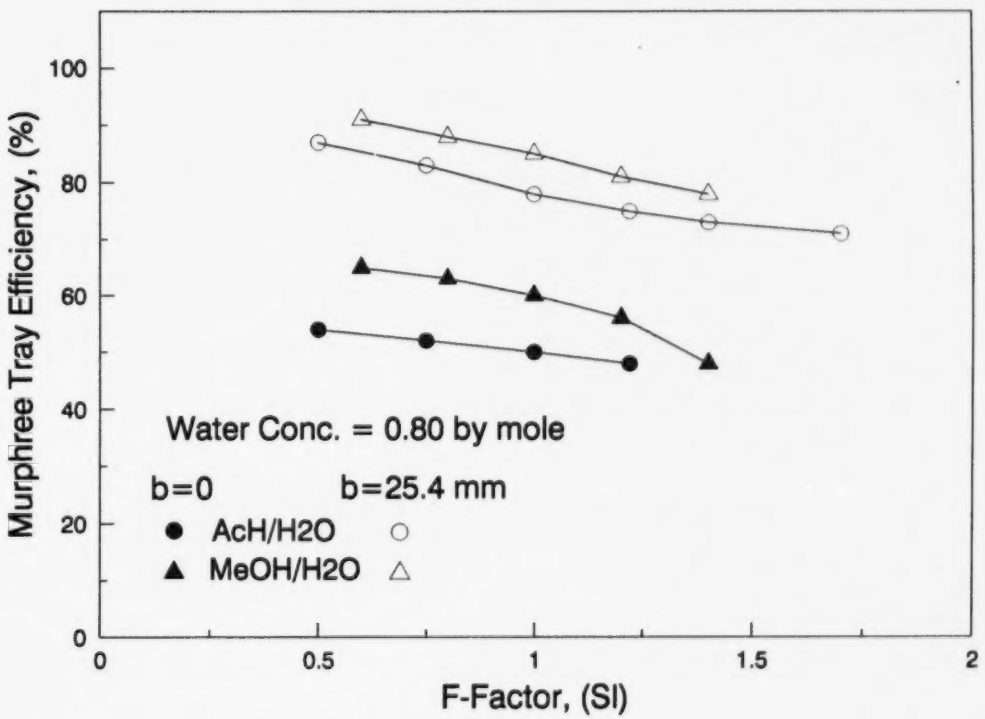

Figure 7-5
Entrainment as a Function of Vapour Velocity
(Air/Water System)

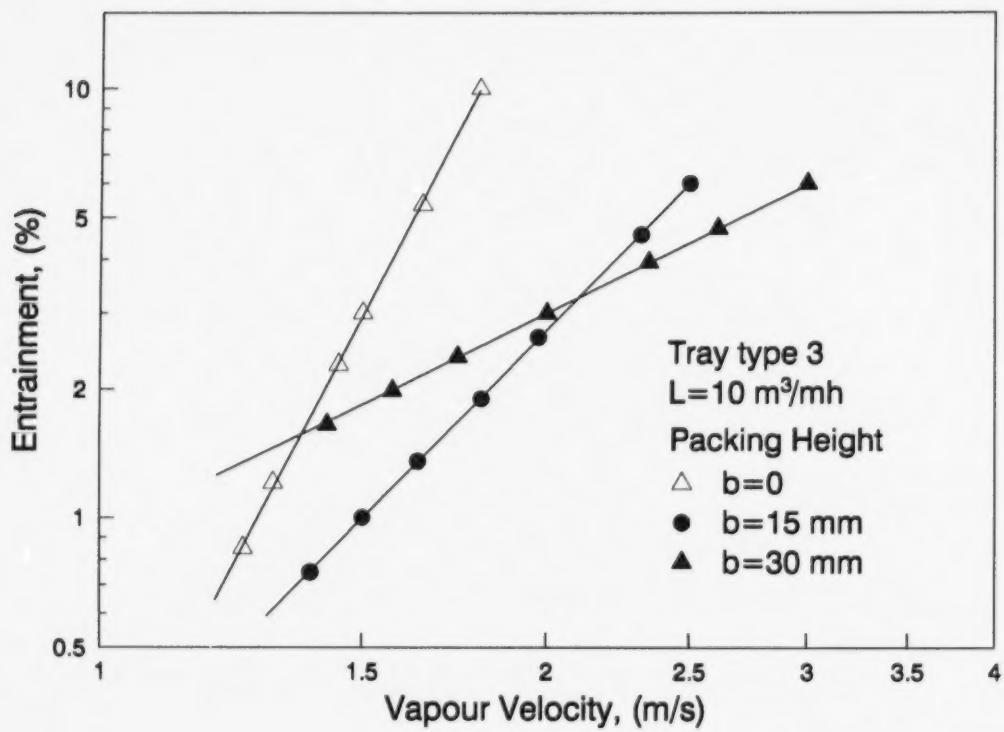

Figure 7-6
Entrainment as a Function of Vapour Velocity
(Air/Water System)

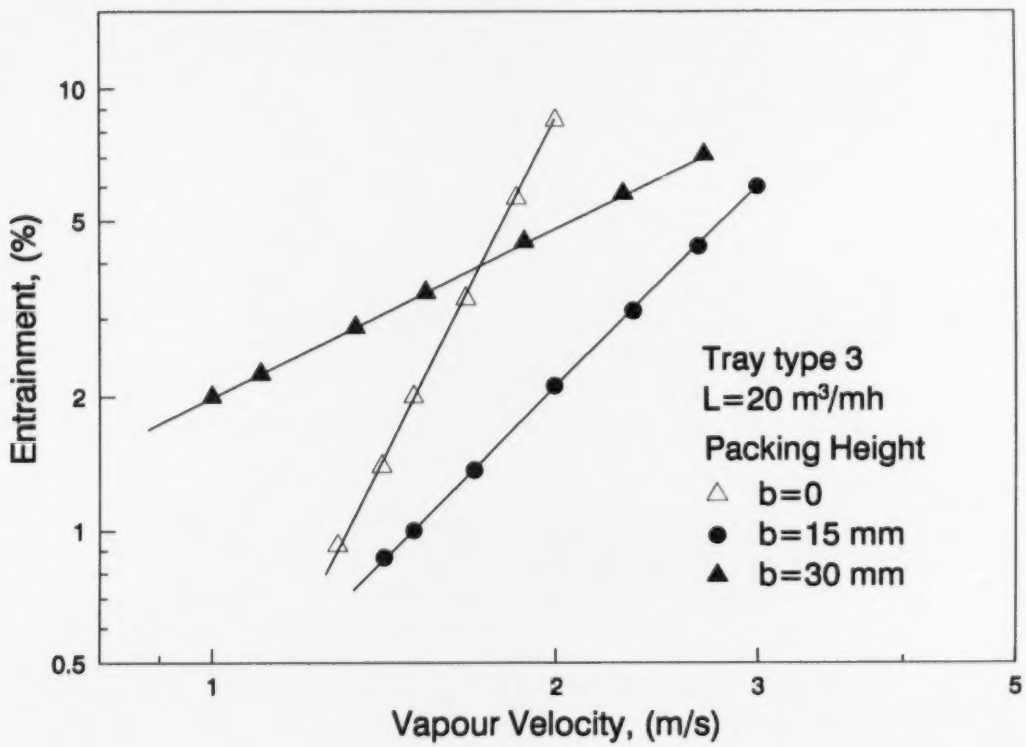

Figure 7-7

Entrainment as a Function of Vapour Velocity
at Different Liquid Flow Rates
(Air/Water System)

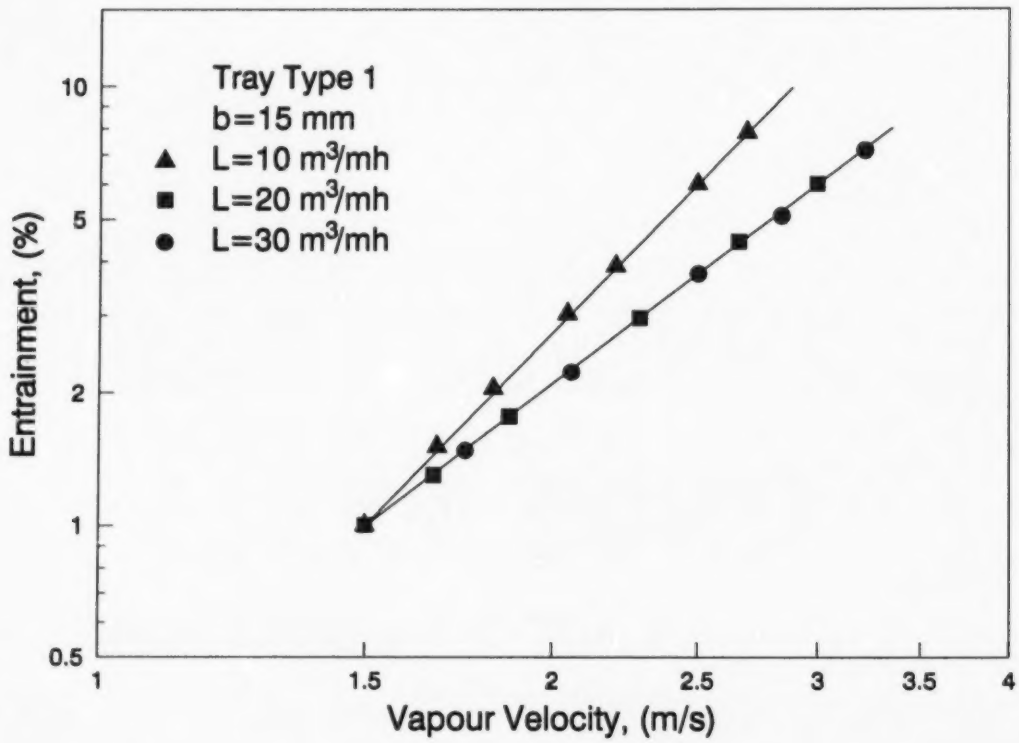

Figure 7-8
Entrainment as a Function of Vapour Velocity
for Different Hole Sizes
(Air/Water System)

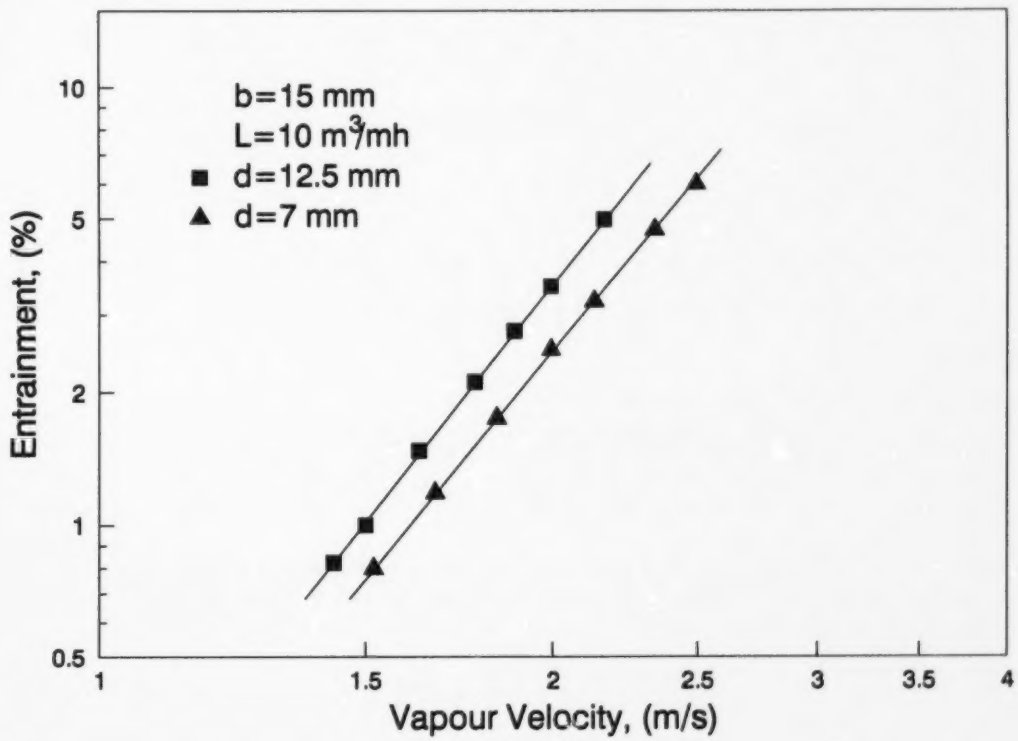

Figure 7-9
Total Pressure Drop as a Function of Vapour Velocity

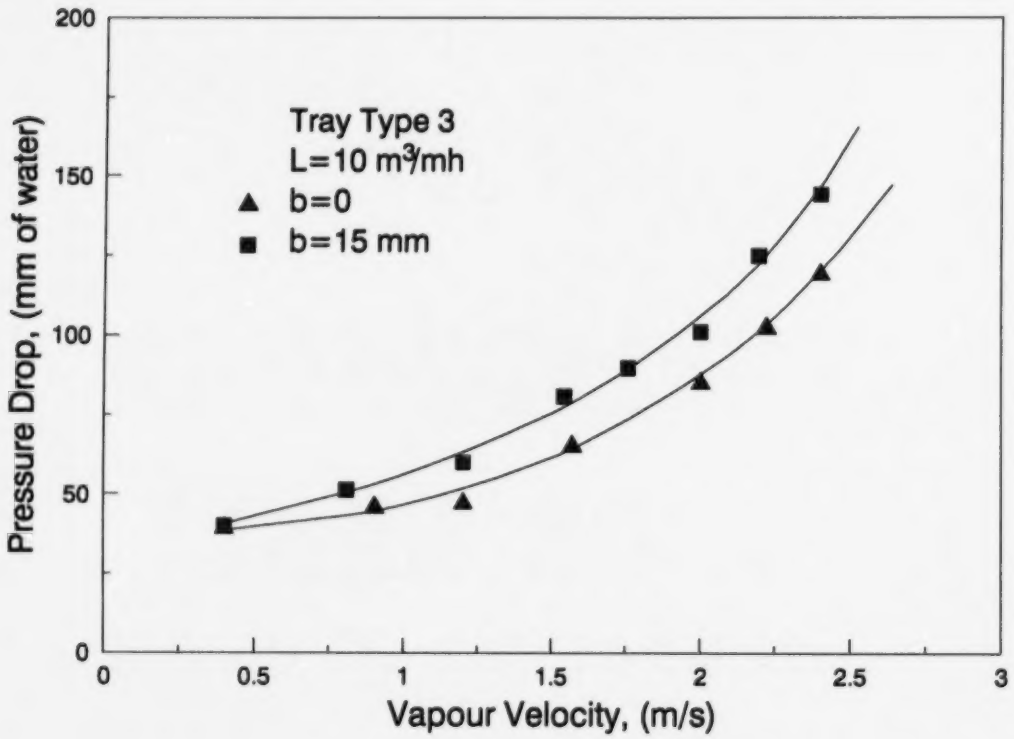

Figure 7-10
Dry Pressure Drop as a Function of Vapour Velocity

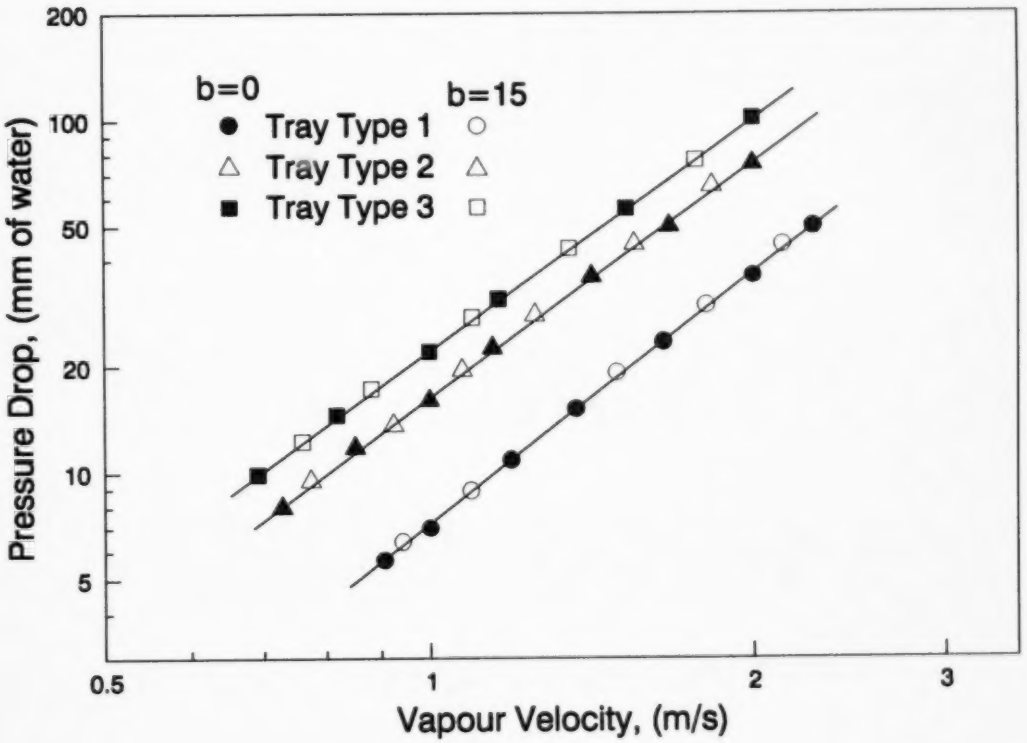

Figure 7-11
Total Pressure Drop as a Function of Vapour Velocity
for Different Hole Sizes

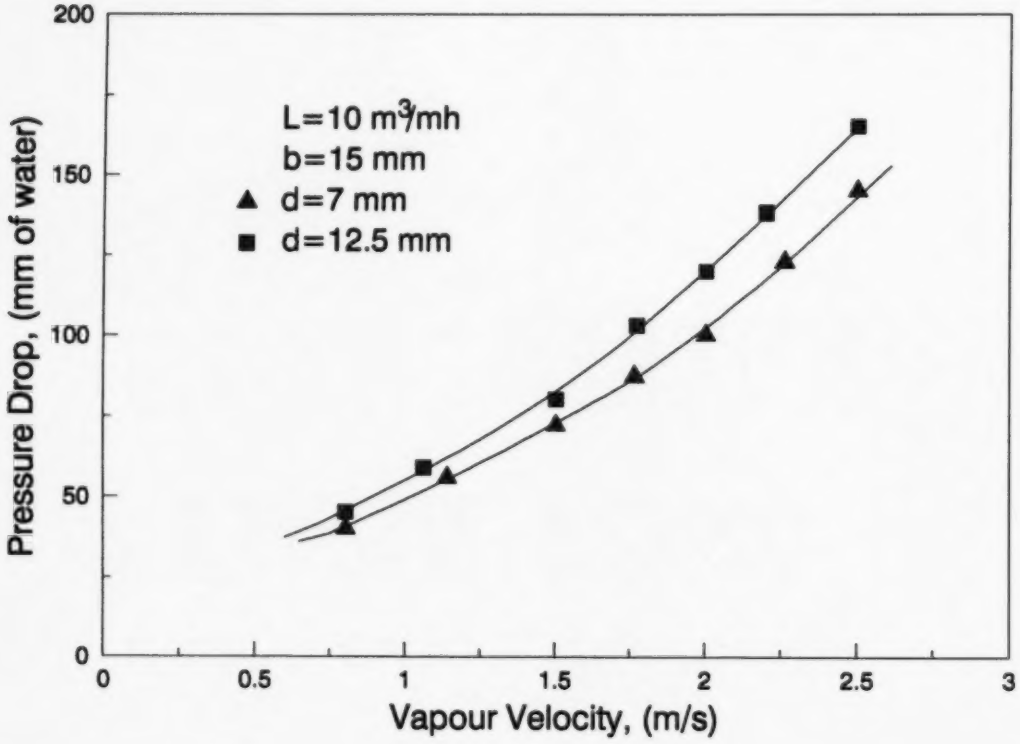

7.6 Literature Cited

Biddulph, M.W. and D.J. Stephens, "Oscillating Behaviour on Distillation Trays", AIChE J. **20**(1), 60-67 (1974).

Biddulph, M.W., J.A. Rocha, J.L. Bravo and J.R. Fair, "Point Efficiencies on Sieve Trays", AIChE J. **37**(8), 1261-1264 (1991).

Fell, C.J.D. and W.V. Pinczewski, "New Considerations in the Design of High Capacity Sieve Trays", The Chem. Engr. (London) **316**, 45-49 (1977).

Jones, J.B. and C. Pyle, "Relative Performance of Sieve and Bubble-Cap Plates", Chem. Eng. Prog. **51**, 424-428 (1955).

Kumar, R. and N.R. Kuloor, "The formation of Bubbles and Drops", Adv. in Chem. Eng. **8**, 255-368 (1970).

Lockett, M.J., G.T. Spiller and K.E. Porter, "The Effect of the Operating Regime on Entrainment From Sieve Trays", Trans. Inst. Chem. Eng. **54**, 202-204 (1976).

Loon, R.E., W.V. Pinczewski and C.J.D. Fell, "Dependence of the Froth-to-Spray Transition on Sieve Tray Design Parameters", Trans. Inst. Chem. Eng. **51**, 374-376 (1973).

Pinczewski, W.V., N.D. Benke and C.J.D. Fell, "Phase Inversion on Sieve Trays", AIChE J. **21**(6), 1210-1213 (1975).

Porter, K.E. and J.D. Jenkins, "Distillation 1979", Institution of Chemical Engineers, London, 5.1/1-5.1/47 (1979).

Prince, R.G.H., A.P. Jones and R.J. Panic, "Distillation 1979", Institution of Chemical Engineers, London, 2.2/27-2.2/39 (1979).

Spagnolo, D.A. and K.T. Chuang, "Improving Sieve Tray Performance with Knitted Mesh Packing", Ind. Eng. Chem. Proc. Des. Dev. **23**, 561-565 (1984).

Zuiderweg, F.J., "Sieve tray - a view on the state of art," Chem. Eng. Sci. **37** (10), 1441-1464 (1982).

Chapter 8

PREDICTING POINT EFFICIENCIES FOR PACKED TRAYS IN DISTILLATION

8.1 Introduction

Photographs taken through the wall of a column typically reveal a bubble size at the wall of about 5 mm (West et al., 1952; Calderbank and Moo-Young, 1960; Calderbank and Rennie, 1962; Rennie and Evans, 1962; Porter et al., 1967; Hobler and Pawelczyk, 1972). For many years, it was believed that this was the characteristic size of bubbles in froth. By comparing measured rates of mass transfer with predictions from mass transfer models, West et al. (1952) deduced a minimum bubble diameter of about 13 mm. Similarly, Garner and Porter (1960) pointed out that for a gas film controlled process, if all the gas passes through the froth as 5 mm diameter bubbles, the plate efficiency would be higher than 99%. But such a high efficiency is rarely found in distillation columns. They estimated that the mean bubble diameter in froth is at least 10 mm to correspond to typically observed point efficiency. Calderbank and Rennie (1962) agreed with this view, and suggested that a portion of gas passes through the froth in the form of very large bubbles and this gas leakage limits the plate efficiencies to the 70 to 80% observed for industrial sieve trays. West et al. (1952), Porter et al. (1967), Lockett et al. (1979), and Ashley and Haseldem (1972) used photographic techniques to show the presence of large bubbles rising rapidly through a swarm of slower moving small bubbles. Burgess and Calderbank (1975), Calderbank and Pereira (1977), who used the "Calderbank probe", reached a similar conclusion. Kaltenbacher (1983) reported that the proportion of the gas passing through the liquid in the

form of large bubbles was about 70 to 90%. The values reported by Porter et al.(1967) were 66 to 87%, and by Ashley and Haselden 68 to 95%. It is evident that the low efficiency of sieve trays is the result of the presence of larger bubbles.

Recently, Prado et al. (1987) determined the bubble size by using probe measurements. They found that the bubble size is bimodal, with large bubbles and small bubbles. Based on the results of probe measurements, Prado and Fair (1990) proposed a fundamental model for predicting sieve tray gas phase and liquid phase efficiency for absorption and desorption systems, but not for distillation systems. In their model for the bulk froth zone the large bubble diameter of 25 mm and the small bubble diameter of 5 mm were used. This further indicated the existence of large bubbles on a sieve tray.

It is expected that higher efficiency will be obtained if the large bubbles can be broken up into small bubbles. Studies of the hydraulic and mass transfer performance of wire mesh packed sieve trays are described in Chapters 6 and 7. It was found that the Murphree tray efficiency increased significantly over a wide range of composition for both surface tension positive and negative systems in a 153 mm diameter distillation column operating in the froth regime. It was also suggested that the increase in efficiency is mainly due to breaking large bubbles into small bubbles by mesh packing.

In this chapter, a model will be described for predicting efficiency of packed trays using the efficiency data for conventional sieve trays. The bubble sizes used in the model were estimated from the photographs taken from the top of the froth on the test tray with and without packing in a 153 mm diameter air/water column. The model is intended to provide a better

understanding of the effect of mesh packing on tray efficiency.

8.2 Model Development

Almost all the models currently available in the literature are empirical and seldom correlated with all the important parameters, such as physical properties and froth structure existing on the tray. The only exception is the model of Prado and Fair (1990, 1987). They obtained models for predicting point efficiencies for systems with all gas phase or all liquid phase resistance on the basis of the dispersion structure and zone-contribution (see Figure 8-1). Their model matched the experimental data very well for the air/oxygen/water system and air/water system used in their study. Such a fundamental model can be modified for predicting the efficiency of distillation systems for trays with and without mesh packing.

Based on the observations of Prado et al. (1987), the dispersion above a sieve tray can be divided vertically into three sections and horizontally into three zones (Prado and Fair, 1990). These sections and zones are shown in Figures 8-1 and 8-2. The individual N_G and N_L in each numbered zone in Figure 8-2 has been modeled by Prado and Fair (1990). They also provided a detailed discussion of each zone. For distillation systems, the point efficiency E_{OG} can be obtained from the individual N_G and N_L shown in Figure 8-2. If a tray operates in the froth regime at low Fa-factors, the mass transfer contribution of the spray zone can be neglected, as proposed by Prado and Fair (1990).

Starting with jetting zone, the point efficiency of this zone, E_{OGFJ} can be given:

$$E_{OGFJ} = 1 - \exp(-N_{OGFJ}) \quad (1)$$

$$N_{OGFJ} = N_{OG1} - \ln(1-E_{OG2}) \quad (2)$$

$$N_{OG1} = 1/(1/N_{G1} + m/N_{L1}) \quad (3)$$

$$E_{OG2} = (1-AJ)\cdot E_{OG2L} + AJ\cdot E_{OG2S} \quad (4)$$

$$E_{OG2L} = 1 - \exp(-N_{OG2L}) \quad (5)$$

$$E_{OG2S} = 1 - \exp(-N_{OG2S}) \quad (6)$$

$$N_{OG2L} = 1/(1/N_{G2L} + m/N_{L2L}) \quad (7)$$

$$N_{OG2S} = 1/(1/N_{G2S} + m/N_{L2S}) \quad (8)$$

where AJ is the volume fraction of small bubbles in the bulk froth zone. Similarly, the point efficiency of the large bubbling zone E_{OGFLB} can be obtained by:

$$E_{OGFLB} = 1 - \exp(-N_{OGFLB}) \quad (9)$$

$$N_{OGFLB} = N_{OG3} - \ln(1-E_{OG4}) \quad (10)$$

$$N_{OG3} = 1/(1/N_{G3} + m/N_{L3}) \quad (11)$$

$$E_{OG4} = (1-AJ)\cdot E_{OG4L} + AJ\cdot E_{OG4S} \quad (12)$$

$$E_{OG4L} = 1 - \exp(-N_{OG4L}) \quad (13)$$

$$E_{OG4S} = 1 - \exp(-N_{OG4S}) \quad (14)$$

$$N_{OG4S} = 1/(1/N_{G4S} + m/N_{L4S}) \qquad (15)$$

$$N_{OG4L} = 1/(1/N_{G4L} + m/N_{L4L}) \qquad (16)$$

The efficiency of the small bubbling zone E_{OGFSB} can be easily obtained:

$$E_{OGFSB} = 1 - \exp(-N_{OGFSB}) \qquad (17)$$

$$N_{OGFSB} = 1/(1/N_{G5} + m/N_{L5}) \qquad (18)$$

Thus the overall point efficiency E_{OG} for a distillation system can be given:

$$E_{OG} = FJ \cdot E_{OGFJ} + FLB \cdot E_{OGFLB} + FSB \cdot E_{OGFSB} \qquad (19)$$

where, according to Prado et al. (1987),

$$FJ = (u_a - u_{a,0})/(u_{a,100} - u_{a,0}) \qquad (20)$$

and

$$u_{a,0} = 0.1\rho_G^{-0.5}\rho_L^{0.692}h_W^{0.132}D_H^{-0.26}A_F^{0.992}L^{0.27} \qquad (21)$$

$$u_{a,100} = 1.1\rho_G^{-0.5}\rho_L^{0.692}h_W^{0.132}D_H^{-0.26}A_F^{0.992}L^{0.27} \qquad (22)$$

$$FSB = 165.65D_H^{1.32}A_F^{1.33} \qquad (23)$$

$$FLB = 1 - FJ - FSB \qquad (24)$$

Equation (19) actually includes three adjustable parameters from the individual models of N_G and N_L in each zone. These parameters are: AJ (small bubble fraction in the bulk froth zone); ψ (adjustment for multiple surface renewals in liquid phase); κ (adjustment to account for mass-transfer enhancement in gas phase). Prado and Fair (1990) found that when:

$$AJ = 0.5372;\ \psi = 2.466;\ \kappa = 3.138,$$

their model is best fitted to the experimental data for the absorption and desorption systems. The large bubble diameter of 25 mm and small bubble diameter of 5 mm in the bulk froth zone was used in their efficiency prediction. For distillation systems, the values of the above three parameters are not known, but can be found by fitting equation (19) to the distillation data obtained in this study.

8.3 Experimental

This study uses the efficiency data from the methanol/water and acetic acid/water systems for trays with and without packing at various Fa-factors and different compositions, as shown in Chapters 6 and 7. An air/water column having the same dimensions as the distillation column used in Chapter 6 was used to reveal the bubble diameters of the dispersion above the test tray. Under dark conditions, using a flash of 1/2000 second duration, photographs were taken from the top of the froth for the tray with and without a bed of 1" mesh packing, under the same operating conditions. Bubble sizes were then estimated from the photographs. The obtained results were used in the efficiency models for trays with and without packing, respectively.

8.4 Results and Discussion

8.4.1 Point Efficiency

Murphree efficiencies, froth height and liquid hold-up for the test tray, with and without packing, were determined at total reflux rates for various concentrations of mixtures and different Fa-factors. The measured

Murphree efficiency is then converted to point efficiency by the AIChE method (AIChE, 1958). The results are shown in Table 8-1 for the methanol/water system and Table 8-2 for the acetic acid/water system, respectively. These results have been discussed in detail in previous chapters.

8.4.2 Bubble diameters

Photographs of the top view of the froth were taken at different Fa-factors under total reflux rates for the test tray with and without packing. Bubbles can be easily identified from the photographs taken at low Fa-factor (Fa=0.5). It was found that for the tray without packing most bubbles have a diameter ranging from 20 to 30 mm, with an average diameter about 25 mm. The small bubbles with a diameter about 5 mm are also seen. But the area occupied by the small bubbles is estimated to be less than 20%. At high Fa-factors, the bubbles become ill-defined and are more difficult to identify. For the tray with a bed of 1" mesh packing, it was found that large bubbles become much smaller. The estimated large bubble diameter is about 10 mm. The proportion of small bubbles (diameter 5 mm) seems about the same as that for the tray without packing. These observations clearly indicate that mesh packing can effectively reduce the large bubble size, hence increase the interfacial area and tray efficiency. The measured bubble sizes from photographs are in good agreement with those back-calculated from measured tray efficiencies in Chapter 7.

8.4.3 Parameter Fitting for the Tray Without Packing

As shown in Figure 8-2, the models for individual N_G and N_L developed

by Prado and Fair (1990) are based on the information from the air/water system. Extrapolation to distillation systems has not been done. The model must be tested against the measured tray efficiency data shown in the Tables 8-1 and 8-2. Nevertheless, equation (19) was directly used to fit the experimental data shown in Tables 8-1 and 8-2. The values of parameter ψ and κ obtained by Prado and Fair (1990) were used, since they are mainly dependent on the froth structure (Prado and Fair, 1990). The value of parameter AJ was found by fitting equation (19) to the experimental data for the two systems at various concentrations (see Tables 8-1 and 8-2). Figures 8-3 and 8-4 show how well the model is fitted to the experimental data for the methanol/water and acetic acid/water system, respectively. The average absolute error is only 1.4% and the maximum error is less than 3.5%. This indicates that the model based on the air/water system can be used for distillation systems with different values of parameter AJ. As shown in Table 8-3, the volume fraction of small bubbles, AJ, depends on the systems and compositions. By carefully examining the physical properties of the system at different concentrations, it was found that all properties at different concentrations are similar except surface tension which changes significantly with concentrations. This suggests that AJ may be a function of surface tension. A computerized regression analysis gave the following correlations with assumption that only surface tension affects AJ:

$$AJ = 0.055\ \sigma^{-0.57} \qquad (25),$$ for the acetic acid/water system,

and $$AJ = 0.016\ \sigma^{-0.97} \qquad (26),$$ for the methanol/water system.

Figure 8-5 shows the relationship between AJ and system surface tension. It seems reasonable that the fraction of small bubbles in the froth increases

as surface tension decreases. Large bubbles with a low surface tension are easier to break up in the intense turbulent velocity field than those with a high surface tension. At a low surface tension, breaking up large bubbles will absorb less surface energy than that at a high surface tension. On the other hand, small bubbles with low surface tension are more stable than those with high surface tension. Equations (25) and (26) give an AJ value of less than 0.25 at surface tension of 0.072 N/m for the air/water system. This result is partially confirmed by photographs which indicate that the small bubble fraction is less than 20%. Figure 8-5 shows that at the same surface tension, AJ of the methanol/water system is larger than that of the acetic acid/water system. This may be because the surface renewal effect enhances the liquid phase mass transfer of the methanol/water system (Chapter 5). As a result, the methanol/water system has a higher point efficiency than the acetic acid/water system at the same surface tension (see Tables 8-1 and 8-2).

8.4.4 Predicting Efficiency for the Packed Tray

It has been shown that equation (19) can be applied to the two distillation systems by using different parameter values of AJ. It may also be suitable for the tray with packing by using different bubble sizes in the model. It has been found that a packed tray generates smaller large bubbles. Therefore, to use the model discussed above, the large bubble diameter of 25 mm should be replaced by the bubble diameter found on the packed tray, about 10 mm. Packing seems to have no effect on small bubble diameter and on the volume fraction of small bubbles. It has been shown that parameters ψ and κ are constant and assumed to be independent of hydrodynamics on the tray

(Prado and Fair, 1990). Thus, the values of parameters found for the tray without packing are still used for the tray with packing to test the model against the measured tray efficiency. The results for the two systems are shown in Figures 8-6 and 8-7. The average absolute error is 2.0%. It can be seen from Figures 8-6 and 8-7 that the model seems to be somewhat under-predicting the tray efficiency for both systems. This suggests that packing may also have effects on the hole activity zone. Because of the addition of packing on the tray floor, some bubbles at holes may not fully reach their usual formation size, as described by Prado et al. (1987), but rather be broken up by the packing into smaller bubbles.

The original models developed by Prado and Fair (1990) for individual N_G and N_L in each zone (see Figure 8-2) are based on information from the air/water system. However, the model may also be applied to distillation systems with different values of AJ for different systems and for trays with and without packing. This may be because the development of the model is based on the fundamental fluid mechanics existing on the tray. It is encouraging that the model has so successfully reproduced the experimental results obtained in distillation for trays with and without packing, and that it seems versatile. Figures 8-8 and 8-9 are the parity plots of measured versus calculated tray efficiency.

It is obvious that the models obtained for trays without packing in this study still have much room for improvement. The models have not accounted for the mass transfer in the spray zone. Therefore, they can be used only at low vapour velocities in the froth regime. Because the large bubble size (25 mm) and small bubble size (5 mm) used in the model were obtained from the air/water system, they are not expected to be suitable for

other systems. It is believed that bubble sizes are functions of system physical properties such as surface tension and densities (Chapter 2). If one uses constant bubble sizes, then the fraction of small bubbles present in the froth AJ will be different for different systems as shown in Section 8.4.3. More experimental data are required to substantiate equations (25) and (26). Only then can the efficiency models obtained in this study be reliably used for other systems.

For an existing column, the point efficiency or Murphree efficiency is usually known. It is important for a designer to know how much improvement the packing can achieve. If the point efficiency E_{OG}, froth height h_f, and liquid hold-up h_l are known, the values of these three parameters can be determined by fitting the model to the known efficiencies. For trays with packing, it is suggested that a large bubble diameter of 10 mm in the bulk froth zone should be used without changing the parameter values. The froth height and liquid height of packed trays should be 20% and 10% higher than that of tray without packing. If the measured efficiency data are not available, they should be calculated by the new efficiency correlations obtained in Chapter 2. Then the improvement in efficiency by mesh packing can be estimated by the method described above.

8.5 Conclusions

Photographs of froth on trays with and without packing have been obtained. Bubble diameters were estimated from those photographs. It was found that with a bed of 1" mesh packing the large bubble diameter is reduced from 25 mm to 10 mm. Based on these results, a model has been obtained for estimating the efficiency of trays with packing from that of

trays without packing. The calculated point efficiencies agree well with experimental data for two systems with different concentrations.

8.6 Nomenclature

A_F = fraction free area, m^2

AJ = fraction of small bubbles present in the bulk froth zone

D_H = tray hole diameter, m

E_{OG} = over all point efficiency, gas composition basis

E_{OGFJ} = E_{OG} corresponding to jetting zone of Figure 1

E_{OG2} = E_{OG} corresponding to zone 2 of Figure 2

E_{OG2L} = E_{OG} corresponding to zone 2 of Figure 2 for large bubbles

E_{OG2S} = E_{OG} corresponding to zone 2 of Figure 2 for small bubbles

E_{OGFLB} = E_{OG} corresponding to large bubbling zone of Figure 1

E_{OG4} = E_{OG} corresponding to zone 4 of Figure 2

E_{OG4L} = E_{OG} corresponding to zone 4 of Figure 2 for large bubbles

E_{OG4S} = E_{OG} corresponding to zone 2 of Figure 2 for small bubbles

E_{OGFSB} = E_{OG} corresponding to small bubbling zone of Figure 1

Fa = active area F-factor, $(kg/m)^{0.5}/s$

FJ = fraction of active holes that are jetting

FLB = fraction of active holes that are issuing large bubbles

FSB = fraction of active holes that are issuing small bubbles

h_W = weir height, m

L = volumetric liquid flow rate, m^3/s m of weir

m = slope of equilibrium line

N_G = number of gas phase transfer units

N_L = number of liquid phase transfer units

N_{OG} = number of overall gas phase transfer units

N_{OGFJ} = N_{OG} corresponding to jetting zone of Figure 1

N_{OG1} = N_{OG} corresponding to zone 1 of Figure 2

N_{OG2L} = N_{OG} corresponding to zone 2 of Figure 2 for large bubbles

N_{OG2S} = N_{OG} corresponding to zone 2 of Figure 2 for small bubbles

N_{G1} = N_G corresponding to zone 1 of Figure 2

N_{L1} = N_L corresponding to zone 1 of Figure 2

N_{G2L} = N_G corresponding to zone 2 of Figure 2 for large bubbles

N_{G2S} = N_G corresponding to zone 2 of Figure 2 for small bubbles

N_{L2L} = N_L corresponding to zone 2 of Figure 2 for large bubbles

N_{L2S} = N_L corresponding to zone 2 of Figure 2 for small bubbles

N_{OGFLB} = N_{OG} corresponding to large bubbling zone of Figure 1

N_{OG3} = N_{OG} corresponding to zone 3 of Figure 2

N_{OG4L} = N_{OG} corresponding to zone 4 of Figure 2 for large bubbles

N_{OG4S} = N_{OG} corresponding to zone 4 of Figure 2 for small bubbles

N_{G3} = N_G corresponding to zone 3 of Figure 2

N_{L3} = N_L corresponding to zone 3 of Figure 2

N_{G4L} = N_G corresponding to zone 4 of Figure 2 for large bubbles

N_{G4S} = N_G corresponding to zone 4 of Figure 2 for small bubbles

N_{L4L} = N_L corresponding to zone 4 of Figure 2 for large bubbles

N_{L4S} = N_L corresponding to zone 4 of Figure 2 for small bubbles

N_{OGFSB} = N_{OG} corresponding to small bubbling zone of Figure 1

N_{OGFSB} = N_{OG} corresponding to small bubbling zone of Figure 1

N_{G5} = N_G corresponding to zone 5 of Figure 2

N_{L5} = N_L corresponding to zone 5 of Figure 2

u_a = superficial gas velocity, based on active area, m/s

$u_{a,0}$ = superficial gas velocity, based on active area at 0% jetting, m/s

$u_{a,100}$ = superficial gas velocity, based on active area at 100% jetting, m/s

x = mole fraction of more volatile component in liquid

Greek Letters

κ = factor that accounts for gas phase mass transfer enhancements

ρ_G = vapour density, kg/m^3

ρ_L = liquid density, kg/m^3

σ = surface tension, N/m

ψ = factor that accounts for multiple surface renewals in the Higbie model

Subscripts

G = gas phase

L = liquid phase

Table 8-1

Experimental Data for Methanol/Water System

x	Fa	Sieve tray h_l	Sieve tray h_f	Sieve tray E_{OG}	Packed tray h_l	Packed tray h_f	Packed tray E_{OG}
0.06	0.6	0.027	0.045	0.50	0.03	0.055	0.86
	0.8	0.026	0.047	0.48	0.03	0.059	0.83
	1.0	0.025	0.050	0.45	0.03	0.062	0.80
	1.2	0.024	0.053	0.41	0.03	0.065	0.76
0.20	0.6	0.027	0.047	0.65	0.03	0.057	0.91
	0.8	0.026	0.050	0.63	0.03	0.060	0.88
	1.0	0.025	0.054	0.60	0.03	0.064	0.85
	1.2	0.024	0.057	0.56	0.03	0.067	0.81
0.40	0.6	0.027	0.050	0.72	0.03	0.064	0.98
	0.8	0.026	0.053	0.69	0.03	0.069	0.95
	1.0	0.025	0.058	0.66	0.03	0.073	0.92
	1.2	0.024	0.061	0.61	0.03	0.076	0.89
0.72	0.6	0.027	0.053	0.79	0.031	0.071	0.99
	0.8	0.026	0.055	0.75	0.031	0.074	0.98
	1.0	0.025	0.060	0.72	0.031	0.077	0.95
	1.2	0.024	0.064	0.67	0.031	0.080	0.93
0.85	0.6	0.027	0.056	0.83	0.031	0.074	0.99
	0.8	0.026	0.059	0.80	0.031	0.078	0.99
	1.0	0.025	0.063	0.77	0.031	0.082	0.99
	1.2	0.024	0.067	0.72	0.031	0.087	0.97

Table 8-2

Experimental Data for Acetic Acid/Water System

x	Fa	Sieve tray h_l	Sieve tray h_f	Sieve tray E_{OG}	Packed tray h_l	Packed tray h_f	Packed tray E_{OG}
0.61	0.5	0.023	0.043	0.61	0.028	0.064	0.97
	0.75	0.022	0.047	0.59	0.028	0.068	0.93
	1.0	0.021	0.051	0.57	0.028	0.072	0.89
	1.22	0.020	0.054	0.55	0.028	0.075	0.85
0.72	0.5	0.023	0.042	0.59	0.028	0.057	0.91
	0.75	0.022	0.045	0.57	0.028	0.060	0.88
	1.0	0.021	0.049	0.55	0.028	0.063	0.83
	1.22	0.020	0.052	0.53	0.028	0.065	0.80
0.82	0.5	0.023	0.040	0.54	0.028	0.050	0.87
	0.75	0.022	0.044	0.52	0.028	0.055	0.83
	1.0	0.021	0.047	0.50	0.028	0.058	0.78
	1.22	0.020	0.050	0.48	0.028	0.061	0.75
0.92	0.5	0.023	0.039	0.48	0.028	0.044	0.73
	0.75	0.022	0.042	0.46	0.028	0.047	0.69
	1.0	0.021	0.045	0.44	0.028	0.050	0.66
	1.22	0.020	0.048	0.42	0.028	0.053	0.64

Table 8-3

Parameter values of AJ

	x	AJ
Methanol/water system	0.06	0.2796
	0.20	0.4696
	0.40	0.5374
	0.72	0.6247
	0.85	0.6891
Acetic acid/water system	0.61	0.4355
	0.72	0.4240
	0.82	0.3720
	0.92	0.3265

Figure 8-1
Hydraulic Model of the Dispersion
Above a Sieve Tray

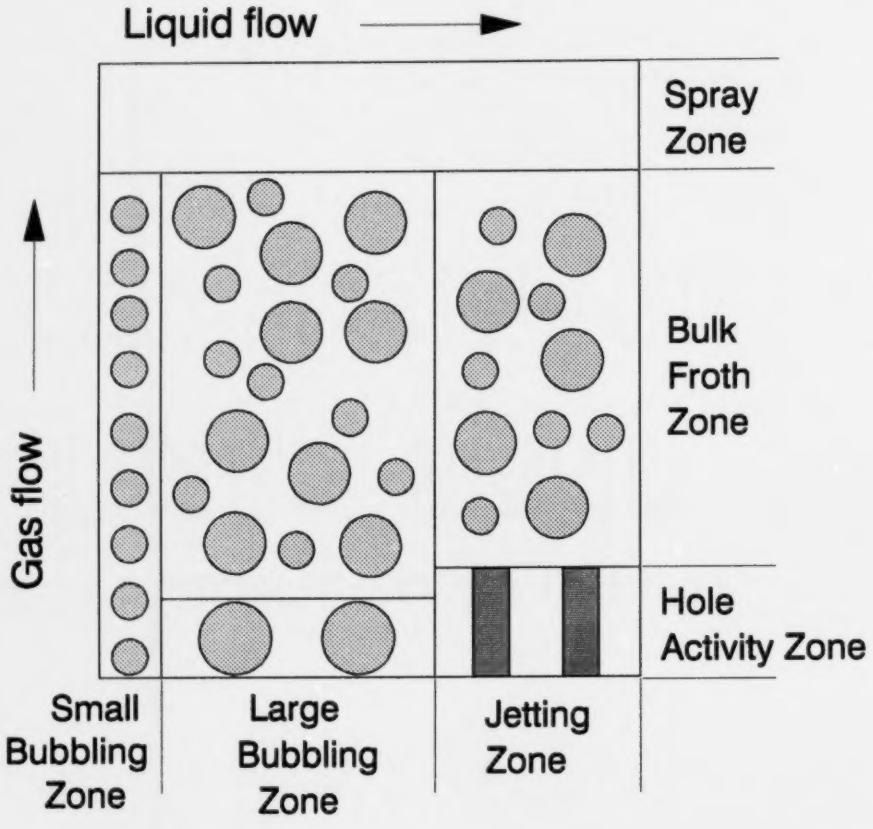

Figure 8-2
Number of Mass Transfer Units
Above a Sieve Tray

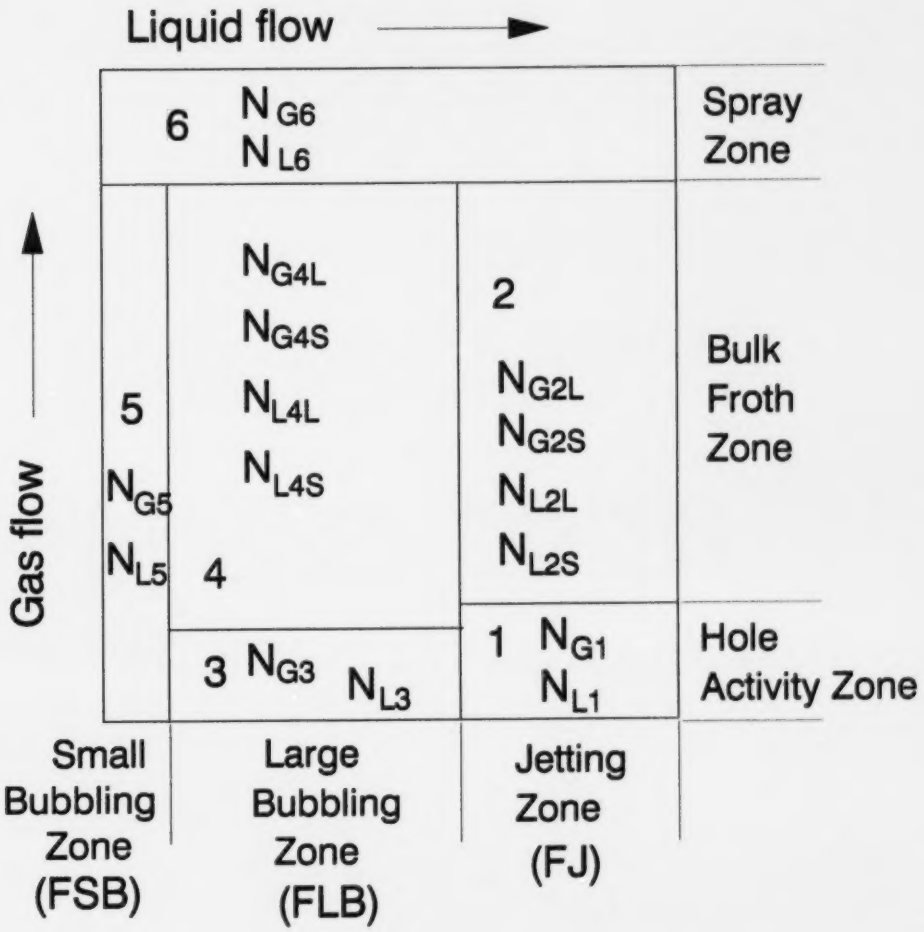

Figure 8-3
Comparison of Experimental and Calculated Mass Transfer Efficiency (Tray Without Packing)

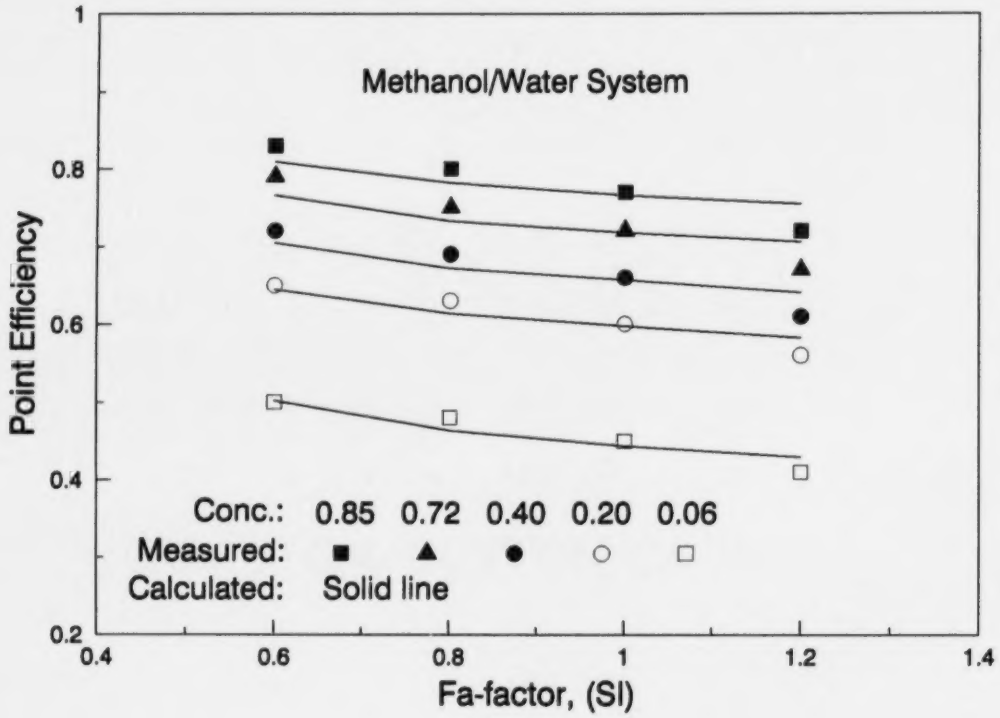

Figure 8-4
Comparison of Experimental and Calculated Mass Transfer Efficiency (Tray Without Packing)

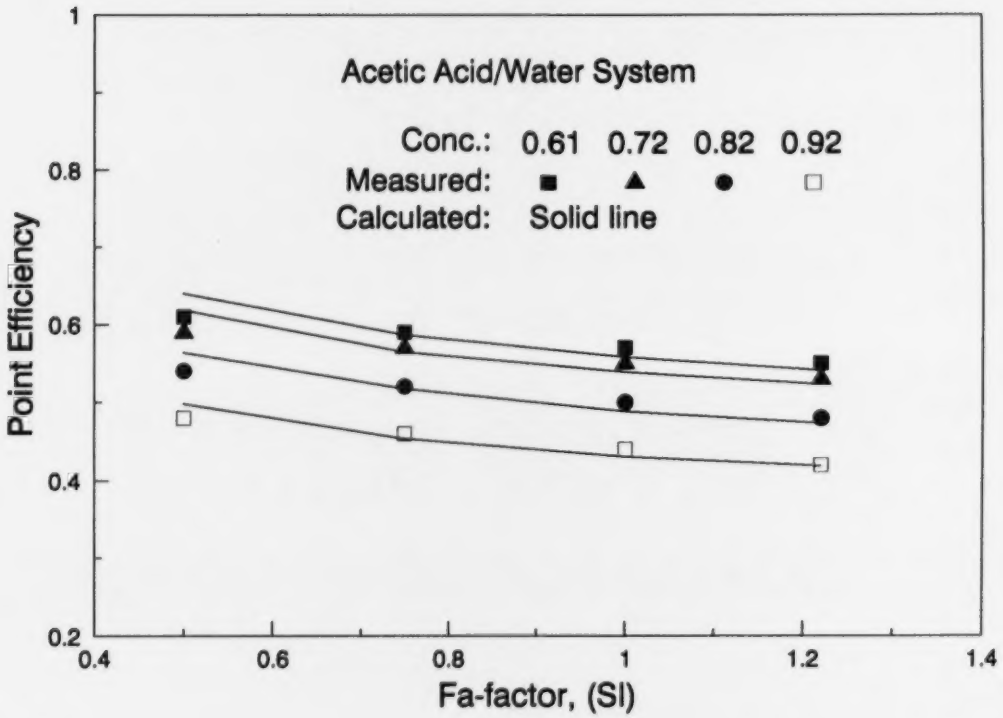

Figure 8-5
Plot of AJ vs Surface Tension

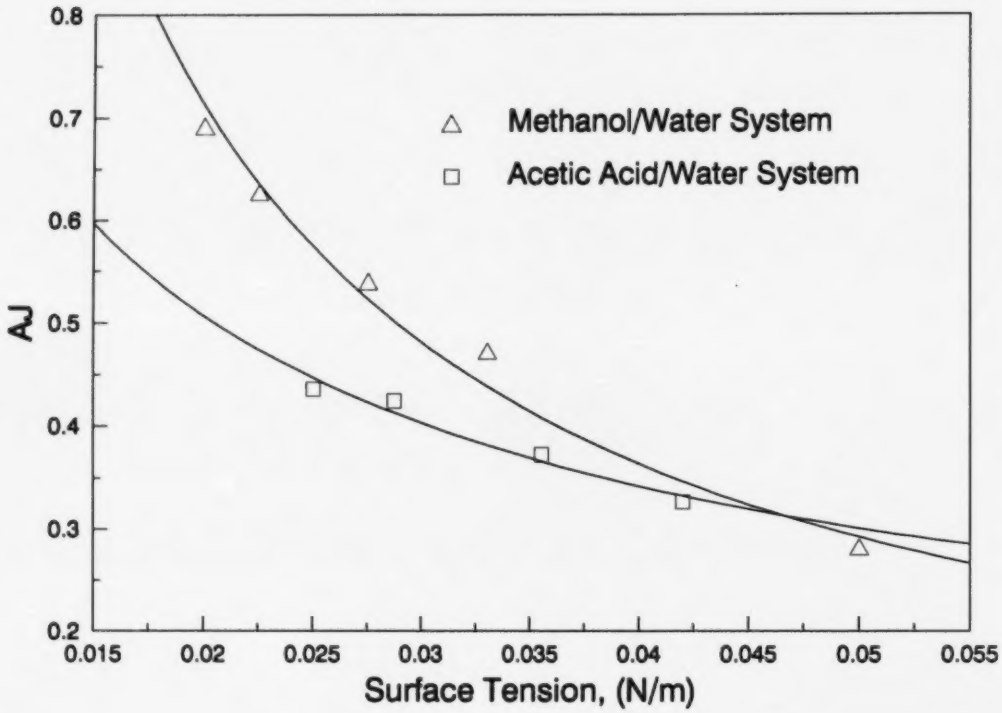

Figure 8-6
Comparison of Experimental and Calculated Mass Transfer Efficiency (Tray With Packing)

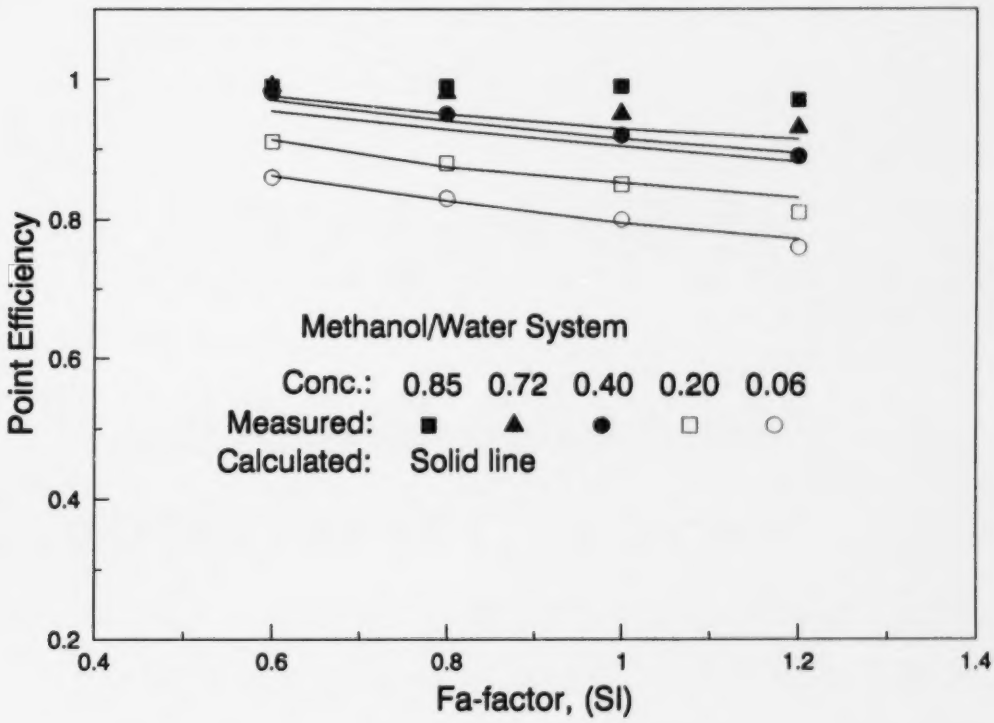

Figure 8-7
Comparison of Experimental and Calculated Mass Transfer Efficiency (Tray With Packing)

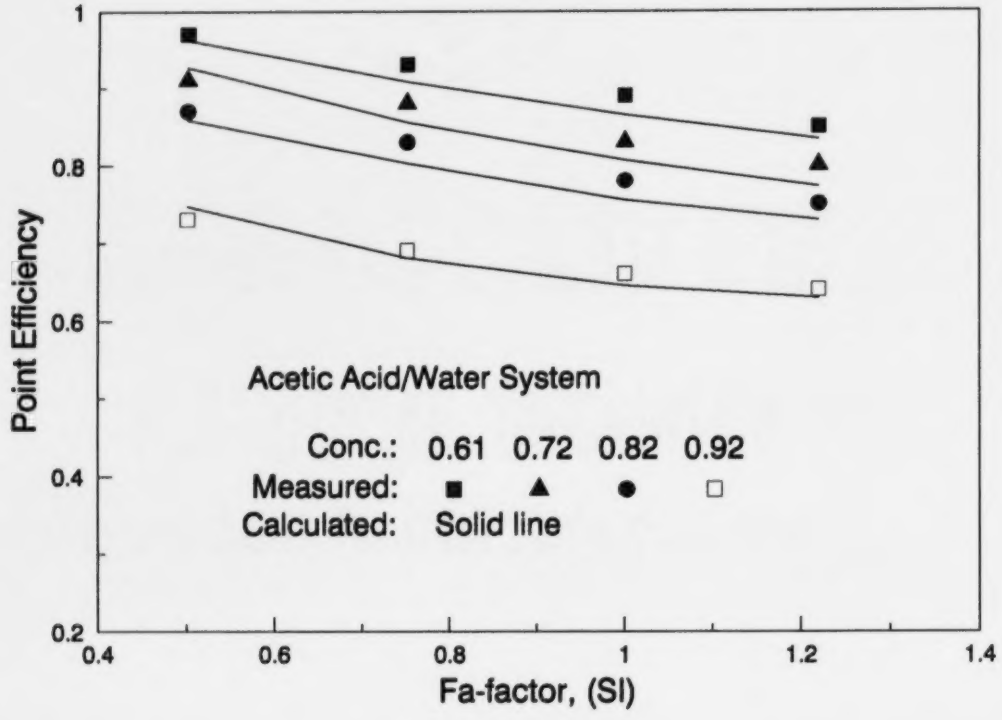

Figure 8-8
Correlation of Tray Efficiency Parity Plot
(Tray Without Packing)

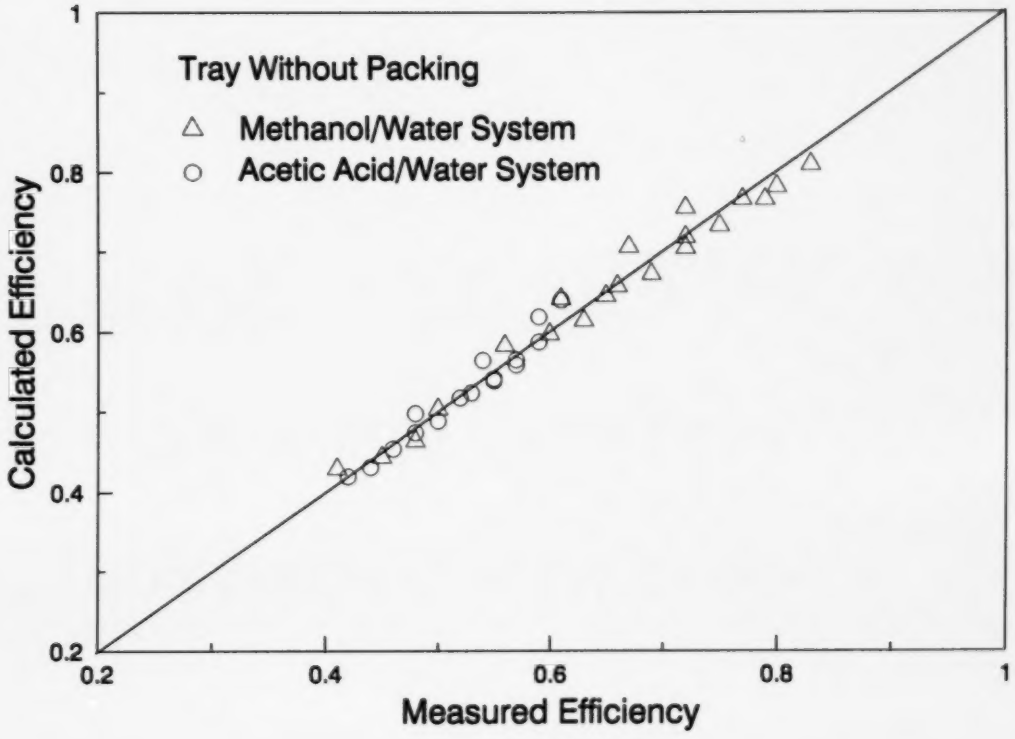

Figure 8-9
Correlation of Tray Efficiency Parity Plot
(Tray With Packing)

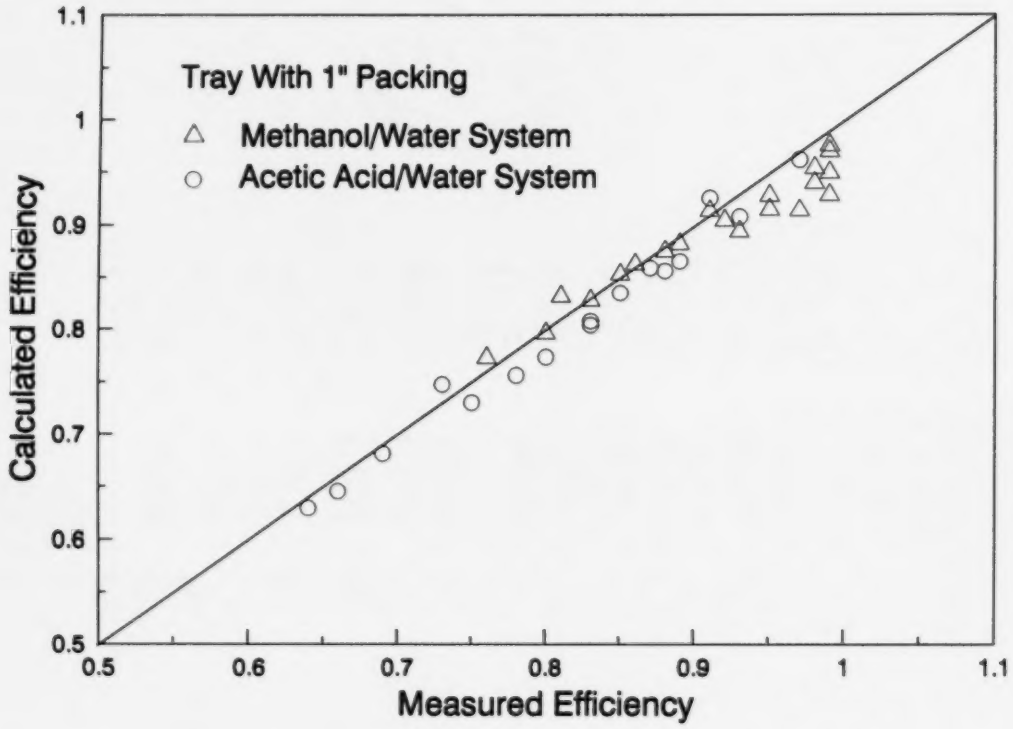

8.7 Literature Cited

AIChE, "Bubble tray design manual", New York (1958).

Ashley, M.J. and G.G. Haselden, "Effectiveness of vapour-liquid contacting on a sieve plate", Trans. Inst. Chem. Engrs. **50**, 119-124 (1972).

Burgess, J.M. and P.H. Calderbank, "The measurement of bubble parameters in two phase dispersions", Chem. Eng. Sci. **30**, 743-750, and 1107-1121 (1975).

Calderbank, P.H. and M.B. Moo-Young, "The mass-transfer efficiency of distillation and gas-absorption plate columns - Part 1", Int. Symp. on Distillation, Inst. Chem. Engrs., Brighton, 59-72 (1960).

Calderbank, P.H. and J. Rennie, "The physical properties of foams and froths formed on sieve plates", Trans. Inst. Chem. Engrs. **40**, 3-12 (1962).

Calderbank, P.H. and J. Pereira, "The prediction of distillation plate efficiencies from froth properties", Chem. Eng. Sci. **32**, 1427-1433 (1977).

Garner, F.H. and K.E., Porter, "Mass transfer stages in distillation", Int. Symp. on Distillation, Ins. Chem. Engrs., Brighton (1960), 43-50.

Hobler, T. and P. Pawelczyk, "Interfacial area in bubbling through a slot", Brit. Chem. Engng. and Proc. Tech. **17**(7/8), 624 (1972).

Kaltenbacher, E., "On the effect of the bubble size distribution and the gas-phase diffusion on the selectivity of sieve trays", Chem. Eng. Fund. **1**, 47-68 (1983).

Lockett, M.J., R.D. Kirkpatrick and M.S. Uddin, "Froth regime point efficiency for gas-film controlled mass transfer on a two-dimensional sieve tray", Trans. Inst. Chem. Engrs. **57**, 25-34 (1979).

Porter, K.E., B.T. Davies and P.F.Y. Wong, "Mass transfer and bubble sizes in cellular foams and froths", Trans. Inst. Chem. Engrs. **45**, T265-T273 (1967).

Prado, M., K.L. Johnson, and J.R. Fair, "Bubble-to-spray transition on sieve tray", Chem. Eng. Prog. **83**(3), 32-40 (1987).

Prado, M., and J.R. Fair, "Fundamental model for the prediction of sieve tray efficiency", Ind. Eng. Chem. Res. **29**, 1031-1042 (1990).

Prado, M., and J.R. Fair, "Fundamental model for the prediction of sieve tray efficiency", Inst. Chem. Engrs. Symp. Series No.**62**, A529-553 (1987).

Rennie, J. and F. Evans, "The formation of froths and foams above sieve plates", Brit. Chem. Engng, **7**(7), 498 (1962).

West, F.B., W.D. Gilbert and T. Shimizu, "Mechanism of mass transfer on bubble plates", Ind. Eng. Chem. **44**, 2470-2478 (1952).

Chapter 9

FOULING OF SIEVE TRAYS

9.1 Introduction

Sieve trays are the most widely used internal in distillation and absorption applications. Numerous studies have been made to better understand tray efficiency, pressure drop, capacity, weeping and entrainment rates. Previous chapters have shown that a bed of mesh packing on sieve trays can increase the tray efficiency significantly. However, fouling may occur on the mesh packing, which in turn may reduce the tray lifetime. Sieve trays are often used where fouling may be encountered. However, not much work has been down in the study of sieve tray fouling and the mechanisms of fouling are not well understood.

Fouling is a phenomenon which occurs with or without a temperature gradient in a great deal of industrial, domestic and natural processes which involve the contact of a fluid with a surface. It may be defined as the accumulation of undesired solid materials at the interface. The presence of foulant in sieve tray holes reduces the hole diameter, consequently, this results in an increase in tray pressure drop and entrainment, and a decrease in capacity and tray efficiency.

It is clear that fouling of sieve trays represents additional energy and maintenance costs. The purpose of this study is to improve understanding of tray fouling, and to provide the opportunity to reduce the cost through the optimum design and operation of tray columns. It would be highly desirable if reliable fouling data could be obtained on full scale

---

A version of this Chapter has been submitted for publication. Chen, G.X., A. Afacan and K.T. Chuang 1993. Chem. Eng. Comm..

commercial sieve tray equipment using the actual fluids. However, it is almost impossible because parameters affecting the fouling vary considerably throughout the equipment and with time. In addition, the properties of the fouling fluid vary considerably due to process and feed stock fluctuations. Furthermore, commercial sieve tray columns are often not equipped with the parameter monitoring devices to permit reliable data acquisition. As a result, knowledge of the fouling processes may be obtained only in the laboratory.

The objectives of this study are: (a) to investigate the mechanisms of crystallisation and particulate fouling on sieve trays; (b) to examine the fouling of sieve trays combined with mesh packing; (c) to develop a mathematical model for predicting the fouling rate in terms of total tray pressure drop as a function of time.

9.2 Background

Fouling is an extremely complex phenomenon. It can be characterized as a combined momentum, mass and heat transfer, and chemical reaction process. Six distinguishable categories have been identified according to the principal process which gives rise to the fouling phenomenon.

1. Crystallisation or precipitation fouling: The precipitation of dissolved substances on the solid surface. Where a solution evaporated beyond the solubility limits of a dissolved salt; or a solution of normal solubility is cooled below its solubility temperature; or a solution of inverse solubility is heated above the solubility limit temperature.
2. Particulate fouling: The accumulation of solids suspended in the process fluid on to a solid surface. In a minority of instances settling by gravity

prevails, and the process may then be referred to as sedimentation fouling.

3. Chemical reaction fouling: Deposits formed at the surface by one or more chemical reactions between reactants contained in the flowing fluid in which the surface material itself is not a reactant.

4. Biological fouling: The deposition and growth of micro-organisms or macro-organisms originating in the process stream on the surface.

5. Corrosion fouling: The surface itself reacts to produce corrosion products which foul the surface and may promote the attachment of other foulants.

6. Freezing or solidification fouling: Fouling due to the freezing of a liquid or some of its higher melting constituents on the surface.

Unfortunately, almost no industrial fouling is due to only one mechanism. Most industrial fouling processes involve several mechanisms such as a combination of crystallisation and corrosion in heavy water sieve tray units (Burrill, 1981).

9.3 Experimental

A glass air-water column having 153 mm diameter, containing three glass sections spaced 0.318 m apart was set up to carry out the tray fouling tests at constant gas velocity to closely simulate a typical sieve tray operation. The schematic diagram of the apparatus is shown in Figure 9-1. The middle tray was a test tray equipped with a manometer for measuring total pressure drop across the tray. The top tray was used to collect the entrainment which was measured by recording time elapsed to fill a container. The bottom tray acted as an air distributor as well as a collector for weeping liquid. Three trays with different hole sizes were used in this study. Detailed dimensions

of the column and the test trays are shown in Table 9-1. The test runs were made at ambient pressures and at steady state conditions. The liquid to the column was pumped through a flow recorder controller and a heater. The dry air was passed through a flow recorder controller, a heater, and if necessary, a saturater. Temperatures of liquid and air were measured by thermocouples. Two sets of test runs, at Fa=1.3 and Fa=2.2, were conducted for each tray. In addition, runs using tray type 1 with different liquid and air temperatures, and humidities were also studied for comparison. During the tests, total pressure drop across the test tray was measured and recorded at desirable time intervals.

In order to study the effect of mesh packing on tray fouling, all tests were repeated with a bed of 1" mesh packing on the tray. The results were compared with those of the same tray without packing.

For easy comparison, a tray lifetime has been defined as the time required for the total pressure drop to increase to 4 times the initial total pressure drop.

9.4 Results and Discussion

9.4.1 Particulate Fouling

Water containing 2 wt.% flour was fed to the column while air saturated with water was entering the air distributor. Because air is saturated with water before entering the column, evaporation of water in the column is avoided. The total pressure drop of the test tray was measured and recorded with time. No change in pressure drop was observed in 48 hours of operation for the three different trays (see Table 9-1 for dimensions) at various Fa-factors. When flour was replaced by a different density solid $Ca(OH)_2$,

the results were identical. When a bed of 1" mesh packing was placed on the tray, no fouling was observed. Visual observations confirmed that the holes and the packing remained clean. These results suggest that fouling with a dirty feed, if occurs, proceeds very slowly. Therefore, tray fouling by the solids in the liquid feed may be studied only over a long experimental period.

9.4.2 Crystallisation Fouling

The tests were carried out with dry air passing through an aqueous solution saturated with $NaHCO_3$ on the test tray. The column was operated under the total reflux rate with fixed air and liquid flow rates. The experimental results obtained are shown in Figures 9-2 to 9-4 for the three trays. Detail experimental conditions for these runs are presented in Table 9-2.

1. Mechanism of Formation

A sketch of the fouling process is shown in Figure 9-5. Crystals became visible around the circumference of the hole on the bottom edge of the tray as seen in (a). They then grew to cover the bottom edge of the holes (step (b) and (c)) and finally reached a formation similar to (d) in which only a very small channel was left for air to pass. It was found that the pressure drop remained unchanged until step (b), at which point the pressure drop began to increase rapidly as seen from Figures 9-2 to 9-4. The top portion of the hole remained clean during the entire experiment. This can be explained by the presence of a thin liquid film on the inside of the holes (see Figure 9-6). This liquid film was confirmed by high speed photography of air flow through a sieve tray hole covered with water by Burril (1981).

The liquid film at the top portion of the hole is renewed between gas bubbles. Because of the high frequency of bubbles, the contact time for the liquid film at the top portion is not long enough to deposit crystals. Once a bubble detaches from the top edge of the hole, new solution from the tray floor replaces the saturated solution and pushes it to the bottom portion of the hole. The saturated solution spreads down the hole to the bottom edge of the tray due to surface tension. The liquid film at the bottom edge of the hole is evaporated by the upward moving gas leaving crystals on the bottom edge of the hole (Figure 9-5 (a)). As crystals accumulate at the bottom of the hole (Figure 9-5 (b) to (d)), the hole becomes partially blocked and the pressure drop begins to increase.

2. Effect of Tray Design and Operating Conditions on Fouling Rates

At an active area Fa-factor (Fa) 1.3, no weeping was observed for trays 1 and 2. It can be seen from Figures 9-2 to 9-4 that increasing the Fa-factors increases the fouling rates and reduces the tray lifetimes. This is because the higher the Fa-factors, the larger the hole air velocities, as a result, the faster the mass transfer rate of water into air. Thus, trays have shorter lifetimes at higher Fa-factors, as shown in Figures 9-2 to 9-4. Because the hole air velocity is inversely proportional to tray open hole area, it can be expected that trays with a larger open hole area will have a longer life time than trays with a smaller open hole area, at fixed Fa-factors. Comparison among Figures 9-2, 9-3 and 9-4 shows that trays with larger hole sizes have longer lifetimes despite with the same open hole area and at the same Fa-factors. This can be explained by the fact that, with the same open hole area, trays with larger hole sizes have a smaller total surface area (ie., circumference) contacting with air. It is obvious that

the smaller the surface area for mass transfer, the slower the mass transfer rates and the longer the tray lifetime.

Figure 9-4 shows that no change in the pressure drop occurred on tray 3 for 10 hours at Fa=1.3 because of tray weeping. Although crystals at the bottom of the tray were found, they were unable to accumulate because of a small amount of weeping through the hole. When a tray begins to weep, the liquid around the bottom edge of the hole is washed down to the next tray. The liquid film at the bottom of the hole is therefore continuously being replaced. This results in no accumulation of crystals in holes. Further tests on a dual-flow tray in the same column revealed that no fouling occurs on dual-flow trays. These results suggest that operating under weeping conditions will eliminate tray fouling due to crystallisation. Weeping, however, reduces the tray efficiency, and thus, operating at these conditions may not be practical. It can be concluded that dual-flow trays could be the best choice for fouling services.

3. Effect of Mesh Packing

As shown in Figures 9-2 to 9-4, a bed of 1" mesh packing on the tray can shorten tray lifetime by 40% for tray 1 to 75% for tray 3. This is due to the depositions on the packing directly above the holes. The depositions were found on the first two layers of packing above the hole openings and in the holes. It was found that before the holes were completely filled by the depositions, the pressure drop had started to increase quickly. This indicates that fouling on the packing is the controlling factor for packed tray lifetime. Comparing Figures 9-2, 9-3, and 9-4, one can find that the fouling of packed trays is less dependent on Fa-factors and hole sizes due to fouling on the packing. These results suggest that the packing reduces

the tray lifetime more at low Fa-factors and for trays with large holes.

3. Effect of Other Factors

Increasing the temperature of the liquid or the air will increase the water evaporation rate, and consequently, will increase the deposition rate. It was found that the lifetime of tray 1 is reduced by 40% when liquid temperature increases from 20^0C to 34^0C. This is shown in Figure 9-7. It was also found that increasing the humidity of the inlet air reduces the fouling rate, presumably due to smaller mass transfer driving force. Tests with air saturated with water indicated no fouling at all conditions. These findings agree with the proposed mechanism of fouling at tray holes.

9.4.3 Mathematical Modeling

Fouling on sieve trays reduces the hole diameter and increases the total tray pressure drop. It is desirable to develop a mathematical model for predicting fouling rate in terms of pressure drops as a function of time. For conventional sieve trays, total pressure drop is given:

$$h_T = h_D + h_L \qquad (1)$$

where h_D is the dry pressure drop and h_L is the hydrostatic head measured from the tray floor. The dry pressure drop can be measured without liquid loads on the tray or can be estimated by using the orifice equation:

$$h_D = \frac{\xi \rho_G U_h^2}{2g\rho_L} \qquad (2)$$

where ξ can be obtained by the equation of Cervenka and Kolar (1973):

$$\xi = \frac{0.94(1-\phi^2)}{\phi^{0.2}(\delta/d_h)^{0.2}} \qquad (3)$$

$$U_h = Q_h/(\pi R^2) \qquad (4)$$

The hydrostatic head h_L can be estimated by equations developed by Bennett et al. (1983). For a fixed tray design and constant liquid and gas load conditions, h_L can be considered constant. Because the fractional open hole area ϕ is small, it may be assumed that $1-\phi^2 \simeq 1$. Substituting equations (2), (3) and (4) into equation (1) gives:

$$h_T = A/R^{4.2} + B \qquad (6)$$

where R is the radius of holes which changes with time when fouling occurs in the holes. "A" and "B" are assumed to be constant for a fixed tray design and at constant liquid and gas loadings. The first term on the right hand side of equation (6) is actually the dry pressure drop, and the second term the liquid pressure drop.

Since fouling is a complex process, the following assumptions were made to simplify the analysis of crystallisation fouling:

1. The liquid film is thin relative to the hole radius;
2. Crystallisation occurs due to evaporation of water only;
3: Evaporation of water inside holes is the rate controlling step;
4. Any heat transfer effect due to evaporation can be neglected;

Evaporation of water from the liquid film in holes can be considered a steady state two dimensional mass transfer problem. In a cylindrical coordinate system as shown in Figure 9-6, a mass balance gives the partial differential equation describing the water concentration in the air:

$$D\frac{\delta^2 W}{\delta r^2} + \frac{D}{r}\frac{\delta W}{\delta r} = U_h \frac{\delta W}{\delta z} \qquad (7)$$

where D: diffusivity of water vapour in air, m^2 / s;

W: concentration of water vapour in air at any r and z, kg H_2O/kg air;

U_h: velocity of air in the sieve hole, m/s, assumed independent of r and z.

The boundary conditions for equation (7) are:

1. $\frac{\delta W}{\delta r} = 0$, at r=0 for all z; 2. $W = W_s$, at r=R for all z.

The initial condition for equation (7) is:

$W = 0$, at z=0 for all r.

If the air has no water vapour at the tray hole inlet, the solution to equation (7) is (Carslaw and Jaeger, 1959):

$$W = W_s - \frac{2W_s}{R} \sum_1^{\infty} \left[e^{-D\alpha_n^2 \frac{z}{U_h}} \right] \left[\frac{Jo(r\alpha_n)}{\alpha_n J_1(R\alpha_n)} \right] \qquad (8)$$

where W_s: saturation of water vapour in air;

R: hole radius at time t, m;

z: distance from hole inlet, m;

r: radial location in hole, m;

α_n: zero for $J_0(R\alpha_n)$, that is $J_0(R\alpha_n) = 0$;

J_0: zero order Bessel function of first kind;

J_1: first order Bessel function of first kind.

The concentration gradient of water vapour in air at the film surface can determine the evaporation rate of water from the film. This rate may be written as:

$$E(z) = D\rho_G \frac{\delta W}{\delta r} \Bigg|_{r=R} \qquad (9)$$

where E(z): evaporation rate at z, kg H_2O /(m^2s);

ρ_G: density of air, kg/m^3.

$(\delta W/\delta r)$ at r=R can be found numerically as a function of (R^2U_h/Dz) from equation (8). When the value of (Dz/R^2U_h) is in the range of 0.001 to 0.1, an empirical expression has been obtained by log-log plot.

$$(\delta W/\delta r) = \frac{W_s}{4R}\left[\frac{R^2U_h}{Dz}\right]^{2/3}, \qquad \text{at r=R.} \qquad (10)$$

In order to evaluate the maximum value of E(z), the maximum $(\delta W/\delta r)$ at r=R should be obtained. It is obvious that the maximum value of $(\delta W/\delta r)$ is at z=0. Unfortunately $(\delta w/\delta r)$ at z=0 is infinite at r=R. But experimental results show that E(z) is finite. Thus, it was obtained by fitting the experimental data of tray 1 at F_a= 1.3. The proper value of $(\delta W/\delta r)$ was found to be:

$$\text{Max}(\delta W/\delta r) = 8\frac{W_s}{R}\left[\frac{R^2U_h}{D}\right]^{2/3}, \text{ at r=R.} \qquad (11)$$

It should be noted that (R^2U_h) is a constant if the run conditions are unchanged. Assuming that all the solute in the evaporating solution deposits on the hole wall where the evaporation takes place, then the deposit rate is simply:

$$N = E\ S \qquad (12)$$

where N: deposition rate of $NaHCO_3$, kg/m^2s;

S: solubility of $NaHCO_3$ at operating temperature, kg $NaHCO_3$/kg H_2O.

Because of the depositions, the radius changes with time and can be expressed as:

$$dR = -\frac{N}{\rho_s}\,dt \qquad (13)$$

where ρ_s: density of solute kg/m^3;

t: time.

Substituting equations (12), (11), and (9) into equation (13) gives:

$$R\ dR/dt = -8D\ \rho_G S(W_s - W_i)\ (R^2 U_h/D)^{2/3}\ /\rho_s \qquad (14)$$

Integration of equation (14) from R_0 to R, and time from t_0 to t, produces:

$$R^2 = R_0^2 - 16D\rho_G S(W_s - W_i)(t-t_0)\ (R^2 U_h/D)^{2/3}\ /\rho_s \qquad (15)$$

Finally the pressure drop can be expressed by substituting equation (15) into equation (6).

$$h_T = \frac{A}{(\ R_0^2 - 16D\ \rho_G S(W_s - W_i)(t-t_0)(R^2 U_h/D)^{2/3}\ /\rho_s\ )^{2.1}} + B \qquad (16)$$

or:

$$h_T = \frac{A\ /\ R_0^{4.2}}{(\ 1\ - 16D\ \rho_G S(W_s - W_i)(t-t_0)(R^2 U_h/D)^{2/3}\ /\rho_s R_0^2\ )^{2.1}} + B \qquad (17)$$

where $(A/R_0^{4.2})$, B and t_0 are determined experimental for each test run. The calculated results are shown in Figures 9-8 to 9-10 together with those measured experimentally for comparison. It can be seen that the model worked well for trays 1 and 2 for all run conditions despite the fact that $(\delta W/\delta r)$ at r=R was obtained by using tray 1 at F_a= 1.3 only. However, the model was unable to predict the pressure drop versus time for tray 3. The reason is that the crystals inside the holes of tray 3 are so thick that they fall off the holes during the test, and thus accurate experimental results can not be obtained.

9.5 Conclusions

Sieve tray fouling due to the deposition of solids was studied experimentally in an air/water column. For an air/water system containing insoluble solids, no fouling was observed for trays with and without packing

during the experimental period of 48 hours. For crystallisation fouling, deposition of solids was found inside holes and at the bottom of the tray. It was found that trays with larger hole sizes have a longer lifetime than trays with small hole sizes despite the same open hole area. For the same tray, the fouling rate is higher at the high gas rates, and no fouling occurs when trays operate under weeping conditions. No fouling was observed for dual flow trays under all conditions. Therefore dual flow trays are recommended for fouling services. A bed of 1" mesh packing on the tray can shorten the tray life by more than 40% to 75% because of fouling on the packing. A mathematical model for predicting crystallisation fouling rate in terms of the total pressure drop was developed. The model could predict the pressure drop versus time for sieve trays with hole diameters less than 10 mm.

9.6 Nomemclature

A =constant

B =constant

D =diffusivity of water in air, m^2/s

d_h =sieve hole diameter, m

E =evaporation rate, kg water/m^2s

F_a = Active area F-factor, $(kg/m)^{0.5}/s$

F_h = Hole F-factor, $(kg/m)^{0.5}/s$

g =acceleration due to gravity, m/s^2

h_D =tray dry pressure drop, cm of liquid

h_L =h_T-h_D, cm of liquid

h_T =total pressure drop across wet tray, cm of liquid

N =deposition rate of $NaHCO_3$, kg $NaHCO_3/m^2s$

Q_h =vapour flow rate of each hole, m^3/s

R_0 =initial radius of sieve hole, m

R =radius of sieve hole, m

r =radial location in hole, m

S =solubility of $NaHCO_3$, kg $NaHCO_3$/kg water

t =time, s

U_h =hole vapour velocity, m/s

W =water concentration in air, kg water/kg air

W_s =saturated water concentration in air, kg water/kg air

z =distance from hole inlet, m

Greek

ξ =coefficient

ρ_G =vapour density, kg/m^3

ρ_L =liquid density, kg/m^3

ρ_S =$NaHCO_3$ density. kg/m^3

δ =thickness of sieve tray, m

ϕ =fraction of open hole area

Table 9-1

Column and Tray Dimensions

Column diameter	0.153 m
Total column cross-sectional area	0.0184 m^2
Active area	0.014 m^2
Downcomer area	0.0022 m^2
Hole diameter	
Tray type 1	4.76 mm
Tray type 2	9.53 mm
Tray type 3	12.7 mm
Open hole area	0.00086 m^2
Tray thickness	2.5 mm
Outlet weir height	0.063 m
Weir length	0.1104 m
Tray spacing	0.318 m

Table 9-2

Run Conditions

Run No.	Tray type	Fa	Packing*	Air Temp.* °C	Liq. Temp.* °C	A/Ro^4 cm of water	B
1	1	1.3	No	20	20	1.8	2.4
2	1	2.2	No	20	20	3.7	2.6
3	1	1.3	Yes	20	20	2.0	3.1
4	1	2.2	Yes	20	20	4.0	3.8
5	2	1.3	No	20	20	2.8	2.6
6	2	2.2	No	20	20	4.2	2.8
7	2	1.3	Yes	20	20	3.1	3.3
8	2	2.2	Yes	20	20	5.1	3.9
9	3	1.3	No	20	20	3.4	2.6
10	3	2.2	No	20	20	5.9	3.0
11	3	1.3	Yes	20	20	4.0	3.4
12	3	2.2	Yes	20	20	6.1	4.0
13	1	1.3	No	20	35	1.8	2.4

* All runs at total reflux using dry air and saturated solution.

* Packing: 1" height mesh packing (York Demister style 431)

Figure 9-1
Schematic Diagram of Experimental Apparatus

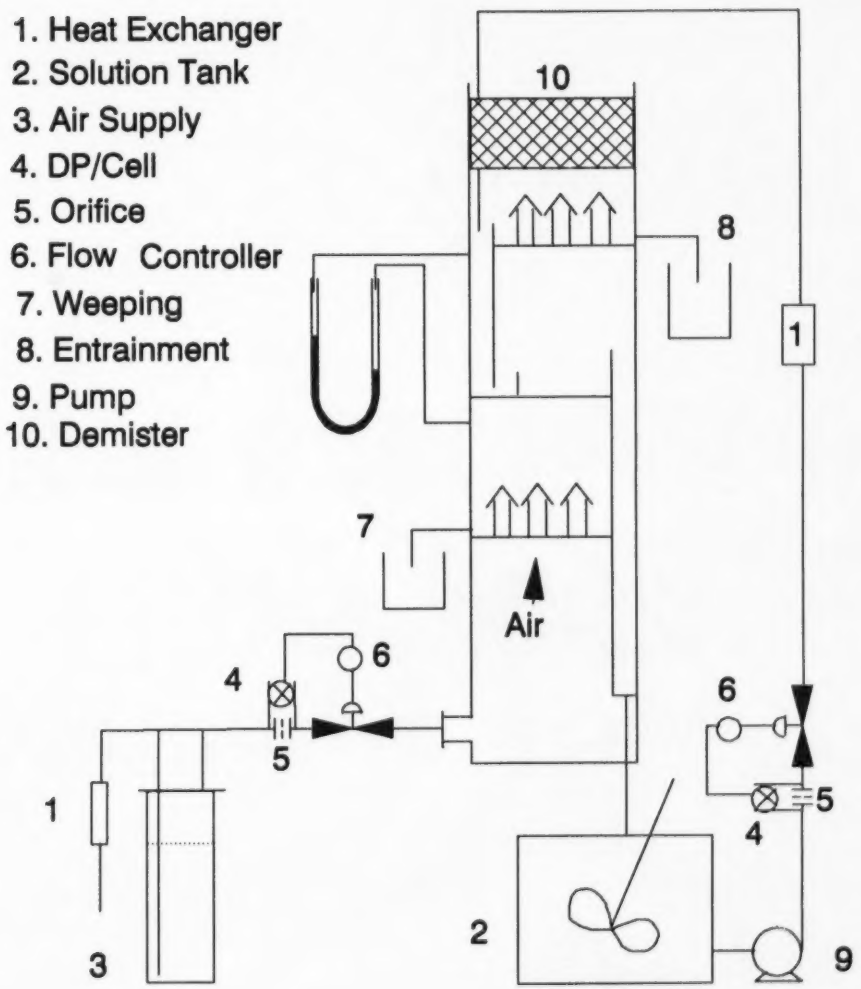

Figure 9-2
Pressure Drop Ratio vs Time for Tray 1 in the Column for Crystallisation Fouling

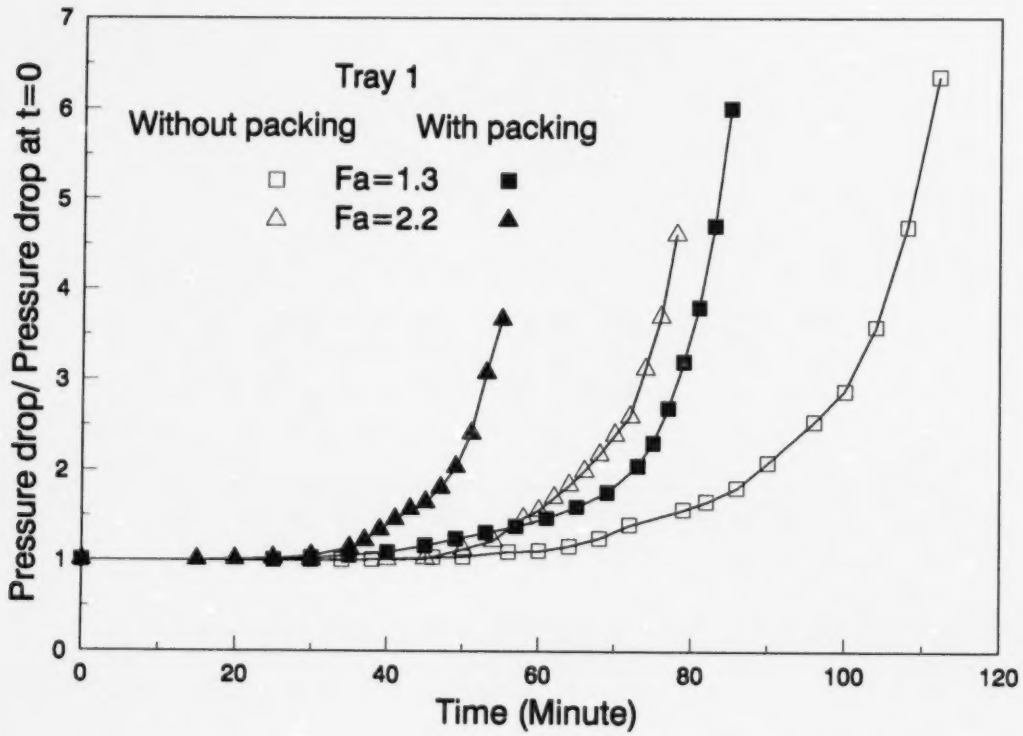

Figure 9-3
Pressure Drop Ratio vs Time for Tray 2 in the Column for Crystallisation Fouling

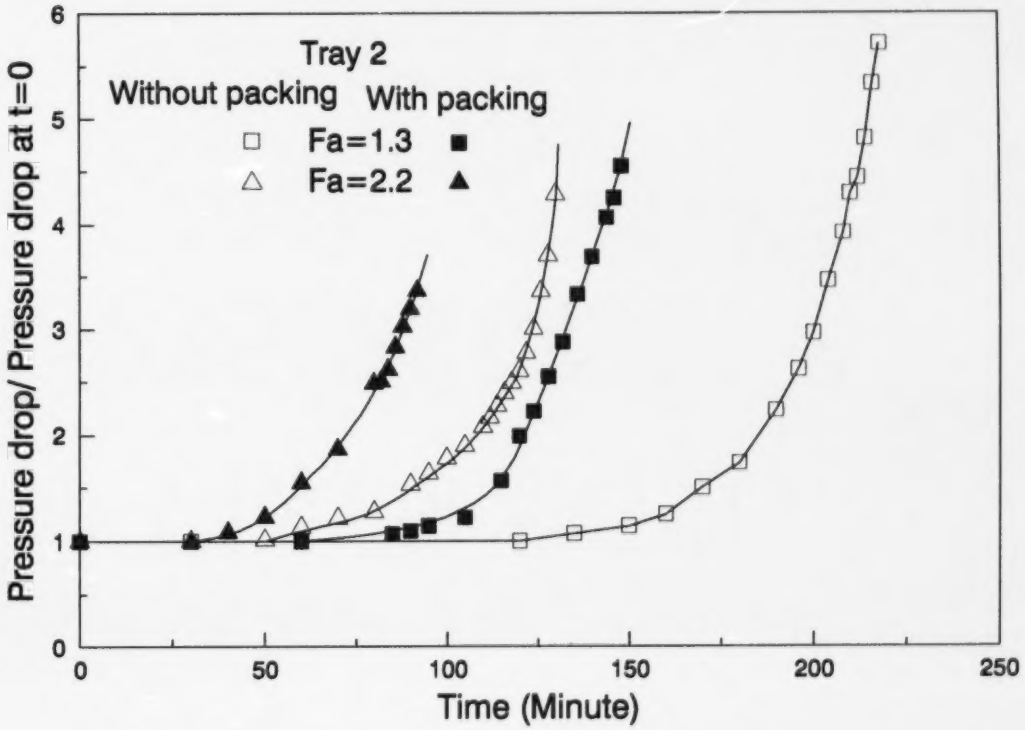

Figure 9-4
Pressure Drop Ratio vs Time for Tray 3 in the Column for Crystallisation Fouling

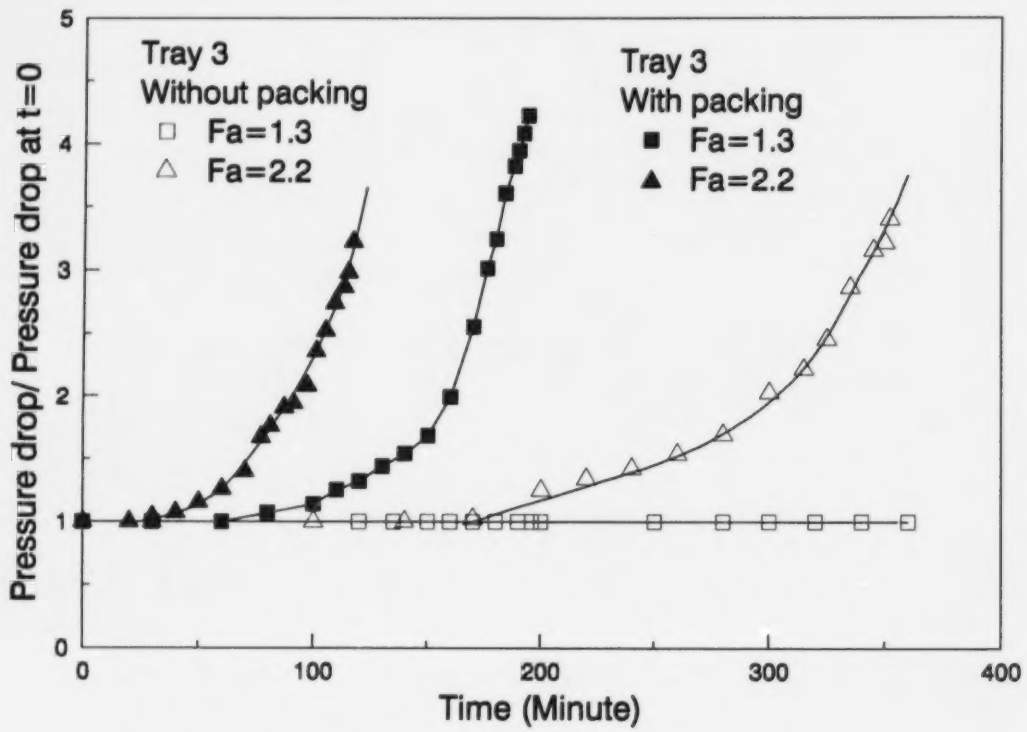

Figure 9-5
Schematic of Visual Observation of Fouling
Processes of a Sieve Tray

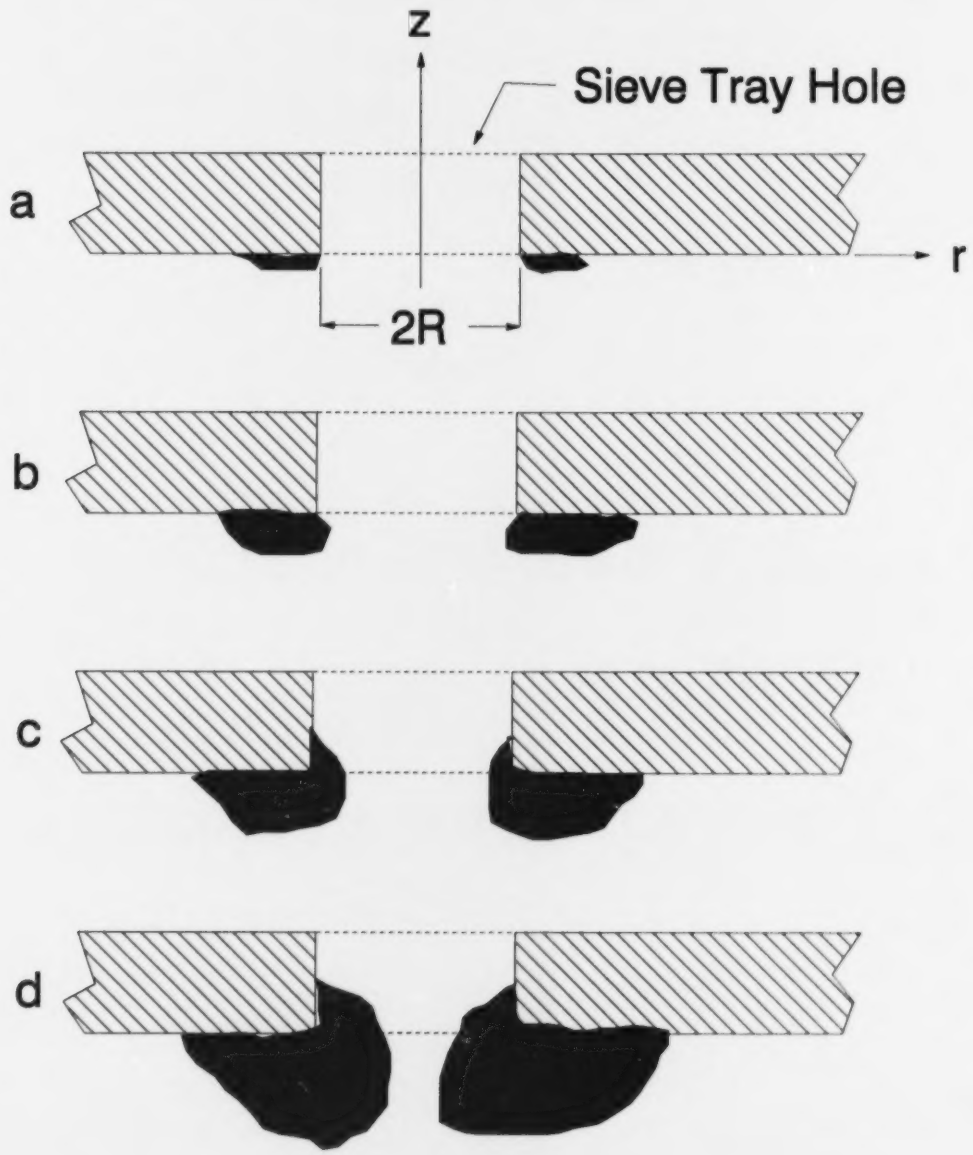

Figure 9-6
Crystallisation Fouling Mechanism in a Tray Hole for the Proposed Model

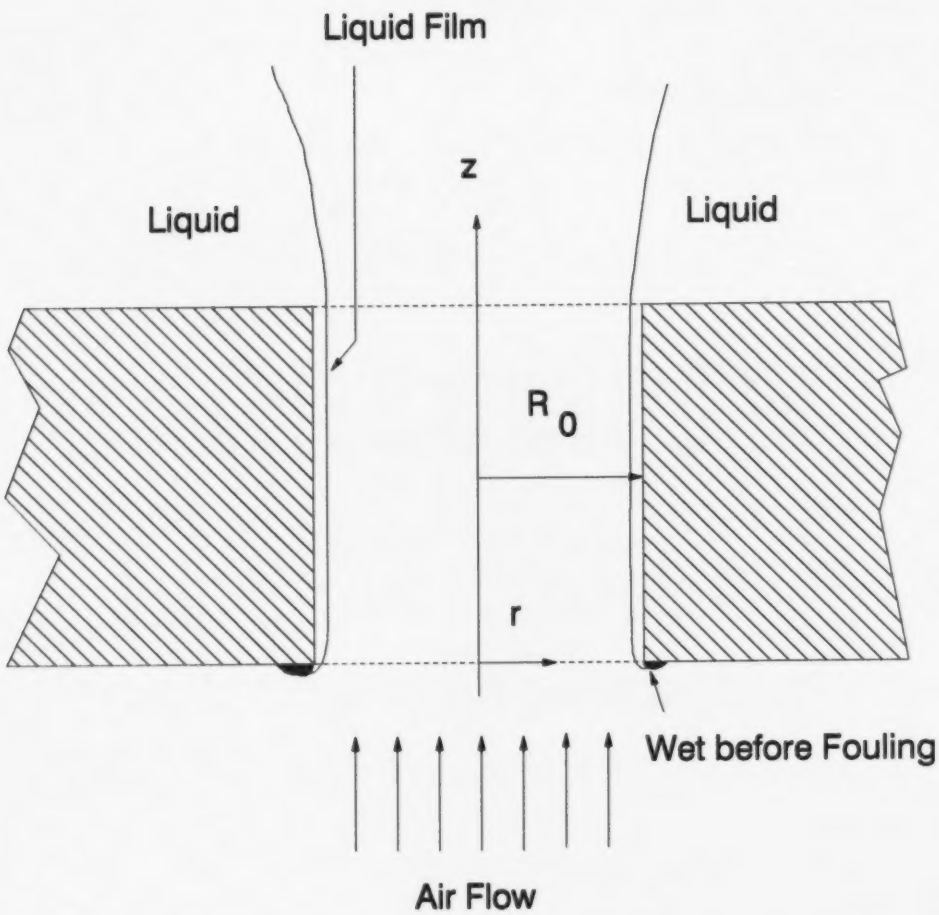

Figure 9-7
Pressure Drop Ratio for Tray 1 at Two Temperatures in the Column for Crystallisation Fouling

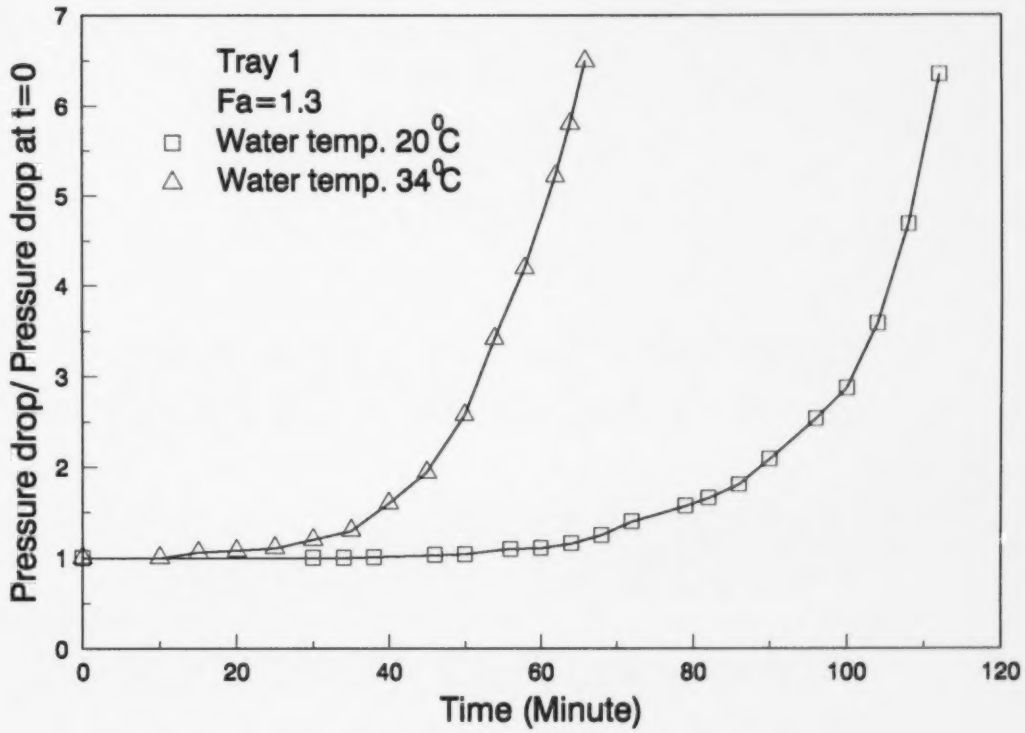

Figure 9-8
Comparison of Experimental and Calculated
Results for Tray 1 for Crystallisation Fouling

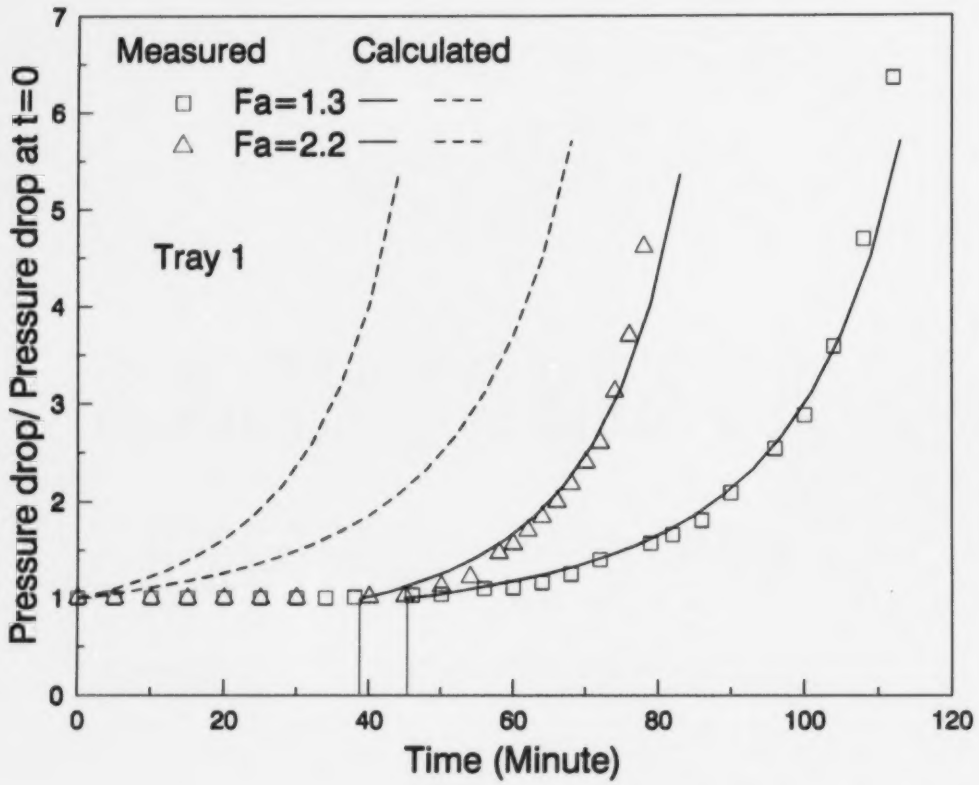

Figure 9-9
Comparison of Experimental and Calculated
Results for Tray 2 for Crystallisation Fouling

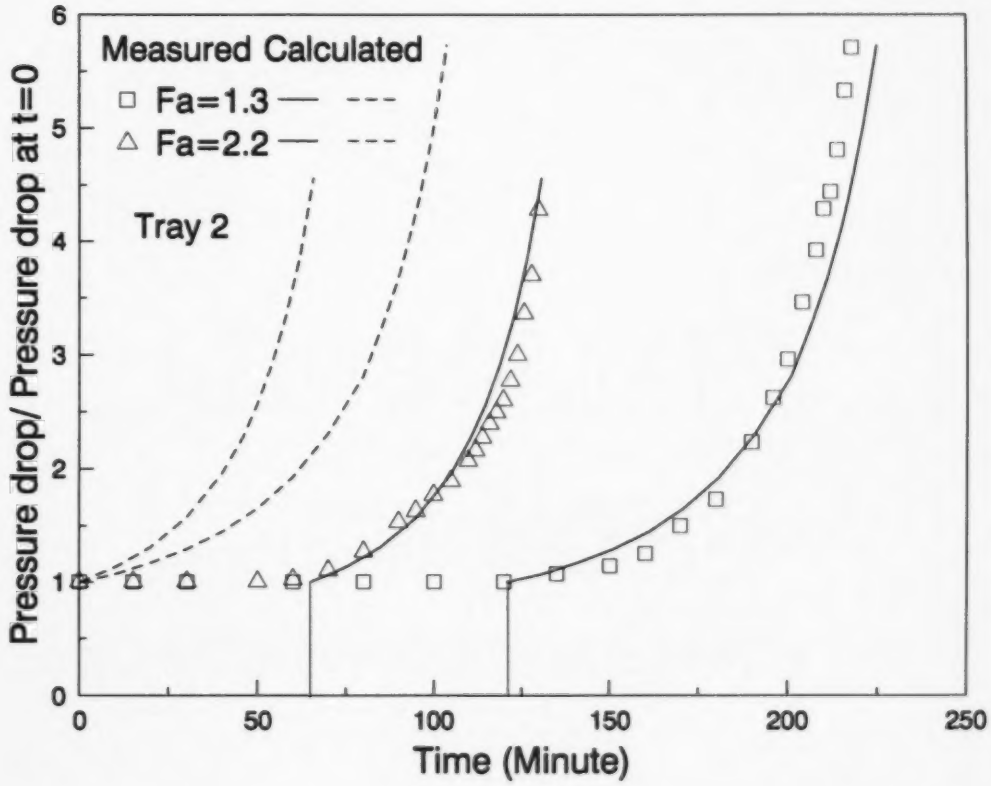

Figure 9-10
Comparison of Experimental and Calculated
Results for Tray 3 for Crystallisation Fouling

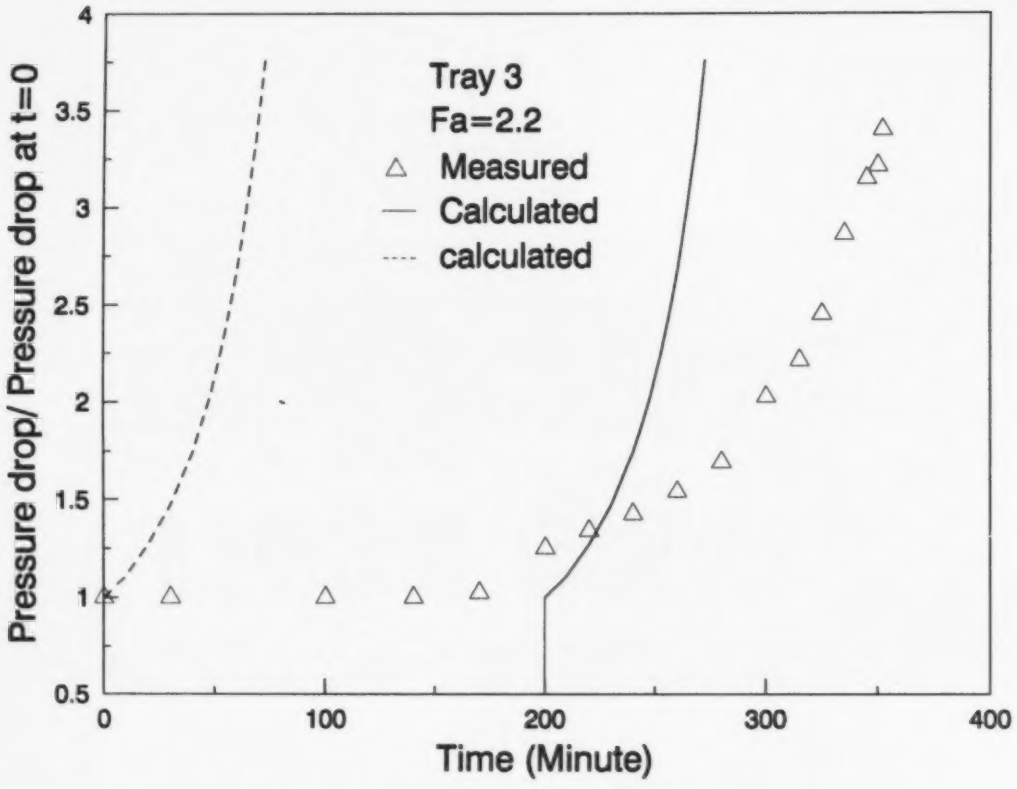

9.7 Literature Cited

Astarita, G. Mass Transfer With Chemical Reaction; Elsevier Publishing Company: New York, 1967.

Bennett, D.L.; Agrawal, R.; Cook, P.J. New Pressure Drop Correlation for Sieve Tray Distillation Columns. AIChE J. **1983**, 29, 434.

Burrill, K.A. Laboratory Studies to Resolve Fouling of Heat Exchangers and Sieve Trays in Canadian Girdler-Sulphide (GS) Heavy Water Plants. in "Fouling of Heat Transfer Equipment": Hemisphere, New York, 1981, 227.

Carslaw, H.A.; Jaeger, J.C. Conduction of Heat in Solids; Oxford Univ. Press: London, 1959.

Cervenka, J.: Kolar, V. Hydrodynamics of Plate Columns 8. Czech. Chem. Comm. **1973**, 39, 2891.

Chapter 10

CONCLUSIONS AND RECOMMENDATIONS

10.1 Introduction

Based on available efficiency data for commercial-scale columns, a new model has been developed for predicting the number of mass transfer units and point efficiency. Using the new efficiency model, the number of liquid and vapour phase mass transfer units in distillation was determined. At the same time, the effects of surface tension and its gradient on tray efficiency were studied. It was found that surface tension and its gradient have strong effects on the number of mass transfer units and on the tray efficiency. New models for estimating the effect of surface tension gradient on tray efficiency have also been obtained.

A new kind of tray called a packed tray has been developed in this study. The mass transfer efficiency of packed trays was determined in a small (0.153 m) distillation column using surface tension positive and negative systems. The hydraulics were measured in an air/water column. By comparing the performance of a packed tray with the performance of the same tray without packing, the effects of mesh packing on tray performance were identified. It was found that a packed tray had many advantages over the tray without packing in a small distillation column.

10.2 Predicting Point Efficiencies

A new semi-empirical model for predicting the number of mass transfer units, hence the tray efficiency, has been developed for distillation. The interfacial area of sieve tray dispersion is estimated by the Levich (1962)

theories, and the mass transfer coefficients are determined by the penetration theory. Two constants that are required to complete the model were obtained by fitting the model to the tray efficiency data of cyclohexane/n-heptane mixtures measured by Fractionation Research Inc (Sakata and Yanagi, 1979). The predicted efficiency and percent liquid-phase resistance are in good agreement with experimental data measured at different flow parameters. The new correlations can be given:

$$N_G = \frac{11}{\mu^{0.1}\phi^{0.14}} \left[\frac{\rho_L F_s^2}{\sigma^2} \right]^{1/3} (D_G t_G)^{0.5} \qquad (1)$$

$$N_L = \frac{14}{\mu^{0.1}\phi^{0.14}} \left[\frac{\rho_L F_s^2}{\sigma^2} \right]^{1/3} (M_G G/M_L L)\ (D_L t_L)^{0.5} \qquad (2)$$

where $t_G = h_L/u_s$; $t_L = t_G\rho_G/\rho_L$; and $F_s = u_s(\rho_G)^{0.5}$

From N_G and N_L, the percent liquid phase resistance can also be obtained.

10.3 Determining N_G and N_L From E_{OG}

Various methods for determining N_G and N_L from E_{OG} were compared. It was found that all methods published in the literature were unreliable. The slope and intercept method may be used only for systems whose N_G and N_L are composition-independent. A new method for obtaining N_G and N_L from E_{OG} has been developed. It was found that the new method can be used for all systems included in this study.

10.4 The Effect of Surface Tension on Tray Efficiencies

Based on accurately determined N_G and N_L, the effect of surface tension

on the number of mass transfer units and tray efficiency was investigated. It was found that surface tension has a strong effect on the number of mass transfer units and tray efficiency. It was also found that a surface tension positive system has a smaller liquid phase resistance than other systems due to surface renewal effects, and hence a higher efficiency. Based on the experimental efficiency data and determined N_G and N_L, most widely used efficiency models were compared. It was found that the new model obtained in this study is much better than any previous models.

10.5 The Effect of The Surface Tension Gradient on Tray Efficiencies

By comparing the efficiency of the methanol/water system with that of the cyclohexane/n-heptane system, it was found that the number of liquid phase mass transfer units of the methanol/water system is much larger, due to surface renewal effects. Based on the penetration theory, models have been obtained for estimating the enhancement of liquid phase mass transfer due to the roll cells caused by the difference in surface tension between the interface and phase bulk. The enhancement factor can be given:

$$\phi = N_L^+/N_L = (10000M/3.856)^{1.3} + (3.856/10000M)^{1.3}/3 \qquad (3)$$

$$M = (x - x_i)\frac{d\sigma}{dx}\ (E_{MV}/E_{OG}) \qquad (4)$$

where N_L is the value calculated from equation (2).

10.6 Mesh Packing Effects on Sieve Tray Performance

10.6.1 Mass Transfer Performance

The mass transfer performance of sieve trays with and without packing

was measured in a 0.153 m diameter distillation column with the methanol/water and the acetic acid/water systems. It was found that by adding a shallow bed of mesh packing, the Murphree tray efficiency was increased by 40 to 50% over a wide range of concentrations in the froth regime. This increase in efficiency can be attributed to much smaller and more uniform bubbles being generated on the packed tray. Models have been developed for estimating the packing effect on tray efficiency.

10.6.2 Interfacial Area and Sauter-Mean Bubble Diameter

The higher tray efficiency of packed trays is mainly due to the smaller and more uniform bubbles on the packed tray. Smaller and more uniform bubbles result in a larger interfacial area and smaller Sauter-mean bubble diameter. By using the experimental data, the interfacial area and Sauter-mean bubble diameter were estimated. It was found that mesh packing reduced the Sauter-mean bubble diameter by as much as 50% and increased the interfacial area up to 2.5 times at low gas velocities. This increase in interfacial area and reduction of bubble diameter are also verified by the photos of froth taken from the air/water simulator and distillation column. It can be concluded that mesh packing can effectively break up the large bubbles into small bubbles in the froth regime.

10.6.3 Entrainment and Vapour Capacity

Entrainment data for trays with different hole sizes with and without mesh packing were obtained in an air/water column. It was found that mesh packing could reduce the entrainment as much as 50 to 70%. The beneficial effect of packing on entrainment became more significant at low liquid loads

and high gas velocities for tray operating in the spray regime. Empirical correlations of entrainment were obtained for the tray with and without packing. It was found that packing reduced the exponent of gas velocity in the entrainment correlations by 40%. If the vapour capacity is defined as at e=10% kg liquid/kg vapour, the vapour capacity of packed trays is about 50 to 80% larger than the capacity of the same tray without packing.

10.6.4 Dry Pressure Drop and Total Pressure Drop

Pressure drop measurements were made in an air/water column. It was found that mesh packing has little effect on the dry tray pressure drop because of large void fraction of mesh packing (97%). But packing did increase the total tray pressure drop by about 15 to 20%. This increase in total tray pressure drop is due to larger liquid hold-up and a larger residual pressure drop which was caused by the extra energy consumed by packing to break up the bubbles. The effect of hole sizes on packed tray pressure drop is similar to that on conventional sieve trays.

10.6.5 Weeping and Turndown Ratio

Tray weeping was found to be greatly reduced by the mesh packing. In the air/water column, it was found that packing eliminated the weeping completely while Fa-factor went to zero because of the large surface tension of water. Consequently, the mesh packing could increase the turndown ratio substantially.

10.6.6 Other Observations

Froth height was measured by visual observation in the distillation

column. It was found that packing increased the froth height by 10 to 20%. It was also found that packing reduced the tray oscillation significantly. It is known that tray oscillation can cause lower froth height, more entrainment and weeping, early spray, and premature flooding. With less oscillation, the liquid hold-up and average liquid and vapour residence time were expected to increase. It is also suggested that the liquid back-mixing of packed trays is greatly reduced. Thus, the Peclet number is increased, especially for systems having a large slope of equilibrium line (m).

10.7 Fouling of Sieve Trays With and Without Packing

Sieve tray fouling due to the deposition of solids was studied in an air/water column. It was found that for the saturated air/water system containing insoluble solids, such as flour and $Ca(OH)_2$, no fouling was found during the experimental period of 48 hours. For crystallisation fouling, the following results were obtained: (1) for a given sieve hole diameter, the fouling rate increases with gas velocities; (2) no depositions were found when the tray operates under weeping conditions, (3) for a given gas velocity, larger sieve holes were found to have higher resistance to fouling, (4) mesh packing on the tray reduced the tray lifetime by more than 40 to 75% because of fouling on the packing. A mathematical model for crystallisation fouling was developed to predict the fouling rate in terms of the total tray pressure drop as a function of time.

10.8 Recommendations for Future Work

10.8.1 Mesh Packing Effect on Liquid Mixing

Tray efficiency falls short of the maximum value because of liquid

back-mixing. Yu et al. (1990) analyzed the liquid RTD profiles on a single-pass sieve tray and indicated a complicated flow pattern, i.e., a central zone of non-uniform flow with parabolic velocity distribution and a segmental zone of slow forward or backward flow with possible circulation. It is possible that packing might improve the liquid flow pattern by reducing the oscillation and waves and, consequently, reducing the liquid back-mixing. Detailed measurements of liquid mixing on trays with and without packing should be made. Then the packing effect on liquid mixing and Murphree tray efficiency could be characterized mathematically.

10.8.2 Effect of Mesh Packing on Tray Efficiencies in Other Flow Regimes

It has been shown that mesh packing can increase tray efficiency in the froth regime. However, sieve trays also operate in the spray regime at high vapour velocities with low liquid loads and in the emulsion regime at high liquid loads with high pressure conditions. The effect of mesh packing on the efficiency in these two regimes is probably different from that in the froth regime. This is because that in the spray regime, bubble sizes are not important to the efficiency. It is liquid droplet sizes which determine the efficiency. A bed of mesh packing on the tray may retard the liquid atomization process and increase the droplet sizes. Thus, it may reduce the efficiency. On the other hand, in the emulsion regime, bubble sizes are small and normally in the range of 5 to 3 mm (Hofhuis and Zuiderweg, 1979). The further reduction of bubble sizes by packing, if any, may be insignificant and have little effect on the efficiency. The definite conclusions on the packing effect on the efficiency in the spray and emulsion regimes can be obtained through the experimental measurements.

10.8.3 Development of Other Kind of Packed Trays

Packing has been found to improve the mass transfer performance of sieve trays. It is likely that packing would also improve the performance of other kinds of trays. One example is a combination of dual flow trays and packing (Chuang et al, 1990). A tray/packing combination is expected to perform better than a tray or packing alone. As one leading expert has said: "a tray/packing combination would be a leading distillation device for the twenty-first century" (Kister, 1991). Much more research is needed to find the optimum tray/packing combinations for different applications.

10.9 Literature Cited

Chuang, K.T, C. Xu, and G.X. Chen, "Gas-liquid contacting apparatus," U.K. Patent Application No. 90 11478.6, Publication No. BG 2232365, Dec. 12, 1990.

Hofhuis, P.A.M., and F.J. Zuiderweg, "Sieve plates: dispersion density and flow regimes," Inst. Chem. Eng. Symp. Ser. No. **56**, 2.2/1 (1979).

Kister, H.Z., Personal Communication, (1991).

Levich, V.G., "Physicochemical Hydrodynamics," Prentice Hall, Englewood, Cliffs, NJ (1962).

Lockett, M.J., "Distillation Tray Fundamentals," Cambridge University Press, (1986).

Sakata, M., and Y. Yanagi, "Performance of a commercial-scale sieve tray," Inst. Chem. Engrs. Symp. Ser. No.**56**, 3.2/21 (1979).

Yu, K.T., J. Huang, J.L. Li and H.H. Song, "Two-Dimensional Flow and Eddy Diffusion on a Sieve Tray", Chem. Eng. Sci. **45**(9), 2901-2906 (1990).

Appendix A

The Top View of Froths on the Tray Without Packing

(Air/water system, Fa=0.4)

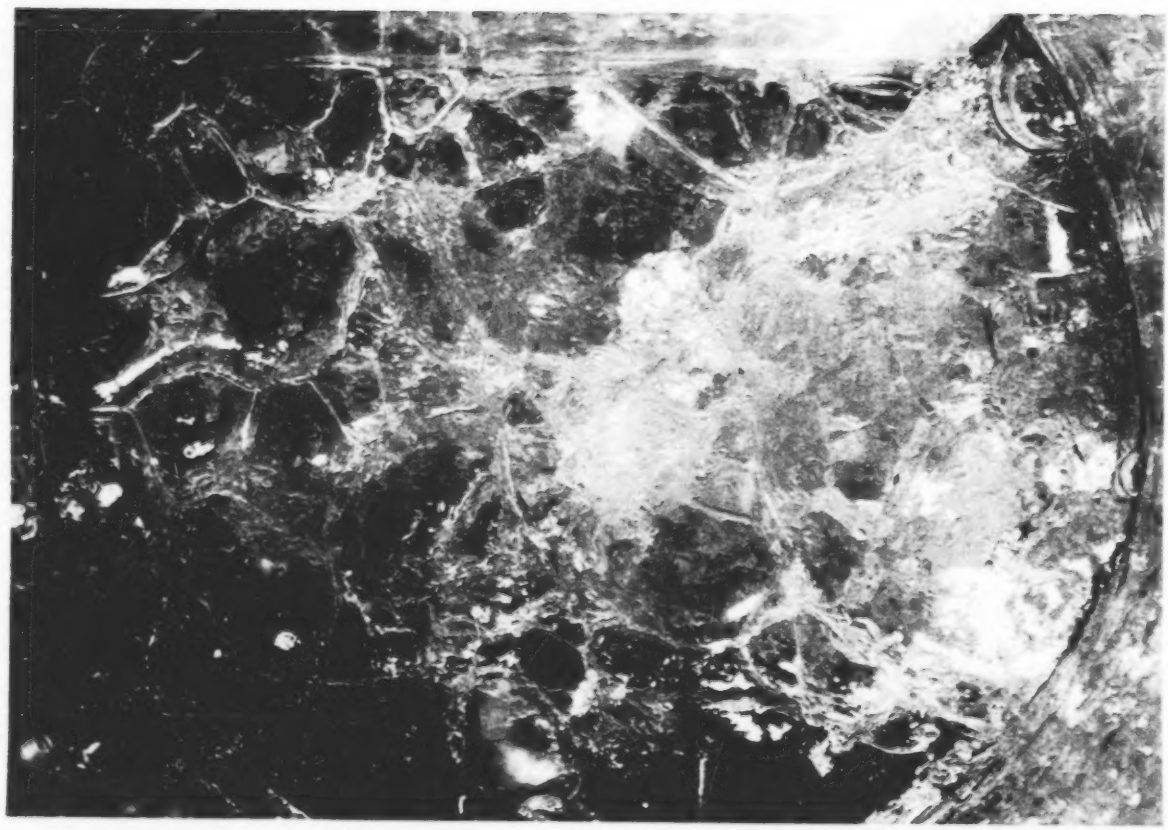

The Top View of Froths on the Tray With 1" Packing
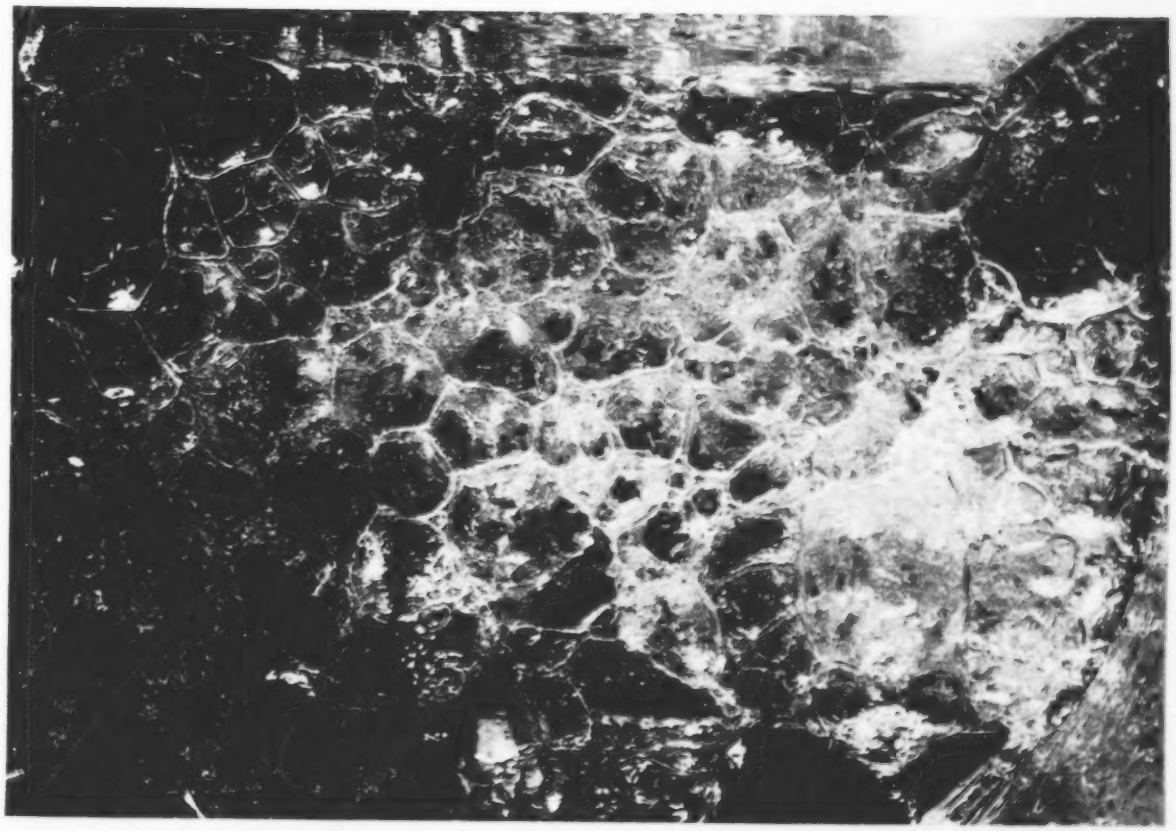
(Air/water system, Fa=0.4)